UNIVERSITY OF OKLAHOMA

GRADUATE COLLEGE

AN ORGANIC GEOCHEMICAL STUDY OF WOODFORD SHALE AND WOODFORD-MISSISSIPPIAN TIGHT OIL FROM CENTRAL OKLAHOMA

A DISSERTATION

SUBMITTED TO THE GRADUATE FACULTY

in partial fulfillment of the requirements for the

Degree of

DOCTOR OF PHILOSOPHY

By

TING WANG
Norman, Oklahoma
2016

AN ORGANIC GEOCHEMICAL STUDY OF WOODFORD SHALE AND WOODFORD-MISSISSIPPIAN TIGHT OIL FROM CENTRAL OKLAHOMA

A DISSERTATION APPROVED FOR THE
CONOCOPHILLIPS SCHOOL OF GEOLOGY AND GEOPHYSICS

BY

_____
Dr. R. Paul Philp, Chair

_____
Dr. Roger M. Slatt

_____
Dr. Michael Engel

_____
Dr. Xingru Wu

_____
Dr. Matthew Herrin

Acknowledgements

I would like to express my sincere appreciation to Dr. R. Paul Philp, my research advisor and committee chairman, first of all for him to accept me to be his Ph.D. student five years ago when I was still a chemistry master student in New Mexico, and moreover for all his time, patience, guidance, mentoring and main financial support throughout the last five years of my PhD research.

I also would like to thank the members of my committee, Dr. Roger M. Slatt, Dr. Michael Engel, Dr. Xingru Wu, and Dr. Matthew Herrin for their encouragement and support, and for their time and valuable suggestions in reviewing this manuscript.

I wish to extend my gratitude to Devon Energy for providing the oils and cores for this project. I also gratefully acknowledge the AAPG Foundation for awarding me the 2014 Grants-in-Aid, and to the ConocoPhillips School of Geology and Geophysics for awarding me the Student Research Grant. These contributions significantly supported this research.

My sincere thanks to Mr. Gene Kullmann and Ms. Vyetta Jordan from the Oklahoma Petroleum Information Center (OPIC) at Oklahoma Geological Survey in Norman, Oklahoma for providing part of the core samples analyzed in this research.

Special thanks for Mr. Brian J. Cardott for training me in organic petrography, especially in vitrinite reflectance measurements, and for providing valuable data for this project. Thank you for your time, disposition, and patience.

I am deeply grateful with all the staff at the Organic Geochemistry Laboratory, especially with Mr. Jon Allen and Mr. Larry Hyde, who always had the patience and

dedication for helping me in innumerable ways to successfully complete my laboratory work. I also wish to extend this acknowledgement to the rest of the staff at the laboratory.

My deepest appreciation is for Dr. Thanh Nguyen and Dr. Yueming Lu. I will never be able to thank you enough for all the help you provided me during all these years. It has been an honor meeting you. I am grateful for your invaluable contribution for this project. I admire your positive attitude, patience and dedication to teach.

I want to thank the staff of the School of Geology and Geophysics, for their assistance, kindness, and for always cheering my days. I also want to thank Mrs. Jody Foote, for all her help in the Youngblood Energy Library, and for also being a friend. I will miss y'all.

Thanks to my classmates and colleagues, especially to Li Liu, Mu Liu, Andrea Miceli Romero, Emillio Torres Parada, Kirellos Sefein for working with me during the my Ph.D. program.

I want to thank my very dear friends Yuqi Zhou, Long Wu, Li Pan, Qiaohua Tan, Chen Chen, Luchao Jin, Jiman Liu, Jing Zhang, Rui Zhai, Hang Deng, Brian Turner, Eli Ester and Richard Brito, for all their support and infinite help, especially during the course of this project.

Finally I want to thank my parents, Zhigang Wang and Xing Huang for their love, encouragement, and support.

Table of Contents

List of Figures

List of Tables

Abstract

A comprehensive organic geochemical analysis was performed on a suite of core samples from the Woodford Shale in Central Oklahoma with the aim of characterizing variations in organic matter source, depositional environments and thermal maturity. A total of 30 oils and condensates produced from the Woodford Shale and Mississippian Limestone in Central Oklahoma were analyzed to determine the origin of these liquids. A total of 168 core samples containing the Woodford and Mississippian sections from 14 wells were subjected to total organic carbon (TOC) and Rock-Eval analysis for geochemical screening, and one sample from each well was analyzed for vitrinite reflectance ($\%R_o$) measurement. Rock samples with good source rock potential (TOC>1.0% wt.) were selected for biomarker and isotope analyses. These analyses were carried out by means of gas chromatography (GC), gas chromatography-mass spectrometry (GC-MS), and gas chromatography-mass spectrometry- mass spectrometry (GC-MS/MS).

Based on the organofacies classification of Pepper and Corvi (1995), the Woodford Shale in this study is a typical marine siliciclastic mudstone (organofacies B), which is supported by the evidence described herein. TOC and Rock-Eval parameters show that the Woodford Shale has excellent source rock potential and is dominated by Type II kerogen indicating a marine origin. Distributions of regular steranes, hopanes and monoaromatic steroids (MAS) point towards a marine siliciclastic depositional environment. Aryl isoprenoids and paleorenieratanes/isorenieratanes suggest the occurrence of episodic periods of photic zone anoxia (PZA) during deposition of the Woodford Shale in this study. In addition, *n*-alkanes, steranes distributions, and the

tentative identification of gammacerane suggest deposition under hypersaline conditions in Central Oklahoma. Source-dependent biomarker parameters indicate that in the area in the proximity of the Nemaha Uplift, the Woodford Shale was deposited under a condition rich in clay content, reflecting the influence of the paleo-Nemaha Uplift. Thermal maturity parameters indicate that the Woodford Shale is immature to marginally mature in Payne County, and shows a progressive increase in maturity towards the southwest following the regional dip. In the area in the proximity of the Nemaha Uplift, the Woodford Shale is in the main stage of oil generation.

Geochemical logs of Pritchard-1 well show a minimal range of vertical variation within the Woodford Shale in this study. The Woodford Shale in this study was subdivided into middle and upper members without the lower member being present based on the integration of geochemical and geological data. The middle Woodford member has the higher TOC values. Pristane and phytane (Pr/Ph) and biomarker ratios suggest the establishment of stronger anoxic conditions during deposition of the middle Woodford member than the upper Woodford member, where the latter may have received an additional siliciclastic organic matter input. In the area in the proximity of the Nemaha Uplift, Pr/Ph ratios indicate deposition under suboxic to dysoxic conditions for the Woodford Shale interval analyzed. Isotope data indicates a marine organic matter source for the Woodford Shale, but $\delta^{13}C$ values do not show significant variations in organic facies, depositional environment, or thermal maturity.

Three conclusions regarding the origin of the liquids in this study are: (i) oils produced from the Woodford Formation and that from the overlying Mississippian Formation share very similar fingerprints suggesting the Woodford Formation and the

overlying Mississippian Formation are connected; (ii) oils produced in the area in the proximity of the Nemaha Uplift (Logan and West Payne Counties) were not only Woodford sourced but also had a Mississippian source contribution based on the presence of abundant extended tricyclic terpanes and other source specific biomarker fingerprint characteristics; (iii) oils sampled from the East of the Cherokee Platform (Central-East Payne County) share strong Woodford source characteristics but were not generated *in-situ* from the Woodford Shale, which is not mature enough in that area, but probably migrated from the Woodford Shale in the deeper part of the Anadarko Basin in Southern Oklahoma. The results of this research are consistent with some new findings reported by Devon geologists that abundant marine coarse-grained biogenic silica (radiolarian-rich chert facies) found in Woodford cores (Central-East Payne County) in this area may be a contributor to good reservoir petrophysical properties suggesting the Woodford Formation may not be the source rock in this area but simply a tight reservoir.

CHAPTER 1

1. INTRODUCTION

Since early 2000s, the "shale revolution" has stimulated tremendous production of oil and natural gas in the United States. Shale resource plays can be either shale-gas or shale-oil. These reservoirs are typically very tight with low porosity and ultra-low permeability values in the nanodarcy range. With the astounding success from shale-gas production in the U.S.A., gas prices have remained low particularly when compared to oil prices since 2009 (Jarvie, 2010). Therefore, subsequent work has been switched from the exploration and development of shale gas plays to shale oil plays (Jarvie, 2010), a "shale oil boom", before crude oil price slumped in September 2014.

According to a projection presented by the International Energy Agency (IEA) in April 2015, it is expected that there will be an increase in the total U.S. production from 11.8 MMBOE/D (million barrels of oil equivalent per day) in 2014 to 13.2 MMBOE/D by 2020 making the U.S. to be the largest crude oil producer in the world instead of Saudi Arabia (IEA, 2015). The increase would be mainly contributed from unconventional resource plays. Shale oil plays are currently undergoing the fastest growth and will account for 18% of total U.S. production by 2030 (IEA, 2015). In the U.S., at least 21 shale oil basins in 20 states have been discovered (Figure 1; EIA, 2015). Oklahoma, with Woodford/Mississippian tight oil production, has been playing a significant role in U.S. total oil production. Excluding federal offshore areas, Oklahoma ranked fifth in crude oil production in the nation in 2014. Moreover, Oklahoma is one of the top natural gas-producing states in the nation, accounting for 7.4% of U.S. gross production and 7.4% of marketed production in 2014 (EIA, 2015). Shale oil has become

an important focal point for both geoscience academia and petroleum industry who have carried out vast amounts of research in order to improve exploration and production strategies.

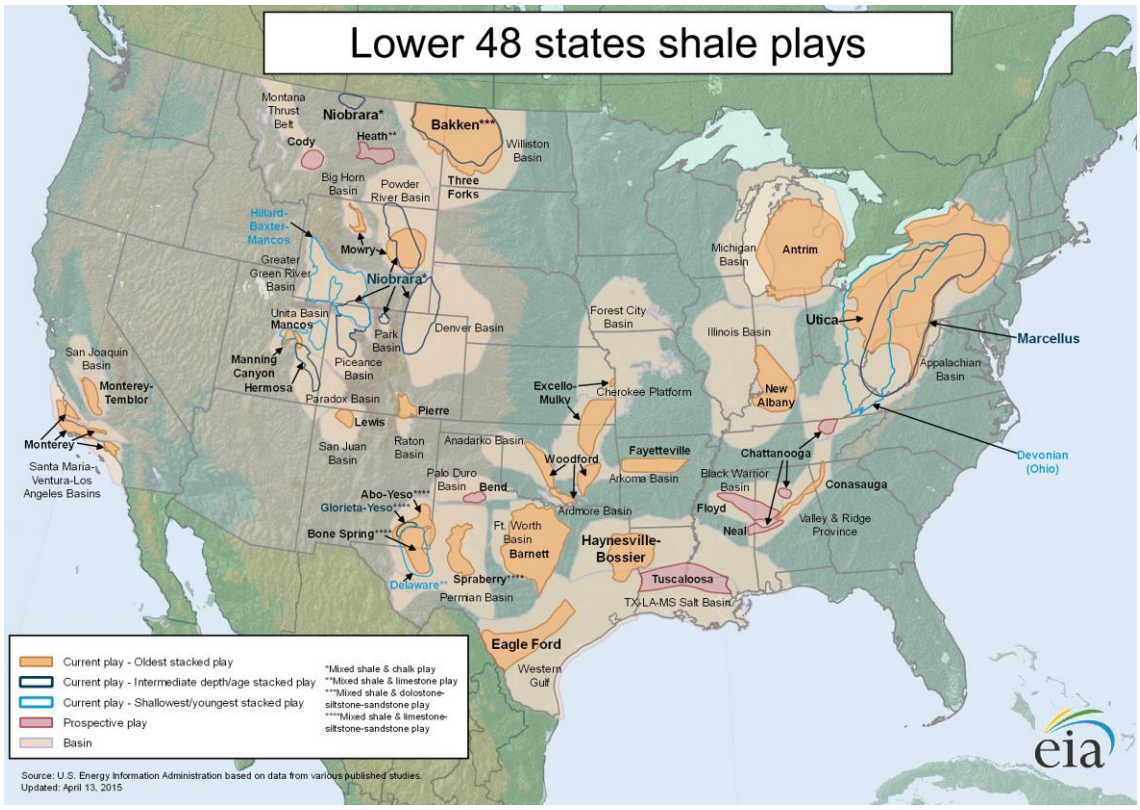

Figure 1. U.S. shale oil plays, lower 48 states (EIA, 2015).

The Late-Devonian to Early-Mississippian Woodford Shale is an organic rich black shale widely distributed over the southern Mid-Continent (Comer and Hinch, 1987; Comer, 1992). It has been proven to be a world-class source rock responsed for 70% to 85% of the conventional hydrocarbon reservoirs in Oklahoma and Kansas (Comer and Hinch, 1987; Burruss and Hatch, 1989; Philp et al, 1989; Jones and Philp, 1990; Comer, 1992; Wang, 1993). Recently it has been an attractive target for unconventional oil and gas exploration and production in Oklahoma and West Texas due to its world famous source rock characteristics (Cardott, 2014a).

Woodford Shale has not only been proven to be an excellent source rock charging conventional reservoirs in Kansas and Oklahoma, but also a frontier for unconventional resource play exploration and production. The unconventional Woodford resource play in Oklahoma (Cardott, 2014a; Kvale and Bynum, 2014; Figure 2), encompasses four regions, namely Anadarko-Woodford, Arkoma-Woodford, Nemaha-Woodford and Southern Oklahoma-Woodford, was estimated to contain 0.24×10^{12} ft^3 of natural gas in place and 70×10^9 bbl of oil in place on the basis of the mass balance calculation indicating a huge potential as unconventional hydrocarbon production target (Comer, 2005). The field production results have already confirmed Comer's estimation. As of July 2010, the cumulative Woodford-only production has been 932 Bcf of gas and 3.7 Mbbl of oil (Cardott, 2012). The dominant hydrocarbon phases produced from the Woodford vary in different structural provinces in Oklahoma (Cardott, 2014a; Kvale and Bynum, 2014; Figure 2). In the Anadarko and Arkoma Basin, the Woodford horizontal wells produce mainly dry gas from over 14,000 ft deep (~4,300 m; ; Cardott, 2014a; Kvale and Bynum, 2014). In areas straddling between the basin and shelf, like the Cana-Woodford Play in Figure 2, the Woodford produces wet gas and condensates. The oil has been commingled produced from the Woodford/Mississippian strata since 2010 on the Anadarko Shelf and Cherokee Platform. From 2004 to 2014 Q1, there were more than 3,100 horizontal and vertical production wells producing hydrocarbon from the Woodford Formation in Oklahoma (Figure 3; Cardott, 2014a). Before the crude oil price plunge since late 2014, there was a sharp increase in the number of Woodford horizontal wells drilled in Oklahoma. As of 2014 Q3, four regions in Oklahoma, were the fastest

growing shale plays in North America, showing a 30% increase in production rates over the previous year (Menchaca, 2014).

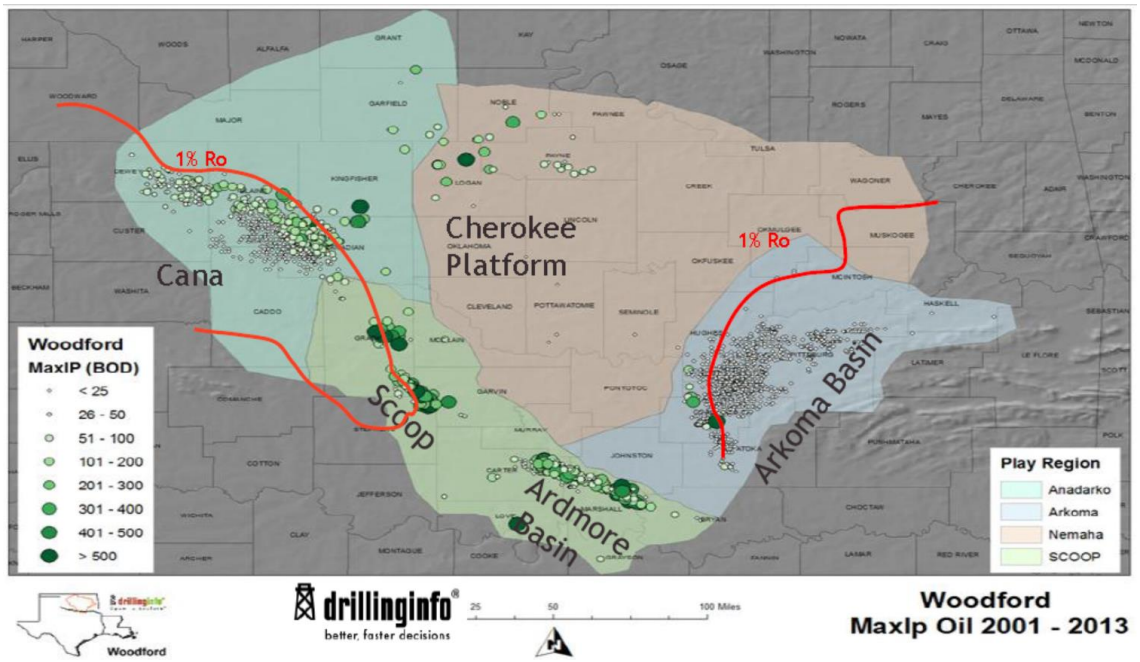

Figure 2. Composite Map of Different Woodford Unconventional Play "Provinces" with Max IP Oil (BOD) and General Thermal Maturity (Kvale and Jamar, 2014)

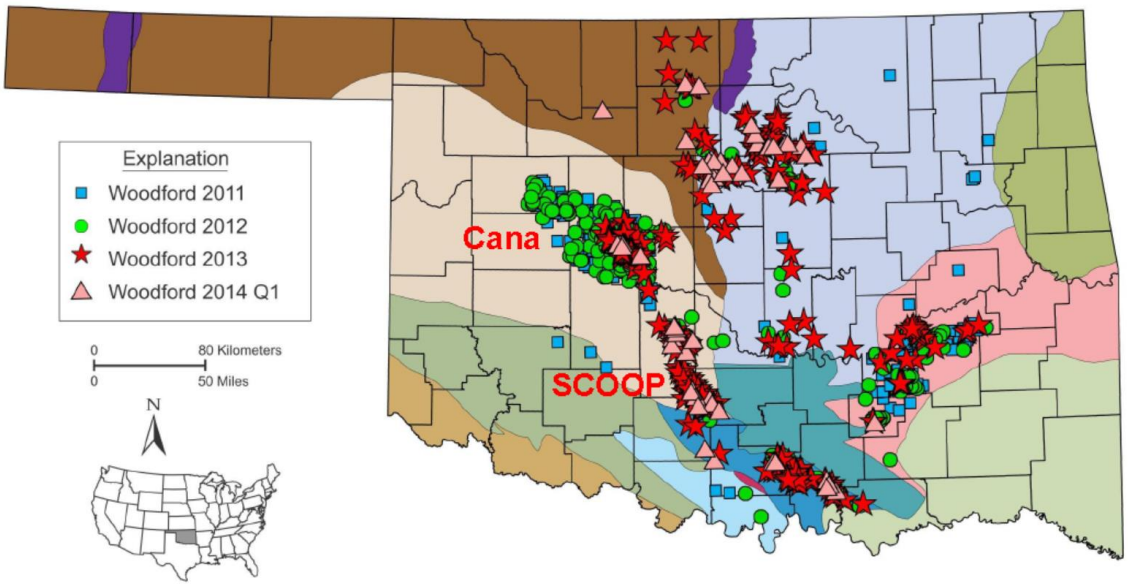

Figure 3. Woodford Production Wells Distribution Map in Oklahoma (modified from Cardott, 2014a).

1.1 General Introduction of Tight Oil Production in Central Oklahoma

In 2009, Devon Energy produced tight oil from the Woodford Formation in Logan and Payne Counties, North-Central Oklahoma (Coffey, 2015). As shown by the Devon operation report of the third quarter of 2014, the net production from the Mississippian-Woodford play (Logan and Payne Counties; Figure 4) averaged a record 21,000 BOE (barrel of oil equivalent) per day, which is a 136% increase compared to the third quarter of 2013. Oil and NGL (natural gas liquid) accounted for nearly 75% of total production (DVN Operation Report Q3 2014). The other players in this area include Marathon, Continental, Sandridge and some other small-size operators.

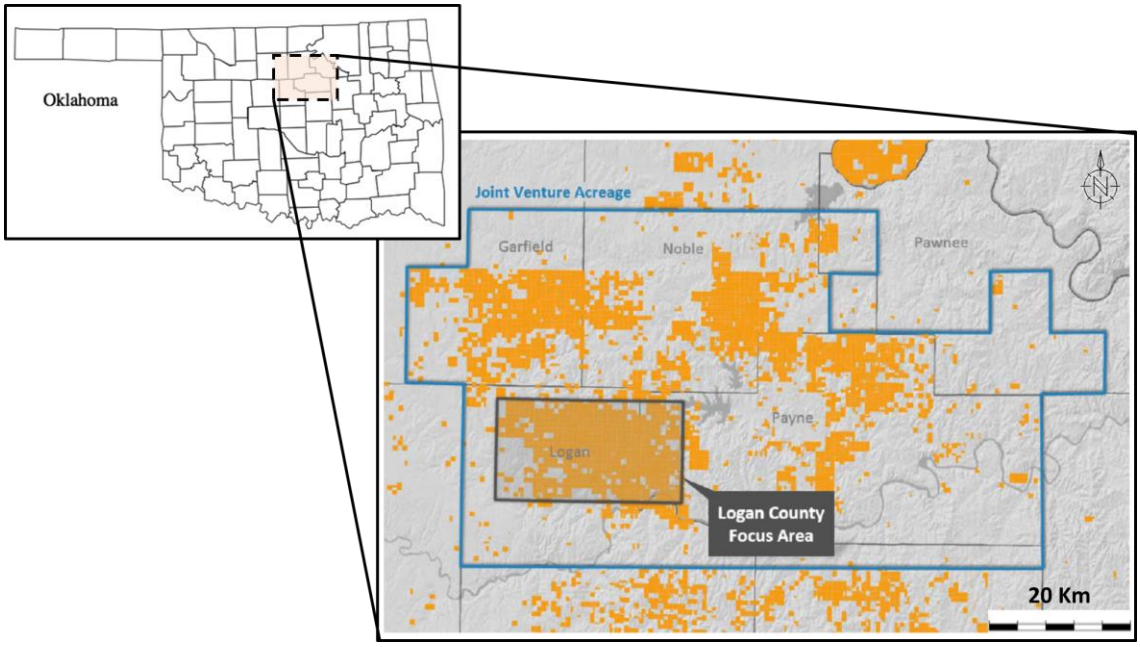

Figure 4. Devon Energy Mississippian-Woodford Tight Oil Play Joint Venture Acreage Map (Devon Acreage in yellow; DVN Operation Report Q3 2014)

1.2 Purpose of Study

The primary objective of this study is to answer two questions: 1) what is the origin of the tight oils: are they generated *in-situ* from the Woodford Shale or migrated; 2) if generated *in-situ*, how could they be generated from immature Woodford Shale; if migrated, how could they charge a very tight shale formation. To answer these questions, it is necessary to evaluate hydrocarbon generation potential of source rocks in the study area as well as examine a detailed geochemical characterization of both crude oils and source rocks to determine several key geochemical parameters including: a) organo- and litho-facies of the potential source rocks and their depositional environment; b) thermal maturity; c) oil-oil and oil-source rock correlations; d) biodegradation if any. The significance of this study for the oil industry will be related to the understanding of the mechanisms of shale oil formation, which in turn will further aid unconventional resource exploration.

1.3 Previous Studies – Literature Review

1.3.1 Previous Studies on General Geology and Petroleum Geology

Since both the Anadarko Basin and Cherokee Platform in Oklahoma are mature giant oil and gas provinces and have been developed over 100 years from 1910s, intensive geological and geophysical studies have been carried out during that period. Those studies have significantly increased the knowledge and understanding of the basin-platform's evolutionary history.

Petroleum exploration in the Cherokee Platform Province began in the 1860's with drilling in Bourbon and Cherokee Counties, Kansas. The first discovery was in 1873 in Allen County, Kansas (Iola field) (Charpentier, 2001). The Anadarko Basin was first

defined in the literature by Gould (1924), although the earliest oil and gas discovery and production occurred in 1917 (Becker, 1927). The geological history, stratigraphy, and structure of the basin have been topics for geological study and speculation since early 20th century (Freie, 1930). Detailed studies of the petrography, paleontology, and facies variation of the Woodford Shale have been conducted by many researchers (Urban, 1960; Hass and Huddle, 1965; Lewan, 1983; Sullivan, 1983; Perry, 1989; Denison et al., 1990; Kelley, 1991; Comer, 1992; Kareem, 1992; Comer, 2005; 2007; 2008; 2009; 2012). Recently many graduate students at the University of Oklahoma have chosen portions of the Woodford Shale in the Anadarko Basin and Cherokee Platform as their target areas for regional geological studies (Miller, 2006; Branch, 2007; Badra, 2011; Althoff, 2012; Chain, 2012; Kilian, 2012; Amorocho Sanchez, 2013; Bernal, 2013; Molinares Blanco, 2013; Mann, 2014; McCullough, 2014; Treanton, 2014; Esther, 2015). An overview of the Woodford Shale from the platform to the basin can be obtained by putting these regional studies together.

Johnson et al. (1989) presented a detailed description of lithology and depositional environments of formations in the Anadarko Basin. The plates (isopach maps of important formations) included in this reference provided valuable information about basin-wide investigation and evaluation of the formations. Rascoe and Hyne (1988) published a book entitled "*Petroleum Geology of the Mid-Continent*", which provided specific information about the stratigraphic and structural data of oil and gas production of the Anadarko Basin and Cherokee Platform. Johnson made a comprehensive review of the geological studies at the Anadarko Basin Symposium held by the Oklahoma Geological Survey in 1988. Other papers presented (1989) at this symposium provided

valuable information, which covered many topics about the geology of the basin (Amsden, 1989; Burruss and Hatch, 1989; Cardott, 1989; Schmoker, 1989; and Northcutt, 2001). Entering into 2000s when the unconventional resource plays became more and more actively exploited in U.S. the Woodford Shale, as one of the "hot shale" targets, was attracting more and more focus from various disciplines of geoscience. Carpentier (2001) presented a detailed description of each element of the major petroleum systems, including reservoirs, source rocks, traps, resource potential and exploration status, in the Cherokee Platform Province. Cardott (2005) made a comprehensive overview of the unconventional energy resource in Oklahoma, including the Woodford Shale, at the Unconventional Energy Resources in the Southern Midcontinent Symposium held by the Oklahoma Geological Survey in 2004.

Many studies have shown that the Woodford Shale should account for more than 85% of commercial oil produced from the conventional reservoirs in Oklahoma and Kansas (Welte et al., 1975; Lewan et al., 1979; Reber, 1989; Burruss and Hatch, 1989). But few publications have strong evidence to prove these oils originated from the Woodford Shale. Previous studies on the petroleum systems thought to be sourced by the Woodford Shale are summarized below.

Comer and Hinch (1987) recognized the expulsion of oil from the Woodford Formation and age-equivalent rocks in Oklahoma and Arkansas by identifying numerous small-scale accumulations of rock extract within mature parts of the Woodford Formation including fractures, stylolites, burrows, nodules, and sandstone lenses, all of which are completely enclosed in the source rock. This work proved the primary migration (expulsion) of hydrocarbon generated from the Woodford Shale.

Another strong piece of evidence showing the Woodford Shale has generated oil *in-situ* is the work by Philp (2013, personal communication). Rock extracts were obtained from the surface fractures of the Woodford outcrop in the McAlister Cemetery Quarry, northern flank of Criner Hill. By correlation of single-ion-mass chromatograms from GCMS analysis, it was concluded that low-thermal-maturity "oil" (rock extract filled in the fractures) had originated from the local Woodford Shale (Cardott, 2014).

Jones and Philp (1989) analyzed oil samples produced from multiple conventional reservoirs of different age and rock extracts of possible source beds. By investigating their GC and GC/MS fingerprint characteristics, it was believed most of these oil samples received a major contribution from the Woodford Shale in the Anadarko Basin and the Viola Group limestone was believed to be the source rock for the oil produced from the Viola Group reservoir (Jones, 1986; Jones and Philp, 1989).

Burruss and Hatch (1989) undertook a detailed geochemical investigation of 104 crude oils and 190 core samples of dark-colored shales from the Anadarko Basin. They distinguished three major oil types, which generally correlated with the reservoir and source-rock age. One of the crude oil types shared the characteristic stable carbon isotope signature and biomarker fingerprints with the Woodford source-rock extracts. This crude oil may have originated from the Woodford Shale in the deep Anadarko Basin (Burruss and Hatch, 1989).

1.3.2 Previous Studies on Woodford Geochemistry

Organic geochemical studies on the Woodford Shale have been conducted by several authors. The maturity of the Woodford Shale was investigated by several studies (Cardott and Lambert, 1985; Schmoker, 1986; Cardott, 1989; Pawlewicz, 1989; Hussain

and Bloom, 1991; Cardott, 2012; Cardott, 2013; Cardott, 2014a; 2014b). Lewan (1983) conducted a hydrous pyrolysis experiment on the Woodford Shale to study the effects of thermal maturation on stable organic carbon isotopes. Schmoker (1986) developed a maturity model for the Woodford Shale in the Anadarko Basin based on a modified Lopatin's TTI (time-temperature index) method. Engel et al. (1988) conducted an organic geochemical correlation of Oklahoma crude oils using R- and Q- mode factor analyses. Hester et al. (1990) mapped TOC of the Woodford Shale in the northwestern part of the Anadarko Basin based on a well log derived TOC calculation method. Kirkland (1992) proposed the Woodford Shale sedimentation in the Anadarko Basin was controlled by the paleo-bathymetry. Lambert (1994) discussed the internal stratigraphy and organic facies of the Devonian/Mississippian Chattanooga (Woodford) Shale in Oklahoma and Kansas. Coming to the 21st century as the "shale boom" overwhelmingly swept across the whole country, the Woodford Shale was re-assessed as a resource play target and geochemistry was integrated with other geoscience disciplines, especially sequence stratigraphy and chemostratrigraphy. The most astonishing finding of this integration was the shale internal heterogeneity. Previously the shale was thought to be uniform stratigraphic sequences in terms of physical and chemical properties. However, more and more evidence demonstrated that a more detailed analysis of these very fine-grained mudrocks can provide greater insight about variations in the depositional and environmental factors that influenced source rock deposition (Hester et al., 1990; Hickey and Henk, 2007; Loucks and Ruppel, 2007; Singh, 2008; Comer, 2008; Slatt et al., 2009a, 2009b, 2009c, 2009d). Several recent studies already demonstrated the usefulness of organic geochemistry as a tool for complementing and refining sequence stratigraphic

frameworks, especially in unconventional shale gas plays. Recently several graduate students at the University of Oklahoma have integrated biomarker analysis with sequence stratigraphy and chemostratigraphy for the Woodford Shale in the Anadarko Basin and Cherokee Platform to investigate the detailed depositional and environmental factors affecting the deposition of mudrocks (Miceli Romero, 2010; Connock, 2015; DeGarmo, 2015). A representative work among these studies is done by Miceli Romero and Philp (2012). They found the presence and extent of photic zone anoxia (PZA) during the deposition of the Woodford Shale and demonstrated the significant lithologic and chemical variability that occurs within shales (Miceli Romero and Philp, 2012).

Moreover, the oil industry and geoscience academia have worked together in order to evaluate the shale play characteristics, including shale type, organic contents, maturity, porosity, permeability, fracability, hydrocarbon content, reservoir thickness, volumetrics, to determine the "sweet spots", play fairways, and producible areas of the potential shale plays (Schmoker, 2002; Schenk, 2005; Gale et al., 2007; Pollastro, 2007; Jarvie et al., 2007 and 2010; Jarvie, 2012a and 2012b). In this regard, geochemistry has played a key role in shale play evaluation. Hester et al. (1990) highly praised the use of organic geochemical data as one of the best tools for characterizing Woodford Shale internal facies. Different approaches and techniques have been used to determine the significant geochemical properties for shale resource play evaluation, including: organic matter type, quantity and provenance; thermal maturity; type of hydrocarbons generated; clay content. This information has been integrated with information from other geoscience and engineering disciplines such as geology, geophysics, petrophysics and reservoir/petroleum engineering to determine shale play potential and attempt to define

petroleum systems for these types of plays (Curtis, 2002; Jarvie et al., 2007; Hill et al., 2007a and 2007b; Philp, 2007; Pollastro et al., 2007; Jarvie, 2012a and 2012b).

CHAPTER 2

2. GEOLOGICAL FRAMEWORK

2.1 The Geological Evolution of the Anadarko Basin, Nemaha Uplift and the Cherokee Platform

2.1.1 Anadarko Basin

During early Paleozoic time, three major tectonic/depositional provinces existed in Oklahoma (Figure 5): the Oklahoma Basin, the southern Oklahoma Aulacogen, and the Ouachita Trough. The Oklahoma Basin, initiated during continental breakup in the Late Precambrian (Miall, 2008), was a shelf-like area that received widespread and thick shallow-marine carbonates interbedded with thin marine shales and sandstones (Johnson et al., 1988; Northcutt et al., 2001). The southern Oklahoma Aulacogen, a west-northwest-trending trough derived from one of the failed rifts during the breakup of the supercontinent Rodinia (Miall, 2008), was the depocenter for the Oklahoma Basin and the precursor of the Anadarko Basin (Johnson et al., 1989; Northcutt et al., 2001). The Ouachita Trough received deep-water sediments, which deposited along a rift located in the southern margin of the North American craton (Johnson et al., 1989; Northcutt et al., 2001).

From Silurian to Middle Devonian clean-washed skeletal limestones, argillaceous and silty carbonates, referred to as the Hunton Group in Oklahoma, were deposited in a shallow marine setting (Northcutt et al., 2001). Epeirogenic uplifts interrupted deposition resulting in two regional unconformities. One unconformity arose during pre-middle Early Devonian (pre-Frisco-Sallisaw unconformity) and the second one during pre-Late Devonian (pre-Woodford-Chattanooga unconformity; Figure 6; Johnson et al., 1989). In

southern Oklahoma the pre-Woodford-Chattanooga unconformity eroded to the Upper Ordovician and in northern Oklahoma the erosion sculpted out Upper Cambrian-Lower Ordovician rocks (Figure 6; Kirkland et al., 1992).

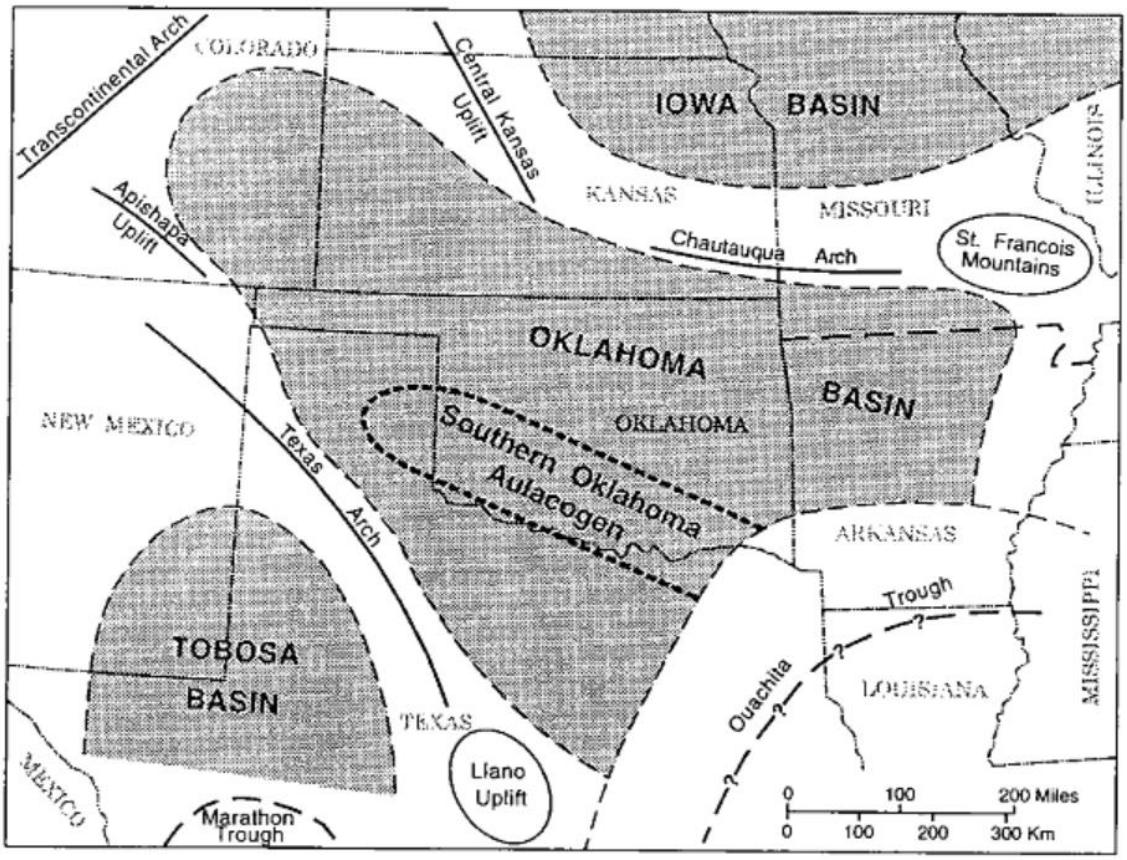

Figure 5. Map of southwestern United States, showing approximate boundary of the Oklahoma Basin and other major features that existed in early and middle Paleozoic time (Northcutt et al., 2001)

During Late Devonian the Woodford-Chattanooga Sea (Kirkland et al., 1992) transgressed from the south-southeast direction, overlying the erosional surface with dark-gray to black silts and clay throughout most of the Oklahoma Basin. The exception took place where the Woodford-Chattanooga Sea advanced across the paleo-highs, which were the source for the Misener Sands. The Misener Sands were derived most likely from reworking of Middle Ordovician Simpson sands in North-Central Oklahoma (Amsden

and Klapper, 1972; Kirkland et al., 1992) and incorporated into the basal sediments of the Misener-Woodford Formation. The Misener-Woodford interval represents an anoxic transgressional episode (Fritz and Beaumont, 2001). Throughout Mississippian time extensive epeirogenic movements continued on the southern Midcontinent (Miall, 2008).

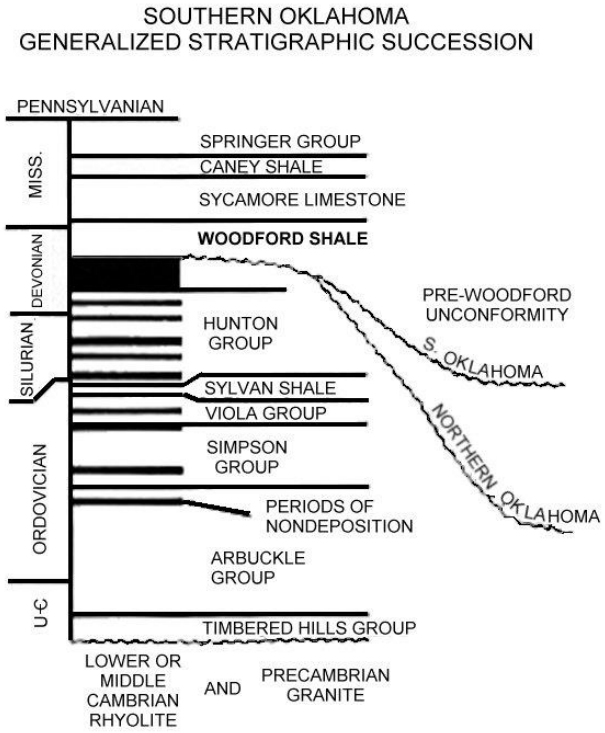

Figure 6. Generalized stratigraphic section for the pre-Pennsylvanian of southern Oklahoma showing periods of non-deposition (black) and extent of pre-Woodford unconformity (Kirkland et al., 1992).

After the regression of the euxinic Woodford-Chattanooga Sea, a warm and oxygenated sea covered the continental region and favored the shallow-marine limestones, carbonate micrites, and later cherty-limestone to develop in this region (Kirkland et al., 1992; Miall, 2008). The Oklahoma Basin, the Ozark Uplift, and the paleo-Nemaha Uplift were the most important structural features that influenced sedimentation during this time (Northcutt et al., 2001). Other regions were mostly low-energy shelves or platforms

(Northcutt et al., 2001). According to Northcutt et al. (2001), these three major Paleozoic structural provinces were finally modified during the Pennsylvanian. The Oklahoma Basin and the Southern Oklahoma Aulacogen evolved into restricted marine basins. The Ouachita Trough was destroyed by the uplift and northward thrusting associated with the Marathon-Ouachita Orogeny. The present-day structural provinces of Oklahoma were generated as a consequence of these events (Figure 7).

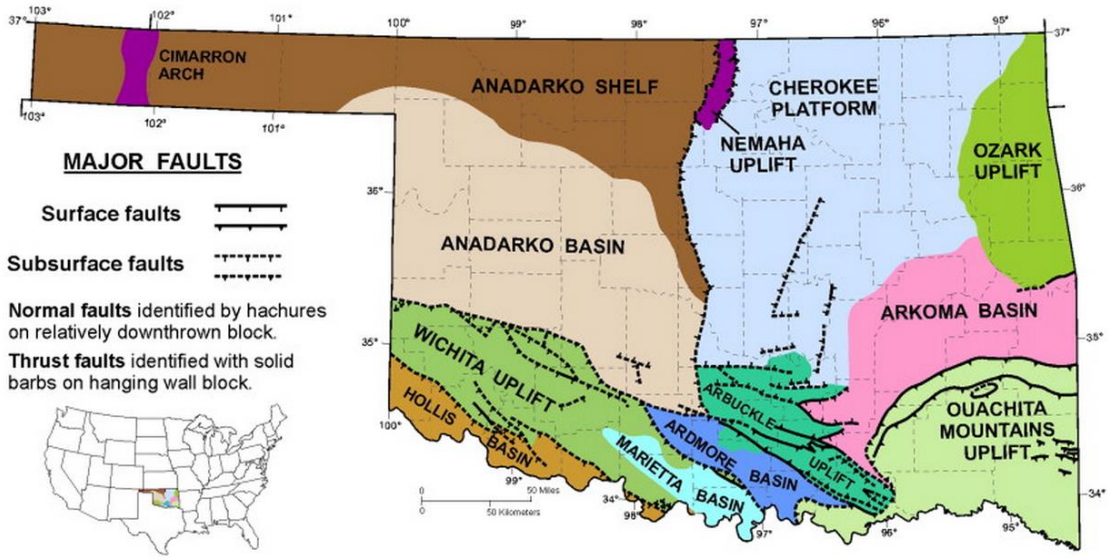

Figure 7. Map showing major geologic provinces of Oklahoma (Cardott, 2012)

2.1.2 Nemaha Uplift

The Nemaha Uplift (also called the Nemaha Ridge or the Nemaha fault zone) is a buried range of the Ancestral Rocky Mountains associated with a granite high in the Pre-Cambrian basement that extends from approximately Nebraska to Central Oklahoma (Figure 8; Gerhard, 2004). It is 550 km long, 30-50 km wide, and about 50 km east of the 1.1 billion years old Midcontinent rift (Gao, et al., 2002). The Nemaha fault zone is the result primarily of transpressional stresses acting episodically over a very long time. The

earliest known movement of the Nemaha fault zone occurred during the Ordovician, while the major deformation of the Nemaha Uplift took place in pre-Desmoinesian and post-Mississippian time (Lee, 1943; Merriam, 1963; Gerhard, 2004).

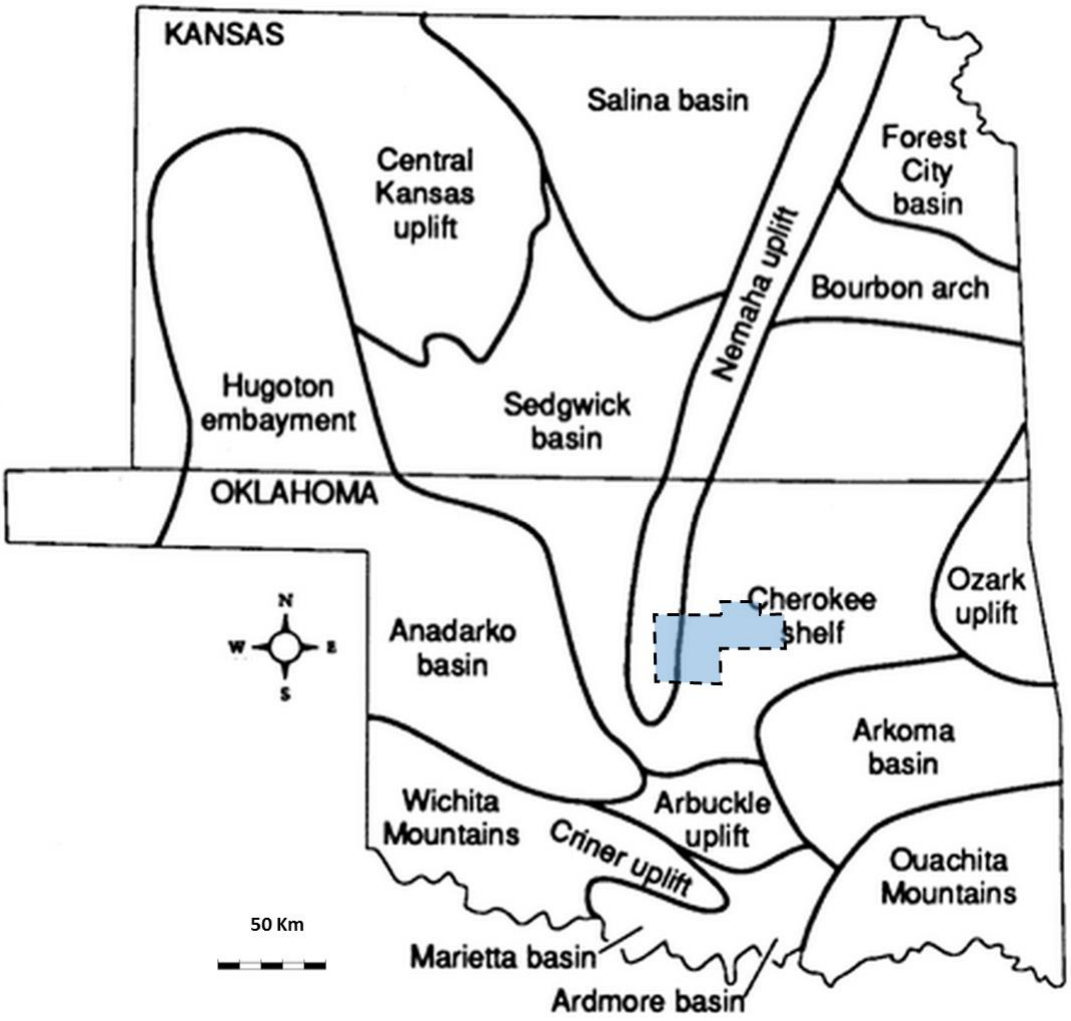

Figure 8. Pennsylvanian tectonic settings in Kansas and Oklahoma showing the Nemaha Uplift Zone (modified from Merriam, 1963; Lardner, 1984; Logan and Payne Counties in light blue area).

Whether or not a paleo-high existed in the vicinity of the present-day Nemaha Ridge zone is a key issue affecting the Woodford internal facies distribution across the Nemaha Uplift along E-W direction in Central Oklahoma. Because paleotopography was

an important factor in the distribution of the Woodford facies (Figure 9; Kvale and Bynum, 2014). The presence of the north-south trending paleo-Nemaha Ridge, which separated the proto-Anadarko Basin and the proto-Arkoma Basin, prevented the distribution of the chert-rich upwelling facies (A chert facies in Figure 9) into the Anadarko Basin but rich in the Arkoma Basin through most of the Woodford deposition (Figure 9; Kvale and Bynum, 2014). Consequently the deep upwelling chert-rich facies decreases rapidly from the Arkoma Basin northward onto the Cherokee Platform, which was also a positive topographic feature for much of the Woodford deposition (Figure 9; Kvale and Bynum, 2014).

2.1.3 Cherokee Platform

The Cherokee platform, extending from southeastern Kansas and part of southwestern Missouri to northeastern Oklahoma, could be considered as part of the stable shelf area of the Arkoma Basin throughout most of the Woodford deposition (Figure 5; Campbell and Northcutt, 2001). It is 235 miles long (north-south by 210 miles wide (east-west) and has an area of 26,500 sq. mi (Charpentier, 2001). In terms of Oklahoma geological history, major sedimentary basins in Oklahoma began to form in the latest Mississippian to earliest Pennsylvanian. In the Late Devonian, the Cherokee Platform was a broad shelf separated from the proto-Anadarko Basin by the paleo-Nemaha Ridge (Figure 5; Northcutt and Campbell, 1996; Campbell and Northcutt, 2001).

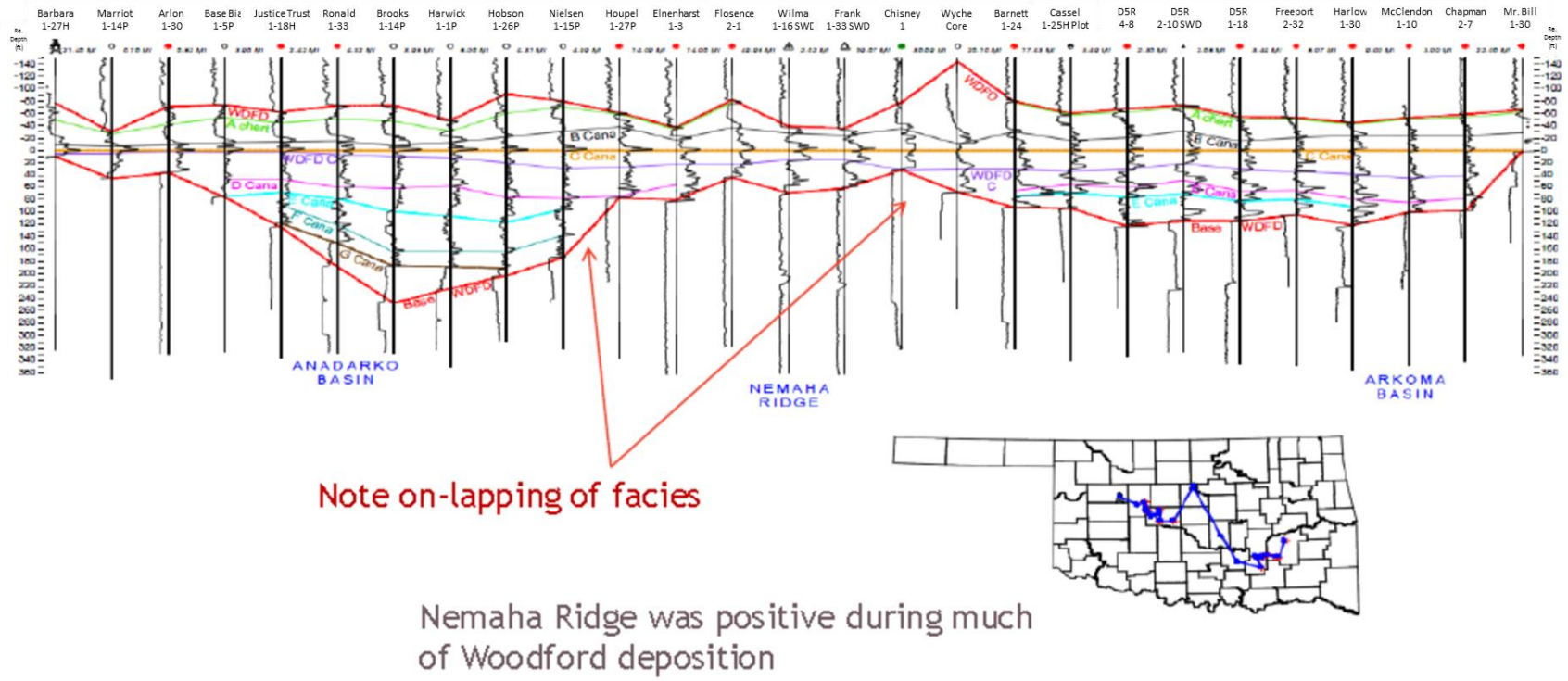

Figure 9. Cross Section extending from the Barbara 1-27 core in the West Cana, Anadarko Basin (left) to the Mr. Bill core to the east in the Arkoma Basin (Kvale and Bynum, 2014; the top of A chert facies marked by light green line, which refers to the chert-rich upwelling facies)

2.2 The Geological Settings and Depositional Environment of the Woodford Shale

2.2.1 Stratigraphy and Structure

The Woodford Shale of Late-Devonian to Early-Mississippian age is an organic-rich black shale widely distributed over the southern Mid-Continent from the Iowa Basin in Kansas to the Permian Basin in West Texas (Comer and Hinch, 1987; Comer, 1992). It was found to be distributed in most of Oklahoma including the Anadarko Basin, the Anadarko Shelf, Cherokee Platform and the Arkoma Basin. On the Cherokee Platform, the Woodford Shale was deposited on a major regional unconformity developed during the late Devonian (Figure 10; Amsden, 1975). It is conformably overlain by limestone and shale of Early Mississippian Age (Figure 10).

The predominant lithology of the Woodford Shale is black shale. Other common lithologies include chert, siltstone, sandstone, dolostone and light-colored shale (Amsden et al., 1967; Amsden, 1975; Comer, 1992). A typical core from the Woodford can contain 30-50% quartz, 0-20% calcite/dolomite, 0-20% pyrite and 10-50% total clay, a variance in mineralogy that occurs on a regional scale and within the stratigraphic section. These differences can have an effect on the porosity and permeability of the interval as they are reported to range from 3-9% and 100 nd - 0.001 md, respectively (Comer, 1991).

The Woodford Shale was uplifted and eroded due to the thrust faulting when the Gondwana Craton collided with the Laurentia Craton during the Ouachita-Marathon-Orogeny (Starting from Middle-to-Late Pennsylvanian until Early Permian), which resulted in the Woodford Shale missing in the southern part of the “Oklahoma Basin”, which was the precursor of the present-day Anadarko Basin. The simplified structural cross section shown below (Figure 11), which is perpendicular to the Anadarko Basin

geometric axis, illustrates the present-day Woodford Shale generally dipping from Northeast to Southwest across the Anadarko Basin (Johnson, 1989).

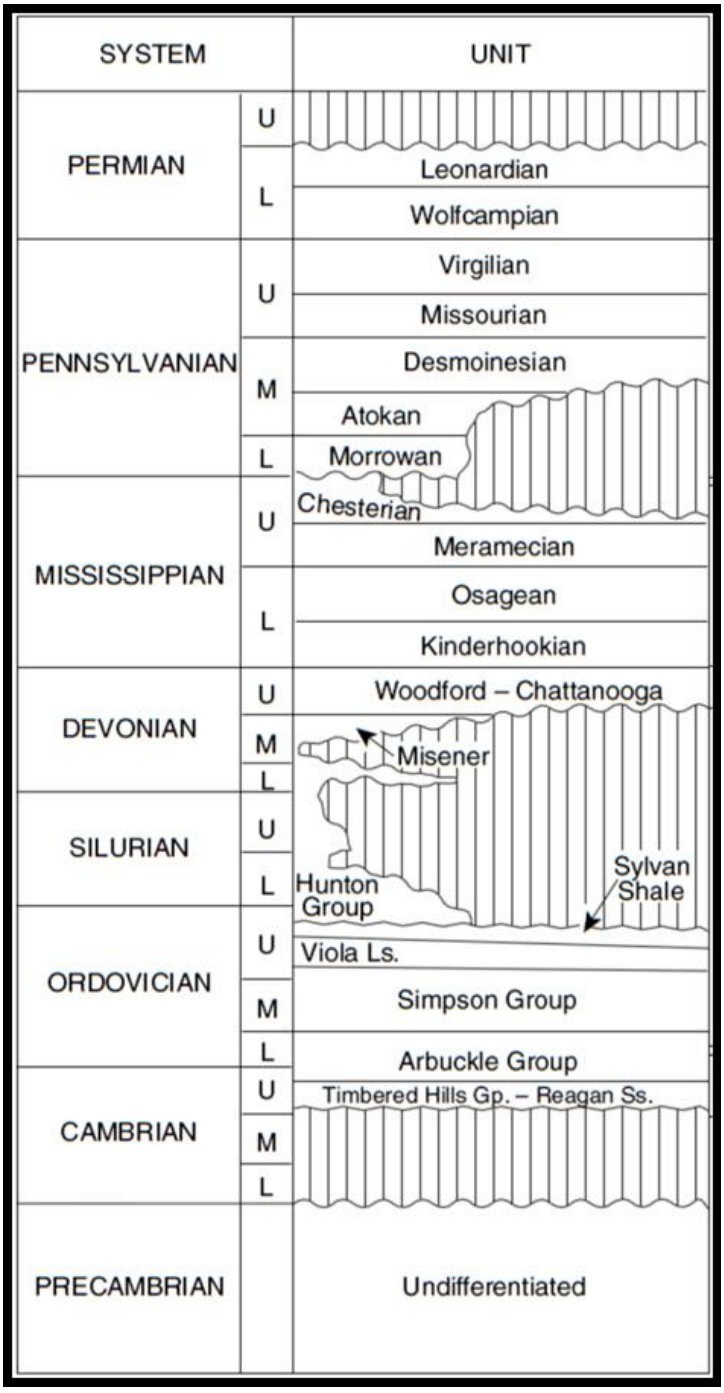

Figure 10. Stratigraphic chart for the Cherokee Platform, North-Central Oklahoma (Charpentier, 2001)

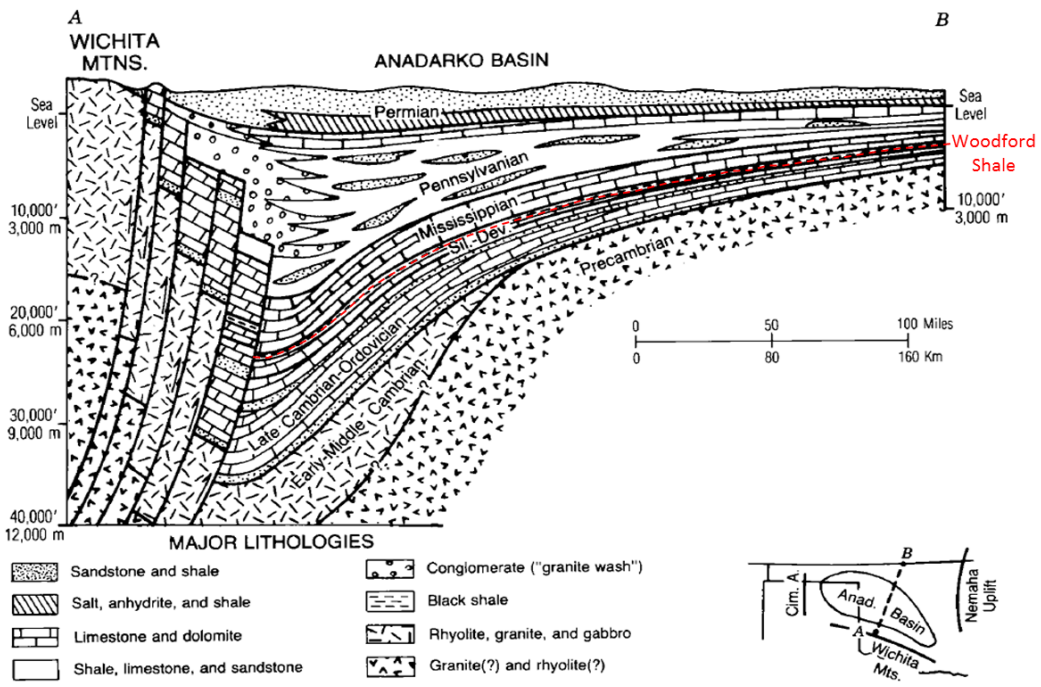

Figure 11. NE-SW structural cross section across the Anadarko Basin (Johnson et al., 1989)

2.2.2 Thickness and TOC Distribution

In Oklahoma, the total thickness of the Woodford Shale, combined with the basal Misener Sands, ranges from near zero to about 125 feet on the northern Anadarko Shelf, 50-150 feet on the Cherokee Platform and increases to around 300 feet at maximum in the Arkoma Basin and more than 900 feet in the depocenter of the Anadarko Basin (Figure 12; Amsden, 1975; Hester et al., 1988; Comer, 1992; 2005; 2008).

A general distribution of organic carbon of the Woodford Shale in Oklahoma is shown below (Figure 13). Except for some locations in the central part of the Ouachita tectonic belt, most of the Woodford contains greater than 0.5% TOC (Comer, 1992). The Anadarko, Marietta and Ardmore Basin, composing the ancestral "Oklahoma Aulacogen" (Ham et al., 1964; Walper, 1977), show a general trend of low TOC in the Northwest and

high (8-10%) in the Southeast (Comer, 1992). Medium TOC contents (4-6%) were found on the northern Anadarko Shelf, the Cherokee Platform, and the axial area of the depocenter of the ancestral "Oklahoma Aulacogen" (Comer, 1992), which is inconsistent with the previously expected TOC general distribution that TOC is usually richest in the depocenter of a basin and decreases from the slope to the shelf.

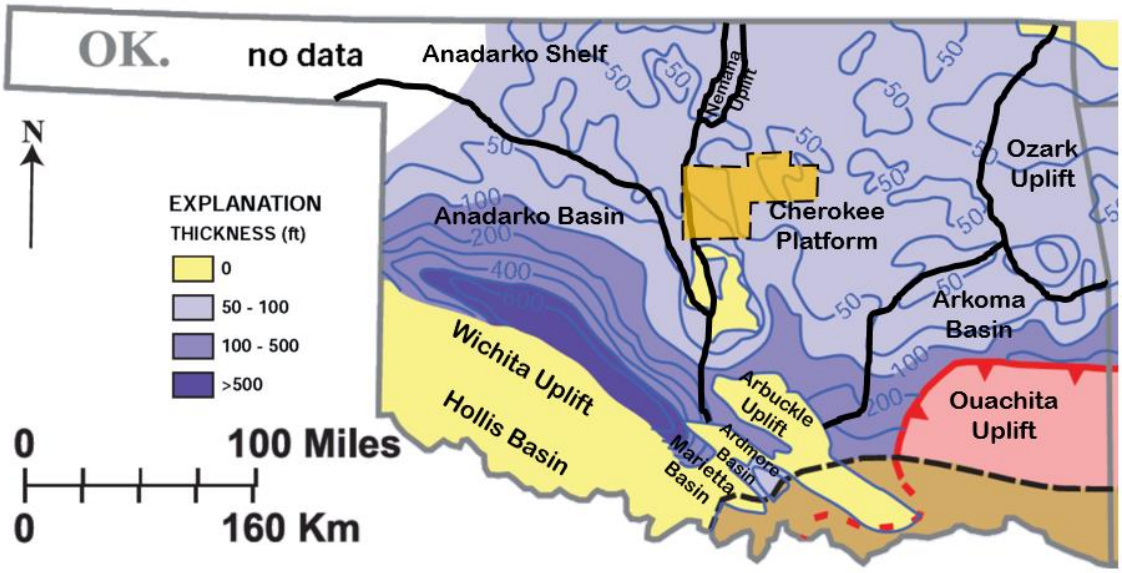

Figure 12. Thickness map of the Woodford Shale in Oklahoma (Logan & Payne Counties in light orange; modified from Comer, 1992 in Comer, 2008).

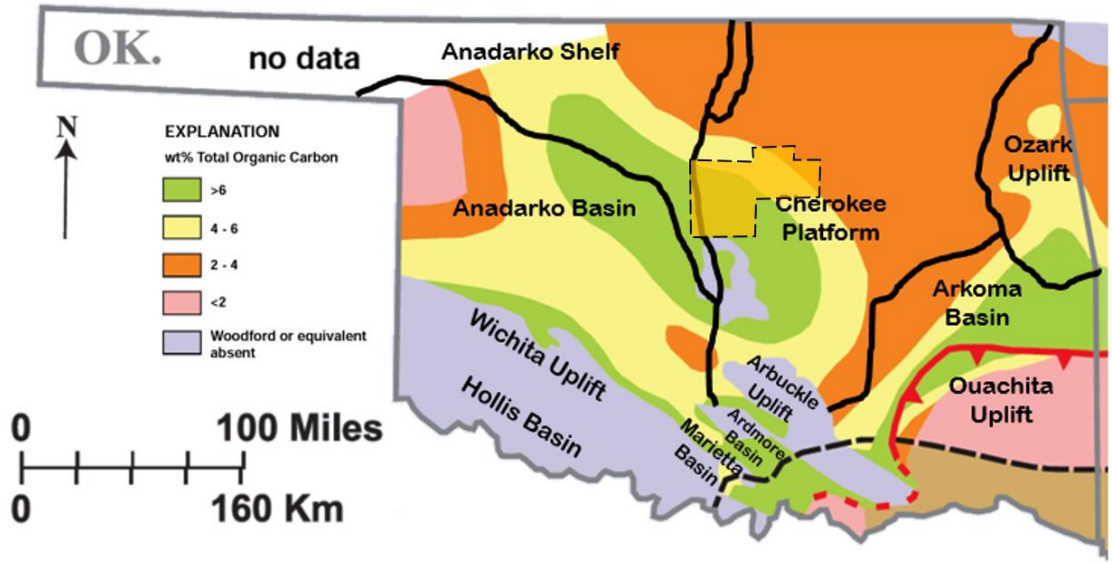

Figure 13. TOC map of the Woodford Shale in Oklahoma (Logan & Payne Counties in light orange; modified from Comer, 1992 in Comer, 2008).

The two parallel Northwest-Southeast trends of high TOC (6-10%) along the Anadarko Basin axis is seemingly consistent with the geometric linear accommodation space of the ancestral "Oklahoma Aulacogen" (Figure 13; Comer, 1992; Comer, 2008). Originating from a failed rift derived from the Pre-Cambrian, the ancestral "Oklahoma Aulacogen" has a Northwest- Southeast trending linear geometry during Late Devonian, which acted as the accommodation space for the Woodford Shale, resulting in the general high TOC distribution trending Northwest- Southeast as well (Figure 13). But the highest TOC band is not overlapping with the thickest Woodford area (Figure 12), which is the depocenter of the ancestral "Oklahoma Aulacogen". On the contrary, the highest TOC band is parallel in between the two second highest TOC trends mentioned above (Figure 13). The reason is probably that the Woodford Shale sedimentation was controlled by the bathymetry as well (Kirkland et al, 1992). It was assumed that the highest TOC was the synthetic result from an appropriate bathymetry, with enough organic matter input and good preservation conditions. In short, too deep a marine environment may bring ocean currents to destroy the organic matter by oxidation and/or dilute the organic richness by inorganic material with ocean currents (Comer, 1992; Comer, 2008). This phenomenon was also found in the Woodford in the Permian Basin (Comer, 1991; Comer, 2005).

2.2.3 Paleogeography

Paleogeography reconstruction of North America (Laurentia) at the beginning of Late Devonian (~385Ma) indicates that Laurentia moved northward during this time and the Southern Mid-Continent were located 15^{o} to 20^{o} south latitude along the western or southwestern continental margin (Figure 14; Blakey, 2008; Comer, 2008; Miall, 2008). Prior to that time, much of the Southern Mid-Continent was subaerially exposed resulting

in a major regional unconformity surface. Back to the beginning of Late Devonian (~385Ma), sea level started to rise as the consequence of the worldwide Late Devonian marine transgression (Haq and Schutter, 2008) and the Woodford was starting to be deposited in the ancestral "Oklahoma Basin" (Figure 14). The "Oklahoma Basin" at that time was a restricted basin developed in an epeiric sea within the passive margin (Figure 14). Coming to Early Mississippian (~360Ma), sea level continued to rise (Haq and Schutter, 2008) and the Woodford Sea covered its maximum deposition area extending into parts of Kansas (Figure 15). The study area, north-central Oklahoma, was in a shallow marine environment, probably the toe of the slope to basin margin (Comer, 2008).

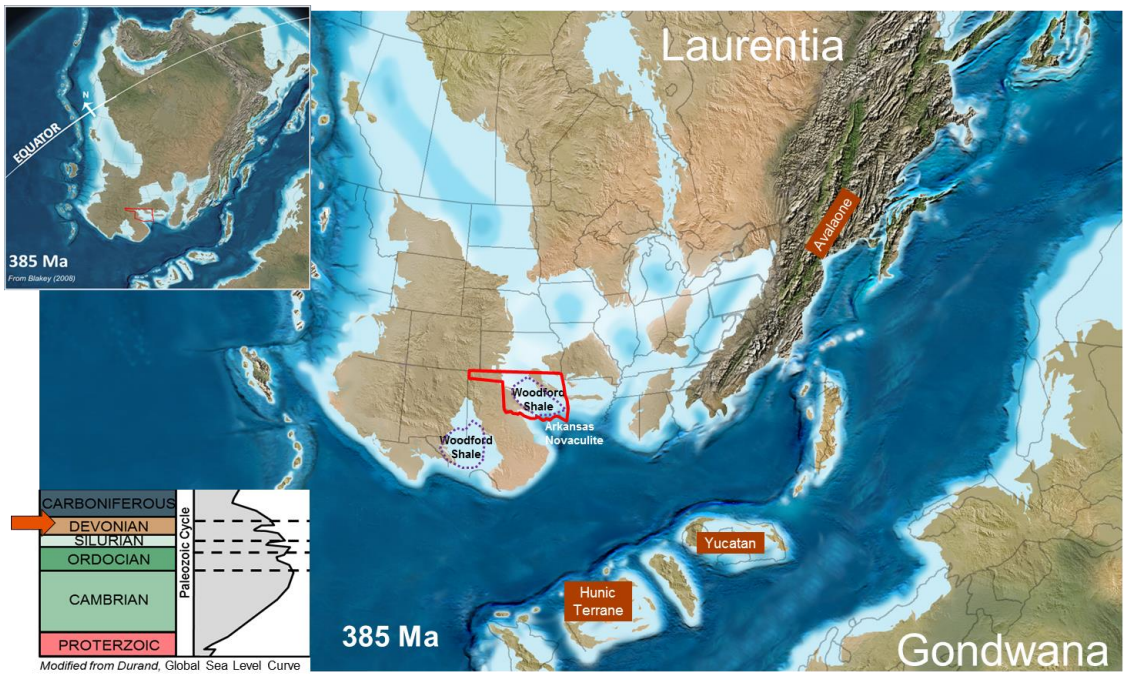

Figure 14. Paleogeography of North America at the beginning of Late Devonian (385Ma) (Oklahoma in red solid line; modified from Blakey, 2013).

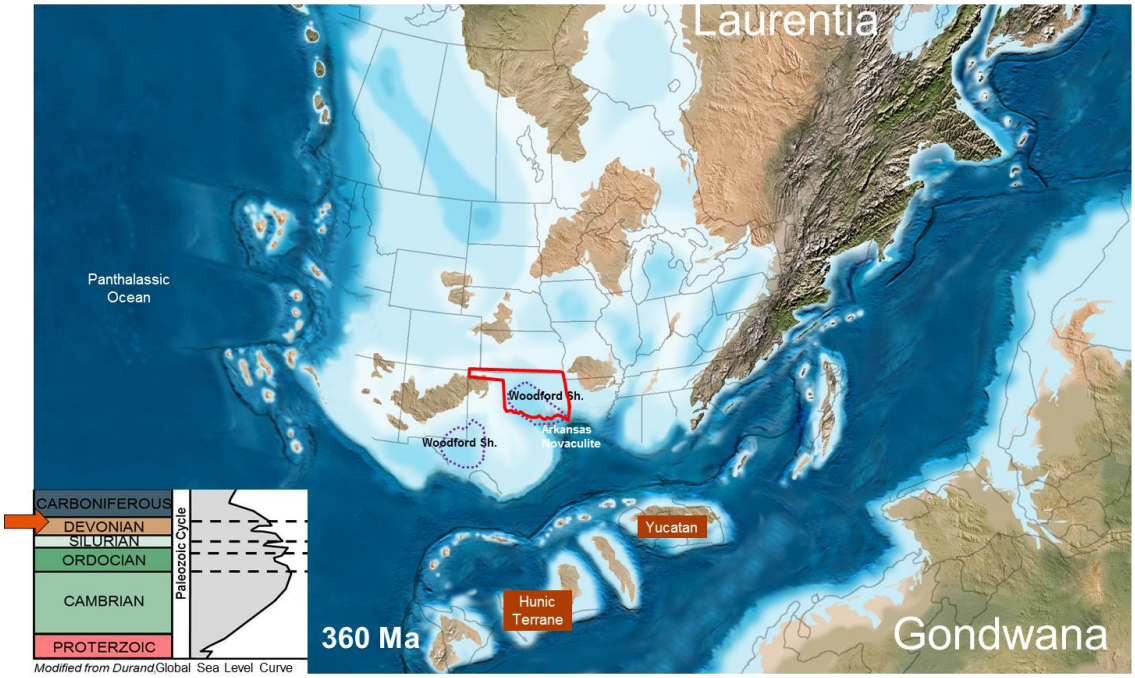

Figure 15. Paleogeography of North America at the beginning of Early Mississippian (360Ma) (Oklahoma in red solid line; modified from Blakey, 2013).

Coastal upwelling along the Late Devonian continental margin were documented by the thick accumulations of biogenic silica (Arkansas Novaculite). The detrital sediments dispersed southward toward the ancestral Anadarko Basin from the paleohighs around the ancestral Ozark Uplift (Figure 16). The regional TOC distribution (Figure 13) can also be used to infer the Late Devonian paleogeography. In general, low TOC contents in the Ozark Uplift and adjacent Cherokee Platform are probably due to dilution by siliciclastic sediments (Figure 16; Comer, 1992; Comer, 2008), which is consistent with other evidence that black shales in this region contain the highest detrital quartz and clay mineral contents (Amsden and Klapper, 1972; Pittenger, 1988). Therefore it indicates the Ozark Uplift was a structural highland when the Woodford Shale deposited (Figure 16; Comer, 1992; Comer, 2008). Mixture of oil-prone type-II amorphous

kerogens and gas-prone type-III structured kerogens were found locally along the Nemaha Uplift indicating there was a topographical highland as terrestrial organic matter source during the Woodford time (Figure 16; Comer, 1992; Comer, 2008). Comer's finding is consistent with Kvale and Bynum based on regional well log correlation of the Woodford internal facies distribution across the Nemaha Ridge zone along the East-West direction (Figure 9; Kvale and Bynum, 2014).

2.2.4 Previous Depositional Models

Numerous publications have interpreted the Woodford Shale as being primarily deposited in a deep marine environment under anoxic condition during global sea level transgression (Kirkland et al., 1992; Comer, 1992; O'Brien and Slatt, 1990; Miceli Romero and Philp, 2012). This interpretation is supported by fossil, sedimentary evidence and biomarker signatures.

Fossil Evidence

Hass and Huddle (1965) reported conodonts, lingula (brachiopods) in the Woodford samples and determined Woodford is of Late-Devonian to Early-Mississippian age based on the fish species the conodonts were derived from. Tasmanites, radiolaria, spores, and hystrichosphaerids (acritarchs) have been identified in the Woodford outcrop from the McAlister Cemetery Quarry, Southern Oklahoma (Kirkland, 1992; Slatt and O'Brien, 2011). These fossil records represent freely floating living creatures (algae and plankton) that sank onto the anoxic sea floor suggesting that the Woodford was deposited in a deep marine environment.

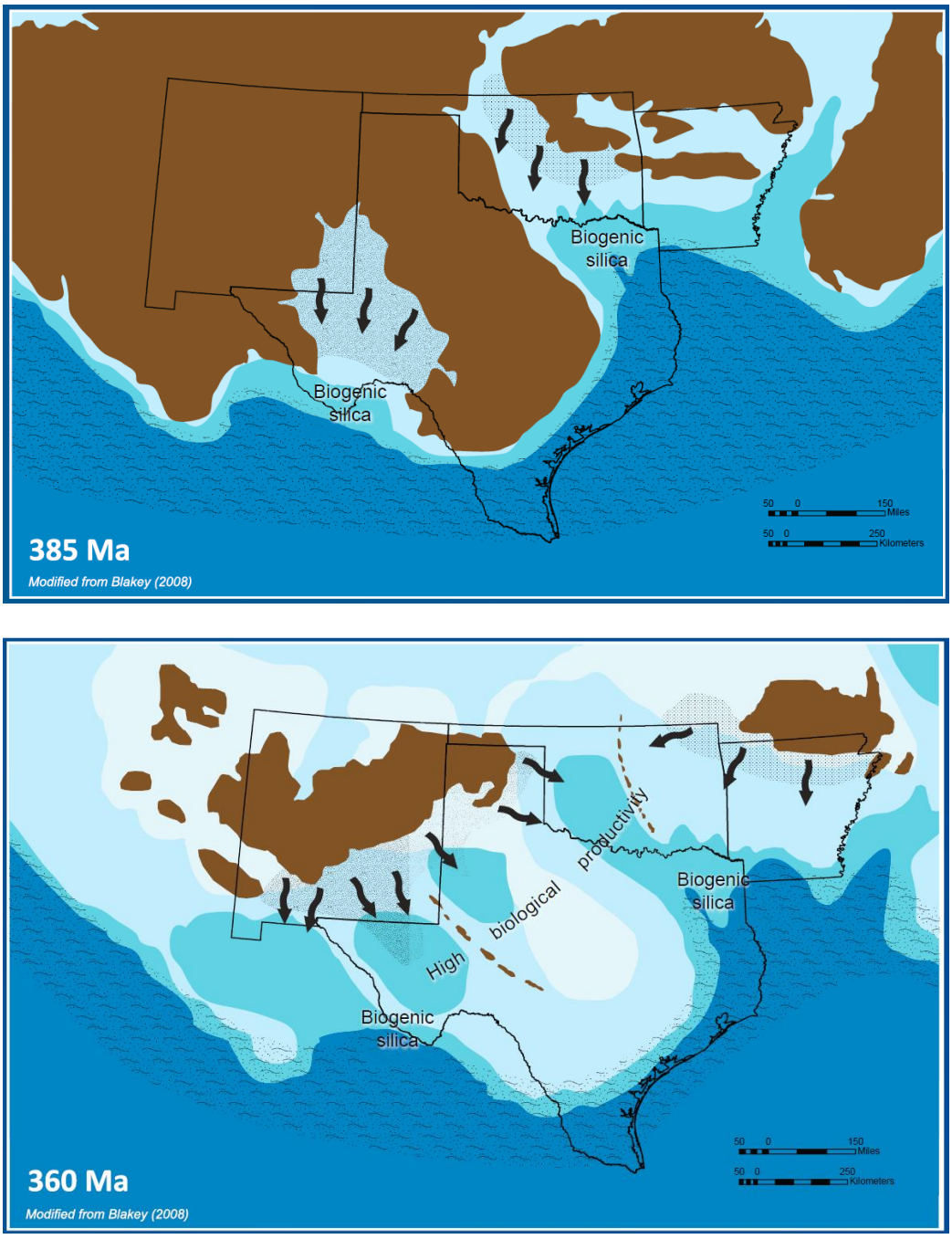

Figure 16. Facies distribution map from 385Ma to 360Ma in the Southern Mid-Continent (modified from Blakey, 2008 in Comer, 2008).

Mineral Evidence

Siliceous- and clay-rich sediments identified from the Woodford Shale samples were interpreted as deposited in a broad intracratonic sea (Figure 16) that was deeper to the southeast and shallower to the northwest (Kirkland et al., 1992; Blakey, 2008; Comer, 2008). The sediments were deposited below storm wave base in an anoxic environment with water density stratification (Kirkland et al., 1992; Miceli Romero and Philp, 2012).

Biomarker Signatures

The molecular fossil records also support the deep marine anoxic environment contributing to the Woodford organic matter preservation. The presence of gammacerane identified from the Woodford Shale extracts indicates the high-salinity conditions and water density stratification in the water column as the organic matter sank to the sea floor (Miceli Romero and Philp, 2012). Moreover, the presence of PZA (Photic Zone Anoxia) in the water column was identified by the aryl isoprenoids found in the Woodford cores extracts (Miceli Romero and Philp, 2012). Aryl isoprenoids have been found derived from isorenieratene, a diaromatic carotenoid pigment derived from the green sulfur bacteria *Chlorobiaceae* (Brown and Kenig, 2004), which need an anoxic water column, hydrogen sulfide and sunlight to photosynthesize (Miceli Romero and Philp, 2012).

Development of Anoxic Bottom Water in the Woodford Sea

To discuss the Woodford depositional model, a key question is how the bottom waters of the shallow Woodford Sea had remained anoxic over ~105 square miles for 25~30 millions of years. Three major models were developed to account for the anoxic bottom waters in the Woodford Sea:

A. Anoxic bottom water derived from oxygen-minimum zone of Late Devonian ocean (Comer and Hinch, 1981; Jones, 1983);

In their model, oxygen-deficient water in the oxygen minimum layer intersects the continental margins most often on the upper slope, where the best potential source rocks are deposited. The modern analog to support this model is that oxygen-deficient water locally reaches onto the shelf, where the shallow upwelling of nutrient-rich water favors the high biological productivity, as in offshore southwest Africa. While, the modern analog to disfavor this model is that the oxygen-minimum zone, in modern oceans, has an oxygen concentration that is dysoxic but not anoxic; the top depth of the oxygen-minimum zone usually occurs at a depth of 1,500-6,500 ft (Schopf, 1980). If the top of the oxygen-minimum zone in the Woodford Sea was at a similar depth-range as in the modern oceans, the anoxic waters may have been at too great a depth to have transgressed far onto the continents (Kirkland et al., 1992). Moreover, currents to transport such water into the epicontinental seas were probably absent. Tyson (1987) argues that epeiric black shales do not represent an expansion of an oxygen-minimum zone into an epeiric sea.

B. Anoxic bottom water developed when a persistent horizontal barrier within water mass, a thermocline, with persistent water column stratification (Hallam, 1967; Kirkland et al., 1992);

The model modified from Hallam (1967) by Kirkland et al. (1992) was that anoxic bottom waters developed when a persistent vertical barrier within the water column prevented transfer of dissolved oxygen from the zone near the surface to the zone near the sea floor. Oxygen was incorporated into surface water by solution of atmospheric

oxygen, a by-product of photosynthesis. This dissolved oxygen was prevented from being carried to the bottom water by persistent density stratification of the water mass. The relative shallowness of the Woodford Sea couldn't satisfy the horizontal ocean currents to occur, so such ocean currents were ineffective to transport the oxygen into the epicontinental Woodford Sea (Irwin, 1965; Hallam, 1981). If the Woodford Sea was much shallower, oxygen dissolved in the surface water might have been in contact with the sediments to degrade the organic matter; if the Woodford Sea was too deep, the ocean currents would have destroyed the euxinic conditions carrying oxygen to degrade the organic matter. Therefore in summary, an intracratonic euxinic Woodford sea with anoxic water bottom, water density stratification and an appropriate water depth (< 500 ft) contributed to the extremely organic-rich source beds in the Mid-Woodford age (Kirkland et al, 1992).

Roberts and Mitterer (1992) proposed another local Woodford deposition model, which is similar to Kirkland's model, to successfully interpret the organic-shale-chert "doublets" lamination commonly found in the Woodford Strata in southern Oklahoma. In their model the two alternating phases of sedimentation are illustrated (Figure 17). The Woodford Sea was a euxinic intracratonic sea with anoxic water bottom and "channels" to connect to the open ocean. Cherts were deposited during relatively short periods of high siliceous productivity as organic carbon-rich siliceous oozes. While, organic-rich shale were deposited over longer time periods with lower levels of siliceous productivity and less dilution of organic matter by siliceous sediments input (Figure 17; Roberts and Mitterer, 1992).

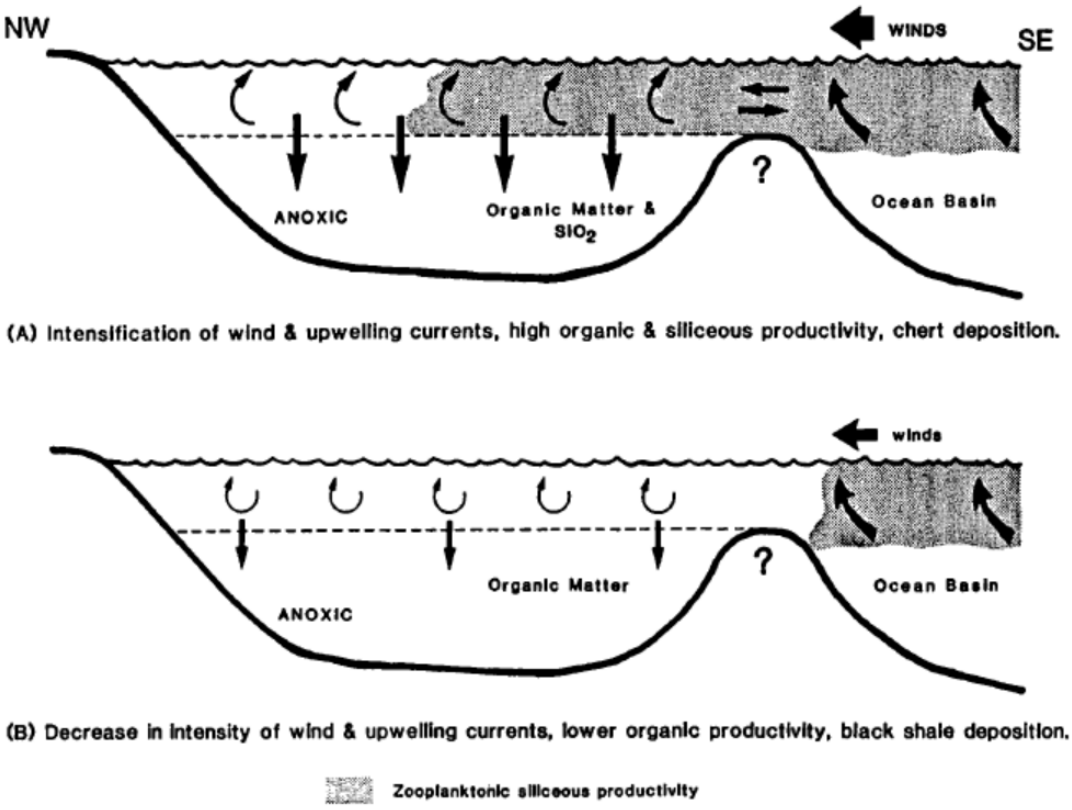

Figure 17. Depositional model for the Woodford Formation in the southern Oklahoma Aulacogen (Roberts and Mitterer, 1992)

C. Upwelling model (Comer, 2008);

Several versions of the upwelling model have been proposed with an attempt to explain the development of anoxic bottom water of the Woodford Sea (Heckel, 1977; Barron and Ettensohn, 1981; Parrish, 1982). The most recent modified upwelling model developed by Comer (2008) has been the most widely accepted model accounting for the Woodford deposition. Comer's model (alternative fair weather and storm sedimentation) successfully explained the formation mechanisms of almost all of the rock records found in the Woodford Shale (Figure 18). Comer (1992; 2004; 2008) mentioned that the Woodford Sea was a classic epeiric sea that transgressed over the southern North American craton during Late Devonian (Figure 16). Deposition of thick novaculite

(biogenic silica) layers along the Late Devonian continental margin shows evidence of upwelling (Comer, 2008). Phosphate-rich strata commonly found in the upper Woodford were supportive evidence for upwelling as well (Kirkland et al., 1992). Comer believed it was not oceanic currents but the arid climate and evaporation of that time to drive upwelling (Comer, 2008; 2012) because the Woodford Sea was not deep enough (<600 ft; Hallam, 1981; Shaw, 1964; Irwin, 1965) to allow the major ocean current systems to transfer large volume of waters. Therefore the Woodford Sea was interpreted as a euxinic intracratonic sea with restricted circulation.

Slightly different from Comer's upwelling model (Comer, 2008), Kvale and Bynum (2014) contributed the major driver on upwelling at that time in the Southern Mid-Continent was not aridity or high evaporation rates proposed by Comer (2008; 2012) but regional deep marine coastal upwelling, which is a function of Hadley circulation and a southeasterly Trade Wind (Kvale and Bynum, 2014).

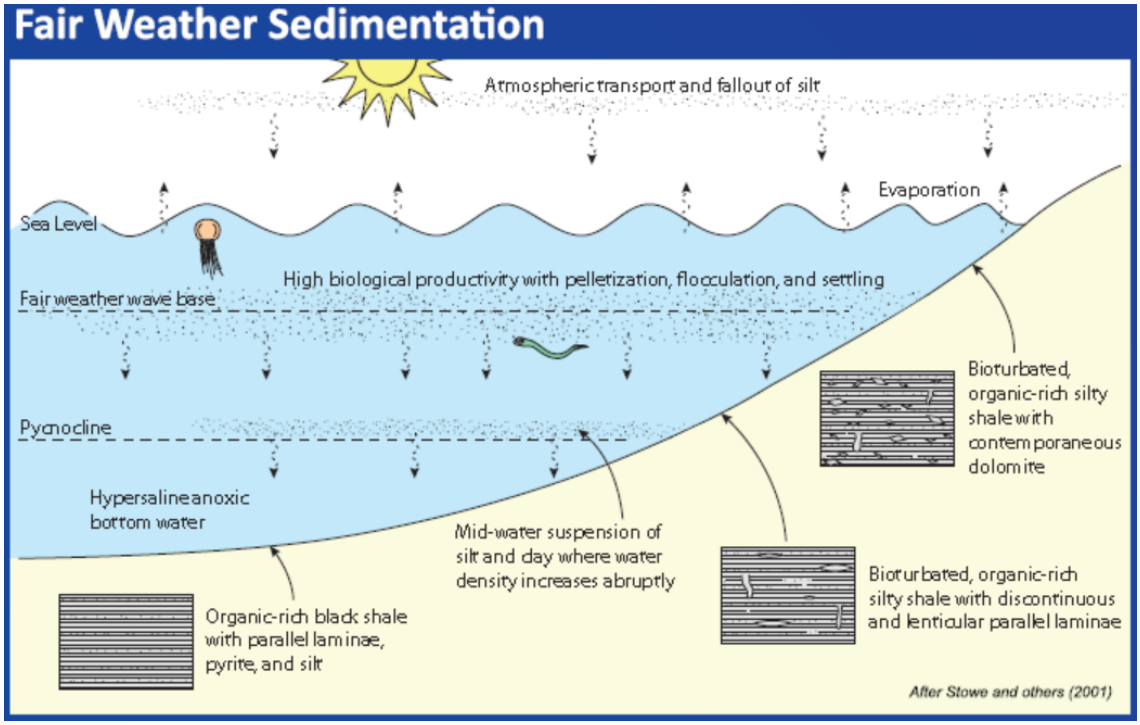

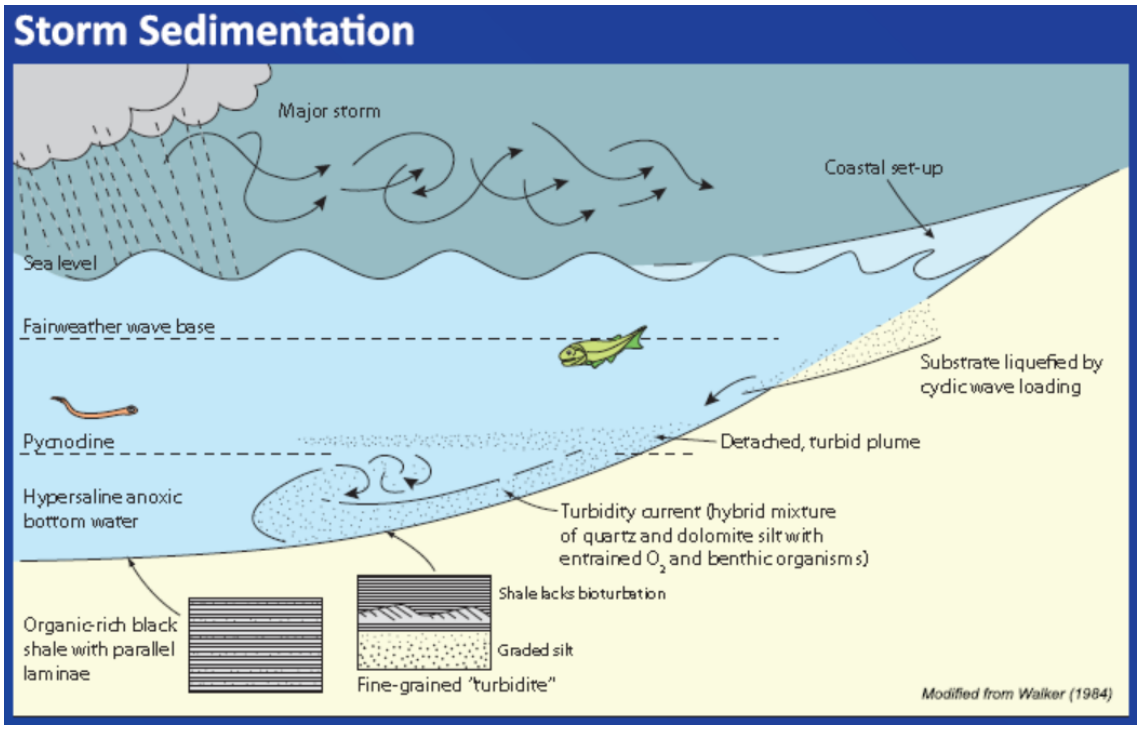

Figure 18. Woodford depositional processes (Comer, 2008)

2.2.5 Chemostratigraphy

Slatt and his Woodford consortium in University of Oklahoma lead a study of Woodford facies variation based on integration of sequence stratigraphy with chemostartigraphy (Turner et al., 2015a and b). They applied recent advances in handheld XRF technology to develop sequence stratigraphic frameworks by comparing chemostratigraphic profiles directly to gamma ray logs and measured stratigraphic sections obtained from the same locations.

In their work, the basic principle to identify a stratigraphic sequence for the Woodford Shale in Central Oklahoma is that an increasing upward gamma ray (GR) log can infer a sea level increase throughout the Middle and Upper Woodford members, and place the maximum flooding surface (MFS) at the GR "spike" between transgressive system tract (TST) and highstand system tract (HST) (Figure 19). A 2nd order MFS

divides rising and falling sea levels by recognition of a transition from a 2nd order TST to a 2nd order HST (Figure 19). Chemostratirgraphy profile with vertical variation of elemental concentration, as sediments source and depositional environmental proxies, refine the sequence stratigraphic framework by identification of 4th order parasequences that represent transgression and regression of the shoreline which occur during an overall higher order TST and HST. The basic idea to interpret a chemstratigraphic profile is that Titanium (Ti), Zirconium (Zr) are associated with deposits from continental source (Pearce and Jarvis, 1992; Pearce et al., 1999). Aluminum (Al) and Potassium (K) are associated with clay minerals and K-feldspar (Pearce and Jarvis, 1992; Pearce et al., 1999). It is well accepted that in terms of hydrodynamics of sediments, clay minerals can travel to a more distal portion of the basin than K-feldsapr grains, which behave similar to sands and silts. Therefore as the concentration of Al and K increase and meanwhile Ti and Zr decrease, it can be interpereted that the depositional environment was increasingly more distal from the clastic detrital sediment source. Silicon (Si) is found in multiple sources, including detrital quartz, clay minerals, feldspars, and biogenic quartz (Pearce and Jarvis, 1992; Pearce et al., 1999). Therefore, it is more common to report the Si/Al ratio (Si/Al) as a supplemental sediment source proxy by integrating with other continental source proxies like the concentration of Ti, Zr, and/or K, Al (Pearce et al., 1999). For example, if Si/Al increases without increasing in Ti or Zr, it can be interpreted as biogenic Si dominated within the measured section, which could be further interpreted as algal bloom if of short duration or a condensed section (CS) if of long time period (Turner et al., 2015a). Strontium (Sr) and Calcium (Ca) are associated with carbonates and phosphates (Banner, 1995). Molybdenum (Mo) and Vanadium (V) are redox

condition indicators (Tribovillard et al., 2006; Algeo and Rowe, 2012). Generally, increases in concentration of Mo and V are associated with a more reducing water column. Sharp changes in the elemental proxies are potential indicators of a stratigraphic surface (Turner et al., 2015a).

By applying this principle, one field site and three cores of the Woodford Shale have been scanned using the handheld XRF to develop a preliminary analysis of the regional variability of chemostratigraphic profiles for the Woodford Shale in Central Oklahoma and setup a regional Woodford sequence stratigraphic framework (Figure 19; Turner et al., 2015b). Esther (2015) used the handheld XRF to determine the elemental profiles for the Woodford core from Prtichard-1 well, which is one well in the data sets of this study and the same well in Turner's regional Woodford sequence stratigraphic framework. She found Ti and Zr curve (continental proxies) both show decrease from 5160 ft to 5155 ft and increase from 5155 ft to 5150ft right above the 2nd order MFS determined from the core GR (Turner et al., 2015b). The "turnover" in continental proxies indicative of a MFS at 5155 ft is consistent with the 2nd order MFS determined from the core GR. Sharp "turnover" found both in K and Al curve (clay proxies) at 5155 ft support the MFS at this depth as well. The concentration of Si covaries with Si/Al, both of which keep constant other than spike at 5155 ft. Si/Al increases from 5160 ft to 5155 ft with decrease in Ti, Zr, K and Al indicating significant biogenic Si within the measured Woodford section. Other than two spikes in calcium curve at 5152 t and 5156 ft, Sr and Ca (carbonate proxies) curve keep constant, which is consistent with that the Woodford in this well is composed of mainly quartz other than several depth from the minerology composition analysis by XRD (Esther, 2015). Regarding redox proxies, Mo curve keeps

relatively constant but V show a general increasing trend from Middle Woodford to Upper Woodford. Mo only precipitates under euxinic conditions (Tribovillard et al., 2006), while V cannot accumulate in the sulfur-rich water column. Therefore this could indicate an upward decline in sulfur in this local Woodford deposition site. The author of this study used Turner's subdivision of stratigraphic sequences and shoreline trajectory for the Woodford in Pritchard-1 to keep consistent with that of regional Woodford sequence stratigraphic framework (Figure 19; Turner et al., 2015b) and put those stratigraphic sequences and shoreline trajectory into the chemostratigraphic profile for Pritchard-1 (Figure 20), which is the referenced stratigraphic sequence to investigate the biomarker profile in Chapter IV.

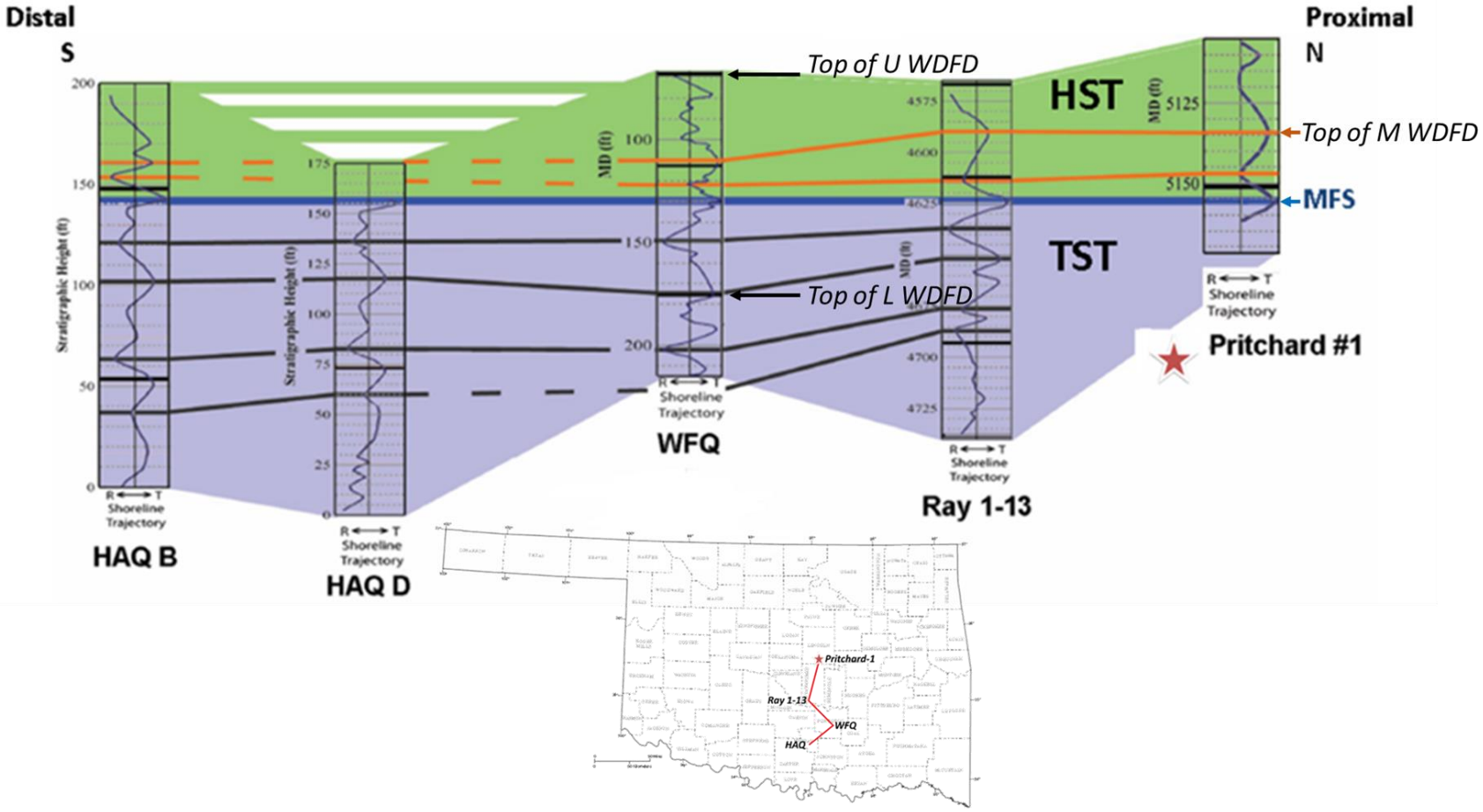

Figure 19. Regional Woodford Chemosequence Stratigraphic Framework in Central Oklahoma (Turner et al., 2015b; TST = 2nd order transgressive system tract; HST = 2nd order highstand system tract; MFS = 2nd order maximum flooding surface)

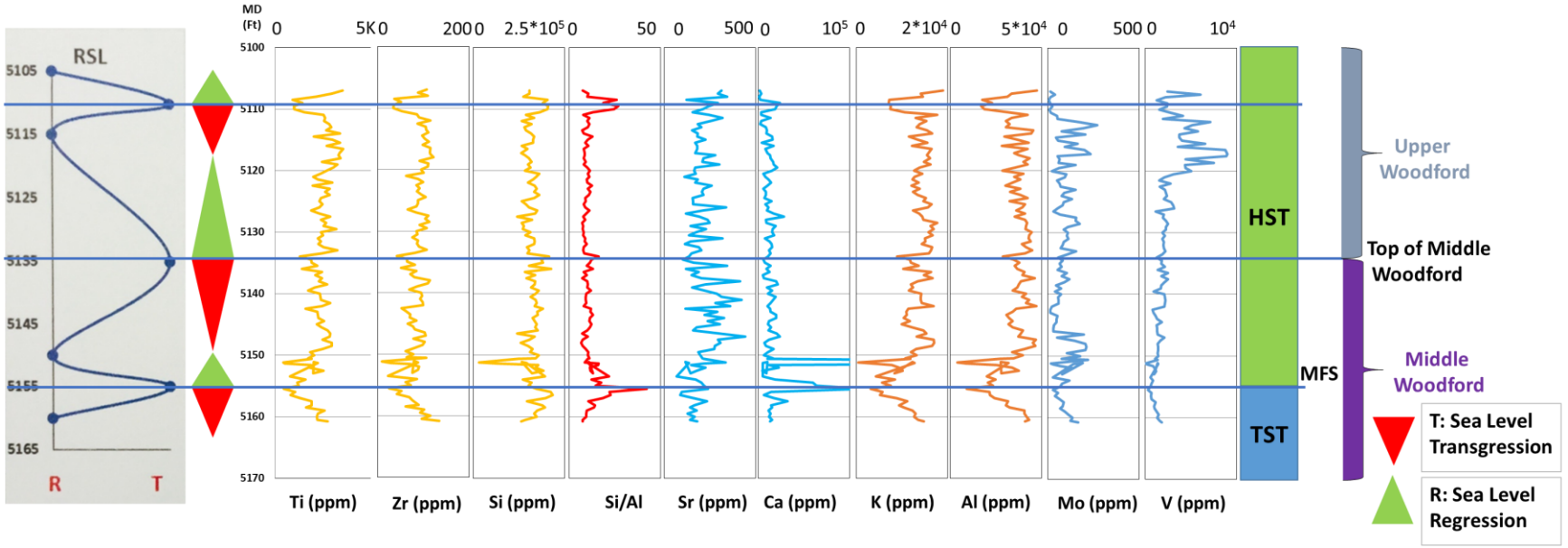

Figure 20. Chemostratigraphic profile of Pritchard-1 Woodford core showing clastic detrital components (Ti, Zr, and Si/Al), clay components (K, Al), carbonates and phosphates (Sr, Ca), and redox condition indicators (Mo, V), whereas green triangles refer sea level regression and red triangles for sea level transgression (RSL = Relative Sea Level) based on chemostratigrapy (elemental data courtesy of Esther, 2015; TST = 2nd order transgressive system tract; HST = 2nd order highstand system tract; MFS = 2nd order maximum flooding surface).

2.2.6 Thermal Maturity

The thermal maturity trends of the Woodford Shale (Figure 21) approximately follow its structural trends. The highest maturities occur in the deep parts of the Anadarko Basin and the Arkoma Basin, which have been in the gas window with the corresponding vitrinite reflectance values as high as 4.0% Ro (Cardott and Lambert, 1985; Cardott, 1989; 2012). The intermediate maturities corresponding to vitrinite reflectance values in the range of 0.6~1.1% VRo occur on the basin flanks and adjacent shelf settings (Cardott and Lambert, 1985; Cardott, 1989; 2012). The least mature areas are located on the structural highlands like the Nemaha Uplift, the area around Arbuckle Mountain Uplift and the Ozark Uplift (Cardott and Lambert, 1985; Cardott, 1989 and 2012). The northwestern Anadarko Shelf and the Cherokee Platform were reported as immature to early-mature based on sparsely distributed vitrinite reflectance measurements (Cardott and Lambert, 1985; Cardott, 1989; 2012). Recent measurements in this research associated with other geological/geochemical evidence suggest an updated Woodford thermal maturity map different from the previous one and will be discussed in detail in Chapter 4.

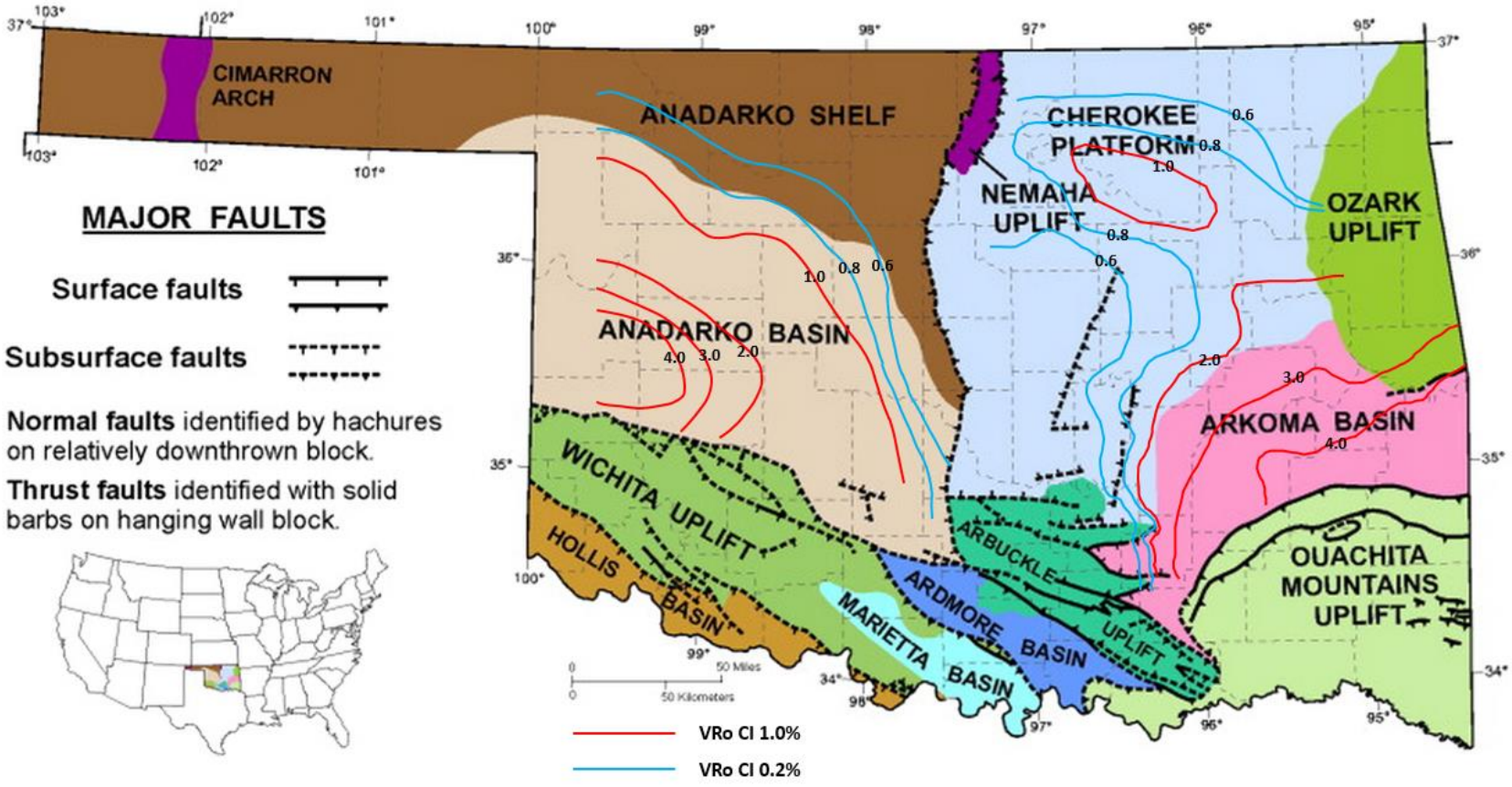

Figure 21. Woodford vitrinite isoreflectance map of Oklahoma (without Woodford in Oklahoma panhandle; modified from Cardott, 2014)

CHAPTER 3

3. SAMPLE PREPARATION AND EXPERIMENTAL METHOD

3.1 Study area and sample locations

In this study, a total of 168 oil and rock samples were collected from wells located throughout the Anadarko Basin, Nemaha Ridge Zone, Cherokee Platform in Central Oklahoma and Southern Oklahoma (Figure 22 and Figure 23, and Table 1). 5 Woodford cores located in the Devon focus production area provided by Devon from 5 different salt water disposal wells were sampled 100~200g of Woodford core plug every 6 feet per each well if allowed. 9 Woodford cores stored in OGS (Oklahoma Geological Survey) OPIC (Oklahoma Petroleum Information Center) core warehouse were sampled 100~200g of Woodford core plug for each Woodford member per each well. The geographic locations of these 9 OGS wells were preferred to choose surrounding the Devon focus production area with an attempt to determine the possible migration pathway if any by oil-to-source-rock correlation. 16 Tight oil samples produced either from Mississippian or Woodford Formation by Devon were sampled. 5 Condensate samples produced from Woodford Formation by Devon were sampled. 9 "Old" oil samples, previously produced from different conventional reservoirs by vertical wells in Southern Oklahoma stored in Dr. Philp's laboratory, which have been proven to be sourced from the Woodford Shale, were analyzed with an attempt to do oil-to-oil correlation.

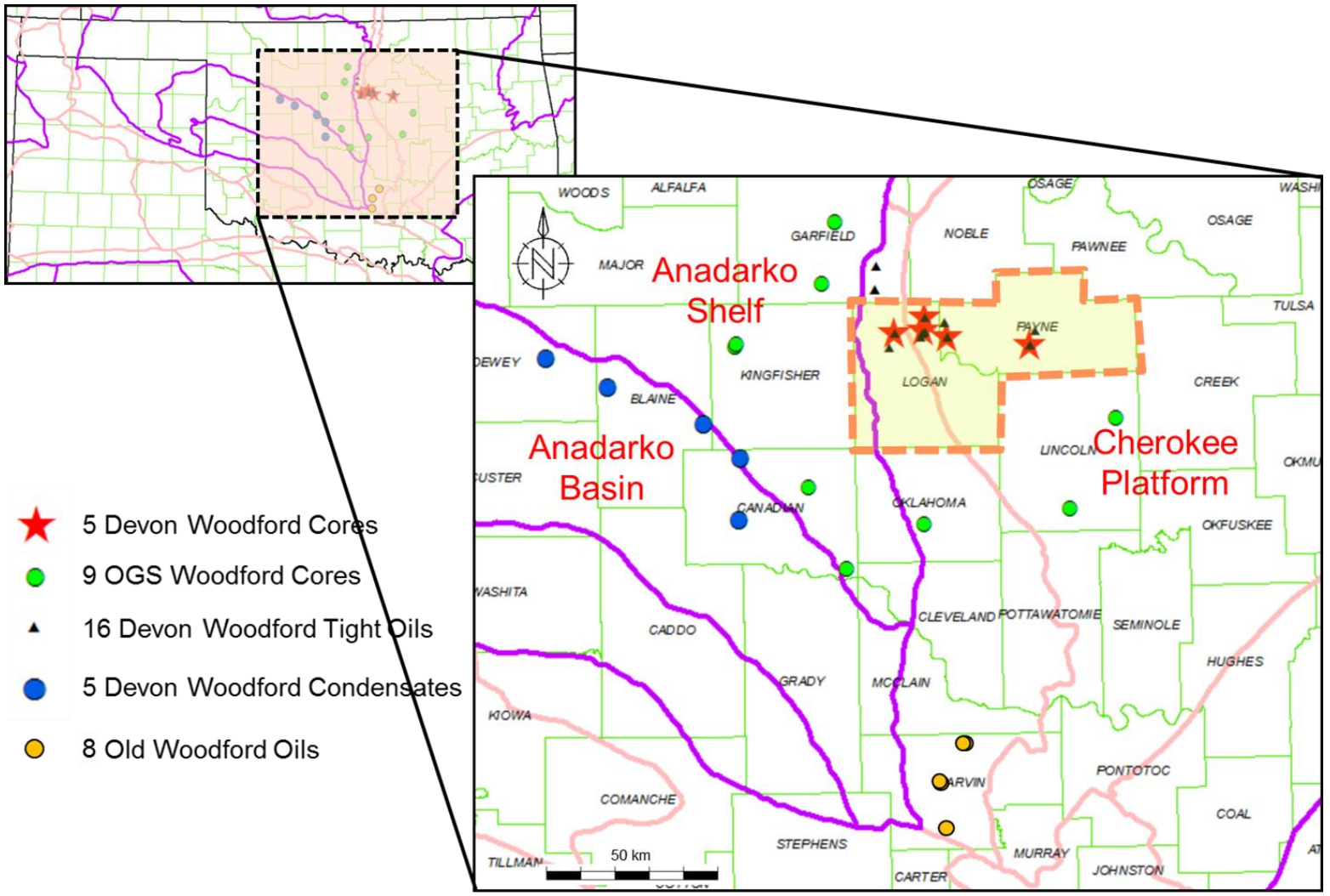

Figure 22. Map of Central Oklahoma showing locations of the samples analyzed in this study (Well names in Table 1)

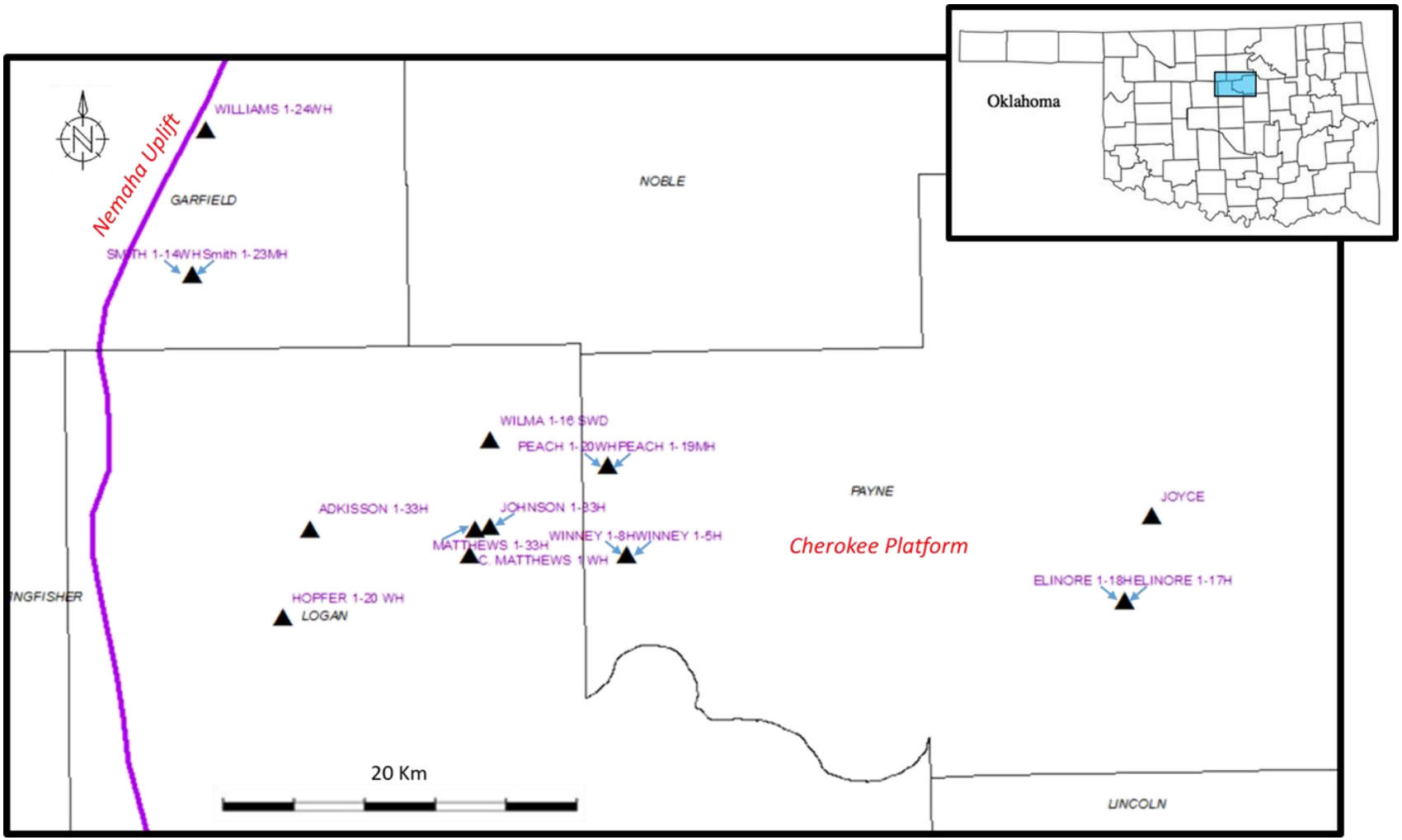

Figure 23. Map of Logan & Payne showing locations of the oil samples analyzed in this study (Well names in Table 1; Logan & Payne County shown in blue in Oklahoma State Map)

Table 1. List of samples for organic geochemical analyses

Well name	Producing Formation	Abbreviation	Sample type	# of samples
Robberson 10-1	NA	A-1	Core	7
Dannehl 2-16	NA	A-2	Core	5
L A Chenoweth-1	NA	A-3	Core	11
Lewis F Pope-1	NA	A-4	Core	10
Effie B York-1	NA	A-5	Core	5
Pritchard-1	NA	A-6	Core	10
Mary Earp-5	NA	A-7	Core	8
Boyd Unit-1	NA	A-8	Core	6
Anderson 12-1	NA	A-9	Core	21
Frank 1-33 SWD	NA	10	Core	11
Wilma 1-16 SWD	NA	11	Core	5
Elinore 1-18 SWD	NA	12	Core	8
Winney 1-8 SWD	NA	13	Core	19
Adkisson 1-33 SWD	NA	14	Core	7
Wion 1-29H	WOODFORD	a	Condensate	1
Lingo 1-13H	MISSISSIPPIAN	b	Condensate	1
Dougherty Bros. 1-18H	NA	c	Condensate	1
Crystal	MISSISSIPPIAN	d	Condensate	1
York 1-2H	WOODFORD	e	Condensate	1
Johnson 1-33H	MISSISSIPPIAN	NA	Oil	1
Matthews 1-33H	MISSISSIPPIAN	NA	Oil	1
Wilma 1-16 SWD	WOODFORD	NA	Oil	1
Elinore 1-18H	WOODFORD	NA	Oil	1
Elinore 1-17H	MISSISSIPPIAN	NA	Oil	1
Winney 1-8H	WOODFORD	NA	Oil	1
Adkisson 1-33H	WOODFORD	NA	Oil	1
Winney 1-5H	WOODFORD	NA	Oil	1
Smith 1-14WH	WOODFORD	NA	Oil	1

Smith 1-23MH	MISSISSIPPIAN	NA	Oil	1
Hopper 1-20 WH	WOODFORD	NA	Oil	1
Peach 1-20WH	WOODFORD	NA	Oil	1
Joyce 1-32 WH	Pennsylvanian Unconformity Sand	NA	Oil	1
Williams 1-24WH	NA	NA	Oil	1
Peach 1-19MH	Bromide (?)	NA	Oil	1
C. Matthews 1 WH	Viola	NA	Oil	1
Ford-1	NA	NA	Oil	1
Thomas James 1-22	NA	NA	Oil	1
Anadarko Taylor 2118	NA	NA	Oil	1
“A”	NA	NA	Oil	1
Ellis Lewis Jet	NA	NA	Oil	1
ST Mary	NA	NA	Oil	1
Albert 1-9	NA	NA	Oil	1
“F”	NA	NA	Oil	1
7-5N-5E	NA	NA	Oil	1

3.2 Experimental

Total Organic Carbon (TOC) determination and Rock-Eval pyrolysis analyses were performed on all rock samples available for this study (Table 1). The rock samples with TOC values greater than 1% were selected for soxhlet extraction. The rock extracts were separated into maltenes and asphaltenes by addition of excess *n*-pentane. The maltene fraction was further fractionated into saturates, aromatics, and NSO fraction by column chromatography. Screening analysis of the saturate and aromatic fractions was performed by gas chromatography (GC). Selected samples were analyzed by gas chromatography-mass spectrometry (GCMS) for biomarker analyses and bulk isotope analysis on isotope mass spectrometer. Oils and condensates were analyzed using GC and GCMS. Rock samples from eleven studied wells were chosen for vitrinite reflectance measurements. Rock-Eval pyrolysis and TOC analyses were carried out at GeoMark Research, Inc. in Humble, Texas and Core Laboratories in Houston, Texas. The remaining geochemical analyses were performed at the University of Oklahoma Organic Geochemistry Laboratories located in Norman, Oklahoma. A summary of the laboratory workflow used in this project is depicted in Figure 24.

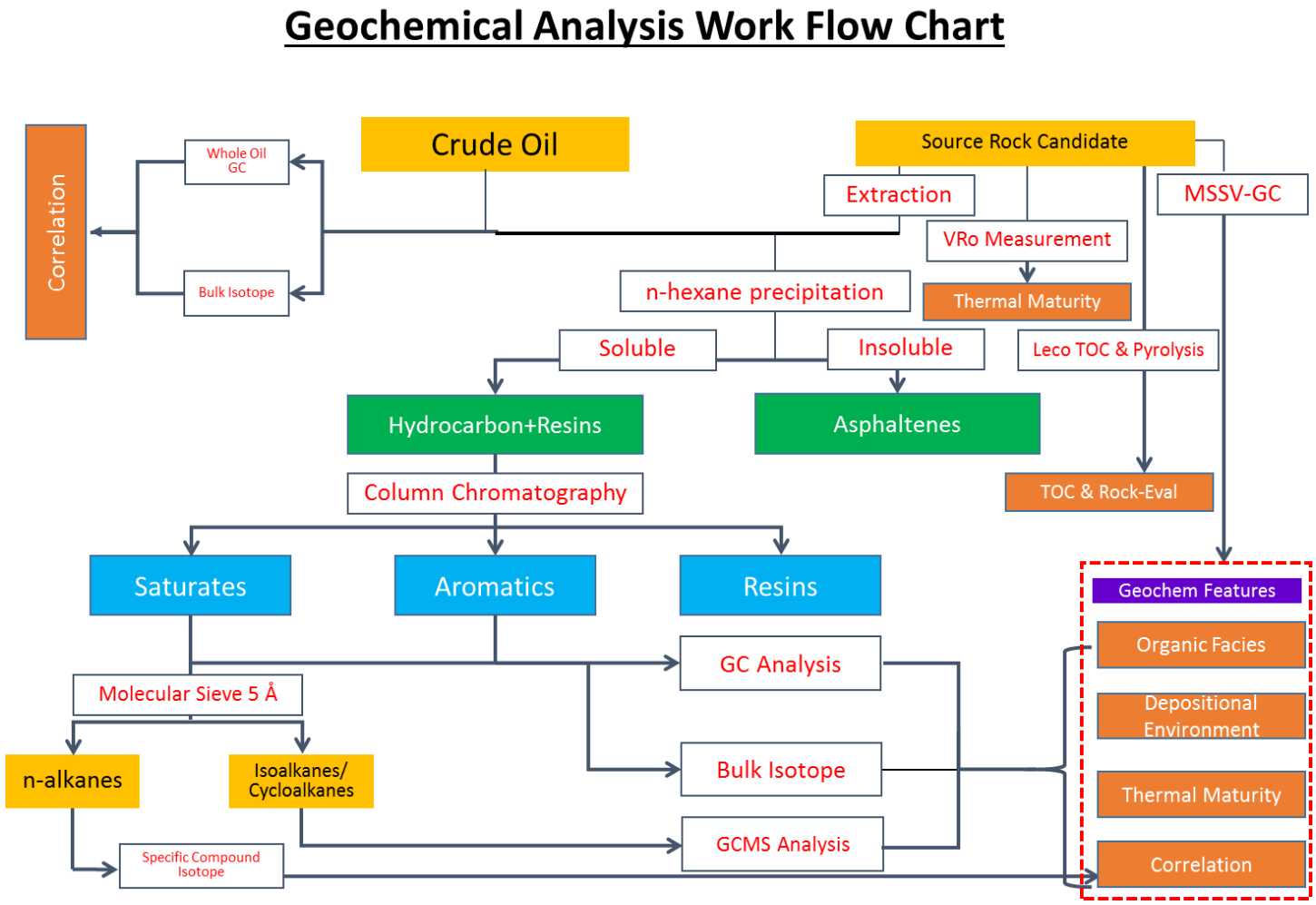

Figure 24. Schematic workflow used for laboratory analyses of the Woodford Shale, whole oil and condensate samples (modified from Miceli Romero and Philp, 2012)

3.2.1 Pre-extraction rock sample treatments

Each rock sample (~100g) was taken from the original core plug and washed with hot water, distilled water and a 1:1 mixture of dichloromethane (DCM) and methanol to remove any possible contaminants (e.g. drilling mud). After the samples were air-dried completely, they were crushed by using a pestle in a porcelain mortar and ground into 60-200 mesh for screening analysis (TOC and Rock-Eval) and soxhlet extraction.

3.2.2 Total Organic Carbon (TOC) and Rock-Eval Analysis

Leco-TOC (Total Organic Carbon) analysis and Rock-Eval pyrolysis were performed on 138 rock samples either at GeoMark Research, Inc. in Humble, Texas or Weatherford Laboratories in Houston, Texas. Approximately 2 grams of crushed rock were used for determination of TOC and Rock-Eval parameters. After pre-screening based on the results of these analyses, source rock samples were chosen for further bitumen extraction and maltenes fractionation.

3.2.3 Vitrinite Reflectance Measurements

Organic petrography pellets for vitrinite reflectance measurement were prepared at the Oklahoma Geological Survey Organic Petrography Laboratories in Norman, Oklahoma under the guidance of Mr. Brian Cardott. The standard dispersed organic pellet were either made from a whole rock or a kerogen concentrate that had been treated with acids to remove minerals.

The kerogen concentrates were made from a whole rock Woodford core sample of ~40g by following Herwig Ganz's procedure. This procedure could be subdivided into several phases: 1) crush the whole rock sample into 18 mesh; 2) remove the bitumen by

Soxhlet extraction; 3) treat by hydrochloric acid (10% HCl) and subsequently hydrofluoric acid (10% HF) to remove carbonates and silicates minerals; 4) neutralize the acidic aqueous solution and filter; 5) air-dry the remaining kerogen grains, which are the kerogen concentrates.

Preparation of dispersed organic pellets from whole rock or kerogen concentrates followed the procedures provided by Mr. Brian Cardott as described below. For each depth, two aliquots of whole rock samples of ~10 grams were ground into 18 mesh and placed in plastic ring forms. A mixture of epoxy resin and hardener (5:1) was centrifuged for 4 minutes to remove the air bubbles and poured into the ring forms until one third full. Each crushed rock sample was poured into its plastic ring form and mixed with the epoxy until all the grains were evenly distributed across the bottom of the ring form. Additional bubble-free epoxy was poured into the ring forms until full. The pellets were left overnight to harden at room temperature.

Dispersed organic pellets were ground and polished using a Buehler Ecomet III Gridding and Polishing Apparatus to remove scratches and obtain a relief-free surface for microscopic analysis. Pellets were polished by using 320, 400, and 600 grit grinding papers with the pressure of 30 psi applied for 4 minutes and tap water as lubricant. Each sample was subsequently rinsed off by distilled water and thoroughly cleaned in an ultrasonic bath with distilled water for 2 minutes. Sample pellets were further polished by using a Buehler Texmet polishing cloth with Wendt Dunnington 0.3μm alumina slurry applied every 40 seconds and distilled water kept tapping as lubricant for 4 minutes. Pellets were then rinsed off with distilled water and thoroughly cleaned in the ultrasonic bath for 2 minutes. Then the pellets were rinsed off with distilled water and air-dried.

After this step, the pellets were polished with Wendt Dunnington 0.05μm alumina slurry following the same steps stated above, and finally placed in a desiccator overnight to dry.

The random vitrinite reflectance measurements were performed using a Vickers M17 Research Model 1 Microscope under oil immersion and reflected white light following the ASTM (2011) organic petrography procedures at the Oklahoma Geological Survey Organic Petrography Laboratories in Norman, Oklahoma under the guidance of Mr. Brian Cardott.

3.2.4 Bitumen Extraction and Fractionation

Before bitumen extraction, the Soxhlet apparatus and cellulose thimbles were pre-extracted for 24 hours using a 1:1 mixture of dichloromethane (CH_2Cl_2) and methanol (CH_3OH) in order to remove contaminants. Then the source rock samples (60g approximately per sample) were introduced into the pre-extracted thimbles to be extracted by the mixture of DCM and methanol (1:1) for 48 hours. The solvent was removed by using a rotary evaporator and the residue containing soluble bitumen was transferred into a glass centrifuge tube. The extract was separated into maltenes and asphaltenes by adding an excess (40:1) of *n*-pentane (C_5H_{12}) and put in a refrigerator overnight to completely precipitate the asphaltenes. After centrifuging for 5 minutes, the maltene fractions were transferred to a 250mL round bottom flask to evaporate the excess solvent until a few milliliters remained which were transferred into a pre-weighed vial. The remaining solvent was finally evaporated until dryness by a gentle nitrogen flow. The asphaltenes remaining in the centrifuge tubes were dissolved in DCM and transferred into pre-weighed vials. The solvent was evaporated and the asphaltene was weighed.

The maltene fraction was diluted in a ratio of 10mg sample per 60uL *n*-hexane (C_6H_{14}) for maltene fractionation by alumina column chromatography. Column chromatography was performed on alumina, which was activated at 550ºC before use and packed in 100ml glass columns. Saturates, aromatics and NSO (nitrogen, sulfur, and oxygen) compounds were fractionated based on differences in polarity of different solvents mixtures and different flow rates.

Columns were dry-packed with a piece of glasswool inserted at the bottom and then 7.5 g of activated alumina (A540-3) on top of the glasswool. Before loading the samples, the column was half filled with *n*-hexane. The column was gently tapped to remove the air bubbles, if any, in the alumina. The maltene fraction (~35mg) diluted within minimum *n*-hexane was introduced to the top of alumina. The saturate fraction was eluted by adding ~17 ml of *n*-hexane to the column without disturbing the alumina surface and then drained at 1 droplet/1.5 seconds; and then the aromatic fraction was eluted with 50 ml of *n*-hexane and DCM (7:3) and drained at 1 droplet/second; finally NSO compounds were eluted with 50ml of DCM and methanol (98:2). Each fraction was weighed on a balance after removing the solvents under nitrogen flow very gently. Saturate and aromatic fractions were diluted into a 3 mg/ml solution for further GC and GC-MS analysis.

The branched and cyclic (B&C) fraction was obtained by removing the *n-alkanes* from the saturate fraction following the procedures modified by Dr. Nguyen after West et al. (1990) using the molecular sieve HI-SIV 3000 purchased from Zeolyst International. The hydrophobic molecular sieve HI-SIV 3000 is activated at 550ºC overnight before it is used to remove n-alkanes from the saturate fraction. A glass wool-plugged Pasteur

pipette was packed with ~2g of HI-SIV 3000 powder and n-pentane was applied under pressure of water-free air to compress the HI-SIV 3000 powder. This step was repeated until the uncompressible HI-SIV 3000 section occupied nearly two-third of the column. Around 10 mg of saturate fraction was dissolved in 1 ml of n-pentane and transferred to the top of the HI-SIV 3000 section and stand for 2 minutes to let the molecular sieve absorb the n-alkanes completely. The water-free air was applied on top of the pipette such that the flow rate of filtrate was about 1 drop per second. The filtrate, which contains branched and cyclic alkanes (B&C fraction), was collected in a 4 ml vial located below the tip of the pipette and n-alkanes retained in the HI-SIV 3000 section. The B&C fraction was diluted into a 3 mg/ml solution for biomarker analyses.

3.2.5 Stable Carbon Isotope Analysis

For 19 crude oil samples, the stable carbon isotope ratios of saturate and aromatic fractions were measured by Mr. Rick Maynard in the isotope laboratory at the University of Oklahoma. Approximately 200-300 ug of each sample is analyzed in a Costech 4010 EA that is equipped with a furnace reactor column packed with the reagents chromium oxide (Costech 011001) and silvered cobalt oxide (Costech 011007) in accordance with the Costech 4010 manual at a furnace temperature of 1000^{o}C. The reduction column is packed with copper reduced wire (Costech 011013) at a temperature of 650^{o}C. The GC column is at a temperature of 55^{o}C.

The samples are weighed on a micro-balance and wrapped in tin capsule (Costech 04107) and then placed in sequence in a Costech zero blank autosampler which is mounted on the elemental analyzer. The samples are purged with high purity helium (99.9999%) to remove air and then analyzed by flash combustion. The resulting sample

peak is carried by a helium stream at a flow rate of 100 ml/min to a Thermo conflo III interface with dilution on which is connected to the ion source of a Thermo Delta V Plus isotope mass spectrometer. The relative stable carbon isotope ratio ($\delta^{13}C$) was reported relative to the Vienna Pee Dee Belemnite (VPDB) scale.

3.2.6 Gas Chromatography (GC)

For whole oil GC analysis, the crude oil sample was diluted into a 1mg/ml *n*-hexane solution and analyzed on an Agilent 6890 series gas chromatograph with a split/splitless capillary injection system and a 100m × 0.25mm (i.d.) J&W Scientific DB-Petro 122-10A6 fused silica capillary column coated with a 0.5µm liquid film. The temperature program started with an initial temperature of 40ºC and 1.5 minutes hold time and increased to 130ºC at a rate of 2ºC per minute and subsequently increased to 300ºC at a rate of 4ºC per minute followed by an isothermal period of 26 minutes for a total run of 115 minutes. C_7 light hydrocarbon analysis were performed using the GC data obtained from whole oil/condensates GC analysis stated above. The isolated fractions, saturates and aromatics respectively, were analyzed using an Agilent 6890 series gas chromatograph with a splitless capillary injector and a 30m × 0.25mm (i.d.) J&W Scientific DB-5 122-5032 fused silica capillary column coated with a 0.25µm liquid film. The injector was set up in the splitless injection mode and the temperature was held at 300ºC. The carrier gas was helium (He) with a flow rate of 1.4 ml/min. The temperature program started with an initial temperature of 40ºC held for 1.5 minute and increased to 300ºC at a rate of 4ºC per minute followed by an isothermal period of 34 minutes for a total run time of 100.5 minutes. The flame ionization detector (FID) temperature was set

at 310ºC. *n*-Alkanes and isoprenoids were identified in each chromatogram by comparing their relative retention times with standards.

3.2.7 Gas Chromatography-Mass Spectrometry (GC-MS)

The GC-MS analyses of the branched and cyclic alkanes (B&C) and aromatic fractions were performed on an Agilent 7890A gas chromatography system coupled with an Agilent Technologies 5975C mass selective detector (MSD) using single ion monitoring (SIM, Table 2). The GC used a 60m x 0.25mm Agilent/J&W Scientific DB-5 122-5562 fused silica capillary column coated with a 0.25µm liquid film. The injected volume of branched and cyclic and aromatic fractions was 1uL per run. The injector temperature was set at 300ºC. The GC temperature program started at 40ºC with 1.5 minutes hold time and was later increased to 300ºC at a rate of 4ºC per minute and then held constant for 34 minutes for a total run time of 100.5 minutes. Samples were run in splitless mode and helium was used as the carrier gas at a flow rate of 1.4 ml/min. Biomarker compounds were determined from fragmentograms corresponding to each ion using relative retention times and by comparison with published data.

For diamondoids analysis in crude oils/condensates, the sample was diluted with pentane in the concentration of 16 mg oil/ ml pentane. The pentane was reported to be a good solvent for adamantanes and diamantanes in terms of high solubility and low boiling point (Reiser et al., 1996). The oil solution was well homogenized in ultrasonic bath for at least 1 min. 1 microliter of the resulting oil solution was injected to Agilent GC-MS to detect adamatanes and diamantanes using SIM mode and key ion fragments:135,136,149 etc. and 188,187,201 etc., respectively. DB-5 MS 60 m x 0.25 mm x 0.25 micron in film

thickness was used. Temperature program started 40ºC and hold it for 1.5 min before ramping 4ºC/ min to 300ºC and holding this temperature for 34 min.

3.2.8 Gas Chromatography-Mass Spectrometry-Mass Spectrometry (GC-MS/MS)

The GC-MS/MS analyses were carried out with a Thermo Scientific Trace 1310 gas chromatography system coupled to Thermo Scientific TSQ 8000 Triple Quadrupole mass spectrometer. Selected parent and daughter ions (For steranes: 372→217; 386→217; 400→217; 414→217; For hopanes: 370→191; 384→191; 398→191; 412→191; 426→191; 440→191; 454→191; 468→191; For tricyclic terpanes: 262→191; 276→191; 290→191; 304→191; 316→191; 318→191; 332→191; 340→191; 360→191; 330→191; 374→191; 388→191; 402→191; 416→191; 430→191; 444→191; 458→191; 444→191; 444→191; 444→191) were used to analyze samples in the selected reaction monitoring (SRM) mode. The GC temperature program is the same as that of the GC/MS system in section 3.2.7. The transfer line temperature was 310ºC. For the MS/MS, the scan time for each daughter ion is 0.025s. The ion source was operated in electron impact mode with a collision energy of 9 eV. The ion source temperature was 250 ºC.

3.3 Quantitative Biomarker Analysis

Quantitation was accomplished by using deuterated *n*-tetracosane ($C_{24}D_{50}$) as internal standard for the saturate fractions and deuterated phenanthrene ($C_{14}D_{10}$) for the aromatic fractions. Each fraction were quantitatively spiked with its internal standard solution before injecting into GC/MS. The relative concentration of the biomarker in the B&C or aromatic fraction was calculated by comparing the peak area of the appropriate biomarker relative to that of the co-injected deuterated internal standard. In this study,

since the ideal standards were not available for each biomarker, it was assumed that the response factors of the analyzed biomarkers on the mass detector would be similar to that of the corresponding internal standards used in this study. In a GC/MS mass chromatogram, the integrated area of each peak represents the abundance of that compound if no significant coelution. Assuming the peak area of internal standard is A_{ISD}, and the peak area of selected compound is A_x. The concentration of internal standard in the mixing solution is $C_{ISD\ mix}$, and the concentration of selected biomarker is C_x. Suppose the volume of sample in each injection was 1μl. The C_x could be calculated as:

$$C_x = A_x C_{ISD\ mix} / A_{ISD} \qquad [1]$$

The concentration of the internal standard in the mixed solution before injected into GCMS ($C_{ISD\ mix}$) was calculated as:

$$C_{ISD\ mix} = \frac{C_{ISD} \times V_{ISD}}{V_{B/A} + V_{ISD}} \qquad [2]$$

C_{ISD} = Concentration of internal standard compound in the original internal standard solution before mixing with B&C or aromatic fraction

V_{ISD} = Total volume of internal standard added to the B&C or aromatic fraction

$V_{B/A}$ = Total volume of B&C or aromatic fraction before mixing with internal standard

In my experiments, C_{ISD} = 0.064mg/ml, $V_{B/A}$ = 200μL and V_{ISD}= 15μL, so:

$$C_{ISD\ mix} = \frac{0.064\ mg/ml \times 15\mu L}{200\mu L + 15\mu L} = 0.00447 mg/ml \qquad [3]$$

Introduced into equation [1], the concentration of biomarker in the saturate or aromatic fraction could be calculated as:

For saturates,

$$C_{bm\,sat} = \frac{C_{ISD} \times V_{ISD}}{A_{ISD} \times V_{B/A}} \times \frac{1}{C_{B/A}} \times A_{bm} \times \frac{m_{B\&C}}{m_{Sat}} \times 1 \times 10^6 \quad [4]$$

For aromatics,

$$C_{bm\,aro} = \frac{C_{ISD} \times V_{ISD}}{A_{ISD} \times V_{B/A}} \times \frac{1}{C_{B/A}} \times A_{bm} \times 1 \times 10^6 \quad [5]$$

where,

A_{bm} = Peak area of the biomarker for quantification

$C_{B/A}$ = Concentration of the B&C or aromatic fraction solution

$W_{B\&C}$ = Weight of the B&C fraction obtained after the molecular sieving (in grams)

W_{Sat} = Weight of the saturate fraction used for the molecular sieving (in grams)

$1x10^6$ = Conversion factor from g to µg

For source rocks extracts, the relative concentration of a specific biomarker is expressed in µg biomarker/g TOC; for crude oil samples, it's expressed in µg biomarker/g whole oil. This allows the comparison of the concentration and distribution of an identical biomarker between oils and source rocks. Below is how to normalize the biomarker concentrations relative to 1g of TOC or whole oil, respectively:

For source rock extracts:

$$C_{bm} = \frac{\mu g\ biomarker}{g\ Saturates} \times \frac{W_{Sat}}{W_{TOC}}$$

and

$$\frac{W_{Sat}}{W_{TOC}} = \frac{\frac{W_{Sat}}{W_{Maltenes}} \times \frac{W_{Maltenes}}{W_{Extract}} \times \frac{W_{Extract}}{W_{Rock}}}{TOC(wt\%)}$$

where

$\frac{W_{Sat}}{W_{TOC}}$ = Weight percentage of the saturate fraction in 1g of total organic carbon (TOC)

$\frac{W_{Sat}}{W_{Maltenes}}$ = Weight percentage of the saturate fraction recovered from the maltenes fraction

$\frac{W_{Maltenes}}{W_{Extract}}$ = Weight percentage of the maltenes recovered from the source rock extract

$\frac{W_{Extract}}{W_{Rock}}$ = Weight percentage of the rock extract recovered from the original source rock sample

$TOC(wt\%)$ = Weight percentage of the total organic carbon contents measured in the source rock sample (in wt. %).

For crude oil samples:

$$C_{bm} = \frac{\mu g\ biomarker}{g\ Saturates} \times \frac{W_{Sat}}{W_{WO}}$$

and

$$\frac{W_{Sat}}{W_{WO}} = \frac{W_{Sat}}{W_{Maltenes}} \times \frac{W_{Maltenes}}{W_{WO}}$$

$\frac{W_{Sat}}{W_{WO}}$ = Weight percentage of the saturate fraction recovered from the one gram g of the whole oil.

$\frac{W_{Sat}}{W_{Maltenes}}$ = Weight percentage of the saturate fraction recovered from the maltenes fraction

$\frac{W_{Maltenes}}{W_{WO}}$ = Weight percentage of the Maltene obtained from the whole oil

Attention should be paid herein is because errors may occur when quantifying biomarker relative concentration from multiple factors. For instance, errors could be introduced during the sample weighing and/or preparing the internal standards of the accurate absolute concentration. Errors may occur when fractionation by column chromatography as well, in which step the experimental operation would affect the relative percentage of each fraction. Moreover, errors could have been resulted from the difference in terms of response factors of the internal standard on the mass detector and each biomarker compound. Consequently, the concentrations of biomarkers in this study should be considered to be relative concentrations.

CHAPTER 4

4. SOURCE ROCK ANALYSIS

4.1 Source Rock Geochemical Screening Analyses

Petroleum geochemistry research has centered on developing applicable criteria and methods to evaluate source rocks associated with exploration prospects or plays (Dembicki, 2009). To evaluate a source rock, three key parameters need to be assessed: 1) what is the total organic carbon (TOC) or the organic richness of the source rock; 2) What is the kerogen type of the source rock and will it generate oil or gas or nothing; 3) What is the thermal maturity of the source rock. The first parameter, organic richness, is one of the prerequisites to determine whether or not it is a prolific source rock. A good source rock should have a high TOC, but not all organic matter is created equal. Some organic matter will generate oil, some will generate gas, and some will generate nothing (Tissot et al., 1974). What type of product would be generated is determined by the original kerogen type. The third parameter, thermal maturity of the source rock, determines the amount of hydrocarbons already generated and the types of hydrocarbons they are.

Prior to any biomarker work to determine organic matter type, depositional environment, or thermal maturity of the source rock, prospective samples should be screened. An effective petroleum source rock must satisfy certain requirements in terms of quantity, quality and thermal maturity of organic matter. It is also considered that prospective source rock samples are free of any contamination from oil-based drilling additives or migrated oils. In the oil industry, a set of geochemical techniques are used for preliminary screening, including, total organic carbon (TOC), Rock-Eval pyrolysis,

vitrinite reflectance (Ro), and petrographic analysis of maceral composition (Philp, 2003).

Subsurface rock samples analyzed in this study were initially screened using Leco-TOC measurements and Rock-Eval pyrolysis. From these data, representative sets of samples were chosen for biomarker and isotope analyses. The definitions of Rock-Eval pyrolysis terms used in the discussion and presented in subsequent figures and tables are shown in Table 2.

Table 2. Parameters, terms, and definitions derived from Rock-Eval pyrolysis analyses (modified from Peters, 1986 and Jarvie et al., 2007)

TOC	Total Organic Carbon	wt.%
S_1	Free volatile hydrocarbons thermally flushed from a rock sample at 300°C (free oil content)	mg HC/g rock
S_2	Products that crack during standard Rock-Eval pyrolysis temperatures (remaining potential)	mg HC/g rock
S_3	Organic carbon dioxide released from rock samples	mg CO_2/g rock
T_{max}	Temperature at peak evolution of S_2 hydrocarbons	°C
HI	Hydrogen Index = S_2 x 100/TOC	mg HC/g TOC
OI	Oxygen Index = S_3 x 100/TOC	mg CO_2/g TOC
S_1/TOC	Normalized Oil Content = S_1 x 100/TOC	
S_2/S_3	Describes type of hydrocarbons generated	Values from 0.00 to >5.00
PI	Production Index = $S_1/(S_1+S_2)$ (or transformation ratio)	Values from 0.00 to 1.00

4.1.1 Organic Richness

Throughout Oklahoma, the Woodford Shale proves to be an excellent potential source rock based on TOC, HI, and thermal maturity. The average TOC for the subsurface rock samples analyzed in this study was shown in Table 3. The spatial distribution of the

average TOC values for the Woodford rock samples from all of the wells in this study was shown in Figure 25. In general, the Woodford Shale shows good to excellent source rock potential based on the guidelines of Peters and Cassa (1994).

Table 3. Average TOC values for the Woodford Shale subsurface rock samples analyzed in this study

Well name	# of samples	Average TOC (wt. %)
Frank 1-33SWD	21	3.4
Elinore 1-18SWD	14	7.5
Wilma 1-16SWD	13	5.9
Winney 1-8SWD	11	3.4
Adkisson 1-33 SWD	9	4.4
Mary Earp – 5	2	7.1
Boyd Unit-1	3	5.4
Dannehl 2-16	5	6.6
Pritchard-1	10	7.1
Robberson Ranch 10-1	4	6.6
Anderson 12-1	19	4.2
Chenoweth-1	8	3.1
York-1	3	4.9
Pope Unit-1	1	5.5

CI = 250’

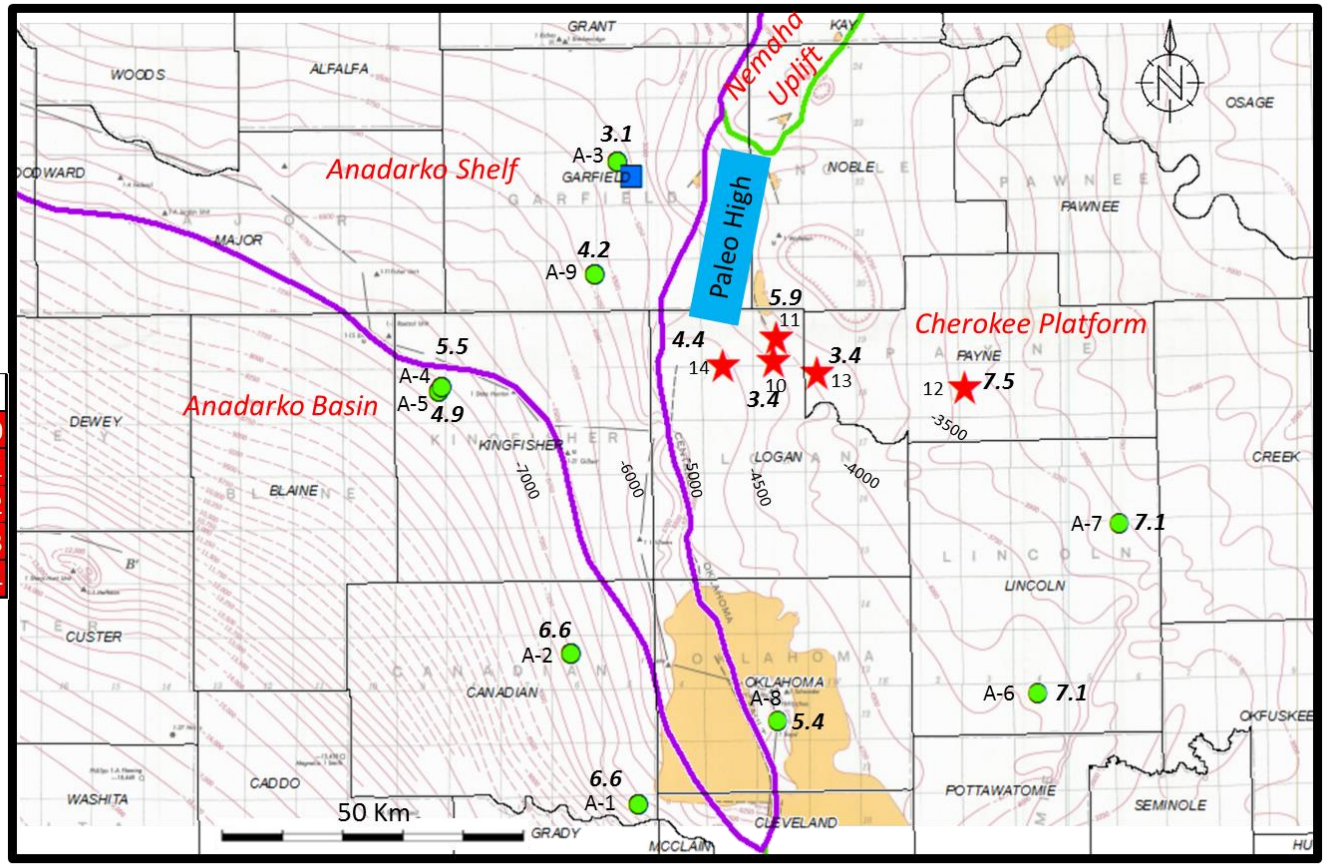

5 Devon Cores	Code
Frank 1-33 SWD	10
Wilma 1-16 SWD	11
Elinore 1-18 SWD	12
Winney 1-8 SWD	13
Adkisson 1-33 SWD	14

9 OGS Wells	Code
ROBBERSON 10-1	A-1
DANNEHL 2-16	A-2
L A CHENOWETH 1	A-3
LEWIS F POPE 1	A-4
EFFIE B YORK 1	A-5
PRITCHARD 1	A-6
MARY EARP 5	A-7
BOYD 1	A-8
ANDERSON 12-1	A-9

Base Map Modified from Amsden, 1975

Figure 25. Woodford Structural Map (in SSTVD) of Study Area with Woodford Rock Average TOC values (*wt. %)* (SSTVD = Sub Sea Total Vertical Depth in feet; TOC = Total Organic Carbon in weight percentage; CI = Contour Increment in feet)

4.1.2 Organofacies and Thermal Maturity Discussion based on Rock-Eval

Before we discuss the organic matter type of the Woodford samples in this study, it is necessary to clarify the definitions of three concepts: organic matter type, kerogen type, and source rock facies. Organic matter type is the type of original organic source matter, such as marine algae or bacteria, freshwater algae or bacterial, and higher plant cuticle, resin or lignin. Kerogen type is the classification of kerogen based on the elemental composition of the hydrogen, carbon and oxygen (Jacobson, 1991). By plotting atomic H/C versus O/C of coal constituents (macerals), van Krevelen (1961) recognized each kind of coal maceral had consistent ratios. These ratios also reflect the hydrocarbon generative potential of the maceral type. Tissot and Welte (1984) extended van Krevelen's work to potential petroleum source rocks by replacing the time-consuming elemental analysis with Rock-Eval analysis. The hydrogen index (HI) and oxygen index (OI) derived from Rock-Eval could be substituted for H/C and O/C to classify different kerogen types (Tissot and Welte, 1984). Source rock facies, also called "Organic Facies" (Jones and Demaison, 1982) or "Organofacies" (Pepper and Corvi, 1995), are mappable subdivisions of a designated stratigraphic unit, distinguished from adjacent subdivisions on the basis of their organic constituents, without regard to the inorganic aspects of the sediments based on Jones and Demaison's definition (1982). Pepper and Corvi (1995) developed the concept of "organofacies" instead of "organic facies" based on their distinct kinetic behavior of typical organofacies. Different from kerogen type, the concept of organofacies is geologically mappable or seismically mappable, which is rarely found on a fine scale and represent sufficiently large stratigraphic thickness and areal extent and have similar organic geochemical properties. Therefore the concept of organofacies

reflects not only the original biological input type but also the preservation processes of the organic matter. Since it has been widely accepted and applied in the oil industry, the concept and classification of organofacies is used in this study to type source rock facies.

Rock-Eval parameters have been used for initial evaluation of the kerogen type and source rock potential by the oil industry for many years. The plot of hydrogen index (HI) versus oxygen index (OI) has been widely used to classify the kerogen types (Tissot et al., 1974; Hunt, 1979; Tissot and Welte, 1984). Therefore, in this study, initially this plot (Figure 26) was used to try to classify the kerogen types of the Woodford samples but failed since this HI vs. OI diagram shows significant variations of HI values among the Woodford samples. The reason why it is confusing for users to classify the kerogen types from a pseudo van Krevelan diagram is because it is a common pitfall to discuss kerogen type with source rock potential together simply by plotting the HI and OI of the source rock samples. However only when the source rock samples are still immature, can the original kerogen type be determined from the HI vs. OI diagram. Source rock potential is totally a different concept. For example, an immature type-III gas-prone kerogen would not have any oil generation potential whatever heat you apply to it (Pepper and Corvi, 1995). It is highly recommended to discuss kerogen type and source rock potential separately. The significant variations of HI values among the Woodford samples in the HI vs. OI diagram could result from the differences in organofacies (Pepper and Corvi, 1995) or differences in thermal maturity. The kerogen type developed by IFP (Tissot and Espitalie, 1975) is classified by the chemical composition, specifically, the HI and OI. If the source rock sample is still immature, the kerogen type could indicate the source rock potential,

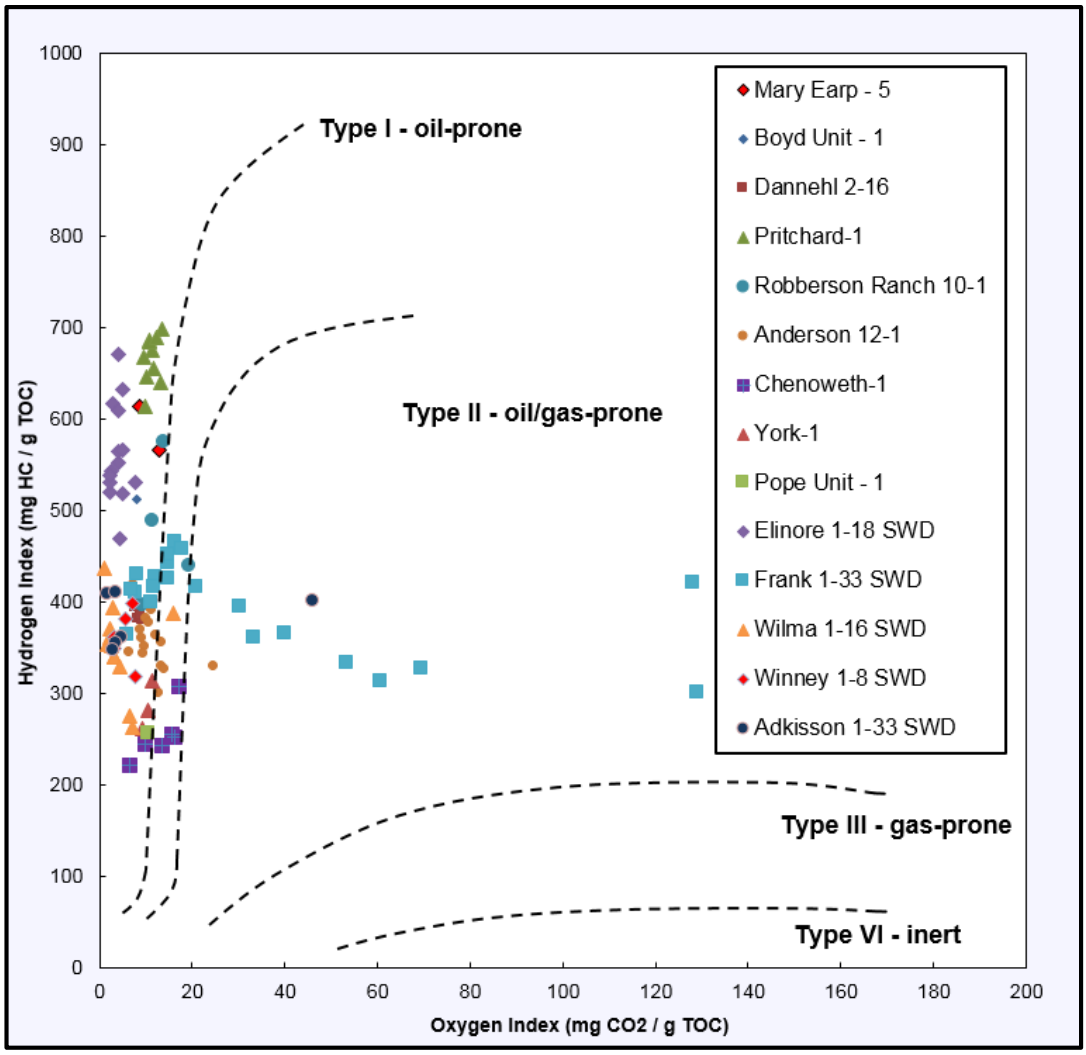

Figure 26. Modified van Krevelen diagram for the Woodford Shale samples

specifically, whether it would generate oil or gas or nothing. But the IFP kerogen type could not provide direct information on organic matter type and depositional environment. There is not a one-to-one relationship between IFP kerogen type and organofacies. An extreme case is you can find type I, II, III and even IV kerogens from an identical organofacies: lacustrine organofacies C (Schamel, 2015;

Figure 27). By IFP definition these are all Type I and Type III kerogens with possible terrestrial (coal/lacustrine) origins. While, the dataset is in fact the lower Green River Formation,

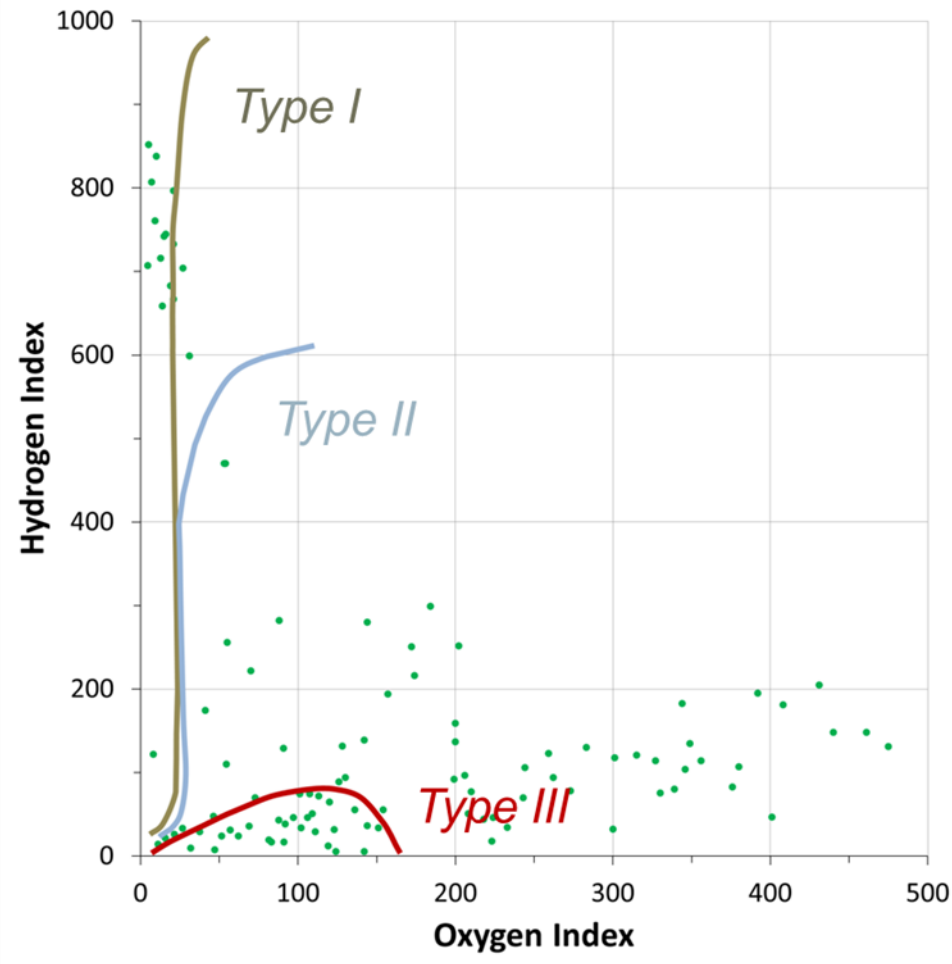

Figure 27. HI vs. OI of Green River Formation lacustrine sediments (modified from Schamel, 2015)

which is a world famous lacustrine mudrock. Based on Pepper's experiments (1995), all these lacustrine mudrock samples have the same generation kinetics with expulsion behavior and proportion of oil to gas generated partly controlled by HI. The data points' spread distribution is because of the samples oxidation. From this case, it is obviously the IFP kerogen type is not an indicator of the source rock depositional environment or source

rock organic matter input type. Therefore the concept of organofacies (Table 4), which is derived from source rock organic matter input type and source rock depositional environment (Figure 28), not only chemical composition, was used in this study to classify source rock facies.

Organofacies can be thought to be a collection of kerogens derived from common organic precursors, deposited in similar environments, and exposed to similar early preservation histories (Pepper and Corvi, 1995). Different from the IFP kerogen type classified upon the chemical composition difference, the concept of organofacies is derived from integration of source rock organic matter input type and source rock depositional environment (Figure 28). For example, a typical organofacies A is marine clay-poor carbonate shale, like the Monterey Shale in California; a typical organofacies B is marine clay-rich siliciclastic shale, like the Woodford Shale in Oklahoma and the Bakken Shale in North Dakota; organofacies C is lacustrine shale, could develop in freshwater lacustrine or saline lakes; organofaices D/E is terrigenous non-marine organic matter rich in wax developed in some ever-wet coastal plains of Mesozoic and younger age; organofaices F is terrigenous organic matter rich in lignin developed in coastal plains of mostly Paleozoic age (Pepper and Corvi, 1995; Table 4).

Organofacies	Descriptor	Principal Biomass	Sulfur Incorporation	Environment/ Age association
A	Aquatic, marine, siliceous or carbonate/ evaporate	Marine algae, Bacteria	High	Marine, upwelling zones, clastic-starved basins (low detrital iron for S scrubbing)
B	Aquatic, marine, siliciclastics	Marine algae, Bacteria	Moderate	Marine, clastic basins
C	Aquatic, non-marine, lacustrine	Waxy freshwater algae, bacteria	Low	Tectonic, non-marine basins: minor on coastal plains
D/E	Terrigenous, non-marine, waxy	Higher plant cuticle, resin, lignin; bacteria OR same but no resin	Low	Some ever-wet coastal plains (Mesozoic and younger)
F	Terrigenous	Lignin	Low	Coastal Plains (mostly Paleozoic)

Table 4. Organofacies classification (modified from Pepper & Corvi, 1995)

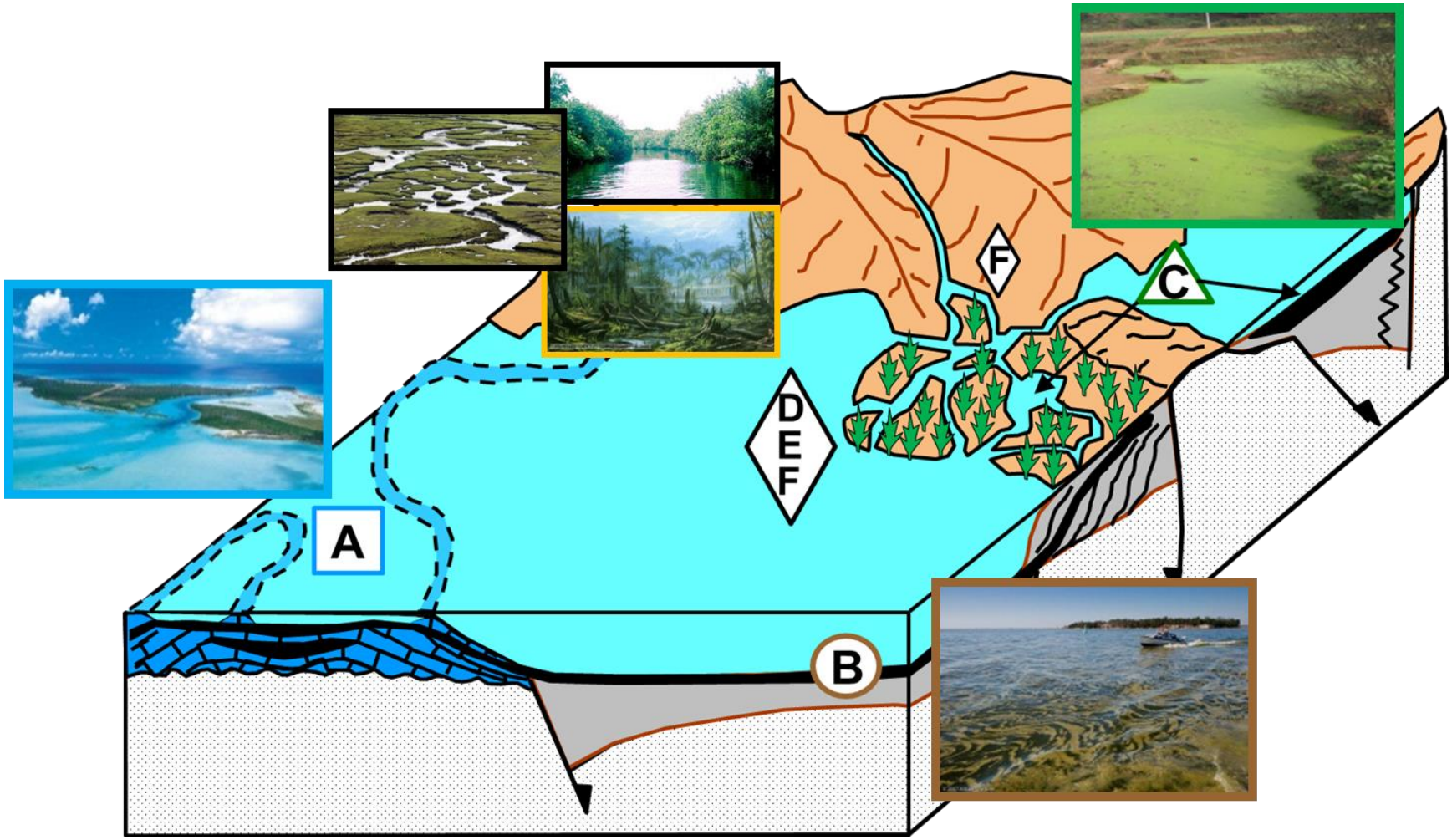

Figure 28. Organofacies depositional environments (modified from Pepper & Corvi, 1995)

The Woodford Shale in Oklahoma is a typical organofacies B – marine clay-rich siliciclastic shale based on three key characteristics found in previous research: 1) marine non-calcareous siliceous mudstone (Amsden, 1975; Kirkland et al., 1992; Comer, 2008; Kvale and Bynum, 2014); 2) low-to-moderate sulfur contents (Jarvie et al., 2007); and 3) high clay mineral contents (Kirkland et al., 1992; Comer, 2008; Kvale and Bynum, 2014). The spread distribution in HI and OI of the Woodford rock samples in this study (Figure 26) is not attributing to organofacies difference but the shale deposition heterogeneity and possible oxidation during organic matter preservation discussed later. Based on the Tmax vs. HI plot (Figure 29), rock samples from most of the studied wells, including Boyd Unit-1, Dannehl 2-16, Roberson Ranch 10-1, Anderson 12-1, Wilma 1-16 SWD, Winney 1-8 SWD, Adkisson 1-33 SWD and some Frank 1-33 SWD show moderate HI values (300-500 mg HC/g TOC) indicating these samples are in the moderate maturity stage. The higher HI values (500-700 mg HC/g TOC) for the samples from Pritchard-1, Elinore 1-18 SWD and Mary Earp-5 are thought to be a result of their low maturity dominantly and not only related to organic matter input. The low vitrinite reflectance values of the Woodford samples from these three wells support their relatively low maturity. In addition, these three wells are located in the east of the study area (Figure 22; on the Cherokee Platform east of the Nemaha Uplift) and the burial depth of the Woodford Shale in these three wells is shallower than in the rest of the wells (Figure 30), which could be additional supporting evidence that the high HI values are mainly as a result of maturity control but not source control. Therefore their major source rock facies is organofacies B of marine origin similar to the majority of the studied wells. The samples with low HI values (200-300 mg HC/g TOC) from Chenoweth-1, York-1 and Pope Unit-1 wells are

interpreted to be of high maturity confirmed by their high vitrinite reflectance values and their deeper Woodford burial depths resulting from the Woodford steeper dipping angle towards the Anadarko Basin (Figure 30). The high OI values for some Woodford samples from Frank 1-33 SWD (up to 140 mg CO_2/g TOC; Figure 26) are probably the result of bioturbation during the Woodford deposition in this well. Another outlier is Anderson 12-1. It is located on the Anadarko Shelf west of the Nemaha Uplift. Its VRo value is close to that from Chenoweth-1 and the location of these two wells are very close. The relatively high HI values (362 mg HC/g TOC in average) could be interpreted as not enough samples to give the true value. Following the dipping trend of the Woodford Shale structure, the Woodford in the studied wells show the lowest HI values (200-300 mg HC/g TOC) on the Anadarko Shelf west of the Nemaha Uplift, medium HI values (300-400 mg HC/g TOC) on the Cherokee Platform east of the Nemaha Uplift, and highest HI values on the Cherokee Platform further east of the Nemaha Uplift, which is eastern-most region of the study area (Figure 30). It seems to be a trend that the Woodford HI values decrease the Woodford burial depth increases, which is not surprising.

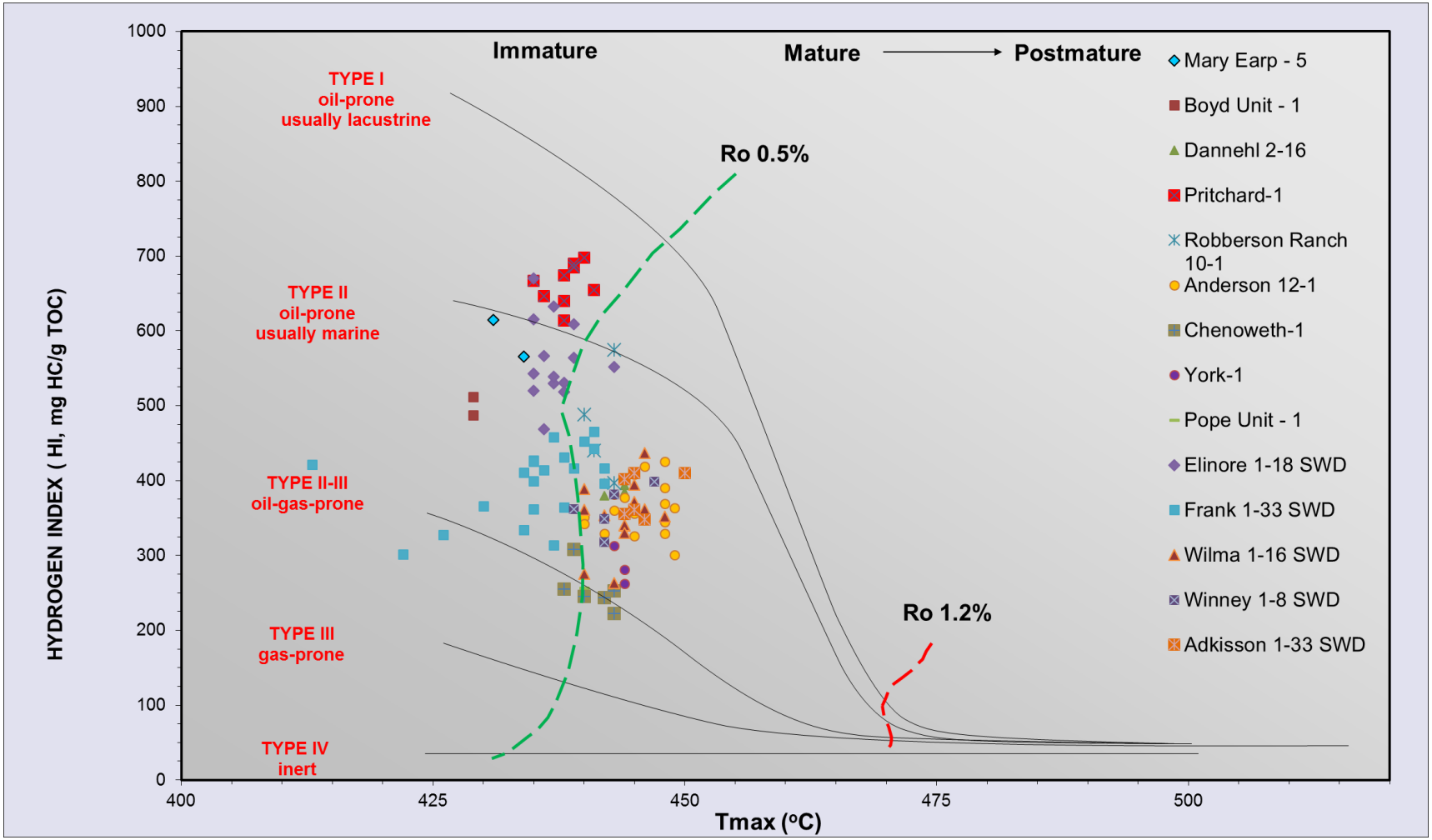

Figure 29. Tmax vs. HI plot showing maturity and kerogen type of the Woodford Shale samples.

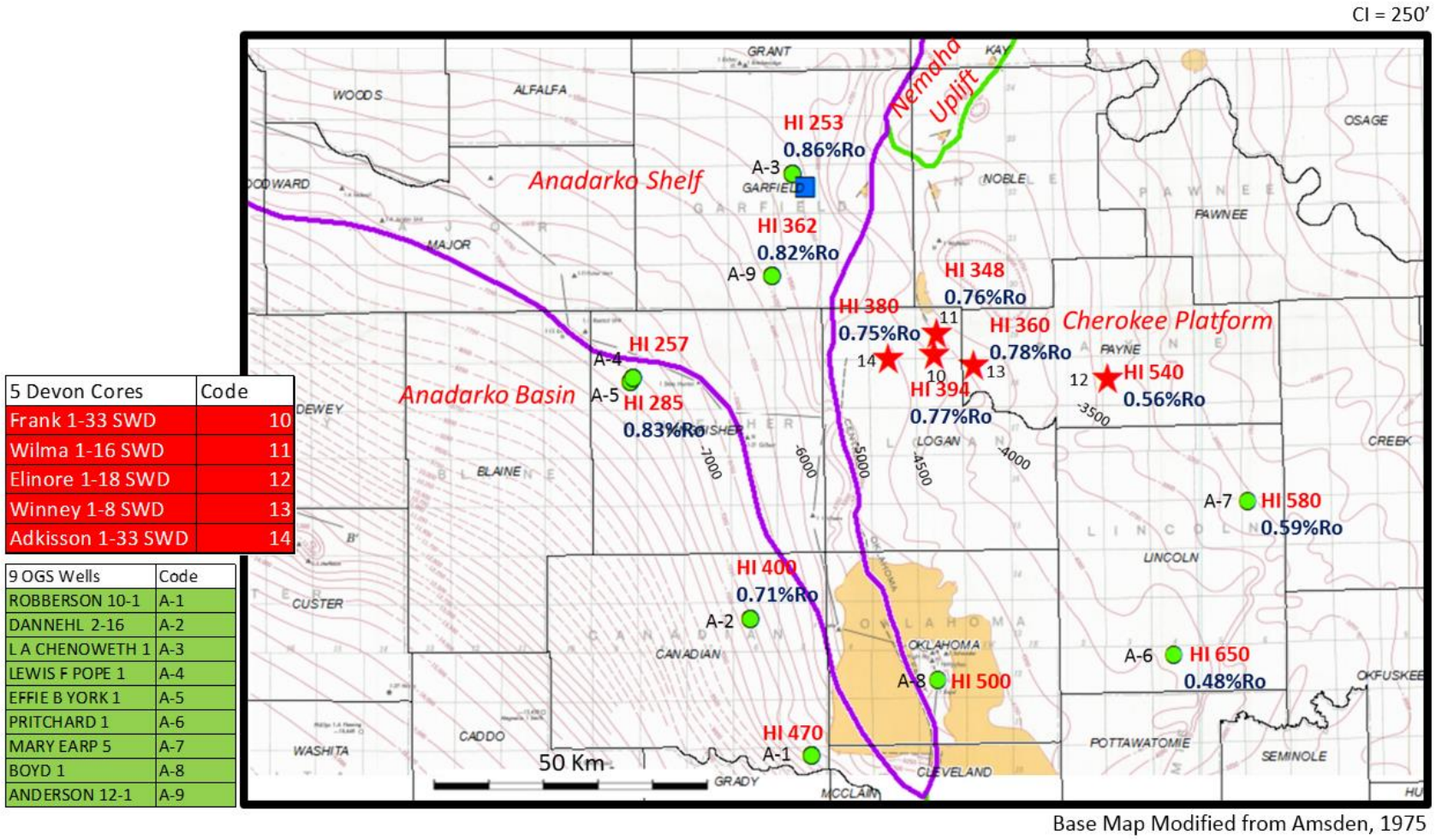

5 Devon Cores	Code
Frank 1-33 SWD	10
Wilma 1-16 SWD	11
Elinore 1-18 SWD	12
Winney 1-8 SWD	13
Adkisson 1-33 SWD	14

9 OGS Wells	Code
ROBBERSON 10-1	A-1
DANNEHL 2-16	A-2
L A CHENOWETH 1	A-3
LEWIS F POPE 1	A-4
EFFIE B YORK 1	A-5
PRITCHARD 1	A-6
MARY EARP 5	A-7
BOYD 1	A-8
ANDERSON 12-1	A-9

Base Map Modified from Amsden, 1975

Figure 30. Woodford Structural Map (in SSTVD) of Study Area with Woodford Rock HI and VRo (measured).

4.1.3 Thermal Maturity from Vitrinite Reflectance Measurements

Vitrinite reflectance ($\%R_o$) has been used as a scale for source rock thermal maturity for years (Philp, 2003; Cardott, 2011, 2012 and 2013), even though there is still controversy on whether or not a vitrinite reflectance value of a source rock could represent its thermal maturity (Cardott, 2011). Two main controversies have been debated by geologists and geochemists in the oil industry. One is the Ro value measures the thermal stress of a source rock but not thermal strain (Cardott, 2011 and 2012). The other is the Ro value is valid only if it is measured from the original vitrinite formed *in-situ* without oxidation but not reworked vitrinite transported into the shale deposits (Cardott, 2011 and 2012).

The reason why the scholars differentiate thermal strain from thermal stress is because in the oil industry people care about thermal strain, which measures the extent of hydrocarbon generation (Is source rock mature enough to generate hydrocarbon? Did it generate oil or gas? How much oil/gas generated?), more than thermal stress, which measures how much heat is applied to the source rock. People found even with a same Ro value, different type of source rock has different thermal strain. For example, a marine carbonate, clay-poor, sulphur-rich source rock (organofacies A) with 0.5% Ro value has generated hydrocarbon but a terrestrial deltaic source rock (organofacies D/E) with 0.5% Ro value is still immature to generate anything (Hunt, 1979; Pepper and Corvi, 1995). That's because vitrinite reflectance, originally derived from coal petrography, measures the percentage of incident light reflected from the surface of vitrinite particles in a sedimentary rock (Dow, 1977; Tissot and Welte, 1984), which is a direct measurement of thermal stress of source rock. The Tmax value, HI value and some biomarker thermal

maturity indicators are direct proxies of thermal strain of source rock. Because they are measured directly from "Products" not "Reactants", if assuming hydrocarbon generation is a sort of chemical reaction.

The other controversy was originally proposed by geologists. Originally Ro values were measured from vitrinites in coals. Obviously these vitrinites are formed *in-situ*. Therefore their Ro values could scale real thermal stress of source rocks. For the other types of source rocks, like marine or lacustrine source rocks, the Ro values would be valid thermal stress proxy only if the vitrinites within them have not been reworked or oxidized before deposition (Cardott, 2012 and 2013).

Vitrinite in the Woodford Shale, common in the lower Woodford member (Urban, 1960; Cardott, 2012), is derived from woody tissue of the progymnosperm *Archaeopteris* (Beck and Wight, 1988 and Anderson et al., 1995). The reason why the author in this research still measured Ro values to represent thermal maturity is because the studied target, the Woodford Shale in North-Central Oklahoma, has been proven to be organofacies B of marine origin. Therefore, in other words, there would be no issues on whether or not thermal stress measured by Ro values is consistent with thermal strain. As long as confirming the vitrinites to be measured are of original status without reworking by organic petrography, the purpose of vitrinite reflectance ($\%R_o$) measurements in this research is to establish a covary trend between Ro values and thermal strain proxies such as HI values. Therefore, in this research, vitrinite reflectance ($\%R_o$) measurements were attempted on more than twenty Woodford Shale samples from eleven different well locations: Pritchard-1, Mary Earp-5, Elinore 1-18 SWD, Frank 1-33 SWD, Adkisson 1-33 SWD, Wilma 1-16 SWD, Winney 1-8 SWD, Chenoweth-1, Anderson 12-1, Dannehl

2-16 and York-1. However, the identification of vitrinite particles with good measurable quality from these whole rock samples, or their isolated kerogen was difficult owing to the scarcity of vitrinite in the Woodford samples. This fact was rather expected since vitrinite is mainly derived from land-plant material (ASTM, 2011). The Woodford Shale was deposited during late Devonian to early Mississippian period, as higher plants were evolving, leading to the low terrigenous input to the Woodford shale. Most of the vitrinite fragments identified were pitted and/or insufficiently-large to obtain a valid measurement. Pitted vitrinite usually shows lower reflectance values due to its pitted surface scattering the reflected light. In addition, it is rather difficult to find a sufficient number of the large vitrinite clasts whose size is greater than the measuring spot of the microscope used for the vitrinite analysis.

From the requirement of organic petrography, a valid Ro value should be based on more than twenty random vitrinite reflectance measurements from a single rock pellet (Barker and Pawlewicz, 1993). Owing to the lack of good vitrinite reflectance measurements, two solutions were applied to obtain valid Ro values. One was to select the Lower Woodford member samples. Based on sequence stratigraphy, the Lower Woodford was deposited as the Woodford Sea started to transgress (Kirkland et al., 1992). In this period, Woodford deposition was relatively close to the land, so there was greater chance for deposition of higher plant derived organic matter input into the Woodford. More good quality of vitrinite fragments were found in the Lower Woodford samples than the Middle and Upper Woodford (Urban, 1960; Cardott, 2012). The other solution to obtain valid Ro values was to concentrate kerogen from the whole rock samples by removing the bitumen and then the mineral matrix with hydrochloric acid and

hydrofluoric acid. By concentrating the vitrinite in this manner, several valid Ro values were obtained based on more than twenty random vitrinite measurements. In the Frank 1-33 SWD 5627.9 feet Woodford sample, thirty five (35) vitrinite clasts were identified and measured, ranging from 0.70 to 0.88%R_o with a random R_o measurement of 0.77%, indicating that in this area the Woodford Shale is approaching peak oil generation. A photomicrograph of a vitrinite clast (0.72%R_o), bitumen (0.44%R_o), and the histogram of random vitrinite reflectance measurement from the same sample is shown in Figure 31. This figure illustrates the variability of macerals and bitumen content observed in the Woodford Shale samples that could potentially lead to errors in the identification and measurement of vitrinite reflectance. One of these common errors would be misidentify bitumen as vitrinite, which would lead to a lower Ro value. This is one possible explanation why the thermal maturity of the Woodford Shale in this study area was underestimated by Cardott (2013 and 2014) compared to the measured results reported in this research.

For the rest of the Woodford pellets, around ten Ro measurements were obtained per sample and could be counted as a qualitative Ro result. A Ro map of the study area was plotted by all the measured Ro values (Figure 30). A general Ro variation trend is obvious and consistent with the NE-SW dipping trend of the Woodford structure in Central Oklahoma. The Woodford in the studied wells show the highest Ro values (0.82-0.86% Ro) on the Anadarko Shelf west of the Nemaha Uplift, medium Ro values (0.75-0.78% Ro) on the Cherokee Platform east of the Nemaha Uplift, and lowest Ro values (0.48-0.59% Ro), which is the eastern-most region of the study area. The Anadarko Shelf and the Cherokee Platform are separated by the Nemaha Uplift Zone. It seems to be a

general trend that the Woodford Ro values increases as the Woodford burial depth increases, and the Woodford HI values decreases as the Woodford burial depth increases as discussed in section 4.1.2. These two trends may indicate the Woodford thermal status on the Anadarko Shelf and Cherokee Platform were controlled by the same tectonic events in the geological history.

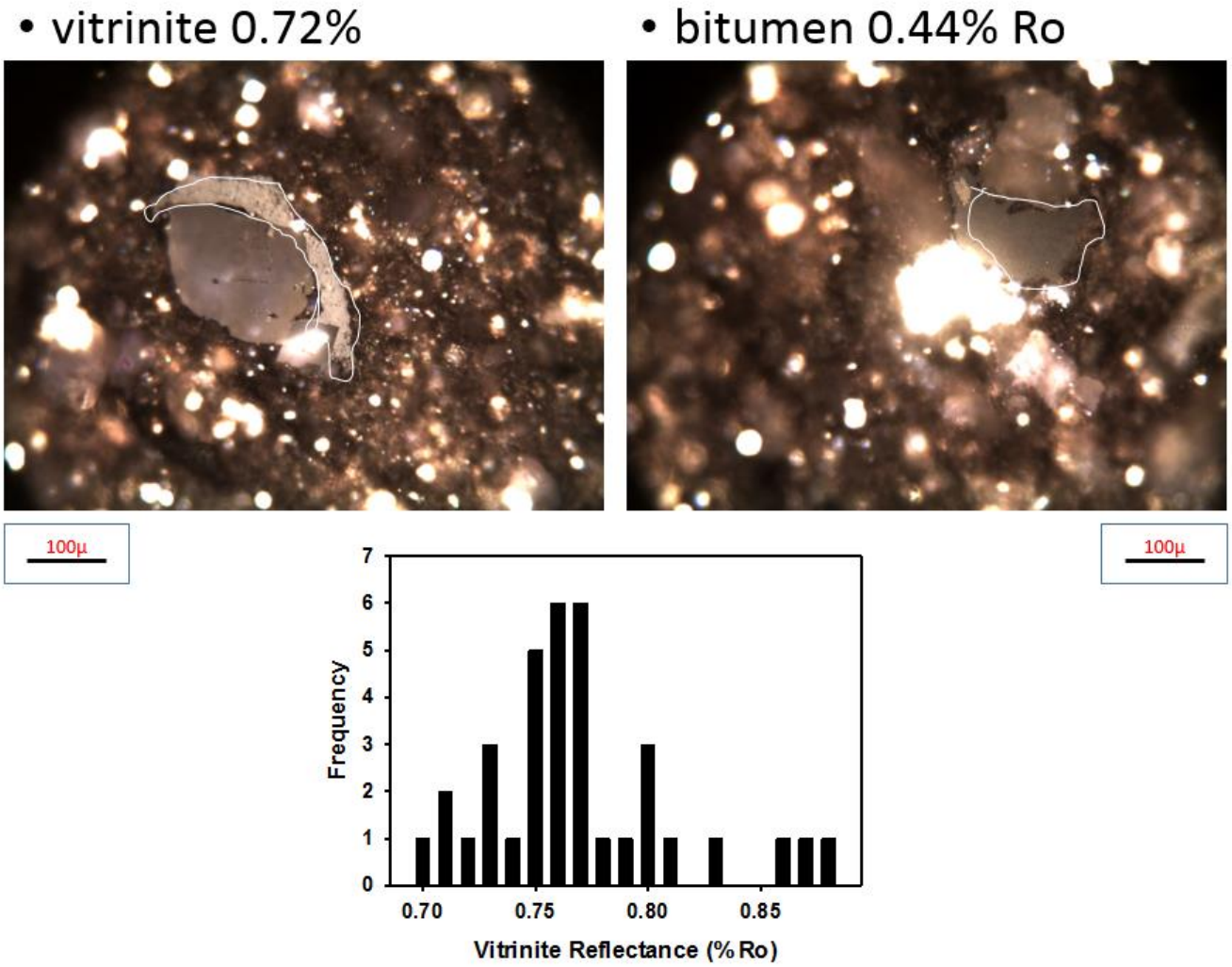

Figure 31. Photomicrographs from the Frank 1-33 SWD 5627.9 feet Woodford Shale sample

4.1.4 Gas Chromatography

4.1.4.1 n-Alkanes distributions

The terrigenous to aquatic ratio (TAR), is a crude parameter used to evaluate the type of organic matter input that compares the high-odd-carbon-numbered *n*-alkanes (terrigenous organic matter) with the low-odd-carbon-numbered *n*-alkanes (marine organic matter; Bourbonniere and Meyers, 1996). The TAR ratio should be used with caution since it was derived from various recent sediment data and is sensitive to secondary processes including biodegradation and thermal maturation (Moldowan et al., 1985; Derenne et al., 1988). The carbon preference index (CPI; Bray and Evans, 1961) compares the odd-carbon-numbered *n*-alkanes (n-C_{25}-n-C_{33}) against the even-carbon-numbered *n*-alkanes (n-C_{24}-n-C_{34}). In general, *n*-alkanes derived from marine organic matter do not show carbon-number preference, whereas *n*-alkanes originating from terrigenous organic matter tend to show odd-carbon-number predominance. Some source rocks developed in hypersaline and carbonate settings at low maturity were reported to show low CPI values due to even-numbered *n*-alkane predominance (Mello et al., 1988). In some cases, CPI can be used to roughly assess thermal maturity. Oils and rock extracts showing CPI values significantly greater than 1.0 (odd predominance) tend to be indicative of low thermal maturity (Peters et al., 2005). In general, both the TAR and CPI ratios are influenced by source and thermal maturity, and additional geochemical parameters need to be incorporated with these ratios when characterizing oils and source rocks.

For the rock samples in this study, gas chromatograms of the saturate fractions of the Woodford rock extracts show only small variations in composition between the

different depths (Figure 32). Several geochemical parameters calculated from the *n*-alkane chromatograms of rock extracts are summarized in Table 5. In the case of the Woodford Shale samples, all of them shows a unimodal distribution towards the low-carbon-number members, and without any preference of even-carbon-numbered *n*-alkanes predominance (Figure 32; Table 5). The Woodford and the Mississippian rock extract samples show a maximum around *n*-C_{15} (Table 5). Several characteristics, including the unimodal *n*-alkanes distribution pattern, *n*-alkane maximum carbon number around *n*-C_{15} and average Pr/Ph ratio in the range of 1 - 2, all point towards a marine origin and the existence of reducing (anoxic) conditions during the source rock deposition. It seems that the TAR ratio of Mississippian extracts (Winney 1-8 SWD 5155', 5166', and C8869 in Table 5) are higher than that from the Woodford. Considering the carbonate depositional settings of the Mississippian rock, this finding is consistent with the other previously reported carbonates source rock organic geochemical studies in Oklahoma and Texas, like the Eagle Ford Shale (Miceli Romero, 2014), the Lower Mississippian Limestone (Kim, 1999), and the Viola Limestone (Wang, 1993). The TAR ratio difference between the Woodford and Mississippian extracts may reflect the depositional environment changing from distal deep marine to proximal carbonate settings. The CPI values of all of the rock samples are close to 1 and could not be used to distinguish the relative amounts of marine/terrigenous input, since they have all already reached equilibrium by thermal maturation.

4.1.4.2 Pristane and Phytane

Pristane (Pr) and phytane (Ph) were identified in the gas chromatograms of the saturate fractions from both the rock extracts (Figure 32). The Pr/Ph ratio has been widely

used for evaluating redox conditions during source rock deposition since their origin is dependent on oxygen availability during diagenesis (Didyk et al., 1978; Sofer, 1984; Waples, 1985). Pr and Ph are primarily derived from the phytyl side chain of the *chlorophyll-a* in phototrophic organisms and bacteriochlorophyll in purple sulfur bacteria (Brooks et al., 1969; Powell and McKirdy, 1973). While, other likely sources, such as unsaturated isoprenoids in zooplankton, higher animals, and archaea, have been found to be precursors for Pr and Ph as well (Blumer et al., 1963; Blumer and Thomas, 1965; Goosens et al., 1984; Rowland, 1990; Bechtel et al., 2007).

Pr and Ph can be generated by two different chemical reactions from the phytyl chain of chlorophyll. Under reducing or suboxic (high Eh) conditions, phytol undergoes hydrogenation and reduction to generate phytane. On the contrary, under oxic conditions (low Eh), pristane was produced by oxidation and decarboxylation of the phytol chain (Tissot and Welte, 1984). Based on this theory, Pr/Ph ratios less than 1 suggest anoxic conditions, whereas Pr/Ph greater than 1 are associated with oxic conditions. Therefore the Pr/Ph ratio could be a proxy in evaluating the redox condition of the depositional environment of the source rock (Didyk et al., 1978; Shanmugam, 1985). But the real world is more complex than the theory above. The utility of Pr/Ph ratio in describing the redox conditions of source rock depositional environment is limited by several factors,

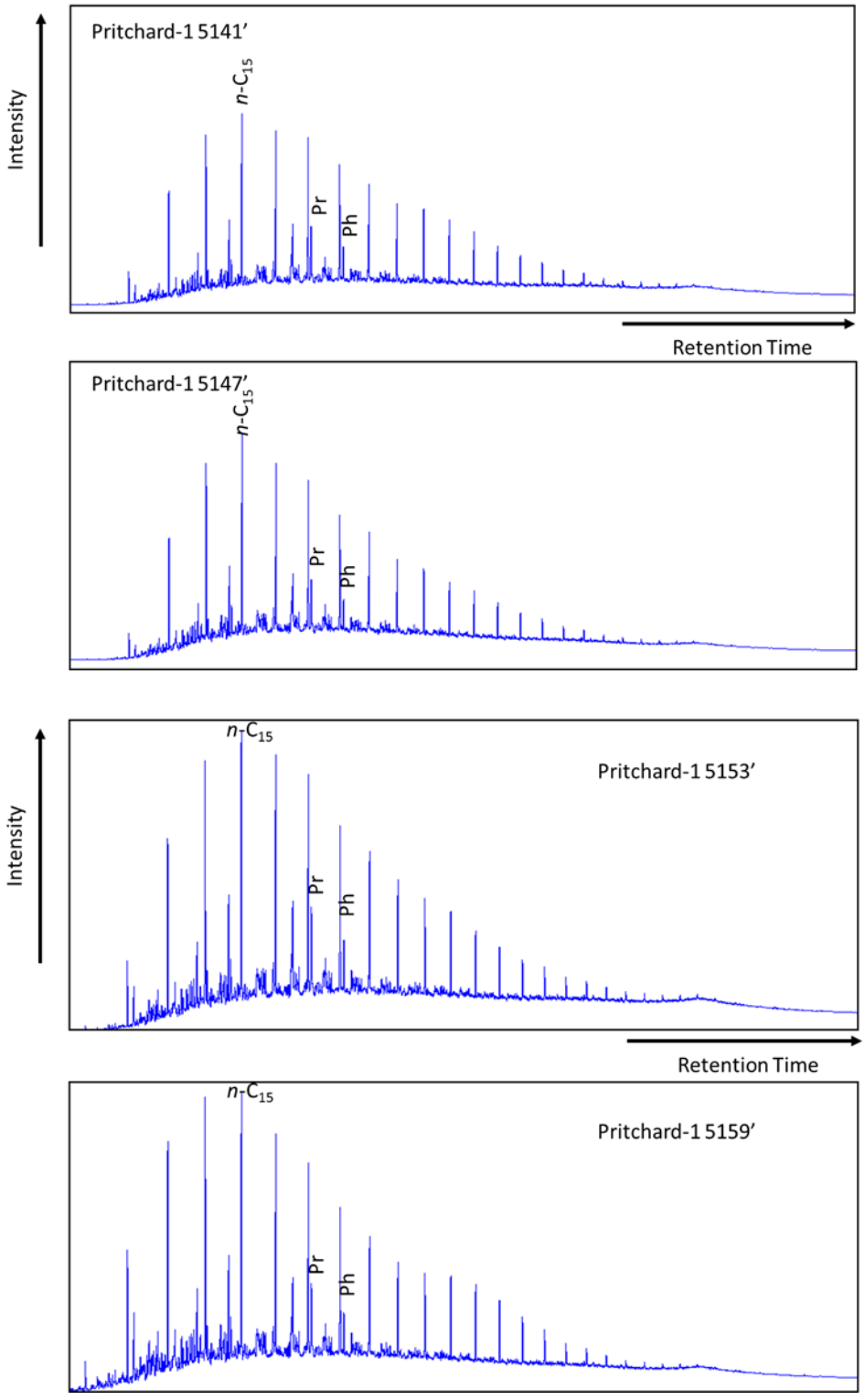

Figure 32. Gas chromatograms of the saturate fractions for the Pritchard-1 Woodford rock extracts (Pr = pristane; Ph = phytane, *n*-C_{15} = C_{15} normal alkane)

Table 5. N-Alkanes parameters derived from the saturate fraction of Woodford Shale and Mississippian Rock extracts

Samples	Formation	Range	n-alkane distribution	n-alkane maximum	Pr/Ph	TAR	CPI
Frank 1-33 SWD	Woodford	*n*-C_{13}-*n*-C_{26}	unimodal	*n*-C_{15}	1.55-2.61	0.03-0.05	0.73-1.10
Wilma 1-16 SWD	Woodford	*n*-C_{12}-*n*-C_{29}	unimodal	*n*-C_{16}	1.22-2.29	0.04-0.08	0.92-1.09
Winney 1-8 SWD	Woodford	*n*-C_{12}-*n*-C_{29}	unimodal	*n*-C_{16}	1.80-1.89	0.05	1.06
Elinore 1-18 SWD	Woodford	*n*-C_{11}-*n*-C_{29}	unimodal	*n*-C_{15}	1.81-1.98	0.02-0.04	1.00-1.14
Adkisson 1-33 SWD	Woodford	*n*-C_{11}-*n*-C_{29}	unimodal	*n*-C_{15}	1.33-1.68	0.03-0.07	0.84-1.03
Pritchard-1	Woodford	*n*-C_{12}-*n*-C_{35}	unimodal	*n*-C_{15}	1.18-2.15	0.03-0.07	0.97-1.04
Anderson 12-1	Woodford	*n*-C_{11}-*n*-C_{39}	unimodal	*n*-C_{14}	1.31-1.91	0.05-0.09	0.99-1.02
Chenoweth-1	Woodford	*n*-C_{12}-*n*-C_{38}	unimodal	*n*-C_{15}	1.73	0.11	1.02
York-1	Woodford	*n*-C_{12}-*n*-C_{36}	unimodal	*n*-C_{17}	0.84-1.08	0.08-0.10	1.01-1.02
Pope Unit-1	Woodford	*n*-C_{11}-*n*-C_{35}	unimodal	*n*-C_{15}	2.24	0.05	1.03
Winney 1-8 SWD 5155	Mississippian	*n*-C_{12}-*n*-C_{30}	unimodal	*n*-C_{15}	1.27	0.22	1.11
Winney 1-8 SWD 5166	Mississippian	*n*-C_{12}-*n*-C_{30}	unimodal	*n*-C_{15}	1.46	0.23	1.06
C8869	Mississippian	*n*-C_{13}-*n*-C_{33}	unimodal	*n*-C_{18}	0.98	0.30	1.18

such as variable precursor origin, different rates of early generation, and interference by higher maturity. Therefore, for rock and oil samples within the oil window, Pr/Ph ratios in the range of 0.8-3.0 are not recommended to indicate specific redox conditions due to the limitation stated above (Peters et al, 2005). It is recommended that Pr/Ph values greater than 3 are associated with terrigenous organic matter input under oxic to suboxic conditions, while Pr/Ph values lower than 0.8 suggest anoxic, hypersaline or carbonate depositional environments (ten Haven et al., 1987).

Overall, the majority of the rock extracts show low Pr/Ph ratios indicating the presence of reducing conditions (anoxia) during source rock deposition (Table 5). Another tool to evaluate variations in redox conditions, organic matter source, maturity, and alteration in source rock extracts and oils is the relationship between Pr, Ph, *n*-alkanes $C_{17,}$ and *n*-C_{18} (Shanmugam, 1985). A cross plot of Pr/*n*-C_{17} versus Ph/*n*-C_{18} for the rock extracts analyzed in this study is shown in Figure 33. This diagram indicates that these samples are mainly composed of marine organic matter mixed with terrigenous input, which is usually developed in a deltaic or near-shore depositional environment. The Woodford or Mississippian source rocks were not developed in a deltaic depositional environment. Moreover, from this plot, there is no obvious interrelationship between the locality of data points and their geographic aspects or geological aspects, either. Such plots derived from *n*-alkane distributions are affected by multiple indigenous and exogenous factors as stated before, which could mask the samples' original geological and/or geochemical properties. Hence additional geochemical data are needed to reveal indigenous differences between samples.

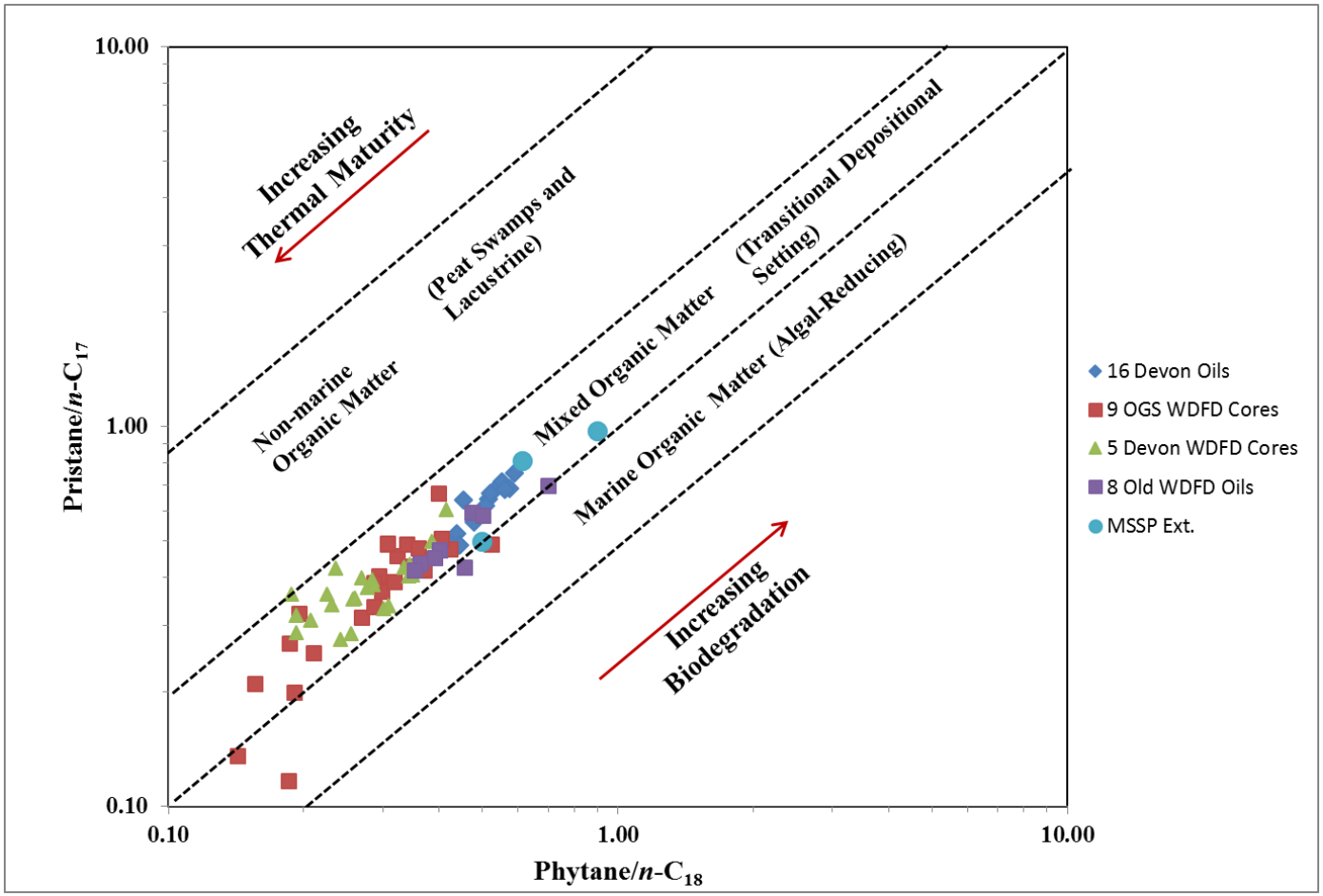

Figure 33. Isoprenoids plot of Pristane/n-C_{17} versus Phytane/n-C_{18} showing redox conditions, maturity, and depositional environments for samples of the Woodford Shale (n-C_{17} = C_{17} normal alkane; n-C_{18} = C_{18} normal alkane)

4.2 Evaluation of Organic Matter Source and Depositional Environments

4.2.1 Steranes (m/z 217)

Steranes originate from sterols, which are compounds found in eukaryotic organisms, mainly algae and higher plants (Tissot and Welte, 1984). Four main families of sterols containing 27, 28, 29, 30 carbon atoms produce four families of regular steranes during diagenesis (Waples and Machihara, 1991). In this study identification of steranes, diasteranes, pregnanes and homopregnanes were performed on the B&C fractions of rock extracts by single ion monitoring (SIM) GC-MS through analysis of the *m/z* 217.3 ion (Figure 34). The *m/z* 217.3 ion mass chromatogram of the Prtichard-1 5147 ft Woodford rock extract shows the steranes distributions of a typical Woodford Shale extracts in the study area (Figure 34). Peak identifications are shown in Table 6. Formulas for calculation of geochemical ratios are displayed in Appendix A. Numerical values of the geochemical ratios calculated are in Appendix D. Biomarkers quantitation results are in Appendix F.

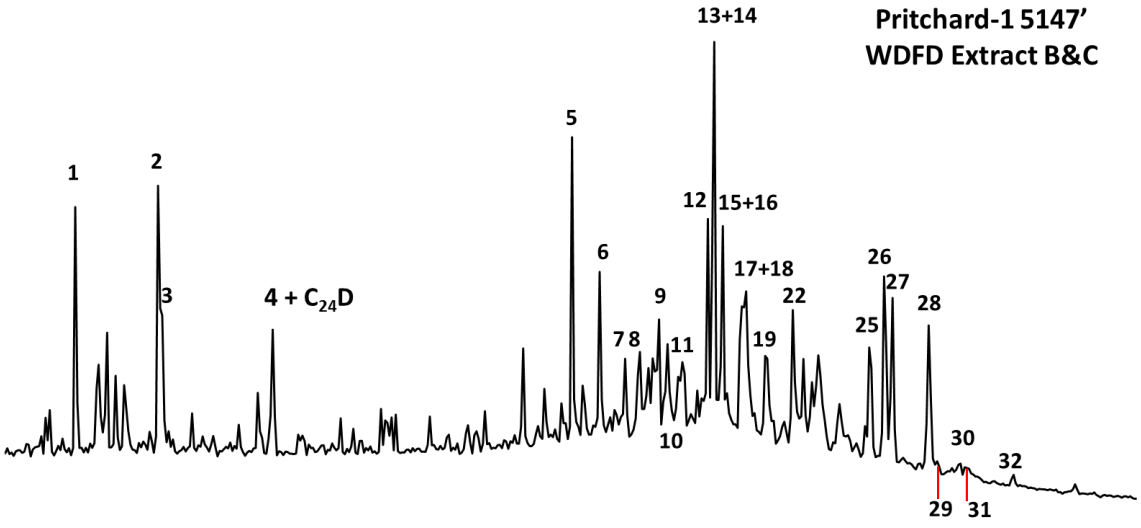

Figure 34. SIM *m/z* 217.3 mass chromatogram showing distribution of steranes in the B&C fraction of Pritchard-1 Woodford rock extract. Peak identification is listed in Table 6.

Table 6. Identification of steranes in the SIM *m/z* 217.3 mass chromatogram of the B&C fraction of Pritchard-1 Woodford rock extract

Peak #	Compound
C_{24}D	Deuterated *n*-tetracosane (ISTD)
1	Diapregnane
2	14β(H),17β(H)-Pregnane
3	Diahomopregnane
4	14β(H),17β(H)-Homopregnane
5	13β(H),17α(H)-Diacholestane (20S)
6	13β(H),17α(H)-Diacholestane (20R)
7	13α(H),17β(H)-Diacholestane (20S)
8	13α(H),17β(H)-Diacholestane (20R)
9	24-Methyl-13β(H),17α(H)-Diacholestane (20S)
10	24-Methyl-13β(H),17α(H)-Diacholestane (20R)
11	24-Methyl-13α(H),17β(H)-Diacholestane (20S)
12	14α(H),17α(H)-Cholestane (20S)
13	24-Ethyl-13β(H),17α(H)-Diacholestane (20S)
14	14β(H),17β(H)-Cholestane (20R)
15	14β(H),17β(H)-Cholestane (20S)
16	24-Methyl-13α(H),17β(H)-Diacholestane (20R)
17	14α(H),17α(H)-Cholestane (20R)
18	24-Ethyl-13β(H),17α(H)-Diacholestane (20R)
19	24-Ethyl-13α(H),17β(H)-Diacholestane (20S)
20	24-Methyl-14α(H),17α(H)-Cholestane (20S)
21	24-Methyl-14β(H),17β(H)-Cholestane (20R)
22	24-Ethyl-13α(H),17β(H)-Diacholestane (20R)
23	24-Methyl-14β(H),17β(H)-Cholestane (20S)
24	24-Methyl-14α(H),17α(H)-Cholestane (20R)
25	24-Ethyl-14α(H),17α(H)-Cholestane (20S)
26	24-Ethyl-14β(H),17β(H)-Cholestane (20R)
27	24-Ethyl-14β(H),17β(H)-Cholestane (20S)
28	24-Ethyl-14α(H),17α(H)-Cholestane (20R)
29	24-Propyl-14α(H),17α(H) -Cholestane (20S)
30	24-Propyl-14β(H),17β(H) -Cholestane (20R)
31	24-Propyl-14β(H),17β(H) -Cholestane (20S)
32	24-Propyl-14α(H),17α(H) -Cholestane (20R)

4.2.1.1 Regular steranes

A ternary diagram based on the distributions of C_{27}, C_{28} and C_{29} 14α(H), 17α(H) 20(R) regular steranes (Figure 36) was used to assess possible variations in depositional environment of the Woodford Shale and Mississippian rock samples by applying a similar approach to that of Moldowan et al. (1985). The idea behind this ternary diagram is that C_{27} steranes (cholestane) are primarily derived from precursors found in plankton and marine invertebrates. C_{28} steranes (ergostane) also originate from similar precursors, although they can be generated from terrestrial organisms as well (Huang and Meinschein, 1979; Moldowan et al., 1985). Similarly, C_{29} steranes (stigmastane) are derived from terrigenous organic matter sources and marine algae (Volkman, 1986). The regular steranes ternary plot for the rock samples (Figure 36) shows that the Woodford and Mississippian rock samples are grouped in slightly different areas of the plot. Either the Mississippian rock samples or the Woodford rock samples are not exactly falling into their corresponding areas on Moldowan's plot (1985; Figure 35), which may be attributed to the data sets for Moldowan to plot was limited back to that time. Data from the oils are discussed in section 5.2.2.1.

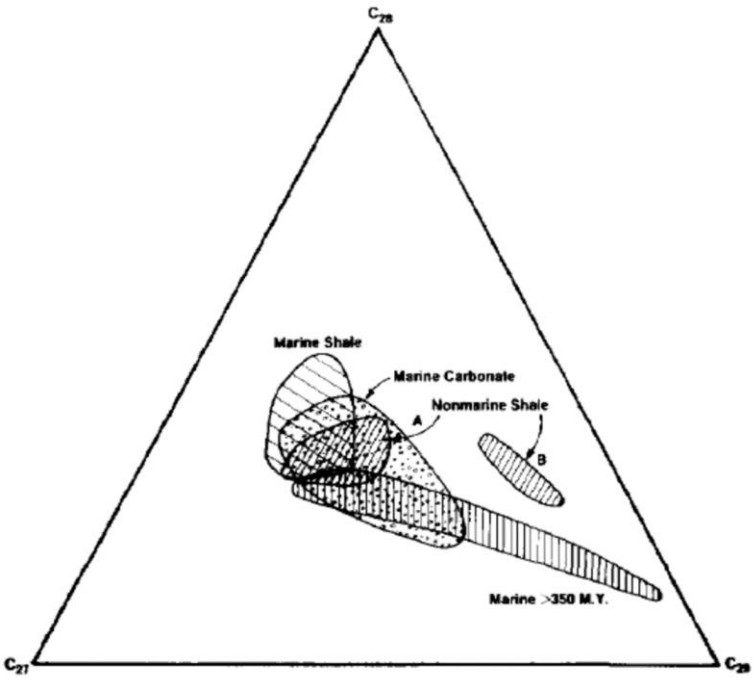

Figure 35. C_{27}-C_{28}-C_{29} regular sterane ternary diagram of oils from known source rocks (Moldowan et al., 1985)

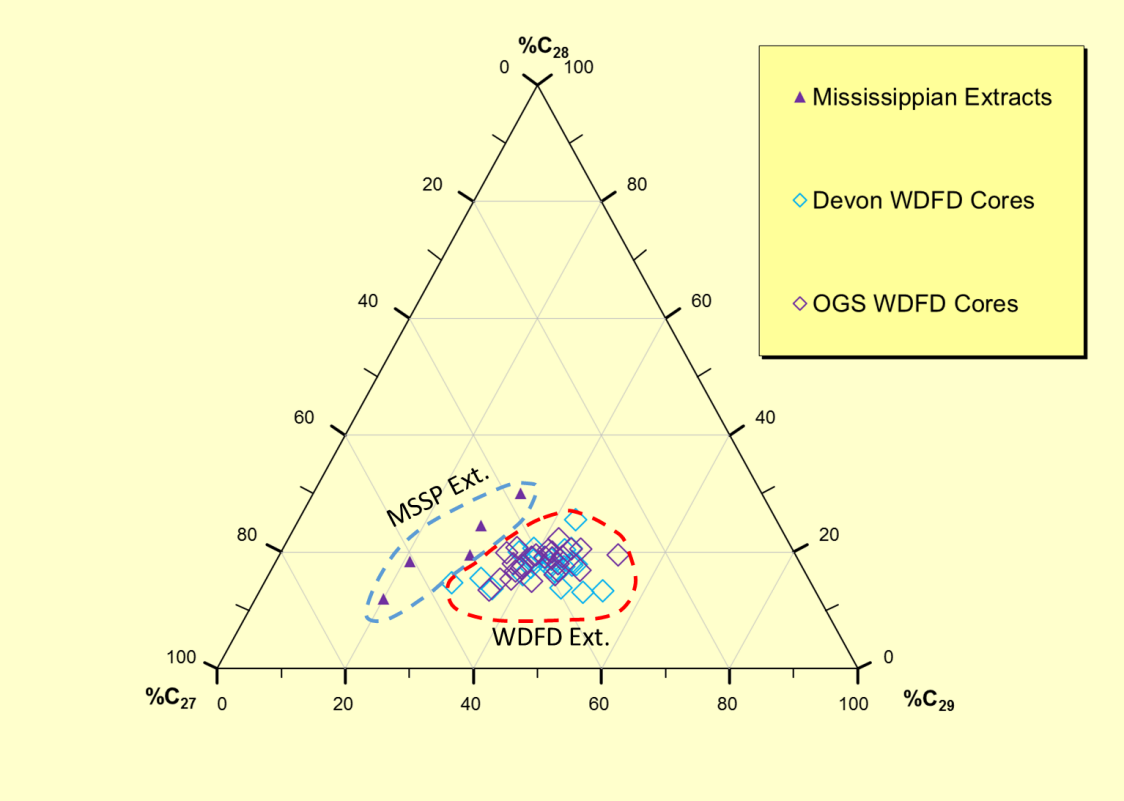

Figure 36. Regular sterane ternary diagram of rock samples using C_{27}, C_{28}, and C_{29} 14α(H), 17α(H) (20R) regular sterane isomers

Another group of steranes used for characterizing marine organic matter source input are the 24-*n*-propylcholestanes. These C_{30} steranes were reported to originate from 24-*n*-propylcholesterols, which are biosynthesized by Chrysophyte, a marine algae of the order *Sarcinochrysidales*, and common in marine invertebrates (Moldowan et al., 1990). As a consequence, C_{30} steranes are specific biomarkers for marine organic matter (Moldowan et al., 1985). C_{30} Steranes were detected in all of the Woodford rock samples analyzed but in variable concentrations.

The internal vertical variation in the Woodford Shale has been discussed by Miceli Romero and Philp (2012). They found AIR (Aryl Isoprenoids Ratio) covaried with Pr/Ph within a core from Wyche Farm Quarry, Southern Oklahoma. Recently Slatt and his Woodford consortium conducted a group of studies of internal Woodford facies variation based on chemostartigraphy (Treanton, 2014; Turner et al., 2015a and b). The current study has attempted to correlate biomarkers variation with chemostratigraphy. The Woodford sub-members subdivision in this study is based on GR log and trace elements concentrations' variation within a regional Woodford chemosequence stratigraphic framework setup by Turner et al. (2015a and b; Figure 19). The Woodford core from Pritchard-1 well has been sampled at 9 depths with an attempt to correlate the biomarker variation with chemostratigraphy. The chemostratigraphic profile of Pritchard-1 Woodford core shows the Upper and Middle Woodford member subdivision and sea level Transgression/Regression (T/R) cyclicity during the Woodford Deposition (Figure 20). Screening the regular sterane based biomarker ratios within the geochemical log, it would be a farfetched attempt to make a correlation between any regular sterane based biomarker ratios' variation and sea level fluctuation (Figure 37). There is not a clear trend

in terms of regular sterane based biomarker ratios' variation changing from Middle Woodford to Lower Woodford probably due to not enough data points being sampled to observe the sea level fluctuations (Figure 37).

The C_{30} sterane index, ratio of $C_{30}/(C_{27}\text{-}C_{30})$ steranes, can be used to investigate marine organic matter input (Molodwan et al., 1985; Peters et al., 1986). Moldowan et al. (1992) found that many oils derived from source rocks deposited under restricted saline to hypersaline lagoonal conditions show lower $C_{30}/(C_{27}\text{-}C_{30})$ steranes than those from open marine systems. Geochemical logs of C_{30} sterane index for the Woodford rock extracts show small variations within the Upper Woodford member (Figure 37) generally pointing to a great marine input in the Upper Woodford Member.

4.2.1.2 Diasteranes (rearranged steranes)

Diasteranes are formed by chemical reduction of diasterenes, which are derived from sterols during diagenesis. This conversion is thought to be catalyzed by acidic sites on clay minerals (Rubinstein et al., 1975), such as montmorillonite or illite, and promoted by acidic (low pH) and oxic (high Eh) conditions in the depositional environment (Moldowan et al., 1986; Moldowan et al., 1991). Therefore, the ratios of diasteranes/steranes are moderately specific for indicating source rock lithology and redox conditions, but are also affected by source rock maturity (Seifert and Moldowan, 1978). At high levels of thermal maturity, rearrangements of steroids to diasterene precursors may become possible, even without clays (van Kaam-Peters et al., 1998). The C_{27} diasterane/C_{27} sterane ratio can help differentiate carbonate and siliciclastic source rocks samples at similar level of thermal maturity (Mello et al., 1988). Low C_{27} diasterane/C_{27} sterane ratios (<0.30) were found to be associated with anoxic clay-poor

or carbonate source rock; whereas high ratios usually indicate clay-rich siliciclastic source rocks. While, this finding is not always true because significant amounts of diasteranes have been reported to be found in some clay-poor carbonate environments (Clark and Philp, 1989), this lithology and redox proxy needs to be used with caution and to be incorporated with other geochemical parameters.

Geochemical logs of C_{27} diasterane/C_{27} sterane for the Woodford Shale samples show lower values of this ratio in the Middle Member, suggesting that this interval has lower clay content relative to the other members (Figure 37). These observations are consistent with the previous findings on the relatively low clay content in the Middle Woodford Member compared to the other members (Bernal, 2013; Molinares Blanco, 2013). Based on the idea of clastics sequence stratigraphy, the Lower Woodford Member was deposited during a transgressive system tract (TST), when the Woodford deposition site was relatively closer to the shoreline, so the Lower Woodford Member has a greater chance to receive clay-rich terrigenous deposits compared to the Middle Woodford Member. It is possible that these clays catalyzed rearrangements of steroids to diasterene precursors.

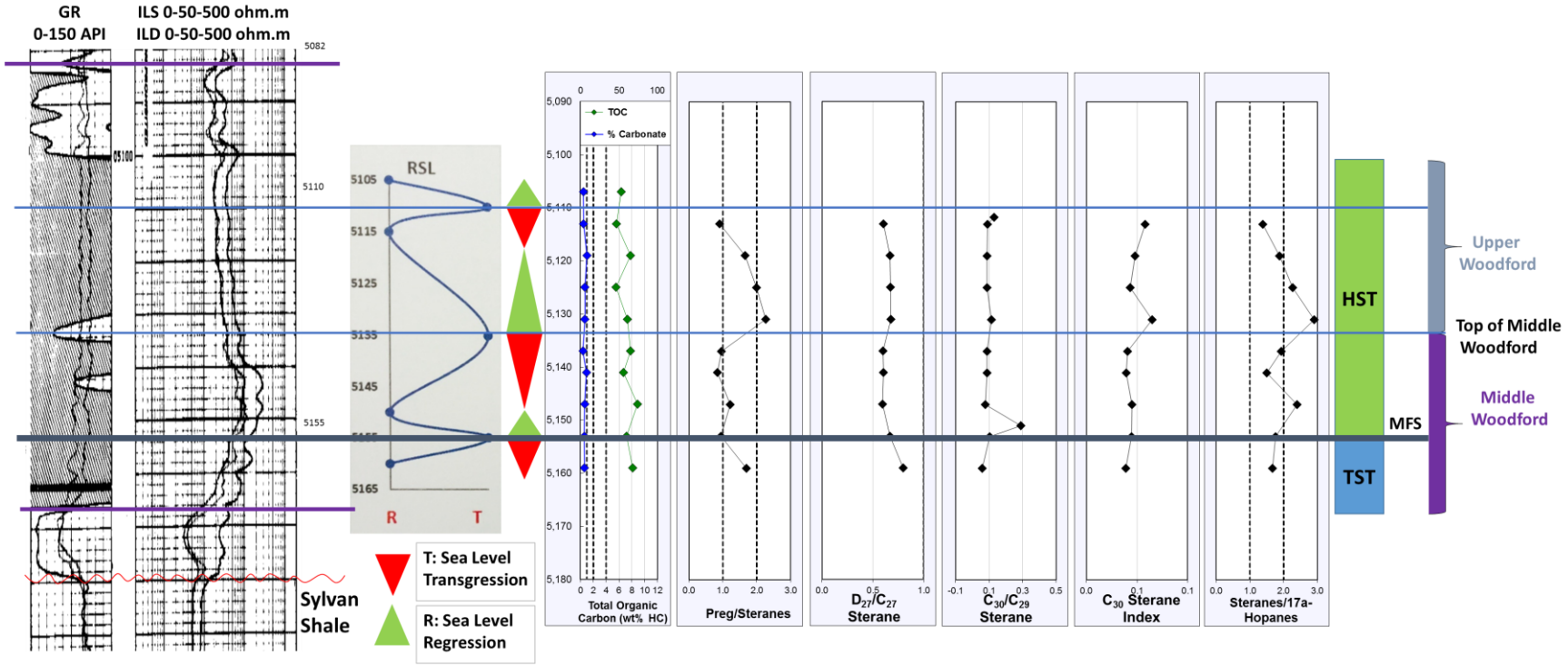

Figure 37. Geochemical logs of steranes ratios for Pritchard-1 Woodford rock samples. Formulas for calculation of ratios are displayed in Appendix A.

4.2.1.3 Pregnanes

Significant amounts of pregnane (C_{20} sterane) and homopregnane (C_{21} sterane) have been detected in bitumen extracted from source rocks deposited in the hypersaline depositional environments (ten Haven et al., 1986). Wang (1993) analyzed rock extracts from the Springer Formation in the Anadarko Basin, Oklahoma and found that pregnanes were more resistant to weathering than regular steranes and diasteranes. Pregnanes can also be produced by degradation of the higher carbon numbered steranes at high maturity levels. Geochemical logs of the pregnane/sterane ratio (Formula for calculation of this ratio is displayed in Appendix A) for the Pritchard-1 well samples show higher pregnane/sterane ratios in the Upper Woodford member, indicating the possibility of hypersaline, anoxic conditions present in the water column during deposition of this unit (Figure 37). Enrichment of pregnane may be attributed to high thermal maturity as reported by Zhang et al. (2014). But in the case of Prichart-1 Woodford samples analyzed, the relatively higher pregnane/sterane ratios associated with the Upper Woodford Member should have nothing to do with high maturity because the Woodford in this well is still immature or at most early mature as discussed in Section 4.1.3. Therefore the higher values for the pregnane/sterane ratio in the Upper Woodford are more likely to represent episodes of higher salinity in the water column during Upper Woodford deposition.

4.2.2 Terpanes (m/z 191)

Terpanes found in petroleum constitute several homologous series of compounds mainly originating from bacterial (prokaryotic) membrane lipids (Ourisson et al., 1982; Alexander, 1983; Tissot and Welte, 1984). Terpane compounds include acyclic, bicyclic,

tricyclic, tetracyclic, and pentacyclic homologous series. Tri-, tetra-, and pentacyclic terpanes were identified in the Woodford Shale rock extracts by analysis of their B&C fractions through SIM/GC-MS of the *m/z* 191.3 ion. Fragmentograms of these compounds are presented in Figure 38 and peak identifications are given in Table 7. Formulas for calculation of geochemical ratios are displayed in Appendix A. Geochemical ratios of terpanes and their relationships with other biomarker groups helped in assessing variations in organic matter source, depositional environment, redox conditions, and thermal maturity for the Woodford Shale rock extracts.

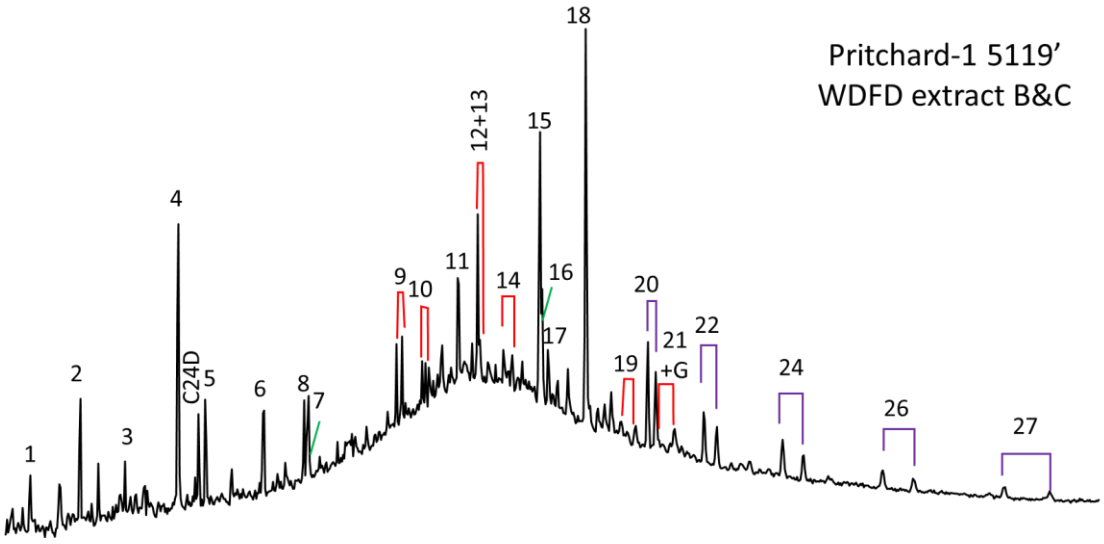

Figure 38. SIM *m/z* 191.3 mass chromatograms showing distributions of terpanes in the B&C fractions of the Pritchard-1 5119 ft Woodford extract. Red brackets denote tricyclic terpane isomers and purple brackets denote homohopane isomers. Peak identification is presented in Table 7.

Table 7. Identification of terpanes in the SIM *m/z* 191.3 mass chromatograms of the B&C fractions

Peak #	Compound
C24D	Deuterated *n*-tetracosane (ISTD)
1	C_{20} Tricyclic terpane (Cheilanthane)
2	C_{21} Tricyclic terpane (Cheilanthane)
3	C_{22} Tricyclic terpane (Cheilanthane)
4	C_{23} Tricyclic terpane (Cheilanthane)

5	C_{24} Tricyclic terpane (Cheilanthane)
6	C_{25} Tricyclic terpanes (Cheilanthanes 22S and 22R)
7	C_{24} Tetracyclic terpane
8	C_{26} Tricyclic terpanes (Cheilanthanes 22S and 22R)
9	C_{28} Tricyclic terpanes (Cheilanthanes 22S and 22R)
10	C_{29} Tricyclic terpanes (Cheilanthanes 22S and 22R)
11	C_{27} 18α(H)-22,29,30-Trisnorneohopane (Ts)
12	C_{30} Tricyclic terpanes (Cheilanthanes 22S and 22R)
13	C_{27} 17α(H)-22,29,30-Trisnorhopane (Tm)
14	C_{31} Tricyclic terpanes (Cheilanthanes 22S and 22R)
15	C_{29} 17α(H),21β(H)-30-Norhopane
16	C_{29}Ts 18α(H)-30-Norneohopane
17	D_{30} 15α-methyl-17α(H)-27-Norhopane (Diahopane)
18	C_{30} 17α(H),21β(H)-Hopane
19	C_{33} Tricyclic terpanes (Cheilanthanes 22S and 22R)
20	C_{31} 17α(H),21β(H)-Homohopanes (22S & 22R)
21	C_{34} Tricyclic terpanes (Cheilanthanes 22S and 22R)
22	C_{32} 17α(H),21β(H)-Bishomohopane (22S & 22R)
23	C_{35} Tricyclic terpanes (Cheilanthanes 22S and 22R)
24	C_{33} 17α(H),21β(H)-Trishomohopane (22S & 22R)
25	C_{36} Tricyclic terpanes (Cheilanthanes 22S and 22R)
26	C_{34} 17α(H),21β(H)-Tetrakishomohopane (22S & 22R)
27	C_{35} 17α(H),21β(H)-Pentakishomohopane (22S & 22R)
28	C_{38} Tricyclic terpanes (Cheilanthanes 22S and 22R)
29	C_{39} Tricyclic terpanes (Cheilanthanes 22S and 22R)
G	Gammacerane

4.2.2.1 Tricyclic terpanes

Since there were probably different biological precursors for tricyclic terpanes less than C_{30} and those greater than C_{30}, according to Wang (1993) and Kim (1999), in this study tricyclic terpane series would be discussed as tricyclic terpanes ($<C_{30}$) and extended tricyclic terpanes respectively ($> C_{30}$). Tricyclic terpanes (cheilanthanes) are thought to be derived from algae and bacterial precursors (Aquino Neto et al., 1981;

Ourisson et al., 1982; Volkman et al., 1989). However, high concentrations of tricyclic terpanes and their aromatic analogs were found in Tasmanites-rich rocks, suggesting the Tasmanites algae as the origin for tricyclic terpanes (Volkman et al., 1989; Azevedo et al., 1992; Simoneit et al., 1993). Philp and Gilbert (1986) identified significant amounts of tricyclic terpanes in marine oils. Moreover, high amounts of C_{19} and C_{20} tricyclic terpanes were reported to be associated with lacustrine saline and marine carbonate environments (Mello et al., 1988). Compared to the hopanes, tricyclic terpanes are highly resistant to thermal maturation and biodegradation. For that reason, these compounds are widely used in source rock characterization, thermal maturity assessment, and oil-to-source rock correlations (Zumberge, 1987). Ratios of tricyclics/17α-hopanes and C_{23} tricyclic/C_{30} hopane have been widely used to differentiate organic matter type by comparing bacterial and/or algal input (tricyclic terpanes) versus prokaryotic contribution (hopanes) in source rock extracts and oils (Waples and Machihara, 1990). SIM m/z 191.3 mass chromatograms show distributions of tricyclic terpanes in the B&C fractions of the Mississippian and Woodford rock extracts in this study (Figure 39). The Woodford rock extracts show higher C_{23} tricyclic/C_{30} hopane ratios in the Middle Woodford Member Shale (Figure 40), indicating a greater marine organic matter input during deposition of this unit, as previously discussed in section 4.2.1.

Biomarker ratios based on tricyclic terpanes are also helpful in investigating depositional environments and differentiating source rock lithology. For example, the C_{22}/C_{21} and the C_{24}/C_{23} tricyclic terpane ratios favor in the identification of rock extracts and oils generated from carbonate source rocks. Rock extracts and oils derived from carbonate source rocks typically show high C_{22}/C_{21} and low C_{24}/C_{23} tricyclic terpane

ratios, while marine shale source rocks show low C_{22}/C_{21} (0.20-0.50) and high C_{24}/C_{23} (0.50-1.00) tricyclic terpanes (J.E. Zumberge, 2000, personal communication in Peters et al., 2005, p. 558). A plot of C_{22}/C_{21} versus C_{24}/C_{23} tricyclic terpane ratios for source rock extracts from the Woodford Shale was shown in Figure 41. From this graph it is suggested that most of these samples are derived from marine shales, with exception of a few Pritchard-1 rock extracts, which are falling in the region of carbonate source rocks.

In this study, the tricyclic terpanes with carbon numbers greater than C_{30} are defined as extended tricyclic terpanes. Their origin is still controversial (Wang, 1993; Kim, 1999; Dutta et al., 2006). The unusually abundant distribution of extended tricyclic terpanes has been reported as one of the most distinct characteristics of Mississippian source rock extracts and Mississippian-sourced oils in Oklahoma (Wang, 1993; Kim, 1999). Kim (1999) preferred to believe the relative abundance of extended tricyclic terpanes ($>C_{30}$) over homohopanes (C_{31}~C_{35}) appeared to be associated with several events of algal bloom during the deposition of Lower Mississippian Limestone (Kim, 1999). The precursors of the tricyclic terpanes were previously thought to be present in *Tasmanites*. But the tricyclic terpanes associated with the *Tasmanites* are tricyclic terpanes containing the carbon number up to C_{30} (Volkman et al., 1989; Azevedo et al., 1992; Simoneit et al., 1993). The extended tricyclic terpanes ($>C_{30}$) may be derived from different organisms than hopanes or tricyclic terpanes ($<C_{30}$) (Wang, 1993; Kim, 1999). The biological precursors for extended tricyclic terpanes ($>C_{30}$) appeared to be related to archaebacterial or algal lipids, whereas specific prokaryotes (primitive organisms) are the major source for sedimentary hopanoids (Peters & Moldowan, 1991).

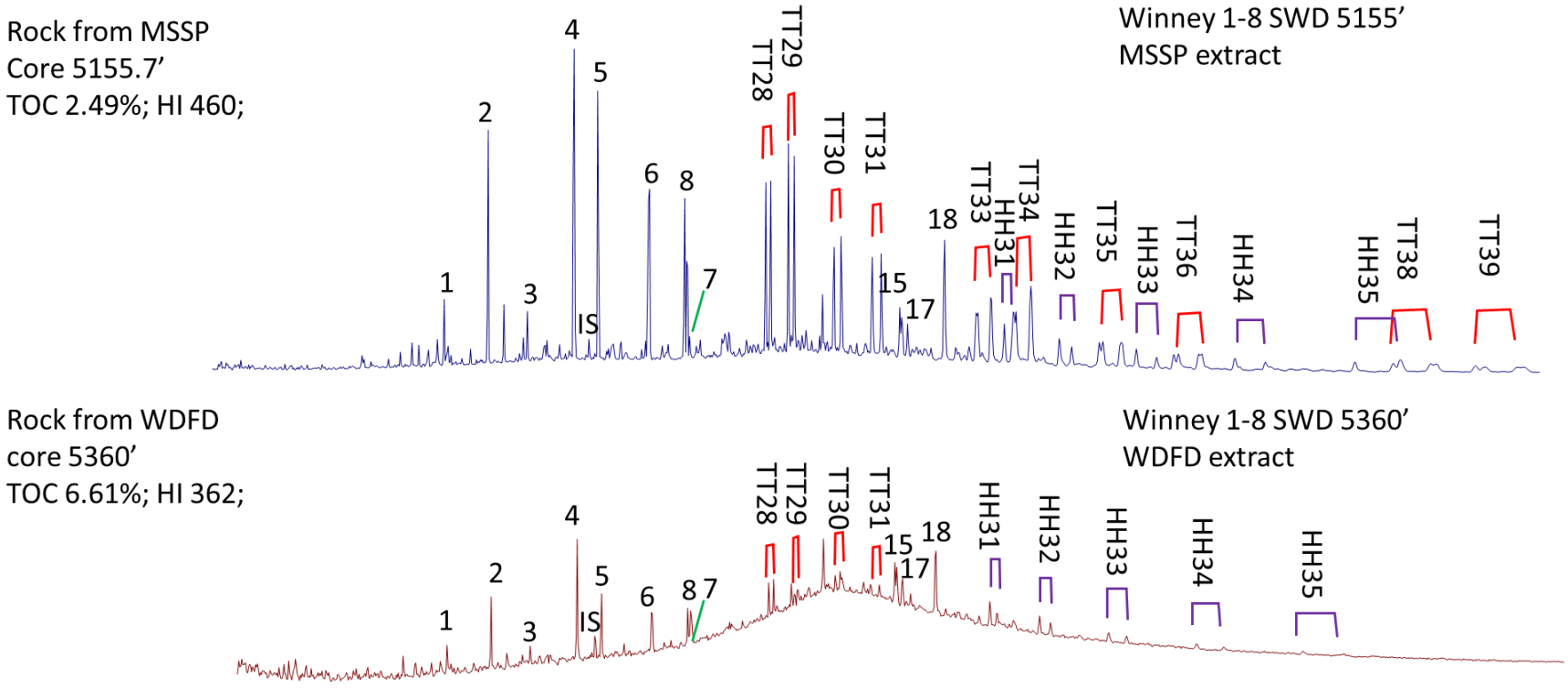

Figure 39. SIM *m/z* 191.3 mass chromatograms showing distributions of tricyclic terpanes in the B&C fractions of the Mississippian and Woodford rock extracts. Red brackets denote tricyclic terpane isomers (TT = Tricyclic Terpane) and purple brackets denote homohopane isomers (HH = Homohopane) (IS: Internal Standard). Peak identification is presented in Table 7.

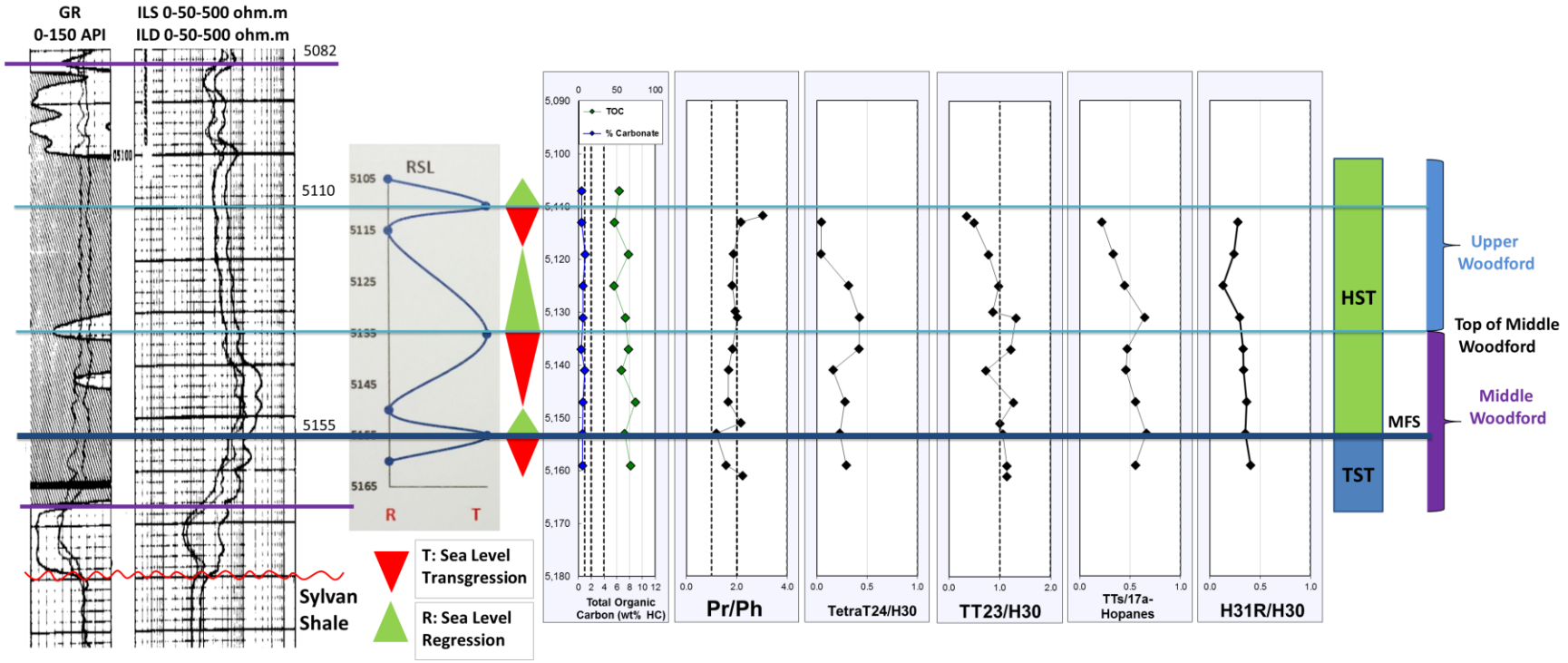

Figure 40. Geochemical logs of biomarker ratios of terpanes for Pritchard-1 Woodford samples. Formulas for calculation of ratios are displayed in Appendix A.

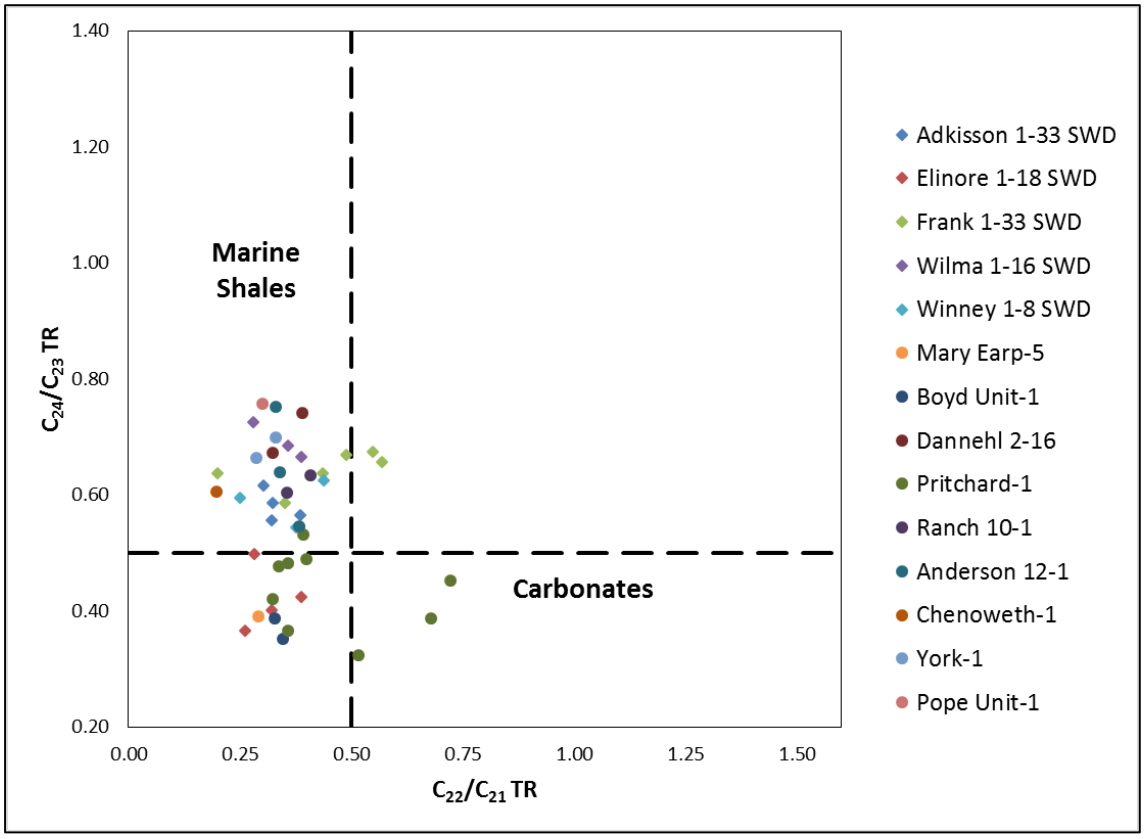

Figure 41. Plot of C_{22}/C_{21} versus C_{24}/C_{23} tricyclic terpanes shows source rock depositional environments for Woodford Shale rock extracts (Dotted lines are used as a guide. Plot template from Peters et al., 2005)

The SIM m/z 191.3 mass chromatograms of two rock extracts are shown in Figure 39, namely Winney 1-8 SWD 5155 ft Mississippian Limestone and 5360 ft Woodford Shale from the same well. From the SIM m/z 191.3 mass chromatograms of the Mississippian rock extract, several characteristics need to be documented: 1) extended tricyclic terpanes (TT33 ~ TT39) dominate over homohopanes (H31 ~ H35) (Appendix G); 2) very abundant tricyclic terpanes (TT28~TT31) (Appendix G). These characteristics are consistent with those previously observed for the Mississippian rocks in Oklahoma by Wang (1993) and Kim (1999).

4.2.2.2 Tetracyclic terpanes

The exact biological origin of tetracyclic terpanes was controversial (Trendel et al., 1982; Aquino Neto et al., 1983; Connan et al., 1986; Clark and Philp, 1989) until Grice et al. (2001) performed the CSIA (compound specific isotope analysis) on C_{24} tetracyclic terpane. What she found is that the stable carbon isotopic composition of the C_{24} tetracyclic terpane is consistant among torbanites from boghead coals, suggesting an origin from hopanoids or terrigenous precursors. Therefore it has been well accepted tetracyclic terpanes derive from hopanes or precursor hopanoids by thermal or microbial cracking. Many publications stated these compounds are more resistant to thermal maturity and biodegradation compared to hopanes (Aquino Neto et al., 1983; Palacas et al., 1984; Connan et al., 1986; Clark and Philp, 1989; Grice et al., 2001). Tetracyclic terpanes range from C_{24} to C_{27} with tentative evidence for its homologs up to C_{35}, where the C_{24} homolog has a widespread occurrence (Aquino Neto et al., 1983). Abundant C_{24} tetracyclic terpanes were believed to be indicative of carbonate and evaporite depositional environments (Palacas et al., 1984; Clark and Philp, 1989). However, this compound was found to be overwhelmingly present compared to the C_{19}~C_{29} tricyclic terpanes in the crude oil samples from the Gippsland Basin (Australia) and was incorrectly believed to originate from terrigenous organic matter (Philp and Gilbert, 1986). Generally, the C_{24} tetracyclic terpane is commonly found, but not that abundant, in most marine oils generated by mudstone to carbonate source rocks (Peters et al., 2005).

In this study, the C_{24} tetracyclic terpane was identified in all of the analyzed rock extracts and oils, and the C_{24} tetracyclic terpane/C_{30} hopane ratio showed small variations within the different Woodford members (Figure 40). Because of the deep marine

depositional environment of the Woodford Shale it is unlikely that the presence of the C_{24} tetracyclic terpane be related to a significant higher plant input. It is possible that these variations are more dependent on lithology than organic facies variations. Significant amounts of C_{24} tetracyclic terpane was reported to be associated with the siliciclastic facies of La Luna Formation (Rangel et al., 2000). A correlation between C_{24} tetracyclic terpane/ C_{30} hopane ratio and C_{27} diasteranes/C_{27} steranes was observed in the Upper and Middle Woodford Member (Figure 37 and Figure 40), suggesting that in this case, the presence of C_{24} tetracyclic terpane may be dependent on clastic input.

4.2.2.3 Pentacyclic terpanes (Hopanes)

Hopanes are pentacyclic terpanes (Van Dorsselacer et al., 1977) that originate from hopanoids present in prokaryotes (bacteria and cyanobacteria) and higher plants but appear to be absent in eukaryotic algae (Ourisson et al., 1979). Bacteria are the major source for sedimentary hopanoids and hence hopanes are found to be ubiquitous in rock extracts and oils worldwide (Peters and Moldowan, 1991). The 17α(H)-norhopane (H29) and the 17α(H)-hopane (H30) are usually the prominent peaks in the *m/z* 191 GC/MS trace and these biomarkers have been used as potential source rock depositional environmental indicators (Waples and Machihara, 1991). All of the Woodford Shale samples analyzed have H29/H30 hopane ratio values lower than 1.0 (Appendix E). When plotted against the $C_{35}S/C_{34}S$ hopanes ratio, the plot of H29/H30 vs. $C_{35}S/C_{34}S$ hopanes can help identify source facies of oils and extracts (Figure 42). According to Peters et al. (J.E. Zumberge, 2000, personal communication in Peters et al., 2005, p. 571), the majority of oils and rock extracts generated from marine carbonates have high $C_{35}S/C_{34}S$ and H29/H30 ratios (>0.8 and >0.6 respectively). Even though this relationship is not clear in

the studied samples (Figure 42), this plot suggests most of the Woodford Shale rock samples are of marine origin.

The C_{31} 22R/C_{30} hopane ratio (31R/30H) is applied to differentiate source rocks of marine versus lacustrine origin. C_{31} 22R/C_{30} hopane ratios greater than 0.25 are associated with marine shale, carbonate, and marl source rocks (p. 569 in Peters et al., 2005; originally from J.E. Zumberge, personal communication, 2000 in Peters et al., 2005). Geochemical logs of this ratio for the Woodford Shale extracts (Figure 40) do not show much variation between the different members. Combination of this ratio with the C_{26}/C_{25} tricyclic terpane ratio, which helps distinguishing marine (0.50-1.40) from lacustrine source rocks (>1.0 J.E. Zumberge, personal communication, 2000 in Peters et al., 2005), the plot of C_{26}/C_{25} tricyclic terpane versus C_{31}R/C_{30} hopane suggests the majority of samples have a marine origin (Figure 43).

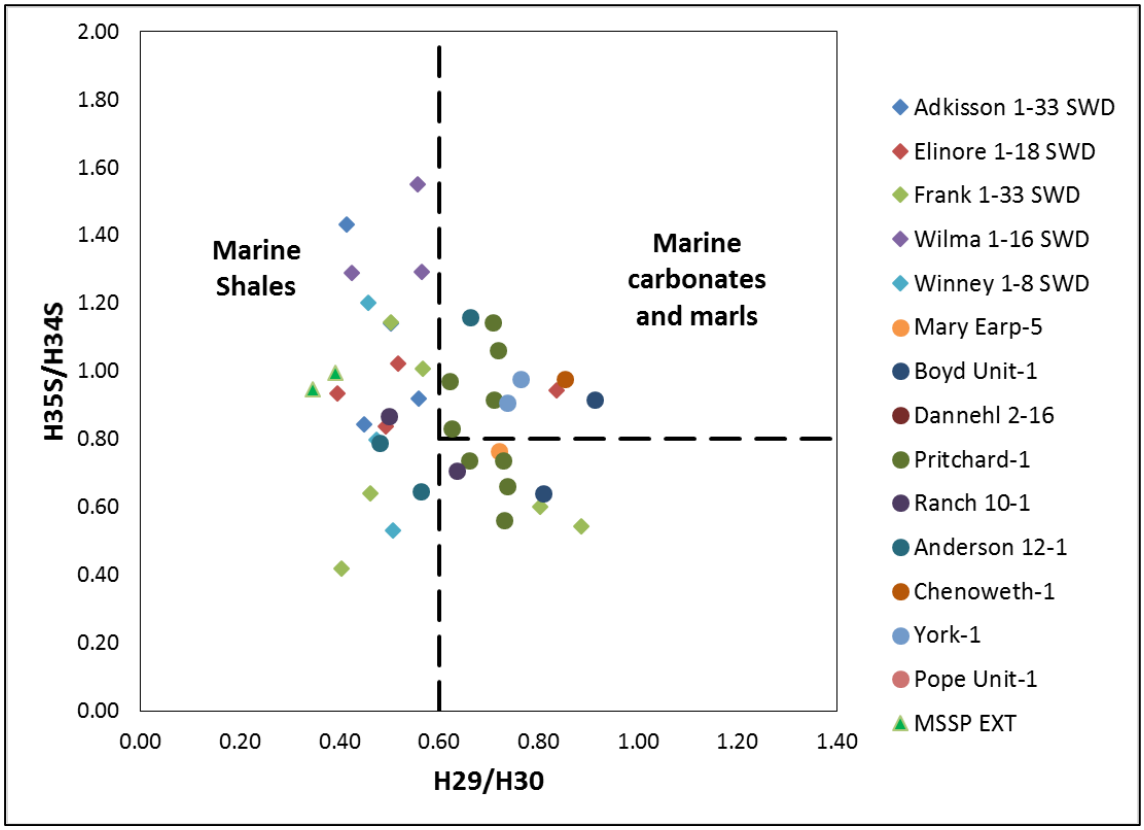

Figure 42. Plot of $C_{35}S/C_{34}S$ homohopanes (H35S/H34S) versus 30-Nor/C_{30} hopane (H29/H30) suggest most of the Woodford Shale rock samples are of marine origin (Dotted lines are used as a guide and do not represent fixed fields on the diagram. Plot template from Peters et al. 2005)

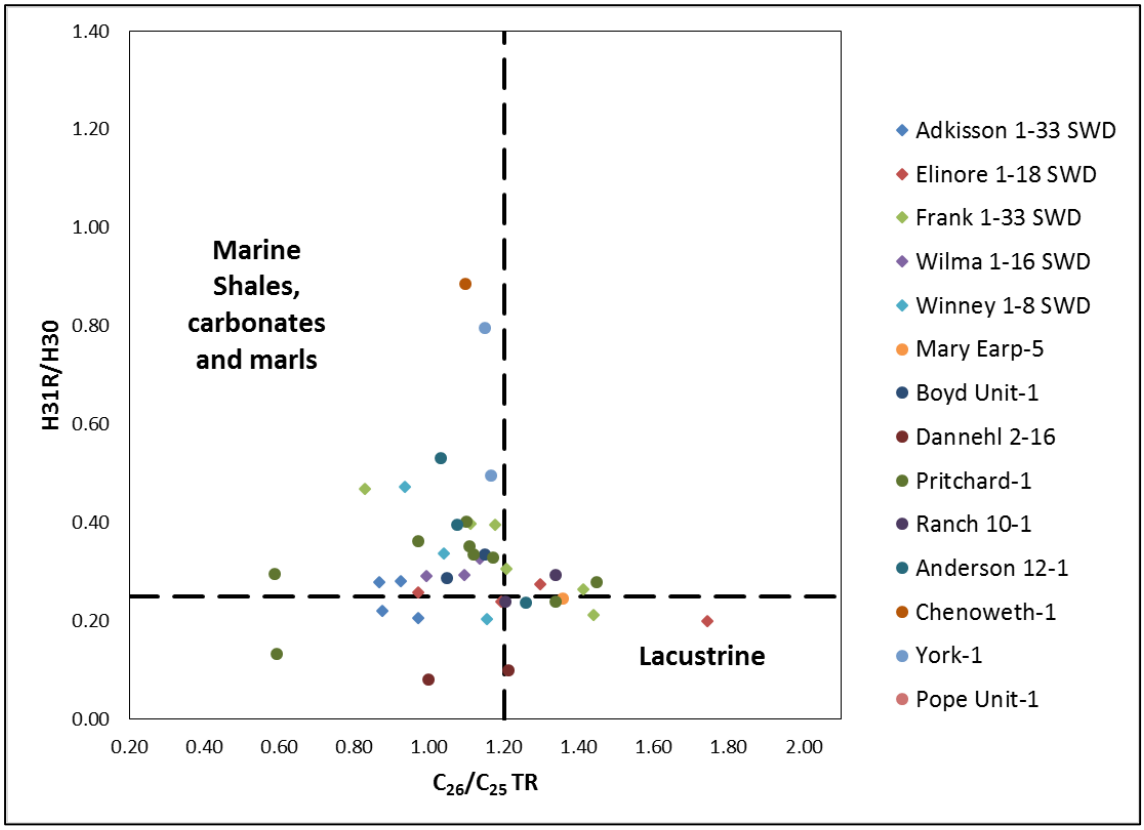

Figure 43. Plot of C_{26}/C_{25} Tricyclic Terpane versus C31R/C30 Hopane shows that the Woodford Shale rock extract are mainly of marine origin (Dotted lines are used as a guide. Plot template from Peters et al., 2005)

Distribution patterns of the extended hopanes or homohopanes (C_{31}-C_{35}) have been widely used to infer redox conditions during source rock deposition. These compounds were thought to be derived from bacteriohopanetetrol or other C_{35} hopanoids (Peters and Moldowan, 1991; Waples and Machihara, 1991). Similar homohopane distribution patterns suggest, but do not prove, a genetic relationship among oil samples. The C_{35} homohopane index, also expressed as C_{35}/C_{34} homohopanes ratios or $C_{35}S/C_{34}S$ hopanes, could be used as an indicator of redox potential in marine sediments during diagenesis. Many published papers suggest high C_{35} homohopanes were indicative of marine carbonates or evaporites (Boon et al, 1983; Connan et al., 1986; Fu Jiamo et al.,

1986; Clark and Philp, 1989). However, many other studies prefer to believe high C_{35}/C_{34} homohopanes ratios are interpreted to be associated with highly reducing (low Eh) marine conditions during deposition (Peters and Moldowan, 1991) due to preferential preservation of the C_{35} homolog (Peters and Moldowan, 1991; Moldowan et al., 1992).

Plots of homohopane distributions for the Elinore 1-18 SWD rock samples analyzed (Figure 44) do not show C_{35} homohopane predominance in any of the Woodford samples. Mississippian Limestone sample (4453 ft) from Elinore 1-18 SWD shows C_{35} homohopane predominance over C_{34}. This finding is consistent with the observation that high C_{35}/C_{34} homohopanes ratios are generally related to marine carbonates source rocks, like the same homohopane distribution pattern found in the Eagle Ford Shale (Miceli Romero, 2014), which is a well-known carbonate source rock in South Texas. Therefore in this study, the C_{35} homohopane predominance is not only associated with anoxic conditions but also the source rock lithology.

Gammacerane, a C_{30} triterpane, was tentatively identified in all the Woodford Shale samples analyzed (Figure 38) but coeluted with C_{34} 22(R)-tricyclic terpanes (Cheilanthanes 22R) in most of the samples. Although the origin of gammacerane is still uncertain, this compound may be formed by reduction of tetrahymanol during diagenesis (ten Haven et al., 1989). The precursor of tetrahymanol was reported to be associated with *Tetrahymena*, a fresh water ciliated protozoan (ten Haven et al., 1989). Consequently, gammacerane is used as a specific biomarker for water-column stratification and hypersaline conditions in marine and non-marine environments (Sinninghe Damsté et al., 1995). The occurrence of gammacerane in the Woodford Shale samples suggests that regional hypersaline conditions and water stratification may have

developed during deposition of these sediments. This observation positively correlated with the low Pr/Ph ratios (section 4.1.4.2) and the predominance of the ββ steranes over the αα steranes (Appendix D), which were reported to be associated with hypersalinity (ten Haven et al., 1988).

4.2.2.4 Diahopanes

The chemical structure of 17α-diahopanes suggests they are probably rearranged products from 17α-hopanes (Corbett and Smith, 1969). It was reported the C_{30} 17α-diahopanes in oil samples may be related to bacterial hopanoid precursors that have undergone oxidation in the D-ring and rearrangement by clay-mediated acidic catalysis (Corbett and Smith, 1969; Moldowan et al., 1991). Many terrigenous source rocks were deposited under oxic to suboxic conditions and are clay-rich. Therefore, it has been widely accepted that 17α-diahopanes originated from bacterial input to sediments containing clays deposited under oxic to suboxic conditions (Volkman et al., 1983). This interpretation is also consistent with the type of highly terrigenous oils found in the Gippsland Basin (Philp and Gilbert, 1986). Therefore the 17α-diahopane/17α-hopane ratio has been widely used as an oxic-suboxic/clay-rich depositional environmental indicator.

A composite map of the Woodford Shale Structure (in SSTVD: Subsea Total Vertical Depth) in Central Oklahoma with average 17α-diahopane/hopane ratios of Woodford cores is shown in Figure 45. These data points could be divided into two groups: Group-A, six wells far from the paleo-Nemaha Uplift, including Elinore 1-18

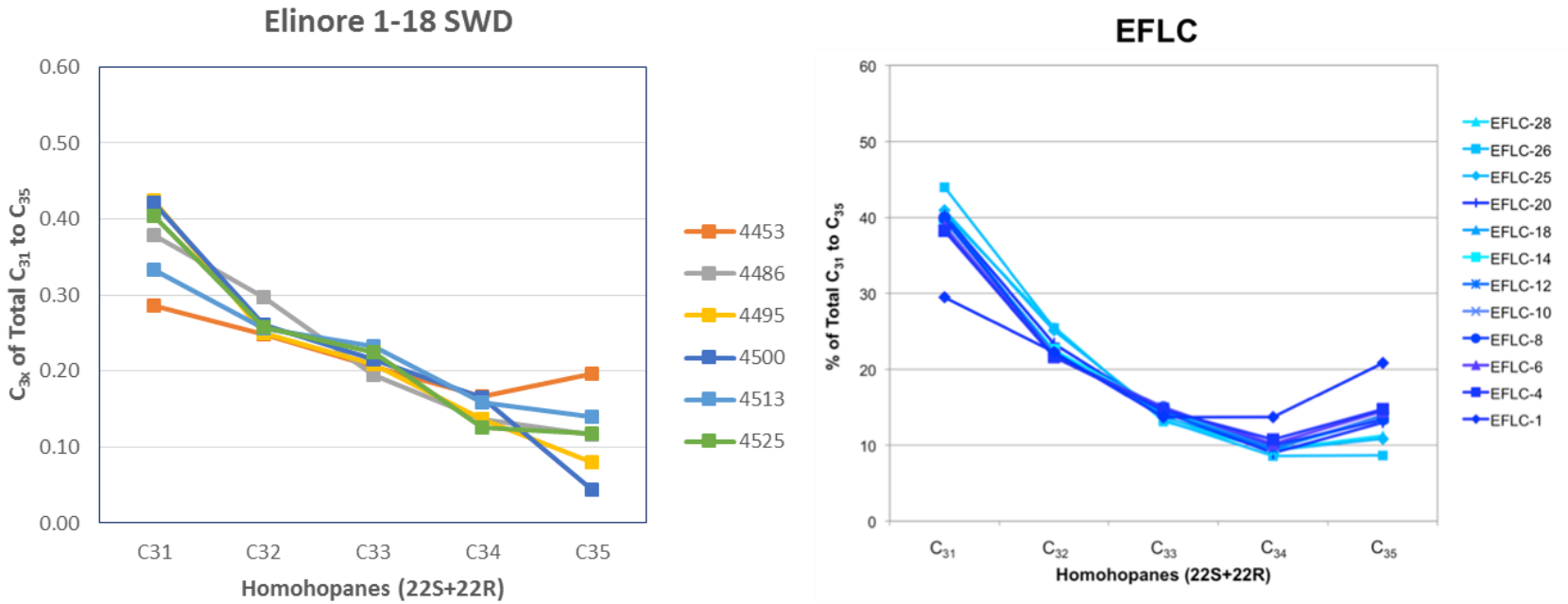

Figure 44. Homohopanes distributions for Woodford rock extracts from Elinore 1-18 SWD well compared with that from the Eagle Ford Shale (Miceli Romero, 2014)

SWD, Mary Earp-5, Pritchard-1, Boyd-1, Roberson Ranch 10-1, and Dannehl 2-16, with a diahopane/hopane ratio below 0.40; and Group-B, the other eight wells closer to the paleo-Nemaha Uplift with a diahopane/hopane ratio greater than 0.40. It would be geologically reasonable to interpret the relatively higher diahopane/hopane ratios from the wells in Group-B to result from the relatively greater amounts of clay-rich terrigenous sources shed from the paleo-Nemaha Uplift into the Woodford deposits at that time. Alternatively, in addition to the clay content necessary to catalyze the acidic arrangements, thermal energy, most probably from the Woodford subsidence, is also a significant control on the transformation. The two wells, Pope Unit-1 and York-1, which were closer to the paleo-Nemaha Uplift and buried deeper towards the Anadarko Basin, have both enough clay source and thermal energy to experience more extensive rearrangement to form diahopanes.

4.2.3 Aryl Isoprenoids and Isorenieratane related compounds (m/z 133+134)

Isorenieratane and many mono-, di-, tri-, and tetra-aromatic compounds originate from the C_{40} diaromatic carotenoid hydrocarbon isorenieratene in green and purple sulfur bacteria in marine sedimentary environments (Grice et al., 1996; Brocks and Summons, 2013). Green sulfur bacteria (GSB) are anoxygenic phototrophs that fix carbon dioxide using the reverse tricarboxylic acid cycle (TCA), leading to biomass that is enriched in ^{13}C (Koopmans et al., 1996a and 1996b). Thus, when ^{13}C-rich isorenieratane and related compounds occur in rock extracts or crude oils, they indicate photic zone anoxia (PZA) during source rock deposition (Summons and Powell, 1987; Clifford et al., 1997).

Aryl isoprenoids found in the source rocks have been reported to originate from *Chlorobiaceae* (green sulfur bacteria) growing under photic zone anoxia (PZA) condition

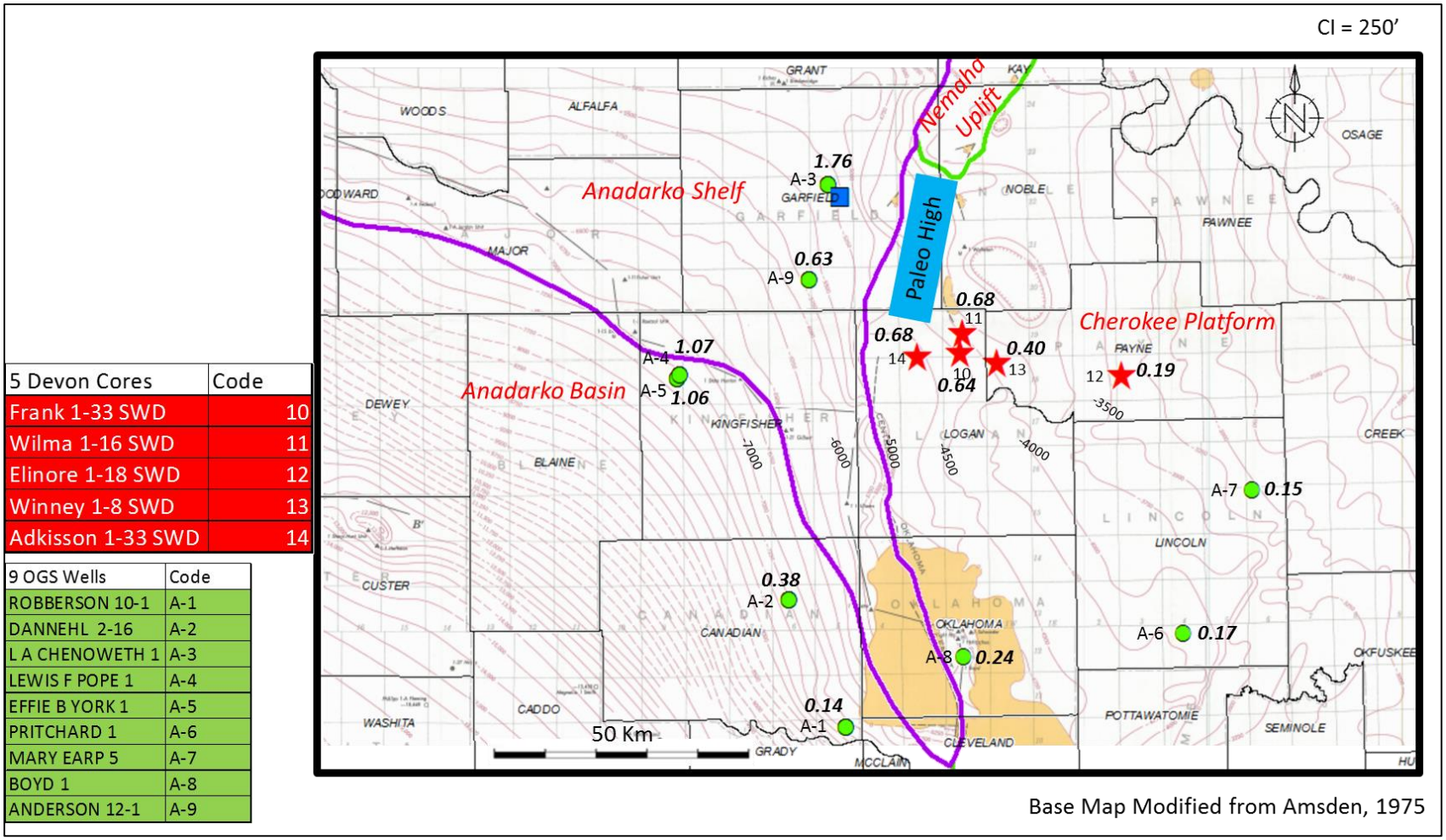

5 Devon Cores	Code
Frank 1-33 SWD	10
Wilma 1-16 SWD	11
Elinore 1-18 SWD	12
Winney 1-8 SWD	13
Adkisson 1-33 SWD	14

9 OGS Wells	Code
ROBBERSON 10-1	A-1
DANNEHL 2-16	A-2
L A CHENOWETH 1	A-3
LEWIS F POPE 1	A-4
EFFIE B YORK 1	A-5
PRITCHARD 1	A-6
MARY EARP 5	A-7
BOYD 1	A-8
ANDERSON 12-1	A-9

Figure 45. Composite map of the Woodford Shale Structure (in SSTVD) in Central Oklahoma with C_{30} 17α-Diahopane/Hopane ratios of the Woodford cores in this study (SSTVD = Sub Sea Total Vertical Depth in feet; Devon condensates not shown due to this ratio couldn't be measured)

(Summons and Powell, 1987; Clark and Philp, 1989; Requejo et al., 1992; Hartgers et al., 1994; Grice et al., 1997; Brown and Kenig, 2004; Schwark and Frimmel, 2004; Miceli Romero and Philp, 2012). *Chlorobiaceae* undergoes photosynthesis within light-penetrating, H_2S-saturated, anoxic waters. Therefore, aryl isoprenoids are good indicators for photic-zone anoxia (PZA), and can be used as a geochemical parameter in paleoenvironmental studies.

Analysis of aryl isoprenoids was performed on the B&C fractions of rock extracts and oils by SIM/GC-MS using ions *m/z* 133.1 and 134.1 (Figure 46). Identification of these compounds was achieved by comparison with reference mass chromatograms published by Brown and Kenig (2004); Schwark and Frimmel (2004); Miceli Romero and Philp (2012). Because of the long acyclic substituent, aryl isoprenoids tend to elute into the saturate fraction, although these compounds have an aromatic ring in their structure (Brown and Kenig, 2004). The compounds identified from the rock extracts in this study included a series of C_{13}-C_{31} aryl isoprenoids. The 2,3,6-trimethyl substituted aryl isoprenoids (*m/z* = 133) were the most abundant in all of the samples, with the 3,4,5-trimethyl isomers (*m/z* = 134) present in lower concentrations. Possible variability of PZA in the Woodford Shale could be characterized by using the aryl isoprenoid ratio (AIR; Appendix A). Schwark and Frimmel (2004) introduced this ratio by analyzing the ratio of the proportions of the short-chain (C_{13}-C_{17}) versus intermediate-chain (C_{18}-C_{22}) aryl isoprenoids. High AIR (3.0) ratios are thought to be associated with episodic PZA, which leads to degradation of the long- and intermediate-chain aryl isoprenoids. Conversely, low AIR (0.5) indicates persistent PZA, which results in preservation of the long-chain aryl isoprenoids (Schwark and Frimmel, 2004).

Most of the samples show AIR greater than 1 or close to 1 suggesting that the Woodford Shale experienced episodic periods of PZA, where shifts of the chemocline occurred periodically but at relatively lower frequency. However, the origin of aryl isoprenoids are still controversial. Koopmans et al. (1996) determined aryl isoprenoids could also have at least two precursors, isorenieratene or β-isorenieratene in *Chlorobiaceae* and β-isorenieratene in the ubiquitous β-carotene. Only if the 2,3,6 trimethyl-substituted aryl isoprenoids are enriched in $\delta^{13}C$, they are indicative of PZA. In the present study, the $\delta^{13}C$ values for the aryl isoprenoids were not determined. Nevertheless, geochemical logs of AIR for the Woodford Shale samples show a positive correlation with Pr/Ph and RSL (relative sea level) change (Figure 47), and aryl isoprenoids were used to tentatively evaluate variations and degree of PZA as a result of sea level fluctuation. As sea level transgressed, both the corresponding Pr/Ph ratio and AIR decreased, which may indicate persistent PZA occurred during the sea level transgressional tract; as sea level regressed, both the corresponding Pr/Ph ratio and AIR increased, indicating episodic PZA (Figure 47).

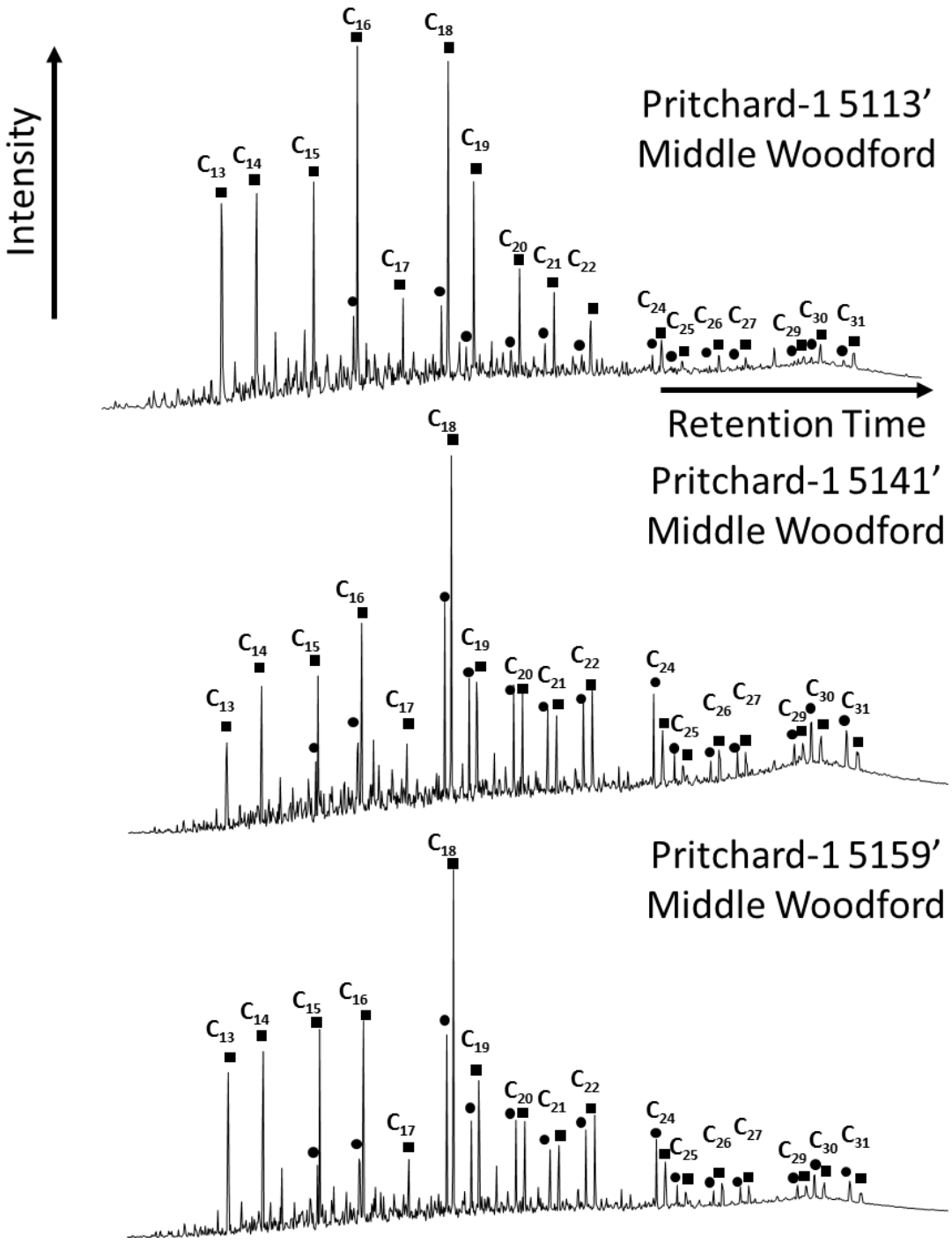

Figure 46. Summed mass chromatograms of *m/z* 133, 134 of the B&C fractions showing the aryl isoprenoids distributions of the Pritchard-1 well Woodford samples (filled squares = 2,3,6-trimethyl substituted aryl isoprenoids, filled circles = 3,4,5- trimethyl substituted aryl isoprenoids. Number of carbon atoms is indicated above each peak)

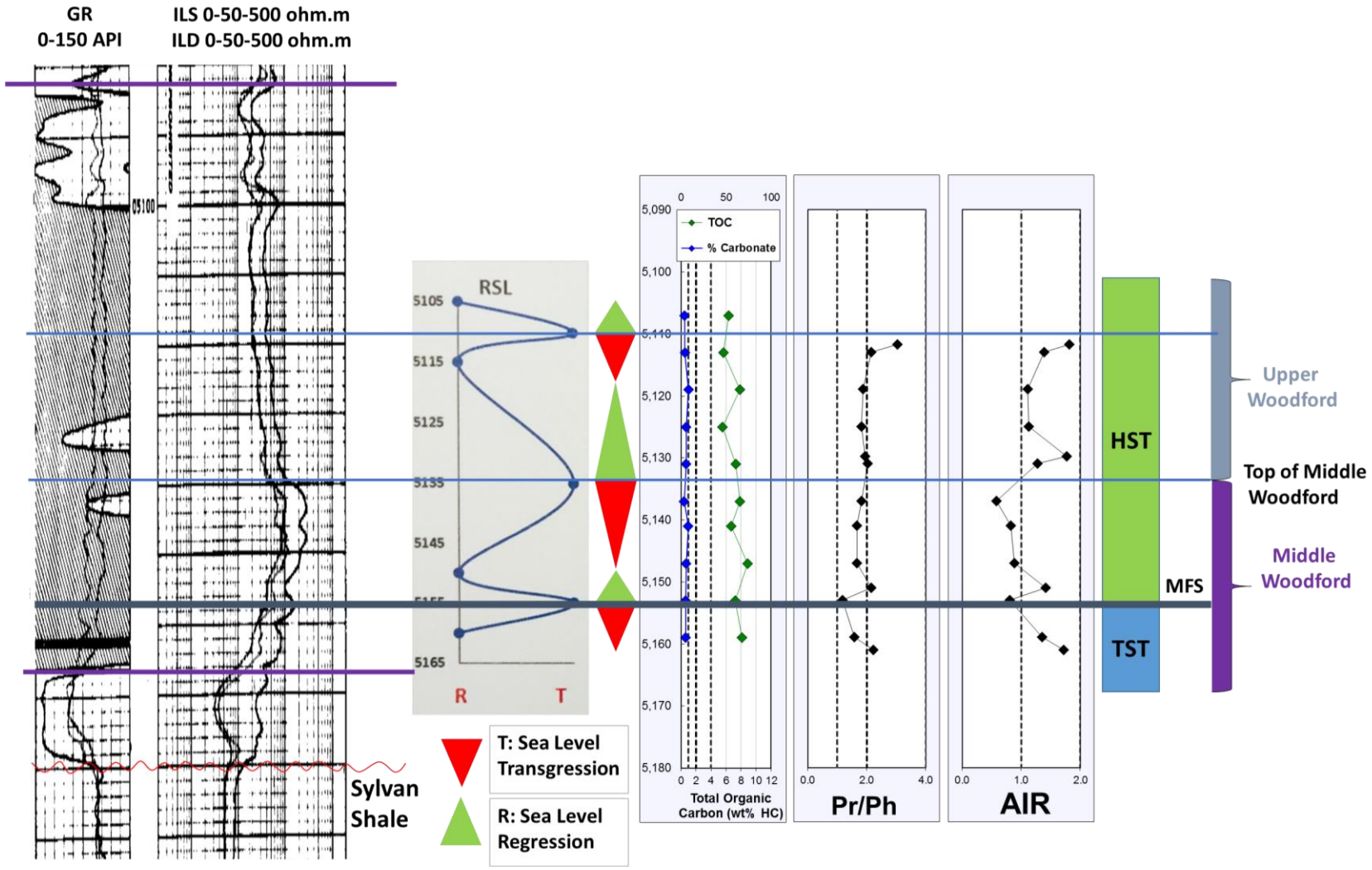

Figure 47. Geochemical logs of aryl isoprenoids ratio for Woodford Shale extracts from Pritchard-1 well.

Isorenieratanes and paleorenieratane, whose detection needed high-temperature GCMS conditions (started at 40ºC with 1.5 minutes hold time and was later increased to 320ºC at a rate of 4ºC per minute and then held constant for 34 minutes for a total run time of 105 minutes), were identified in the aromatic fractions of selected oil samples and rock extracts. Analysis of paleorenieratanes and isorenieratanes was performed on the aromatic fractions of the oils by SIM/GC-MS using the ion *m/z* 134.1 (Figure 48). Identification of these compounds was achieved by comparison with reference mass chromatograms published by Brown and Kenig (2004); Schwark and Frimmel (2004); Miceli Romero and Philp (2012); and Connock (2015). Paleorenieratanes and isorenieratanes were found either in Woodford extracts or Mississippian extracts (Figure 48), which suggests paleorenieratanes and isorenieratanes are not source-specific only for the Woodford Shale but PZA may occur not only during the deposition of the Woodford Shale but also the Mississippian Limestone as well.

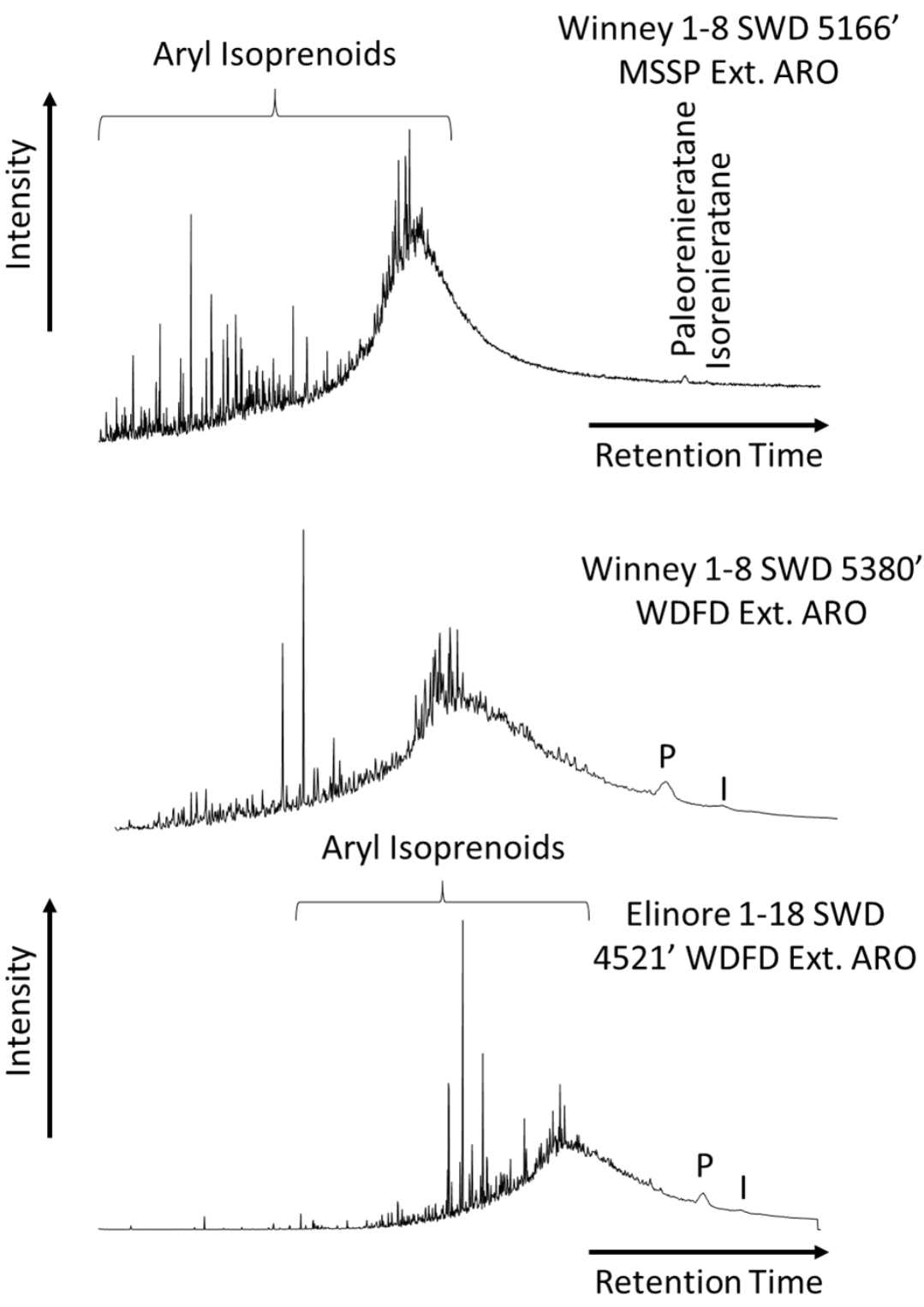

Figure 48. Mass chromatograms of *m/z* 134 of the aromatic fractions showing the paleorenieratane and isorenieratane related compounds distributions of the rock extracts in this study (P = Paleorenieratane; I = Isorenieratane)

4.3 Evaluation of Thermal Maturity

4.3.1 Steranes (m/z 217)

Biological precursors of steranes, which are sterols in living organisms, only have the R configuration at C-20. The R isomer gradually converted to a mixture of R (biological product) and S (thermal product) during source rock thermal maturation. The sterane isomerization ratio, reported as the C_{29} 20S/(20S+20R) sterane ratio provides a useful tool for thermal maturity assessment. The C_{29} 20S/(20S+20R) sterane ratio increases from 0 to about 0.5 with increasing thermal maturity, and reached equilibrium at 0.52 to 0.55 (Seifert and Moldowan, 1986). This ratio is not recommended for use within the oil window but is more specific for immature to early mature stages. Moreover, organic facies variation and secondary alteration, such as weathering and biodegradation, may also influence this maturity parameter. Another maturity proxy based on sterane ratios, the C_{29} ββ/(ββ+αα) sterane ratio, does not have this problem. Furthermore, its equilibrium would be reached at higher maturity levels compared to the C_{29} 20S/(20S+20R) sterane ratio. With increasing thermal stress, the C_{29} ββ/(ββ+αα) ratio would increase from near-zero to about 0.7 with equilibrium being reached at about 0.67 to 0.71. Correlation between the C_{29} ββ/(ββ+αα) and C_{29} 20S/(20S+20R) sterane ratios are commonly used to assess thermal maturity of oils and rock extracts (Figure 49; Seifert and Moldowan, 1986). From the cross plot (Figure 49), there is not a good correlation between these two maturity parameters in this study area. The data points are for the most part separated due to difference in the C_{29} ββ/(ββ+αα) ratio rather than C_{29} 20S/(20S+20R) sterane ratios. One interpretation is that organic facies change may affect the C_{29} 20S/(20S+20R) sterane ratios, which mask the true maturity variations. After plotting the C_{29} ββ/(ββ+αα) sterane ratios on the map, a geological reasonable interpretation is apparent.

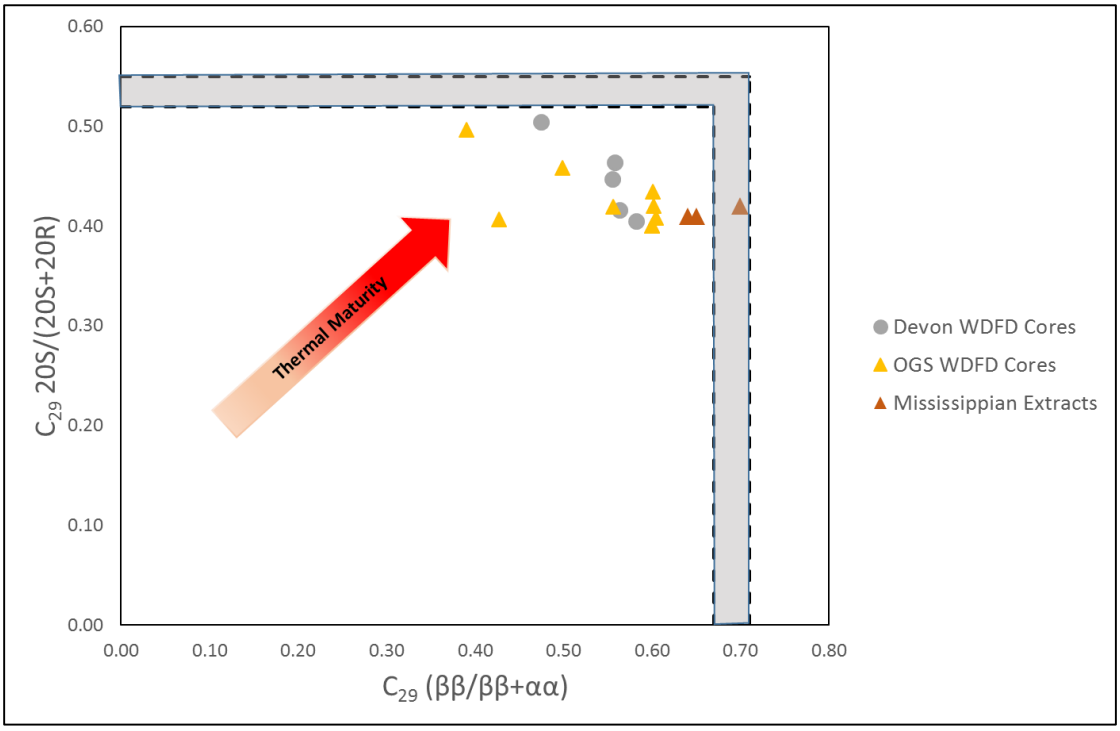

Figure 49. Plot of C_{29} 20S/(20S+20R) steranes versus C_{29} ββ/(ββ+αα) steranes showing variations in thermal maturity for the Woodford Shale source rocks and liquids (Gray area represents end points of isomerization. Plot template from Peters, 1999)

The composite map of the Woodford Shale Structure (in SSTVD: Sub Sea Total Vertical Depth in feet) in Central Oklahoma with HI values and C_{29} ββ/(ββ+αα) steranes ratios (Figure 50) divides the samples into three groups: the Woodford Shale in four wells, including Elinore 1-18 SWD, Mary Earp-5, Pritchard-1 and Boyd-1, which are located in the eastern-most region of the study area, are less mature than the others based on their C_{29} ββ/(ββ+αα) steranes ratio (0.44) and their HI values. Among the other ten wells, the Woodford samples in the four Devon wells located besides the Nemaha Uplift have an intermediate C_{29} ββ/(ββ+αα) sterane ratio of 0.56, and those Woodford samples in the western most five OGS wells have the relatively highest C_{29} ββ/(ββ+αα) sterane ratio of 0.58. Generally, C_{29} ββ/ (ββ+αα) sterane ratio increases as the Woodford burial depth increases, which suggests the Woodford structure is the primary control on maturity. The vitrinite reflectance (VRo) values

measured from the Woodford cores also support this conclusion as discussed in section 4.1.3. The Woodford Shale in the studied wells show the relatively highest Ro values (0.82-0.86% Ro) on the Anadarko Shelf west of the Nemaha Uplift, medium Ro values (0.75-0.78% Ro) on the Cherokee Platform right besides east of the Nemaha Uplift, and show the lowest Ro values (0.48-0.59% Ro) on the Cherokee Platform, east of the Nemaha Uplift, consistent with the C_{29} ββ/ (ββ+αα) sterane ratios. The Anadarko Shelf and the Cherokee Platform is separated by the Nemaha Uplift Zone. The Woodford in these two structural provinces may have gone through different thermal histories. There may not be 1:1 correlation between Ro value and the C_{29} ββ/(ββ+αα) sterane ratio for the Woodford samples in the study area, But it shows a general trend of the C_{29} ββ/(ββ+αα) sterane ratios covarying with the measured vitrinite reflectance.

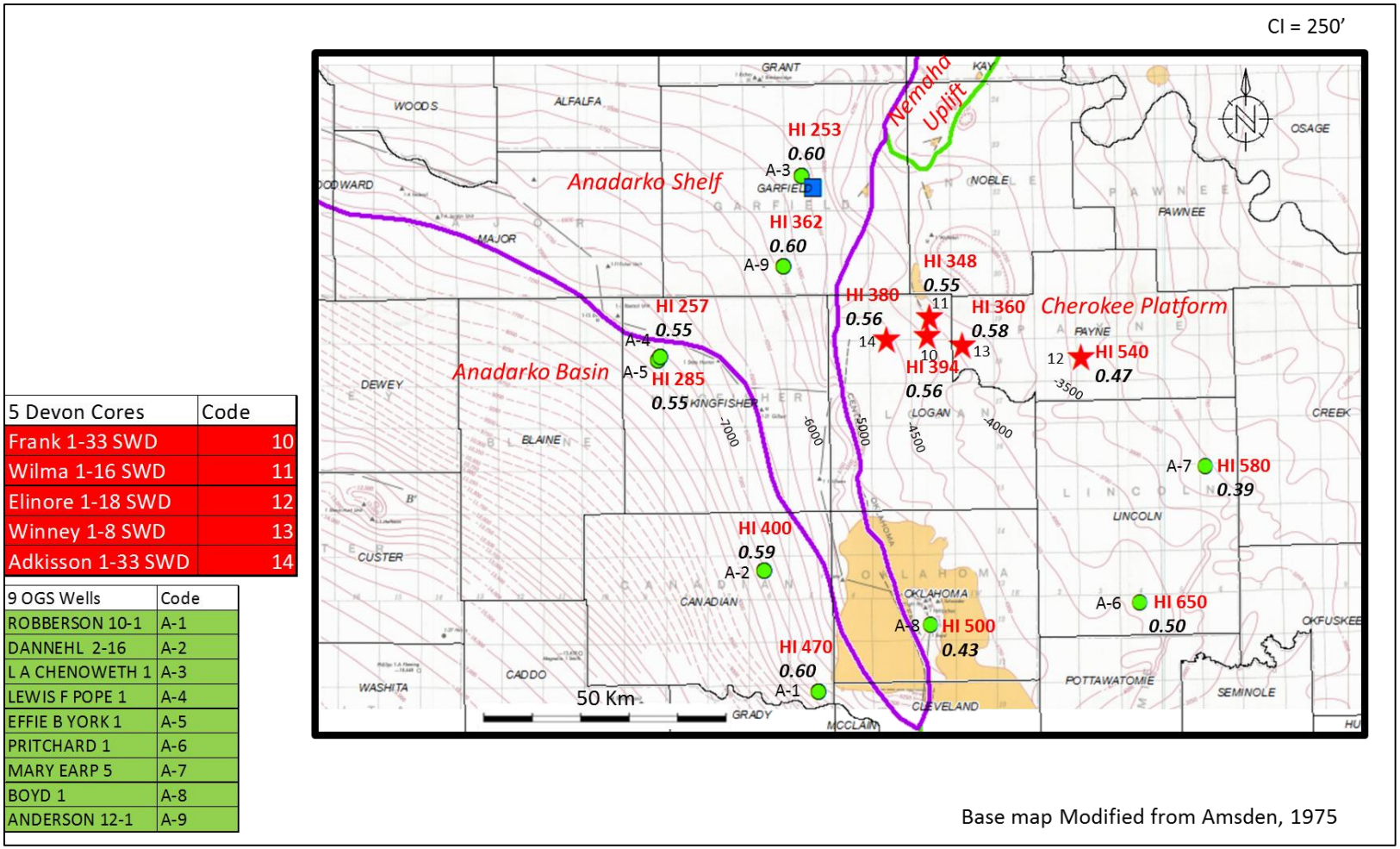

5 Devon Cores	Code
Frank 1-33 SWD	10
Wilma 1-16 SWD	11
Elinore 1-18 SWD	12
Winney 1-8 SWD	13
Adkisson 1-33 SWD	14

9 OGS Wells	Code
ROBBERSON 10-1	A-1
DANNEHL 2-16	A-2
L A CHENOWETH 1	A-3
LEWIS F POPE 1	A-4
EFFIE B YORK 1	A-5
PRITCHARD 1	A-6
MARY EARP 5	A-7
BOYD 1	A-8
ANDERSON 12-1	A-9

Figure 50. Composite map of the Woodford Shale Structure (in SSTVD) in Central Oklahoma with HI values and C_{29} ββ/(ββ+αα) sterane ratios showing variations in thermal maturity for the Woodford Shale source rocks (SSTVD = Sub Sea Total Vertical Depth in feet; CI = Contour Increment in feet)

Table 8. Average sterane isomerization ratios for the Woodford Shale rock extracts and liquids (ND = not determined; *not averaged)

Sample	# of samples	C_{29} 20S/(20S+20R)	C_{29} ββ/(ββ+αα)
Adkisson 1-33 SWD	6	0.46	0.56
Elinore 1-18 SWD	7	0.50	0.48
Frank 1-33 SWD	9	0.42	0.56
Wilma 1-16 SWD	5	0.45	0.56
Winney 1-8 SWD	5	0.40	0.58
Mary Earp-5	2	0.50	0.39
Boyd Unit-1	2	0.41	0.43
Dannehl 2-16	3	0.40	0.60
Pritchard-1	9	0.46	0.50
Roberson Ranch 10-1	2	0.41	0.60
Anderson 12-1	3	0.42	0.60
Chenoweth-1	1	0.43	0.60
York-1	2	0.42	0.56
Pope Unit-1	1	0.40	0.60
Adkisson 1-33H	*	0.46	0.67
Smith 1-14H	*	0.43	0.64
Winney 1-8H	*	0.40	0.64
Elinore 1-18H	*	0.43	0.53
Johnson 1-33H	*	0.48	0.63
Smith 1-23MH	*	0.48	0.66
Wilma 1-16SWD	*	0.39	0.62
Winney 1-5H	*	0.41	0.65
Matthews 1-33H	*	0.40	0.67
Williams 1-24 WH	*	0.44	0.69
Peach 1-19 MH	*	0.41	0.65
Joyce 1-32 WH	*	0.46	0.56
Hopfer 1-20 WH	*	0.45	0.67
Peach 1-20 WH	*	0.45	0.68
C. Matthews 1-8 WH	*	0.46	0.64
Ford-1	*	0.42	0.56
Thomas James 1-22	*	0.44	0.60
Anadarko Taylor 2118	*	0.48	0.61

A	*	0.47	0.62
Ellis Lewis Jet	*	0.43	0.60
F	*	0.44	0.61
7-5N-5E	*	0.40	0.57

4.3.2 Terpanes (m/z 191)

4.3.2.1 Hopanes

The C_{32} 22S/(22S+22R) ratio is a maturity parameter based on the change in epimer ratios of the C_{32} 17α(H)-homohopanes during source rock thermal maturation. The biological configuration of the homohopane precursor is the 22R and during the early stages of source rock maturation, isomerization at the C-22 position gradually converted the C_{32} homohopanes to a mixture of 22R and 22S epimers (Peters and Moldowan, 1991). The 22S/(22S+22R) ratio increases from 0 to equilibrium ratios of approximately 0.57 to 0.62 (early oil window) with no additional thermal maturity information being available after equilibrium is reached. Almost all of the Woodford Shale samples (Figure 51) show their 22S/(22S+22R) ratios in the range of 0.53-0.59 (Table 9) to be approaching to the equilibrium range in the early oil window. From the other biomarker maturity proxies and maturity indicators, it is reasonable to infer the samples' maturity in this study have all entered the early oil window.

Table 9. Average C_{32} 22S/(22S+22R) hopane ratios for the Woodford Shale rock extracts and the studied oils (*not averaged)

Sample	# of samples	C_{32} 22S/(22S+22R)
Adkisson 1-33 SWD	6	0.53
Elinore 1-18 SWD	7	0.55
Frank 1-33 SWD	9	0.56
Wilma 1-16 SWD	5	0.53
Winney 1-8 SWD	5	0.55

Mary Earp-5	2	0.55
Boyd Unit-1	2	0.59
Dannehl 2-16	3	0.56
Pritchard-1	9	0.55
Roberson Ranch 10-1	2	0.57
Anderson 12-1	3	0.59
Chenoweth-1	1	0.56
York-1	2	0.53
Pope Unit-1	1	ND
Adkisson 1-33H	*	0.61
Smith 1-14H	*	0.56
Winney 1-8H	*	0.57
Elinore 1-18H	*	0.59
Johnson 1-33H	*	0.64
Smith 1-23MH	*	0.63
Wilma 1-16SWD	*	0.61
Winney 1-5H	*	0.69
Matthews 1-33H	*	0.59
Elinore 1-17H	*	0.61
Peach 1-19 MH	*	0.56
Joyce 1-32 WH	*	0.59
Hopfer 1-20 WH	*	0.62
Peach 1-20 WH	*	0.56
C. Matthews 1-8 WH	*	0.62
Ford-1	*	0.60
Thomas James 1-22	*	0.60
Anadarko Taylor 2118	*	0.60
A	*	0.54
Ellis Lewis Jet	*	0.58
F	*	0.59
7-5N-5E	*	0.59

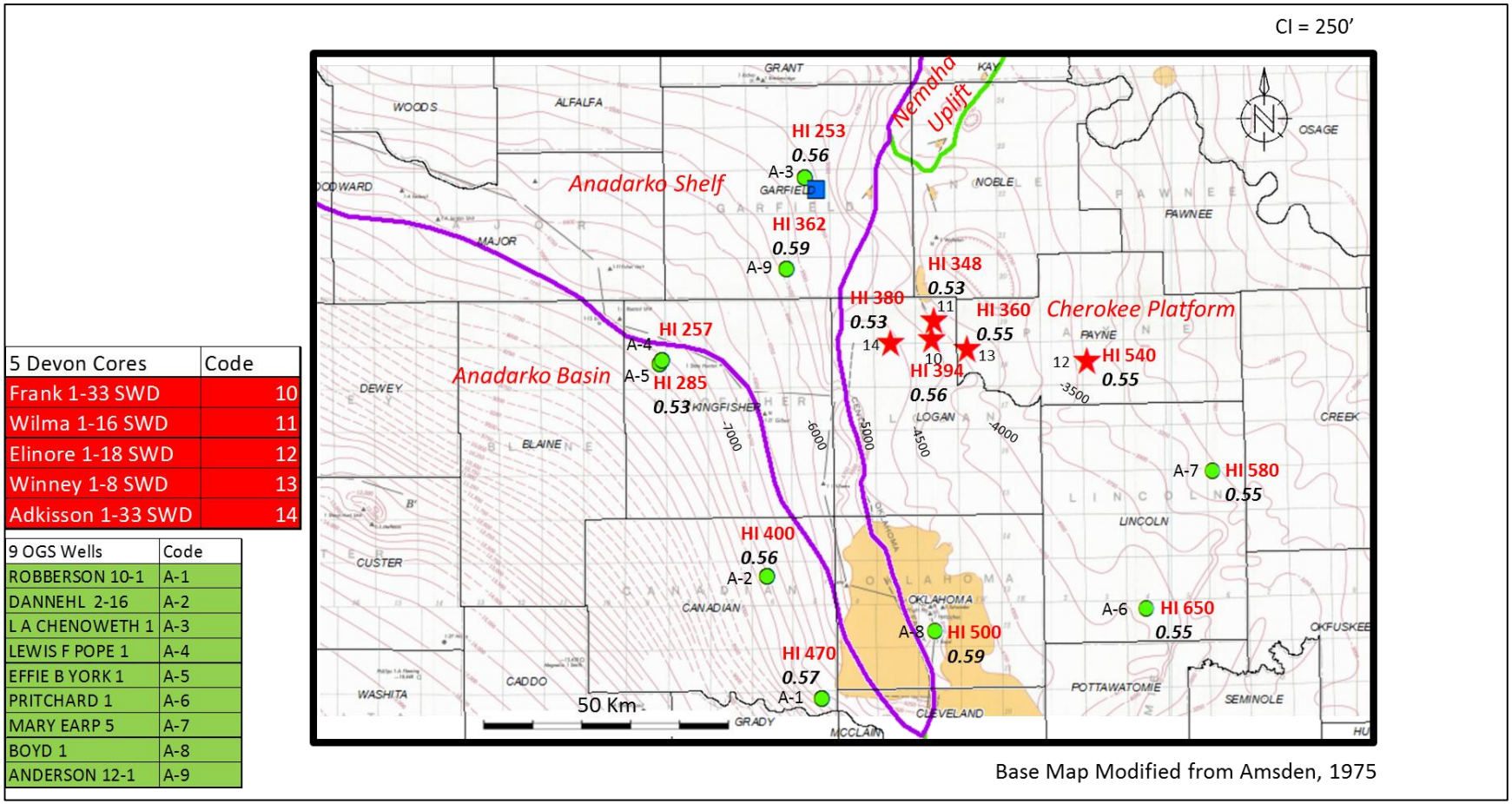

5 Devon Cores	Code
Frank 1-33 SWD	10
Wilma 1-16 SWD	11
Elinore 1-18 SWD	12
Winney 1-8 SWD	13
Adkisson 1-33 SWD	14

9 OGS Wells	Code
ROBBERSON 10-1	A-1
DANNEHL 2-16	A-2
L A CHENOWETH 1	A-3
LEWIS F POPE 1	A-4
EFFIE B YORK 1	A-5
PRITCHARD 1	A-6
MARY EARP 5	A-7
BOYD 1	A-8
ANDERSON 12-1	A-9

Figure 51. Composite map of the Woodford Shale Structure (in SSTVD) in Central Oklahoma with HI values and C_{32} 22S/(22S+22R) hopane ratios showing thermal maturity of the Woodford Shale source rocks (SSTVD = Sub Sea Total Vertical Depth in feet; CI = Contour Increment in feet; HI = Hydrogen Index; Devon condensates not shown due to this ratio couldn't be measured)

The abundance of hopanes in *m/z* 191 trace could be used as a crude thermal maturity proxy for the Woodford rock extract as well. Regular hopanes have been found to be depleted compared to other terpane compounds in extracts of the Woodford Shale by several published papers (Jones, 1989; Wang, 1993; Kim, 1999). The hopane depletion in the Woodford extracts was thought to be associated with the types of source materials, which are living organisms that contain abundant long-chain lipids that yield large amounts of normal alkanes and aromatics but contain low concentrations of terpane or sterane precursors (Wang, 1993). Immature Woodford outcrop samples (Miceli Romero, 2012) and early mature subsurface Woodford cores in this study (for example, Mary Earp-5, Pritchard-1 and Elinore 1-18 SWD) contain more abundant regular hopanes than mature Woodford cores (Table 10). Screening a series of Woodford rock extracts of different thermal maturity (Figure 52; Table 10), the preliminary conclusion based on the variation in terms of the absolute concentration of terpanes of the Woodford core extracts with different thermal maturity is that the regular hopanes (H29 ~ H35) have been thermally degraded during source rock maturation (Figure 52). The data sets of this study provided a good chance to investigate relative concentration changes with thermal maturation of the regular hopanes (Figure 52). It suggests the relative proportion of regular hopanes (H29 ~ H35) versus tricyclic terpanes (TT23 ~ TT29) decreases as maturity increases since tricyclic terpanes are known to be more thermal resistant than the regular hopanes (Aquino Neto et al., 1983; Peters et al., 1990).

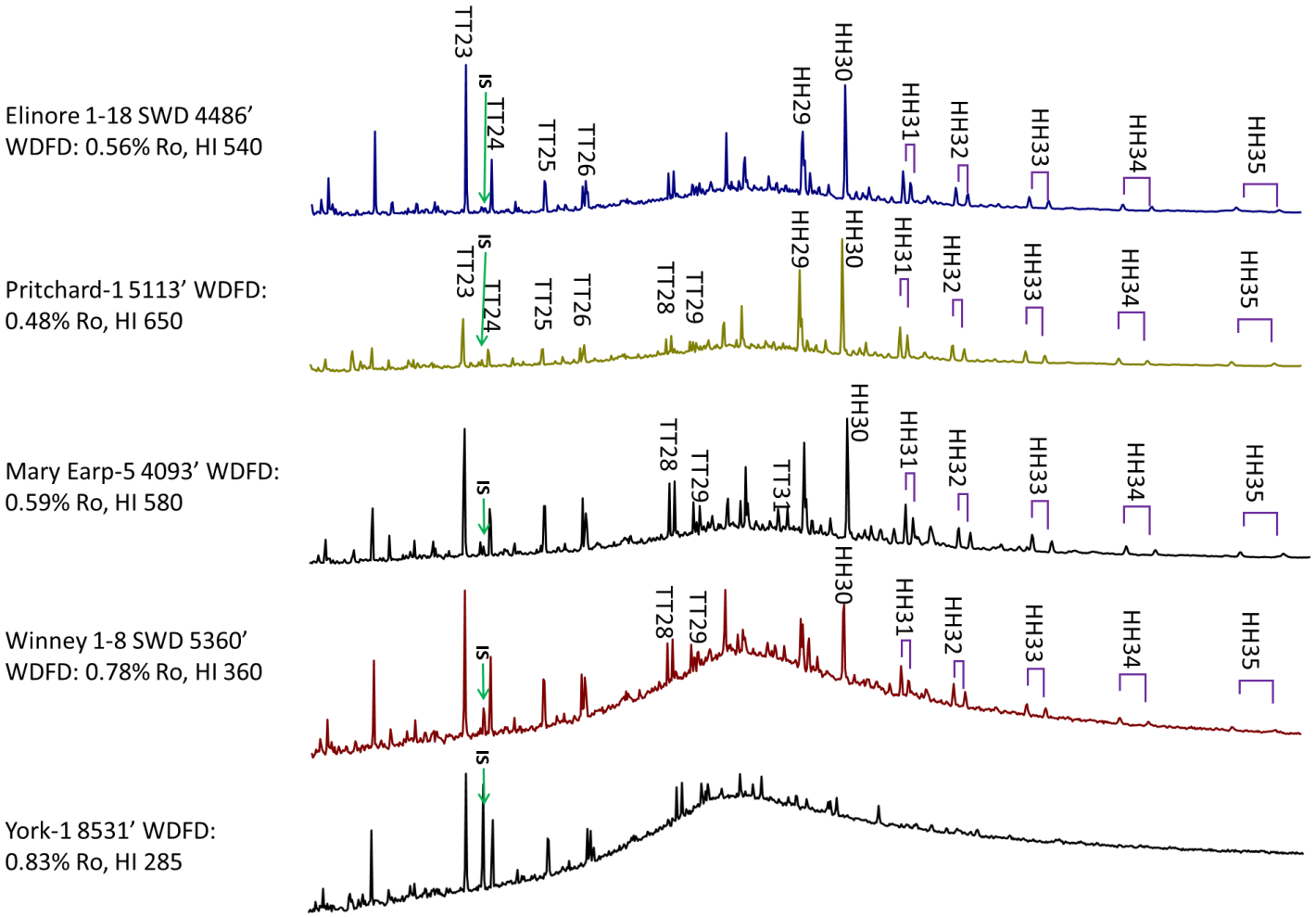

Figure 52. SIM *m/z* 191.3 mass chromatograms showing hopanes relative concentration change with thermal maturation in the B&C fractions of the Woodford rock extracts

Table 10. Absolute Concentrations of Terpanes (m/z 191) of selected Woodford cores extracts with different thermal maturity (Concentrations are expressed as µg biomarkers/g TOC)

Well Name	Depth/ft	VRo%	TT19	TT20	TT21	TT22	TT23	TT24	TT25	TT26	TT28S	TT28R	TT29S	TT30S	Tm	TT30R	TT31S	TT31R	H29
Elinore 1-18 SWD	4486	0.56	1.72	3.32	8.32	2.18	13.98	5.11	5.56	6.64	2.89	2.67	2.18	1.68	4.65	1.67	1.88	1.08	12.69
Pritchard-1	5113	0.48	0.21	0.56	0.74	0.38	2.10	0.68	0.85	1.23	0.41	0.41	0.31	0.37	1.25	0.32	0.40	0.30	3.00
Mary Earp-5	4093	0.59	0.14	0.42	0.92	0.27	2.34	0.91	1.21	1.65	0.91	0.83	0.51	0.54	0.97	0.56	0.54	0.46	1.70
Winney 1-8 SWD	5360	0.78	0.16	0.23	0.43	0.19	0.83	0.52	0.58	0.54	0.28	0.32	0.24	0.22	0.21	0.26	0.26	0.17	0.33
York-1	8531	0.83	0.01	0.01	0.03	0.01	0.04	0.03	0.03	0.03	0.01	0.01	0.01	0.01	0.01	0.00	0.01	0.01	0.01

Well Name	Depth/ft	VRo%	29Ts	D30	H30	TT33S	TT33R	H31S	H31R	H32S	H32R	H33S	H33R	H34S	H34R	H35S	H35R
Elinore 1-18 SWD	4486	0.56	4.07	3.01	15.2	N.D.	2.02	4.43	3.64	3.67	2.65	2.12	2.02	1.70	1.22	1.60	0.88
Pritchard-1	5113	0.48	0.85	0.49	4.23	0.00	0.63	1.42	1.18	0.85	0.71	0.74	0.628	0.532	0.468	0.609	0.495
Mary Earp-5	4093	0.59	0.51	0.36	2.36	0.45	0.39	0.72	0.52	0.56	0.46	0.53	0.393	0.371	0.277	0.284	0.394
Winney 1-8 SWD	5360	0.78	0.26	0.28	0.66	N.D.	0.14	0.33	0.31	0.27	0.21	0.22	0.14	0.16	0.15	0.09	0.10
York-1	8531	0.83	0.01	0.01	0.01	0.00	0.00	0.004	0.005	0.00	0.00	0.003	0.003	0.002	0.003	0.002	0.003

4.3.2.2 Ts and Tm

17α-22,29,30-trisnorhopane (Tm) and 18α-22,29,30-trisnorneohopane (Ts) are two terpanes frequently used to assess maturity level from immature to postmature stage (Seifert and Moldowan, 1978). Tm becomes less stable than Ts as thermal maturity increases. Consequently, the Ts/(Ts+Tm) ratio can be used as a maturity proxy, but with strong dependence on source. For example, this ratio was observed to increase at lower Eh and decrease at higher pH in terms of depositional environment for the Lower Toarcian marine shales from southwestern Germany (Moldowan et al., 1986). It has been also observed that oils from carbonate source rocks were shown to have unusually low Ts/(Ts+Tm) ratios compared with those from siliciclastic shales (McKirdy et al., 1983; 1984; Rullkötter et al., 1985) Therefore this ratio is better to be used for samples of similar lithology and organic facies (Moldowan et al., 1994).

The composite map of the Woodford Shale Structure (in SSTVD: Sub Sea Total Vertical Depth in feet) in Central Oklahoma with HI values and Ts/(Ts+Tm) ratios (Figure 53) shows the Ts/(Ts+Tm) ratio increases as HI decreases and the Woodford burial depth increases, acting like the C_{29} ββ/(ββ+αα) sterane ratio discussed in section 4.3.1, which suggests the Woodford structure is the primary control on maturity as mentioned before.

CI = 250’

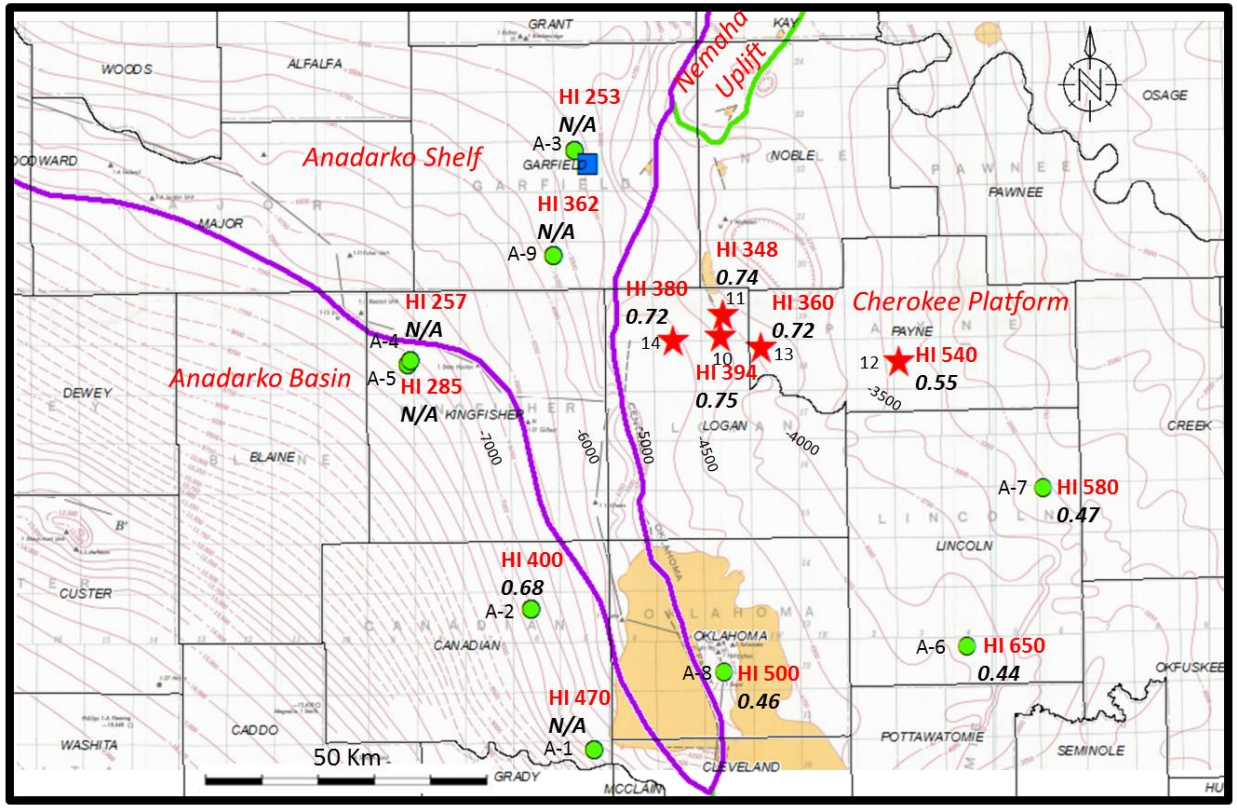

5 Devon Cores	Code
Frank 1-33 SWD	10
Wilma 1-16 SWD	11
Elinore 1-18 SWD	12
Winney 1-8 SWD	13
Adkisson 1-33 SWD	14

9 OGS Wells	Code
ROBBERSON 10-1	A-1
DANNEHL 2-16	A-2
L A CHENOWETH 1	A-3
LEWIS F POPE 1	A-4
EFFIE B YORK 1	A-5
PRITCHARD 1	A-6
MARY EARP 5	A-7
BOYD 1	A-8
ANDERSON 12-1	A-9

Base Map Modified from Amsden, 1975

Figure 53. Composite map of the Woodford Shale Structure (in SSTVD) in Central Oklahoma with HI values and Ts/(Ts+Tm) ratios showing thermal maturity of the Woodford Shale source rocks (SSTVD = Sub Sea Total Vertical Depth in feet; CI = Contour Increment in feet; HI = Hydrogen Index; N/A = Not Available)

4.3.3 Phenanthrenes

Phenanthrenes, methylphenanthrenes and dimethylphenanthrenes were determined in the aromatic fraction of rock extracts and oils by SIM/GC-MS monitoring the ions *m/z* 178.3, 192.3, and 206.3 (Figure 54). A number of ratios derived from the distributions of phenanthrenes and substituted phenanthrenes have been widely used as biomarker thermal maturity indicators (Radke and Welte, 1981; Radke et al., 1984 and 1986). The methylphenanthrene indices (MPI-1 and MPI-2) are the most commonly used ratios. The ratio of the 2- and 3-methylphenanthrenes relative to the 1- and 9-methylphenanthrenes increase with increasing temperature and burial (Radke et al., 1982). Radke and Welte (1981) found a positive correlation between MPI-1 and vitrinite reflectance for samples within the oil window (0.65-1.35%R_o), and a negative correlation for samples of high thermal maturity (1.35-2.00%R_o). Based on these observations, Radke and Welte (1981) derived two equations for R_o calculation, which can be used to estimate thermal maturity for rock extracts and oils (Appendix A).

MPI-1:

$$MPI\ 1 = 1.5 \times \frac{[2-MP+3-MP]}{[P+1-MP+9-MP]}$$

Calculated vitrinite reflectance:

For 0.65 to 1.35%R_o: R_c = 0.60 MPI-1 + 0.40

For 1.35 to 2.00%R_o: R_c = -0.60 MPI-1 + 2.30

Values of MPI-1 ratios were obtained for the Woodford rock samples in this study, and used to calculate a vitrinite reflectance equivalent (Rc) value (Figure 55). The equation from Radke and Welte (1981) which corresponded to low maturity levels was used to calculate vitrinite reflectance values for the Woodford rock samples. The vitrinite

reflectance equivalent (Rc) values calculated from the MPI-1 parameters of the Woodford rock samples in this study show no covariance with any geological or geochemical parameters (Figure 55). This anomalous behavior may be attributed to the fact that the relationship between MPI-1 and vitrinite reflectance was based on shale and coals containing type III organic matter (Radke and Welte, 1983). As a result it may not be directly applicable for the other types of source rocks, such as the Woodford Shale, containing mainly type II organic matter. Lithology of the source rock can also affect MPI ratios. It was reported by Cassani et al. (1988) that high MPI-1 values corresponded to high carbonate content in the La Luna Shale but did not reflect the true maturity level.

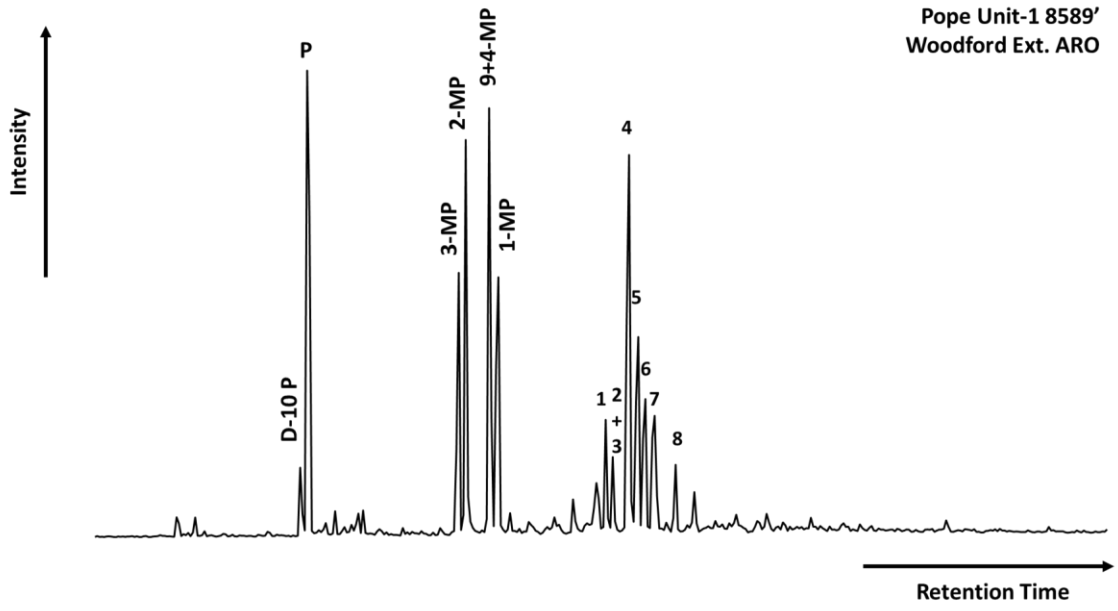

Figure 54. Summed mass chromatograms of *m/z* 178.2, 192.3, 206.3, 188.2 ions showing distributions of phenanthrenes compounds in the aromatic fractions of sample Adkisson 1-33 H Oil. Peak identification is presented in Table 11.

Table 11. Identification of phenanthrenes in the SIM mass chromatograms of *m/z* 178.3, 192.3, 206.3 of the aromatic fractions

Peak #	Compound
D-10 P	Deuterated Phenanthrene (ISTD)
P	Phenanthrene
3-MP	3-Methylphenanthrene
2-MP	2-Methylphenanthrene
9+4-MP	9+4-Methylphenanthrene
1-MP	1-Methylphenanthrene
1	Dimethylphenanthrene
2	Dimethylphenanthrene
3	Dimethylphenanthrene
4	1,3+2,10+3,9+3,10-Dimethylphenanthrene
5	1,6+2,9+2,5-Dimethylphenanthrene
6	1,7-Dimethylphenanthrene
7	2,3-Dimethylphenanthrene
8	1,9+4,9+4,10-Dimethylphenanthrene

CI = 250’

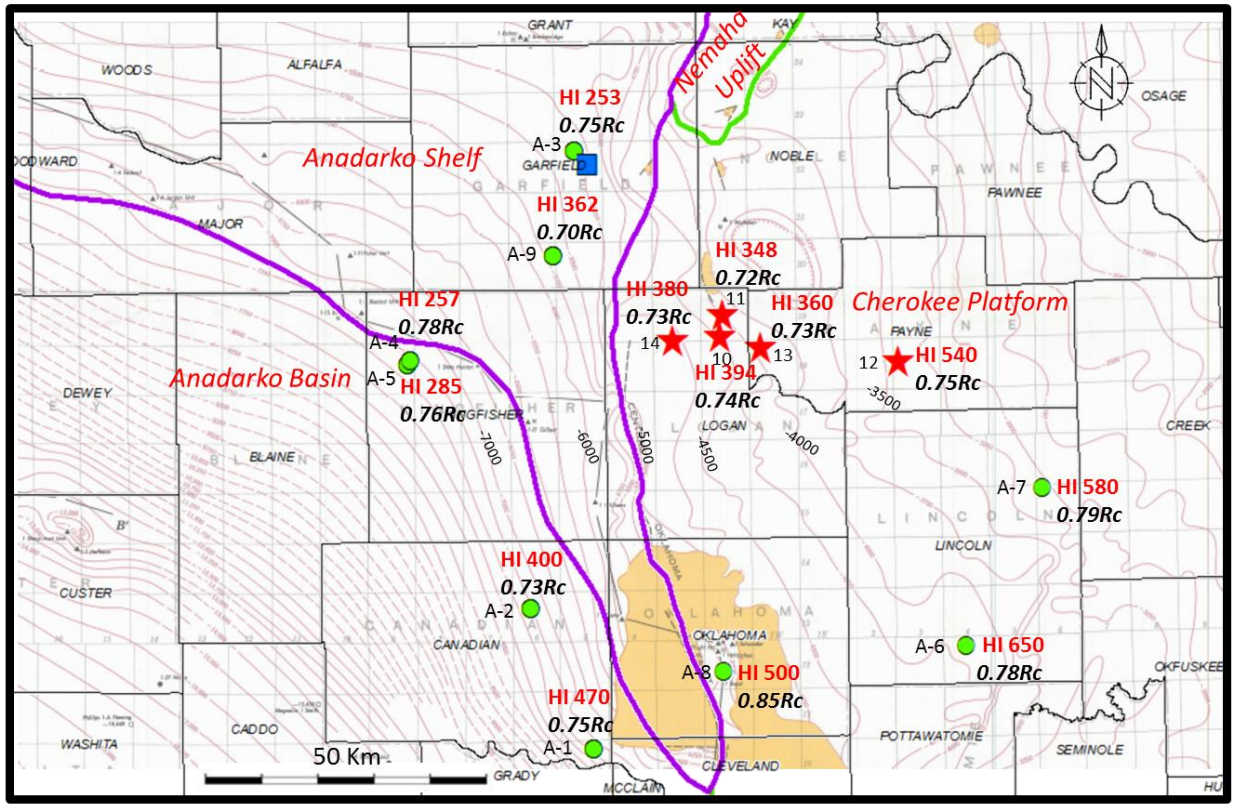

Base Map Modified from Amsden, 1975

5 Devon Cores	Code
Frank 1-33 SWD	10
Wilma 1-16 SWD	11
Elinore 1-18 SWD	12
Winney 1-8 SWD	13
Adkisson 1-33 SWD	14

9 OGS Wells	Code
ROBBERSON 10-1	A-1
DANNEHL 2-16	A-2
L A CHENOWETH 1	A-3
LEWIS F POPE 1	A-4
EFFIE B YORK 1	A-5
PRITCHARD 1	A-6
MARY EARP 5	A-7
BOYD 1	A-8
ANDERSON 12-1	A-9

Figure 55. Composite map of the Woodford Structure (in SSTVD) in Central Oklahoma with HI values and the vitrinite reflectance equivalent (Rc) values calculated from the MPI ratios of the Woodford Shale samples (SSTVD = Sub Sea Total Vertical Depth in feet; CI = Contour Increment in feet; HI = Hydrogen Index)

CHAPTER 5

5. OIL GEOCHEMISTRY

5.1 Oil Geochemical Screening Analyses

5.1.1 Gas Chromatography

5.1.1.1 n-Alkanes distributions

For the crude oil samples, the gas chromatograms of the saturate fractions show only small variation in composition (Figure 56). Several geochemical parameters calculated from the *n*-alkane chromatograms of crude oil samples are summarized in Table 12. The crude oil samples show a unimodal distribution towards the low-carbon-number members, and without any preference of even-carbon-numbered *n*-alkanes predominance (Figure 56). The oil samples have *n*-alkanes maximum around either *n*-C_{14} or *n*-C_{15}. The other characteristics, including the unimodal *n*-alkane distribution pattern, *n*-alkane maximum carbon number around *n*-C_{14} or *n*-C_{15} and average Pr/Ph ratio around 1.5 (Table 12), all suggest these crude oils have a marine origin, deposited under a reducing (anoxic) conditions.

5.1.1.2 Pristane and Phytane

Overall, the majority of the oil samples show low Pr/Ph ratios indicating the presence of reducing conditions (anoxia) during source rock deposition (Table 12). The cross plot of Pr/*n*-C_{17} versus Ph/*n*-C_{18} for the rock extracts and oils analyzed in this study was shown in Figure 57. This diagram indicates that these samples are mainly composed of marine organic matter mixed with minor amounts of terrigenous input.

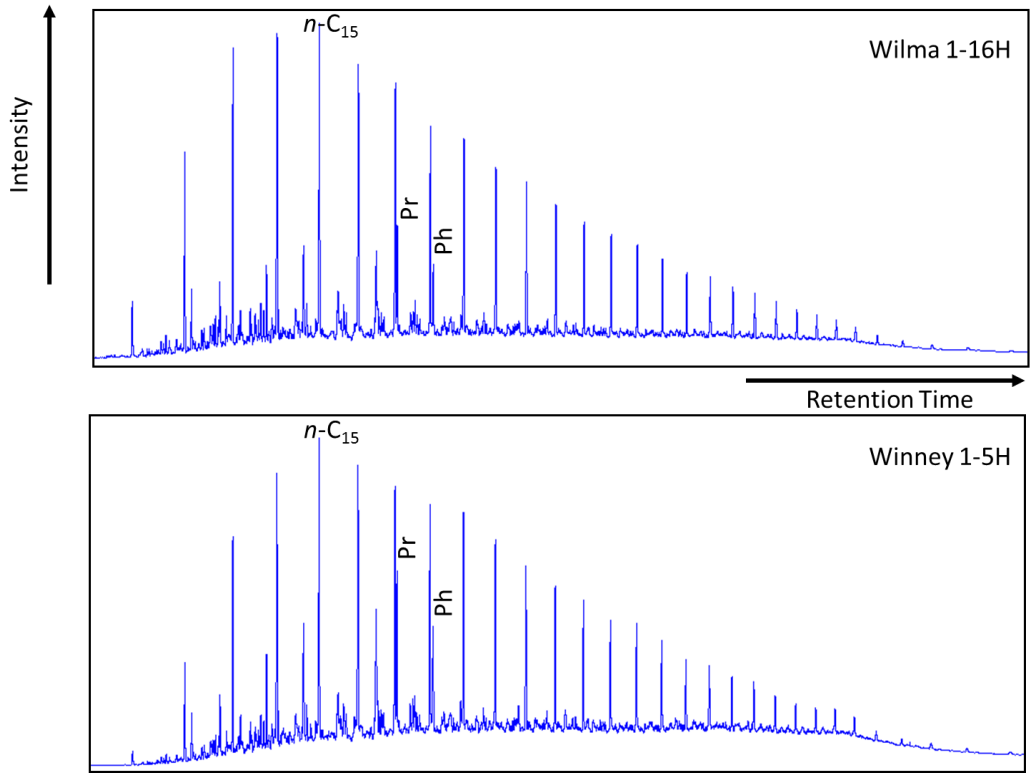

Figure 56. Gas chromatograms of the saturate fractions of two Woodford tight oil samples (Pr = pristane; Ph = phytane, n-C_{15} = C_{15} normal alkane)

Table 12. n-Alkanes parameters derived from the saturate fraction of the oils (ND = not determined)

Samples	Range	n-alkane distribution	n-alkane maximum	Pr/Ph	TAR	CPI
Smith 1-23H	*n*-C_{11}-*n*-C_{30}	unimodal	*n*-C_{15}	1.41	0.17	0.98
Wilma 1-16H	*n*-C_{11}-*n*-C_{30}	unimodal	*n*-C_{15}	1.51	0.20	0.96
Matthews 1-33H	*n*-C_{11}-*n*-C_{30}	unimodal	*n*-C_{15}	1.41	0.31	0.99
Winney 1-5H	*n*-C_{11}-*n*-C_{30}	unimodal	*n*-C_{15}	1.50	0.23	0.97
Smith 1-14H	*n*-C_{11}-*n*-C_{30}	unimodal	*n*-C_{15}	1.50	0.18	0.96
Johnson 1-33H	*n*-C_{10}-*n*-C_{30}	unimodal	*n*-C_{14}	1.50	0.44	1.00
Elinore1-18H	*n*-C_{11}-*n*-C_{30}	unimodal	*n*-C_{15}	1.45	0.21	0.99
Winney 1-8H	*n*-C_{11}-*n*-C_{30}	unimodal	*n*-C_{15}	1.52	0.18	0.98
Adkisson 1-33H	*n*-C_{10}-*n*-C_{30}	unimodal	*n*-C_{15}	1.49	0.32	0.99
Elinore 1-17H	*n*-C_{12}-*n*-C_{30}	unimodal	*n*-C_{16}	1.53	0.22	0.98
Williams 1-24WH	*n*-C_{11}-*n*-C_{30}	unimodal	*n*-C_{14}	1.52	0.14	0.97
Peach 1-19H	*n*-C_{12}-*n*-C_{30}	unimodal	*n*-C_{15}	1.55	0.20	1.02
Joyce 1-32H	*n*-C_{12}-*n*-C_{30}	unimodal	*n*-C_{15}	1.68	0.28	1.05
Hopfer 1-20H	*n*-C_{11}-*n*-C_{30}	unimodal	*n*-C_{15}	1.69	0.21	0.94
Peach 1-20WH	*n*-C_{11}-*n*-C_{30}	unimodal	*n*-C_{15}	1.51	0.24	0.94
C. Matthews 1-8WH	*n*-C_{11}-*n*-C_{30}	unimodal	*n*-C_{15}	1.51	0.27	0.98
Williams 1-24WH	*n*-C_{11}-*n*-C_{30}	unimodal	*n*-C_{14}	1.52	0.14	0.97

Ellis Lewis Jet	*n*-C_{11}-*n*-C_{30}	unimodal	*n*-C_{15}	1.63	0.07	0.96
Thomas James 1-22	*n*-C_{11}-*n*-C_{30}	unimodal	*n*-C_{15}	1.49	0.19	ND
F	*n*-C_{11}-*n*-C_{30}	unimodal	*n*-C_{15}	1.38	0.19	1.01
7-5N-5E	*n*-C_{11}-*n*-C_{30}	unimodal	*n*-C_{15}	1.14	0.19	0.92
Ford-1	*n*-C_{11}-*n*-C_{30}	unimodal	*n*-C_{15}	1.14	0.27	0.91

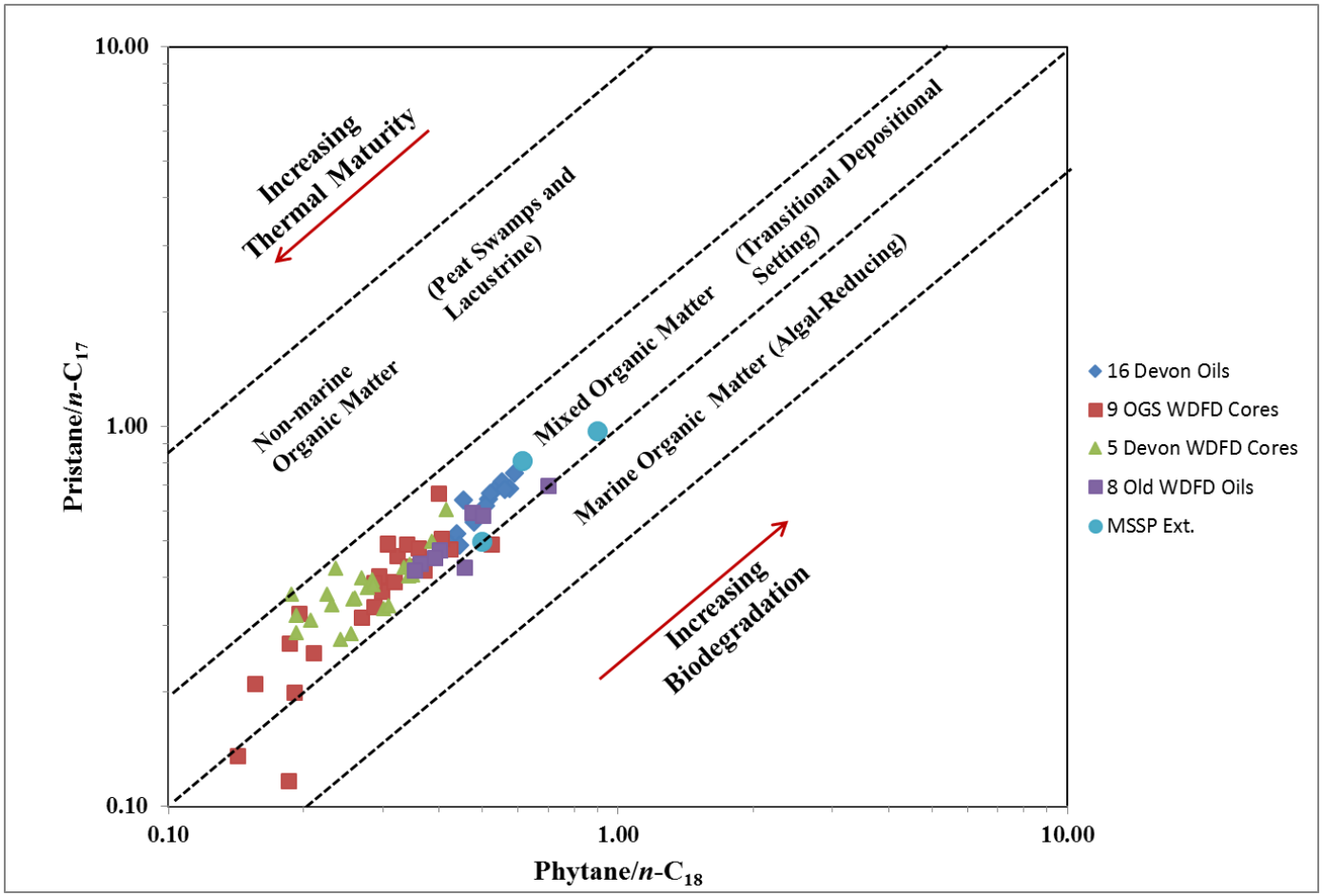

Figure 57. Isoprenoids plot of Pristane/n-C_{17} versus Phytane/n-C_{18} showing redox conditions, maturity, and depositional environments for samples of the Woodford Shale (n-C_{17} = C_{17} normal alkane; n-C_{18} = C_{18} normal alkane)

5.1.1.3 C_7 Light hydrocarbon analysis

Light hydrocarbons (C_4-C_9) are a significant portion of most crude oils but they are not biomarkers since their carbon skeletons are too short to preserve the origin/precursor information on their parent organic molecules in living organisms (Hunt, 1984 and 1995). Most light hydrocarbons form by breakdown of larger molecular precursors during catagenesis (Mango, 1990 and 1994; Walters et al., 2003). Some isomers may have direct biological origins or may be cleaved from biomarkers, but there are so many possible precursors that they cannot be traced to a specific biological origin (Mango, 1994). Nevertheless, light hydrocarbons contain considerable information on their source, thermal maturity and their post-expulsion history (Mango, 1997). Thermal maturation can change the composition of light hydrocarbons, such as iso-alkanes convert to n-alkanes during maturation (Hunt, 1984; Mango, 1991 and 1997). Other than that, various secondary processes can change the abundance of light hydrocarbons in crude oils. Late-stage generation, reservoir cracking, and various migration processes, including evaporative fractionation, phase separation, and admixture of condensates, can increase light hydrocarbons (Mango, 1997). On the contrary, biodegradation, water washing, thermochemical sulfate reduction (TSR), and evaporation can remove light hydrocarbons (Mango, 1997).

Many C_6-C_7 light hydrocarbons can be used to determine thermal maturity, and indicate various reservoir alteration processes. Thompson (1987) B-F diagram summarized several reservoir alteration factors, namely evaporative fractionation, maturation, water washing and biodegradation, in a plot of aromaticity ratio (toluene/n-heptane, B) versus paraffinity ratio (n-heptane/methylcyclohexane, F). Thompson

proposed that evaporative fractionation initially results in a decrease in F and an increase in B. Subsequent evaporative fractionation will result in a rapid increase in B. The other alteration processes can also be characterized by applying the same idea, like iso-alkanes convert to n-alkanes during thermal maturation, water washing will prefer to remove toluene than n-heptane, and n-heptane will be biodegraded prior to methylcyclohexane. Compared to the Devon tight oils falling into the unaltered "Normal Oil" field, the Woodford-sourced oils produced in conventional reservoirs from Southern Oklahoma have been altered and are more mature based on the Thompson B-F diagram (Figure 59), which is consistent with the observation from the isoheptane versus n-heptane ratio diagram (Figure 60).

Walters et al. (2003) proposed an empirical isoheptane ratio (I) versus heptane ratio (H) diagram based on the C_7 ratios measured for oils/condensates from the North Sea to investigate the thermal maturity of oils/condensates in a plot of isoheptane ratio (2-methylhexane + 3-methylhexane)/∑(dimethylcyclopentanes)) versus heptane ratio (100*n-C_7/∑ (cyclohexane through methylcyclohexane) , H). This diagram (Figure 60) shows all of the Devon tight oils are in the range of 0.85 ~ 1.1 %Ro. Most of the conventionally produced oils from Southern Oklahoma are in the range of 1.1 to 1.5%Ro except Anadarko Taylor 2118, which is a condensate, close to 1.5%Ro. These observations seem reasonable since the conventionally produced oils from the Pauls Valley, Southern Oklahoma were thought to be migrated from deep part of the Anadarko Basin (Jones, 1989). In other words, they were generated at a higher thermal stage. Another possibility would be the composition of light hydrocarbons already changed during over twenty year's storage.

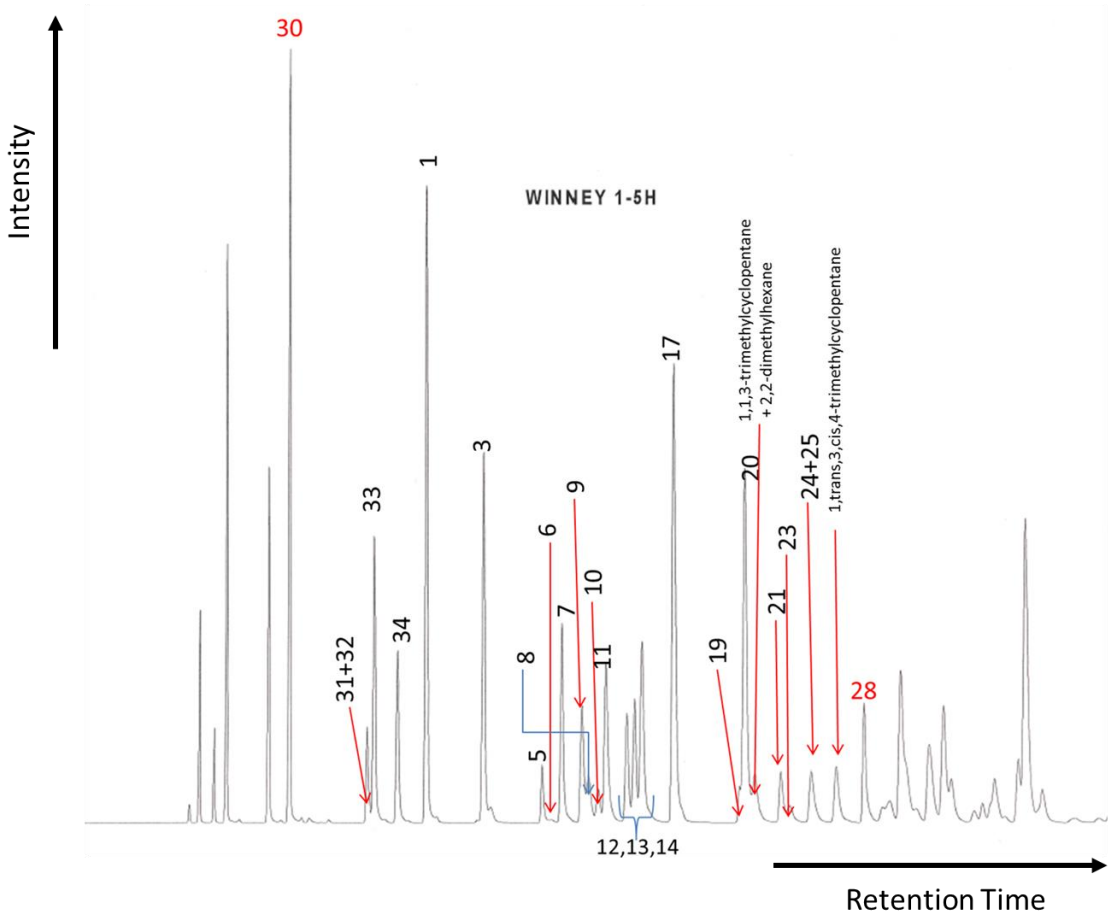

Figure 58. Whole oil gas chromatogram of Winney 1-5H oil showing light hydrocarbon distribution (Peak identification is listed in Table 13)

Table 13. Light hydrocarbon compounds identification

Peak #	Compound	Abbreviation
1	n-Hexane	n-C6
2	2,2-Dimethylpentane	2,2-DMP
3	Methylcyclopentane	MCP
4	2,4-Dimethylpentane	2,4-DMP
5	Benzene	B
6	3,3-Dimethylpentane	3,3-DMP
7	Cyclohexane	CH
8	2,3-Dimethylpentane	2,3-DMP
9	2-Methylhexane	2-MH

10	1,1-Dimethylcyclopentane	1,1-DMCP
11	3-Methylhexane	3-MH
12	Cis-1,3-Dimethylcyclopentane	C1,3-DMCP
13	Trans-1,3-Dimethylcyclopentane	T1,3-DMCP
14	Trans-1,2-Dimethylcyclopentane	T1,2-DMCP
15	3-Ethylpentane	3-EP
16	2,2,4-Trimethylpentane	2,2,4-TMP
17	n-Heptane	n-C7
18	2,2-Dimethylhexane	2,2-DMH
19	Cis-1,2-Dimethylcyclopentane	C1,2-DMCP
20	Methylcyclohexane	MCH
21	Ethylcyclopentane	ECP
22	2,5-Dimethylhexane	2,5-DMH
23	2,4-Dimethylhexane	2,4-DMH
24	1,2,4-Trimethylcyclopentane	1,2,4-TMCP
25	1,2,3-Trimethylcyclopentane	1,2,3-TMCP
26	2,3,4-Trimethylpentane	2,3,4-TMP
27	2,3,3-Trimethylpentane	2,3,3-TMP
28	Toluene	Tol
29	Isooctane	i-C8
30	n-Pentane	n-C5
31	2,2-Dimethylbutane	2,2-DMB
32	2,3-Dimethylbutane	2,3-DMB
33	2-methylpentane	2-MP
34	3-methylpentane	3-MP

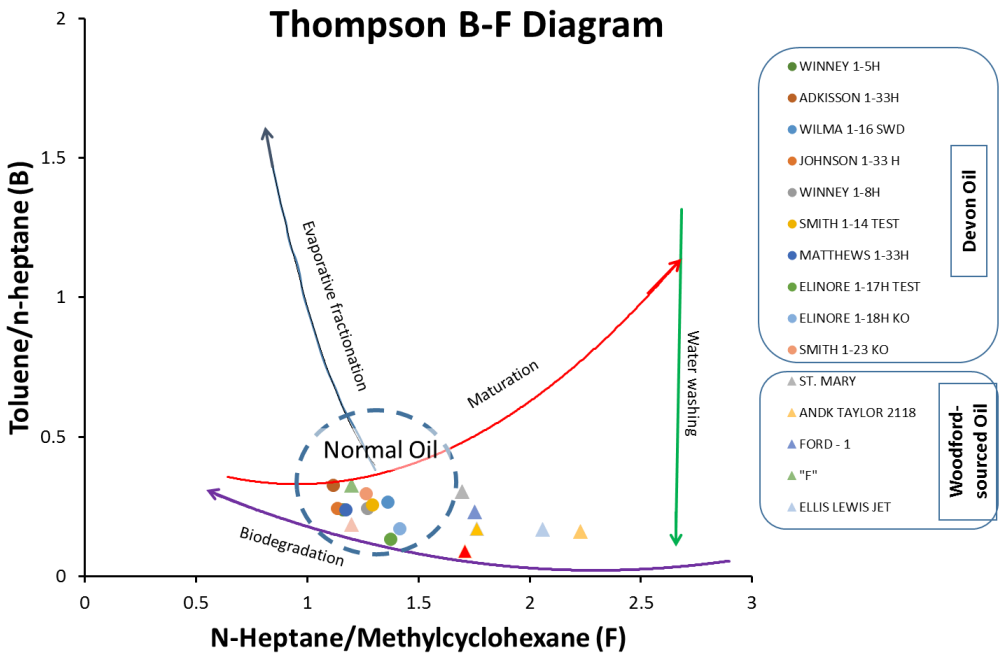

Figure 59. Thompson B-F Diagram summarizing reservoir alteration factors for the oils

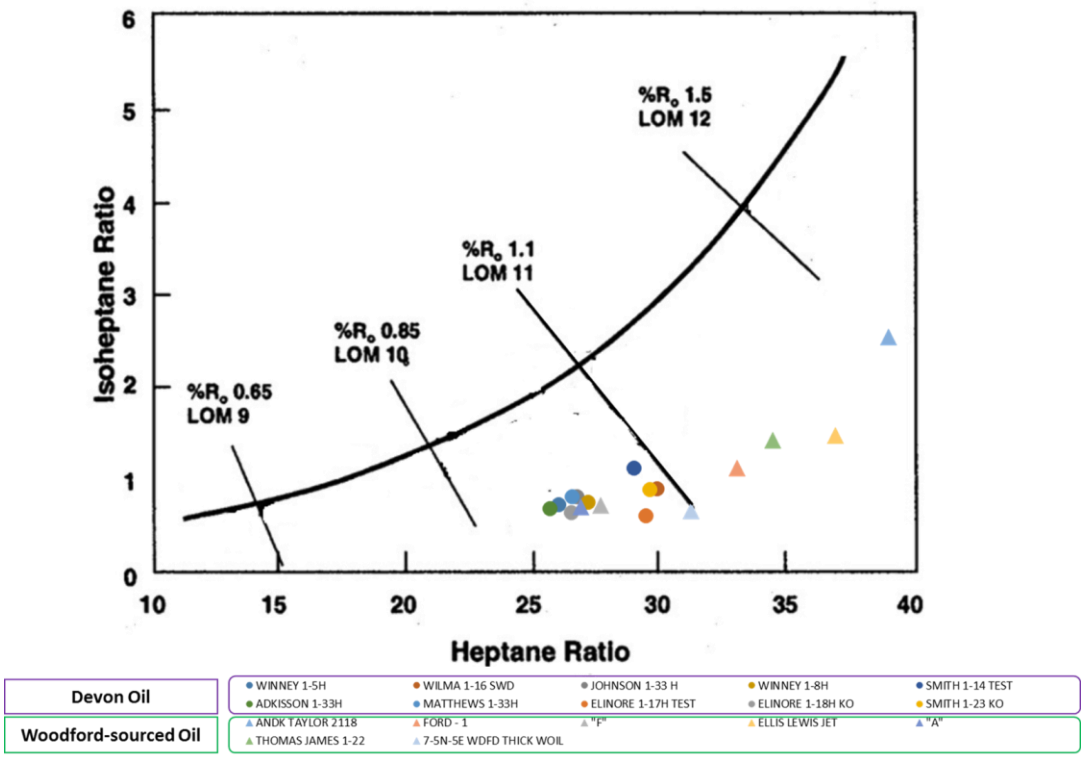

Figure 60. Isoheptane versus heptane ratio diagram showing the maturity of the oil samples (plot template from Walters, 2003; 5 condensates at high maturity stage out of scope)

5.1.2 Isotope Analysis

Stable carbon isotopes have been widely used to correlate crude oils and source rock extracts. Physical and chemical processes during organic matter production and preservation cause variations in stable isotope composition. Bulk stable carbon isotope composition analysis of saturate and aromatic fractions for crude oils and source rock extracts have been widely used to indicate the source of crude oils. Different organic matter types have distinct responses in the stable isotope composition (Sofer, 1984; Andrusevich et al., 1998).

In this study the bulk stable carbon isotope composition of saturate and aromatic fractions were measured for 10 Devon oils and 7 conventionally produced Woodford-sourced oils. Cross plots of $\delta^{13}C$ of aromatic fractions versus $\delta^{13}C$ of saturate fractions for the oil samples were used to correlate with the possible source rocks in Oklahoma based on their data points locality in this plot (Figure 61). In terms of stable carbon isotope signature, the extracts of Simpson group shales are characterized by both saturate and aromatic fractions having values in the range of -32 to -29 per mil, although two samples have values of about -27 per mil (Figure 61). The origin of this wide range of carbon isotope values has been discussed by Hatch et al. (1987). In their opinion, the wide range in $\delta^{13}C$ for oils and rock extracts reflect a major, positive excursion (6-9 per ‰) in organic matter $\delta^{13}C$ composition in late Middle Ordovician rocks (Hatch et al., 1987). The positive excursion in organic matter $\delta^{13}C$ is a possible result of increased organic matter productivity and/or preservation during that time (Hatch et al., 1987). The Woodford Shale extracts show the carbon isotope composition of the saturate and aromatic fractions ranges from -30 to -29 per mil and the carbon isotope composition of the Pennsylvanian

shale extracts is relatively enriched in $\delta^{13}C$ values for saturate and aromatic fractions ranging from -29 to -25 per mil. Two Mississippian Limestone extracts show the $\delta^{13}C$ values around -30.4 per mil for the saturate and the aromatic fractions. These two Mississippian Limestone data points are encompassed by the Woodford Shale data points. The majority of 10 Devon crude oils and 7 conventionally produced Woodford-sourced oils share the carbon isotope composition of the saturate and aromatic fractions ranging from -31 to -30 per mil, which is within the approximate range of the Woodford Shale extracts' $\delta^{13}C$ values. The conclusion here is the oil samples analyzed in this study more closely resemble the Woodford/Mississippian rocks than the Simpson Group or the Pennsylvanian shale in terms of stable carbon isotope composition.

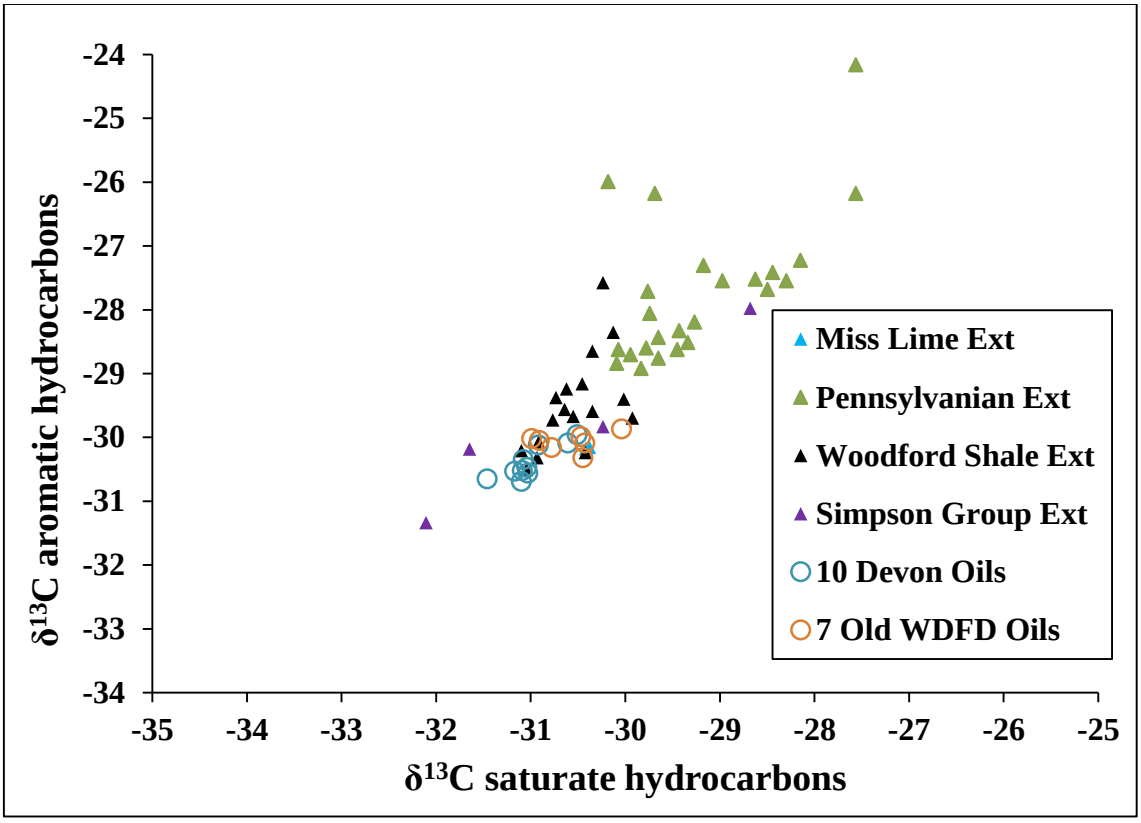

Figure 61. Carbon stable-isotope compositions of saturated- and aromatic-hydrocarbon fractions of rock extracts and crude oils from the Anadarko Basin and Cherokee Platform, grouped by geologic age of source rock (template and

data points of Simpson Group, Woodford Shale and Pennsylvanian rock extracts from Burruss and Hatch, 1989)

5.2 Evaluation of Organic Matter Source and Depositional Environments

5.2.1 Steranes (m/z 217)

The mass chromatogram of *m/z* 217.3 for the 7-5N-5E Woodford-sourced oil sample shows the steranes distributions of a typical Woodford-sourced oil produced from the conventional reservoirs in Southern Oklahoma (Figure 62). The stereoisomers of C_{27}-C_{30} steranes and diasteranes are resolved with help of GC-MS/MS (Figure 63). Peak identification is shown in Table 6. Formulas for calculation of geochemical ratios are displayed in Appendix A. Numerical values of the geochemical ratios calculated are in Appendix D. Biomarkers quantitation results are in Appendix F.

5.2.1.1 Regular steranes

The regular 14α(H), 17α(H) (20R) steranes ternary plot for the oil samples (Figure 64) shows that the oils produced in Payne County and the "Old Woodford Oils" produced in Southern Oklahoma are grouped together falling into the Woodford extract area (denoted by red dash line) of the plot, indicating a common genetic relationship. The oils produced in Logan County cluster in the Mississippian extract area (denoted by blue dash line) of the plot except several oil samples, namely C. Matthews 1-33H, Adkisson 1-33H, Johnson 1-33H and Smith 1-14H, are in the boundary between the Mississippian and Woodford extracts areas, which suggest these oils have both the Woodford and Mississippian source contribution. More of the correlation studies are discussed in section 5.4.

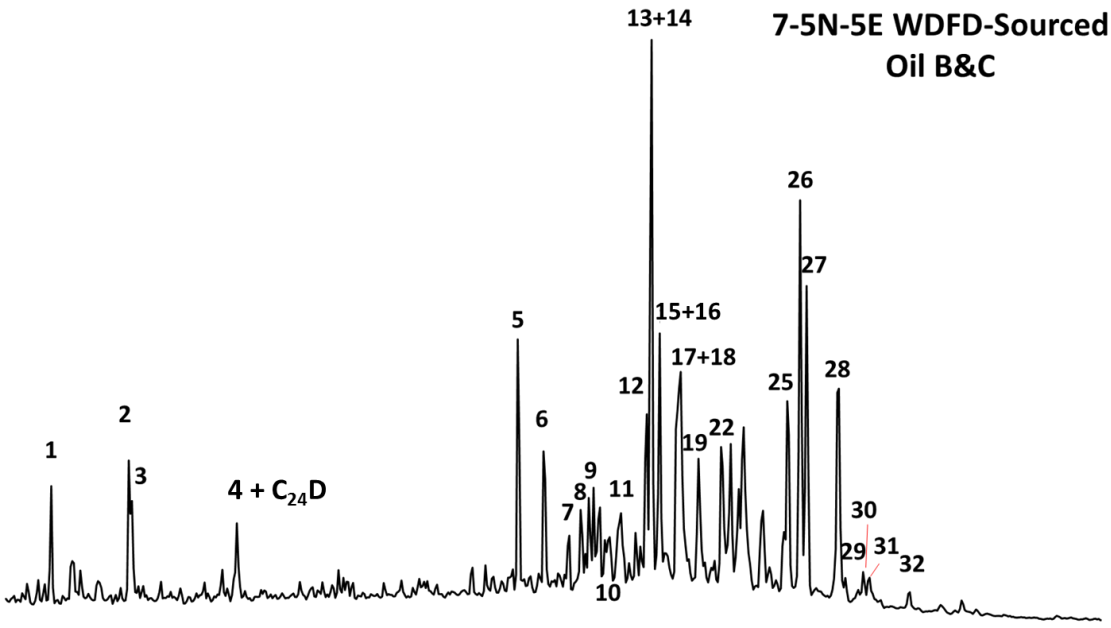

Figure 62. SIM *m/z* 217.3 mass chromatogram showing distributions of steranes in the B&C fraction of 7-5N-5E oil sample. Peak identification is listed in Table 6.

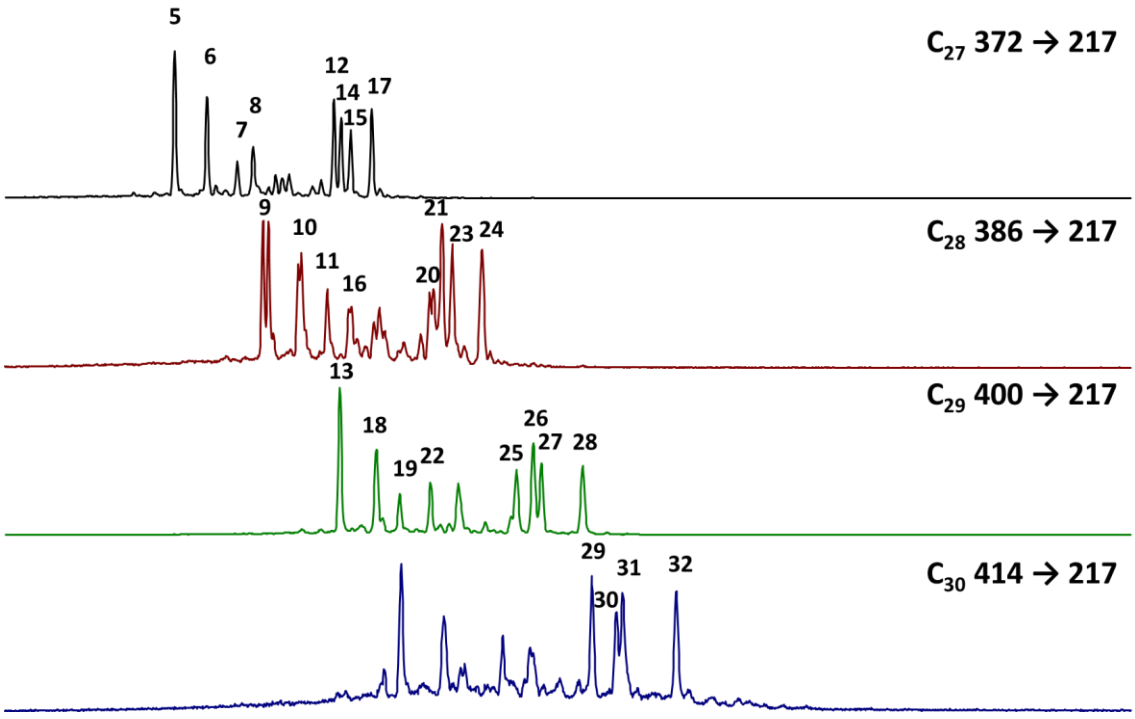

Figure 63. GC-MS/MS chromatograms showing the distributions of C_{27}-C_{30} steranes in the B&C fraction of the 7-5N-5E oil sample. Peak identification is presented in Table 6.

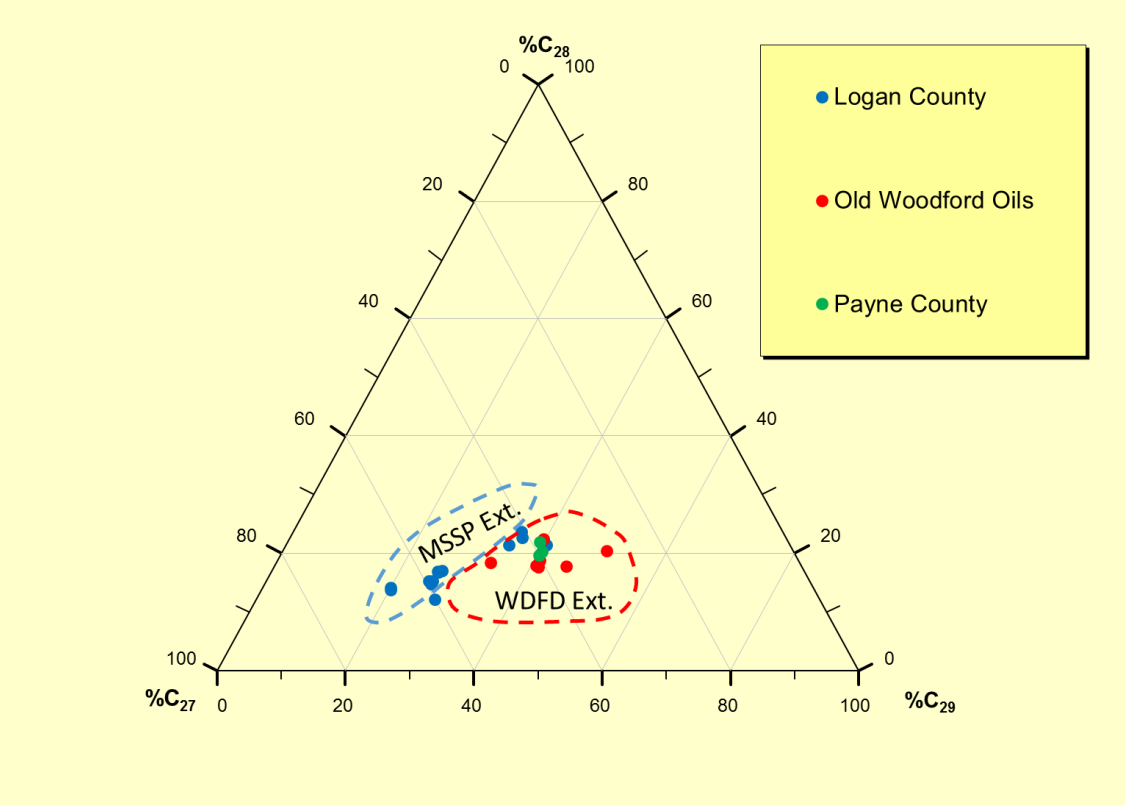

Figure 64. Regular sterane ternary diagram of oil samples using C_{27}, C_{28}, and C_{29} 14α(H), 17α(H) (20R) regular sterane isomers

C_{30} Steranes (24-*n*-propylcholestanes) were detected in all of the crude oil samples analyzed but in variable concentrations (Appendix F), which indicates at least the source rock of these oil samples have marine organic matter input. By plotting the data points of this study onto the $\%C_{34}$ Homohopanes vs. $\% C_{30}/(C_{27}\text{-}C_{30})$ steranes crossplot (Figure 65), and considering no significant evaporitic interval found in the proximity of the Mississippian/Woodford formations in the study area, these oil samples (whatever source rock generated them) are not the typical oil sourced by evaporitic hypersaline source rocks, as reported by Moldowan et al. (1992). It is more geologically reasonable to interpret the possible source rocks for these studied oil samples are falling

in the transition zone from open marine to increasing restricted depositional environments.

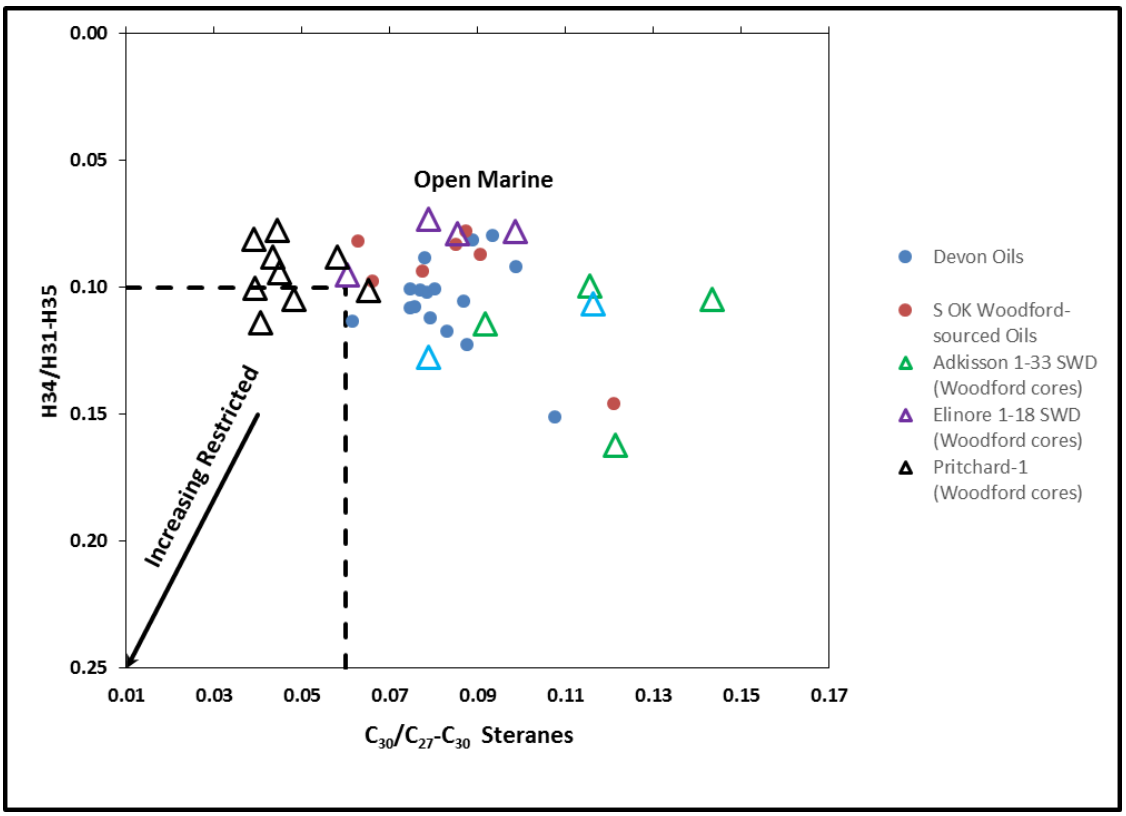

Figure 65. Plot of %C_{34} Homohopanes versus % C_{30}/(C_{27}-C_{30}) steranes shows the possible source rocks' depositional environments for the oil samples in this study (Dotted lines are used as a guide. Plot template from Moldowan et al., 1992)

5.2.1.2 Diasteranes (rearranged steranes)

The majority of the C_{27} diasterane/C_{27} sterane ratios of the studied oil samples are within the range of 0.40~0.60, typical for marine siliciclastic shales (0.30~0.80) as reported by Mello et al., (1988). By plotting this ratio onto the well location map there is not an obvious relationship between the ratios and their geographic locations or geological aspects (Figure 66). Considering the possibility of multiple sources for the oil samples and multiple factors (including clay content, thermal maturity and/or

biodegradation) affecting this ratio, it's problematic to infer the lithology or source rock type only based on the C_{27} diasterane/C_{27} sterane ratios of oil samples here.

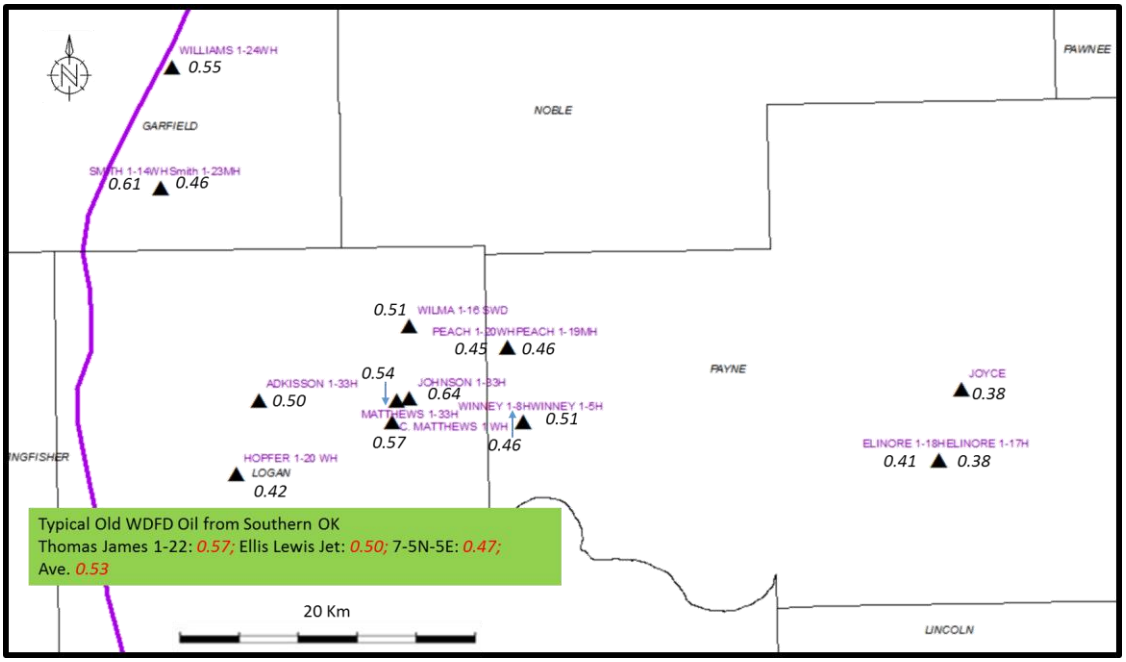

Figure 66. Map of Logan and Payne with C_{27} diasterane/C_{27} sterane ratios of the oil samples in this study

5.2.2 Terpanes (m/z 191)

Tri-, tetra-, and pentacyclic terpanes were identified in the studied oils by analysis of their B&C fractions using SIM/GC-MS of the *m/z* 191.3 ion. Fragmentogram of these compounds is presented in Figure 67. Peak identifications are in Table 7. Formulas for calculation of geochemical ratios are given in Appendix A. Geochemical ratios of terpanes and their relationships with other biomarker groups helped in assessing variations in organic matter source, depositional environment, redox conditions, and thermal maturity for the studied oils.

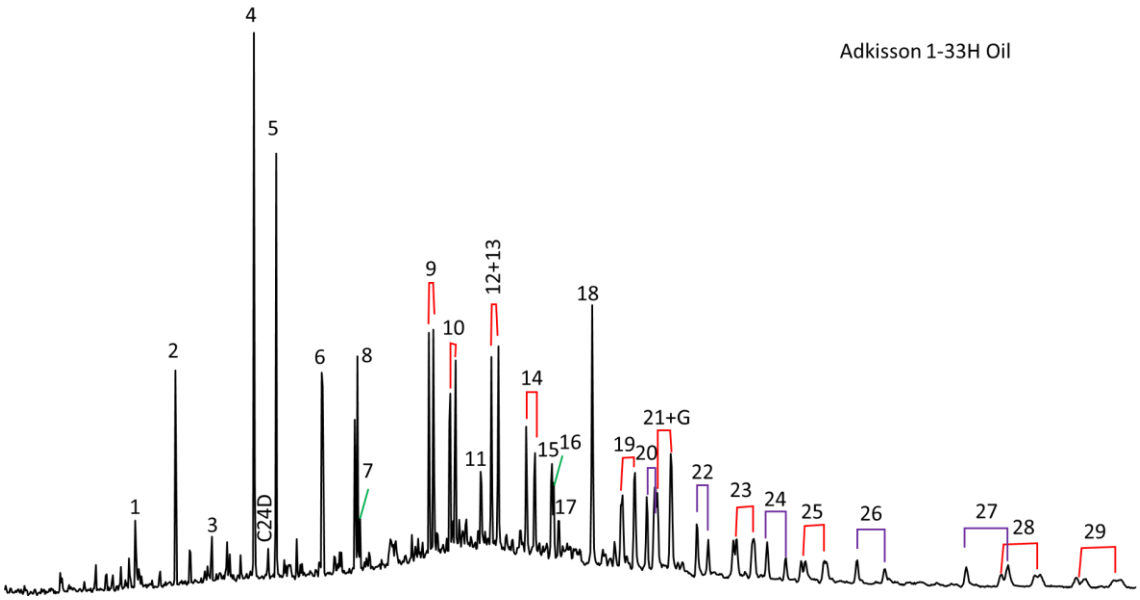

Figure 67. SIM *m/z* 191.3 mass chromatograms showing distributions of terpanes in the B&C fractions of the Adkisson 1-33H oil sample. Red brackets denote tricyclic terpane isomers and purple brackets denote homohopane isomers. Peak identification is presented in Table 7.

5.2.2.1 Tricyclic terpanes

A plot of C_{26}/C_{25} TR versus $C_{31}R/C_{30}$ Hopane for the oil samples in this study was shown in Figure 68. From this graph it is suggested that all of these oil samples are generated from marine shale, carbonates or marls but not lacustrine source rocks. A plot of C_{22}/C_{21} versus C_{24}/C_{23} tricyclic terpane ratios for the oil samples in this study was shown in Figure 69. From this graph it is suggested that all of these oil samples are generated from marine shale. These two commonly used plots based on the tricyclic terpanes ($<C_{30}$) could only differentiate the oil samples sourced by marine versus non-marine at the bulk property level. A detailed characterization of the possible source rocks' organic matter input and depositional environments for the oil samples in this study was carried out by investigating the extended tricyclic terpanes ($>C_{30}$) discussed below.

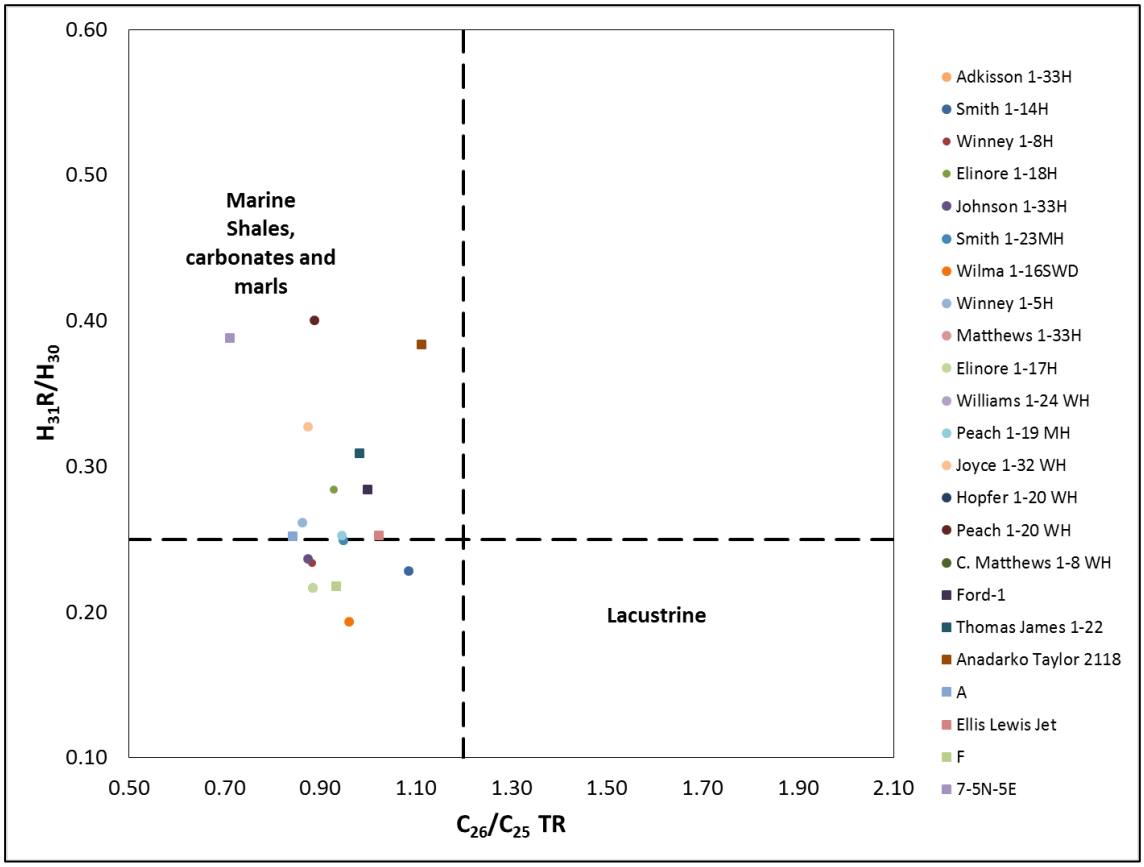

Figure 68. Plot of C_{26}/C_{25} TR versus $C_{31}R/C_{30}$ Hopane shows the possible source rock depositional environments for the oil samples in this study (Dotted lines are used as a guide. Plot template from Peters et al., 2005)

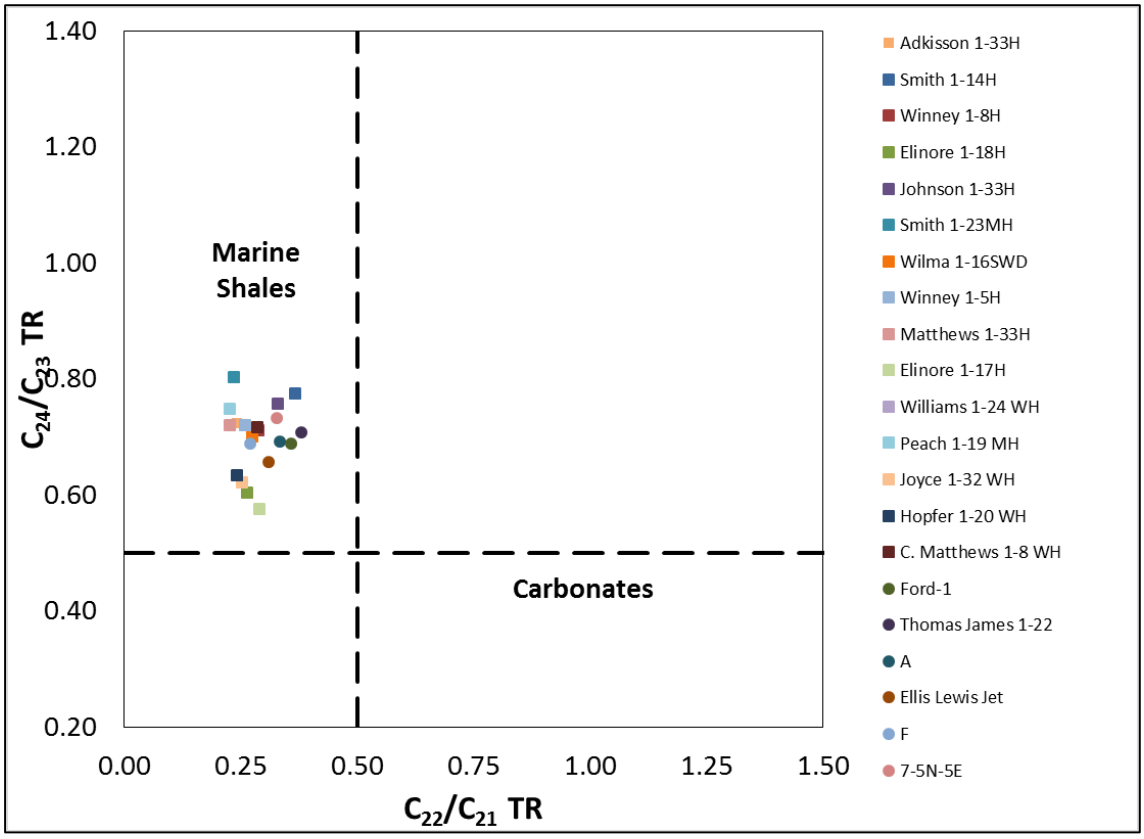

Figure 69. Plot of C_{22}/C_{21} versus C_{24}/C_{23} tricyclic terpanes shows the possible source rock depositional environments for the oil samples in this study (Dotted lines are used as a guide. Plot template from Peters et al., 2005)

The SIM m/z 191.3 mass chromatograms of three oil samples were shown in Figure 70: including two recently produced tight oil samples from Devon Energy, namely Adkisson 1-33H oil, Elinore 1-17H oil, and a typical Woodford-sourced oil produced in conventional reservoir from Southern Oklahoma. These two oil samples are two representative end-members in terms of their *m/z* 191 fingerprints. One end-member is Adkisson 1-33H oil. The other end-member is Elinore 1-17H oil. The characteristics of *m/z* 191 fingerprints of Adkisson 1-33H oil include: 1) extended tricyclic terpanes (TT33 ~ TT39) dominate over homohopanes (H31 ~ H35) in the same chromatographic region (Appendix G); 2) unusually abundant tricyclic terpanes (TT28 ~ TT31) (Appendix G); 3)

relatively higher (29Ts+D30)/H30 ratio (Appendix F). While, comparing with Adkisson 1-33H oil, the characteristics of *m/z* 191 fingerprints of Elinore 1-17H oil are: 1) extended tricyclic terpanes (TT33 ~ TT38) could be detected until C_{38} but homohopanes (H31 ~ H35) still dominate over extended tricyclic terpanes (TT33 ~ TT38) in this range (Appendix G); 2) abundant tricyclic terpanes (TT19 ~ TT31), especially distinct distribution pattern of TT28 ~ TT31 (Appendix G); 3) Ts/Tm ratio close to 1; 4) relatively lower (29Ts+D30)/H30 ratio and C_{30} diahopane sparsely detectable than C_{30} regular hopane. 7-5N-5E oil, as one of the representative Woodford-sourced conventionally produced oil in Southern Oklahoma, shows the characteristics of a typical Woodford-sourced oil, similar to the Elinore 1-17H oil. As discussed previously in section 4.2.2.1, several characteristics documented from the SIM m/z 191.3 mass chromatograms of the Mississippian rock extracts in this study are: 1) extended tricyclic terpanes (TT33 ~ TT39) dominate over homohopanes (H31 ~ H35) (Appendix G); 2) very abundant tricyclic terpanes (TT28 ~ TT31) (Appendix G) are consistent with that of the Mississippian rock in Oklahoma reported by Wang (1993) and Kim (1999). The unusually abundant distribution pattern of extended tricyclic terpanes has been suggested as one of the most diagnostic characteristics of Mississippian source rock extracts and Mississippian-sourced oils (Wang, 1993; Kim, 1999). The tricyclic terpanes abundance and distribution patterns found in the oil samples of this study are source specific, which suggests the oil with abundant extended tricyclic terpanes, like the Adkisson 1-33H oil, have Mississippian source rock contribution. On the contrary, the oil without abundant extended tricyclic terpanes, like the Elinore 1-17H oil, does not have significant Mississippian source rock contribution.

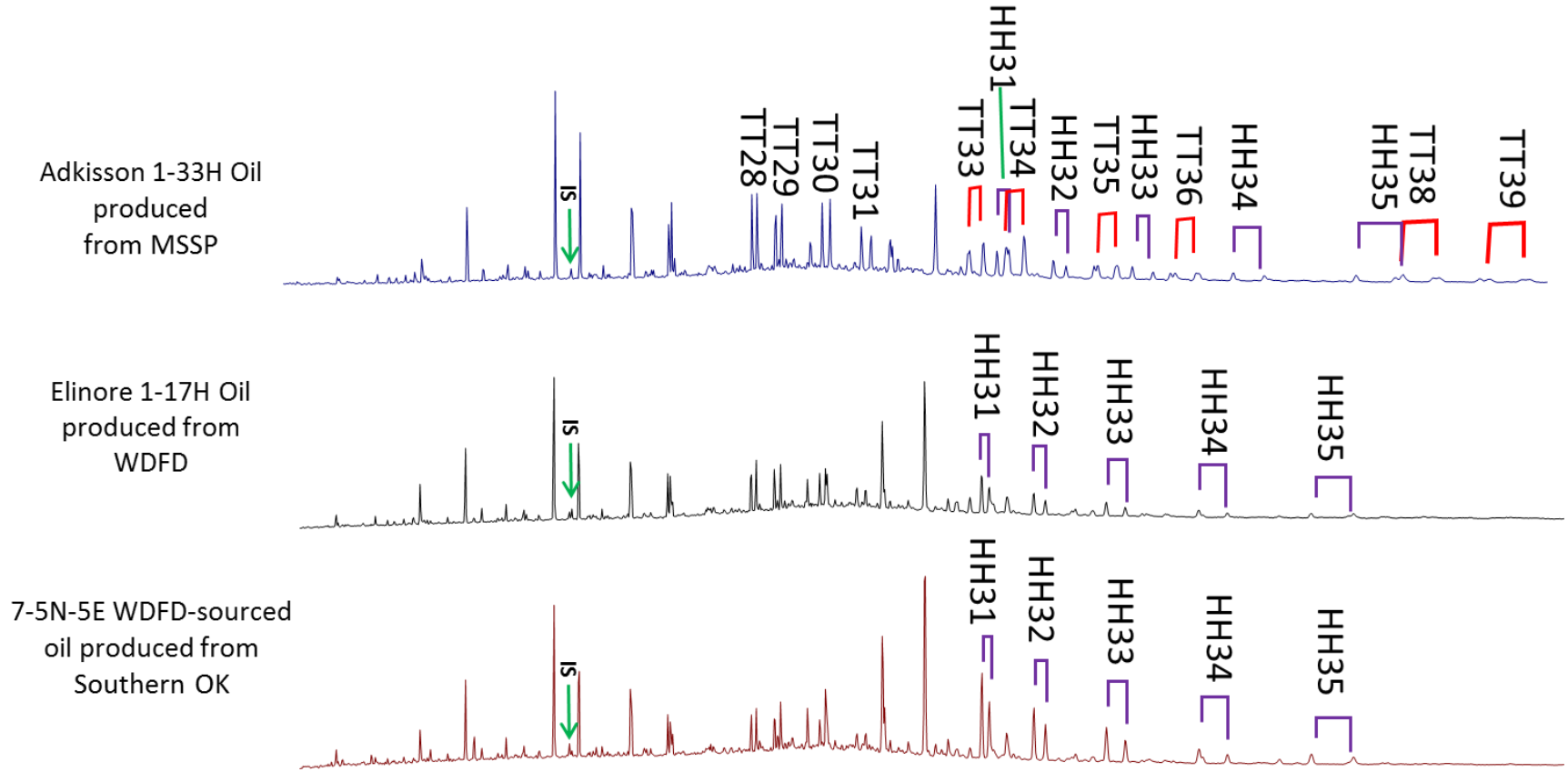

Figure 70. SIM *m/z* 191.3 mass chromatograms showing distributions of terpanes (tricyclic terpanes and homohopanes) in the B&C fractions of the studied oil samples. Red brackets denote tricyclic terpane (TT) isomers and purple brackets denote homohopane (HH) isomers.

5.2.2.2 Pentacyclic terpanes (Hopanes)

All of the oil samples analyzed have H29/H30 hopane ratio values lower than 0.60. When compared to the $C_{35}S/C_{34}S$ hopanes ratio, the H29/H30 can help identify source facies of oils and extracts (Figure 71). This plot suggests most of the oil samples in this study are of marine shale origin (Figure 71).

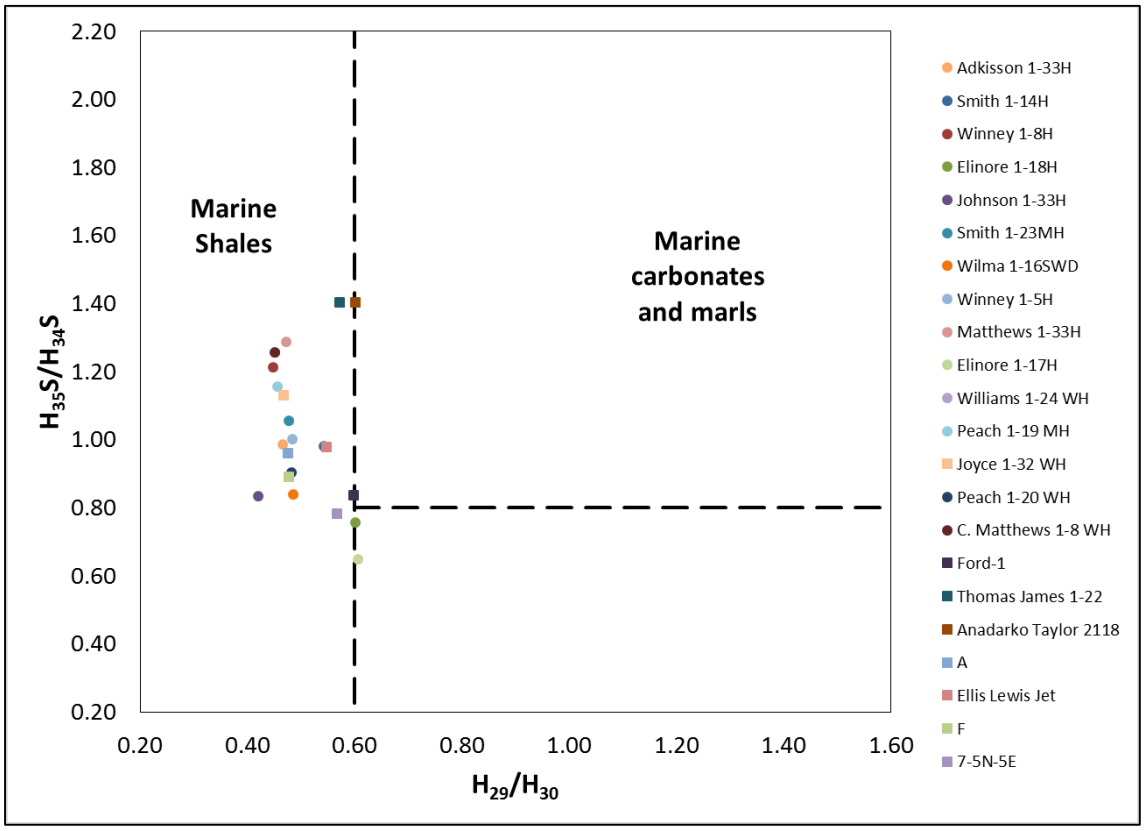

Figure 71. Plot of $C_{35}S/C_{34}S$ homohopanes versus 30-Nor/C_{30} hopane suggest most of the oil samples in this study are of marine shale origin (Dotted lines are used as a guide and do not represent fixed fields on the diagram. Plot template from Peters et al. 2005)

From the plots of homohopane distributions some oil samples show strong C_{35} homohopane elevation, including: Matthews 1-33H, Winney 1-8H, Smith 1-23MH, Peach 1-19MH, Wion 1-29WH; some show mild C_{35} homohopane elevation, including:

Adkisson 1-33H, Peach 1-20WH; and some show stair-like pattern, including: Joyce 1-32WH, Peach 1-20WH, Elinore 1-17H, and Elinore 1-18H. Besides C_{35} elevation, some show C_{32} elevation as well, like Winney 1-5H, Wilma 1-16SWD, Peach 1-19MH, Smith 1-14H (Figure 72).

From the plots of homohopane distributions for the Woodford-sourced oil samples produced in Southern Oklahoma (Figure 72) only one oil sample, Ellis Lewis Jet, shows strong C_{35} homohopane elevation; the others all show mild C_{35} homohopane elevation, including: Ford-1, "F", 7-5N-5E, "A", and Thomas James 1-22. In terms of C_{31}-C_{34} homohopanes distribution patterns, they all show a commonly found stair-like pattern. Since we already know these oils were sourced by the Woodford, a commonly found stair-like pattern in C_{31}-C_{34} homohopanes distribution with a mild C_{35} elevation would be suggested as a homohopane distribution characteristic for a typical Woodford-sourced oil. Based on that, Joyce 1-32WH, Peach 1-20WH, Elinore 1-17H, and Elinore 1-18H share more of the "Woodford-sourced oil" pattern. The other oil samples either have a strong C_{35} elevation, which may relate to highly reducing environment or marine carbonate source rock; or have a C_{32} elevation, which may suggest another oil family.

Gammacerane, a C_{30} triterpane, was tentatively identified in all of the oil samples in this study but coeluted with C_{34} (22R)-Tricyclic terpanes (Cheilanthanes 22R) in most of the oil samples. The occurrence of gammacerane in these oil samples suggests that regional hypersaline conditions and water stratification may have developed during deposition of their source rocks. This observation positively correlated with the low Pr/Ph ratios (section 4.1.4.2) and the predominance of the ββ steranes over the αα steranes

(Appendix D), which were reported to be associated with hypersalinity (ten Haven et al., 1988).

5.2.2.3 Diahopane

Based on the C_{30}- diahopane/hopane ratios on the map (Figure 73), it is clear that tight oil samples can be divided into two groups: Group A clusters the three samples in the eastern-most region of the study area with diahopane/hopane ratio below 0.10, including Joyce 1-32 WH, Elinore 1-17 H and Elinore 1-18 H; and Group B encompasses the fourteen oil samples located closer to the Nemaha Uplift with a diahopane/hopane ratio above 0.10. The oils produced in southern Oklahoma, which have been reported to be sourced from the Woodford Shale (Jones and Philp, 1990), have an average diahopane/hopane ratio of 0.10, which is closer to that of the three oil samples in the eastern-most region of the study area. Since this ratio is probably indicative of source rock lithology (clay content) as discussed previously in section 4.2.2.4, this observation may suggest the possible source rocks for the oils with low diahopane/hopane ratios, including Joyce 1-32 WH, Elinore 1-17 H, Elinore 1-18 H and the oils produced in southern Oklahoma, were deposited under clay-poor environment, while the source rocks for the oils with higher diahopane/hopane ratios, which were produced in the proximity of the paleo-Nemaha Uplift, were deposited under clay-rich environment.

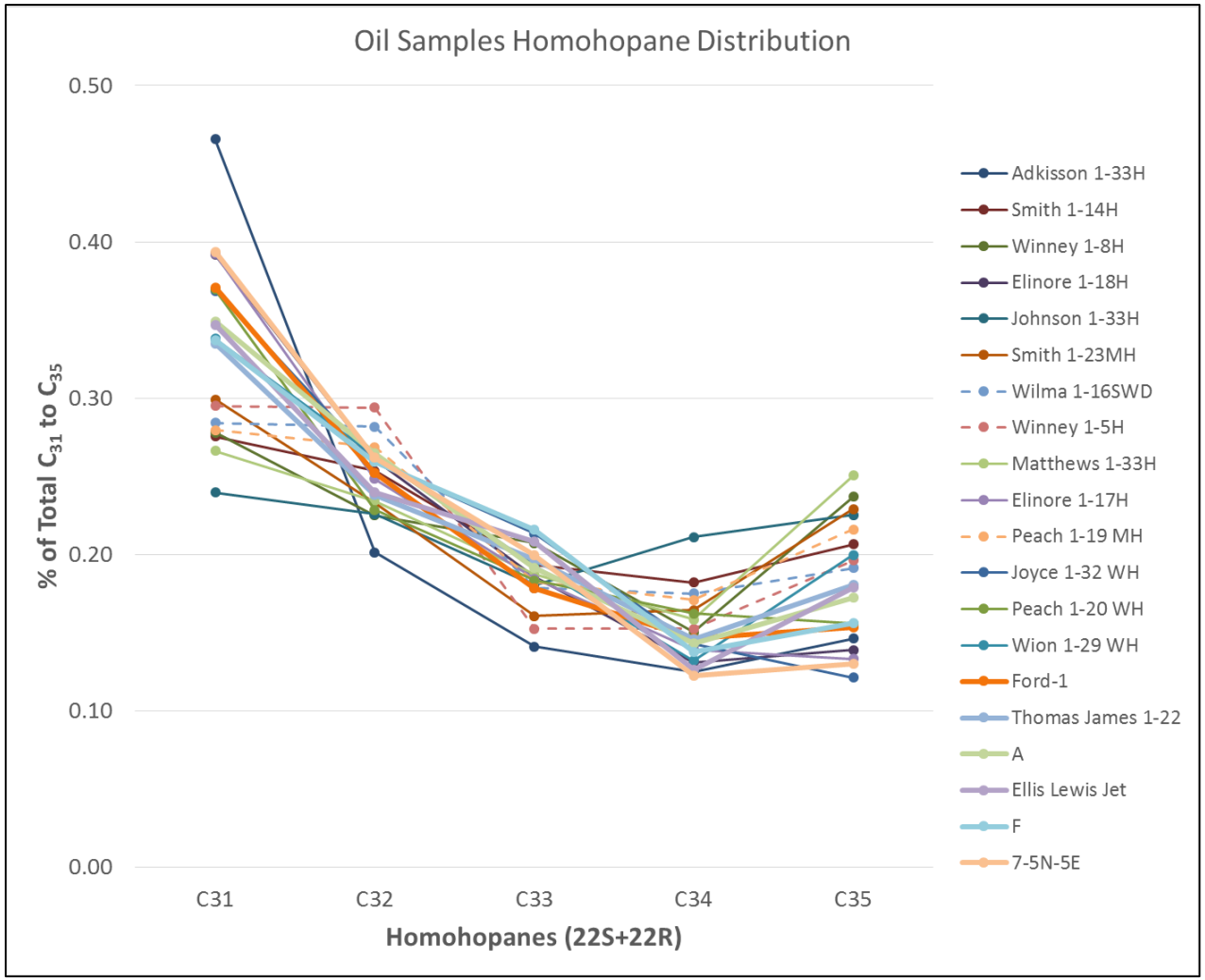

Figure 72. Homohopanes distributions for the oil samples in this study (Plot template from Picha and Peters, 1998

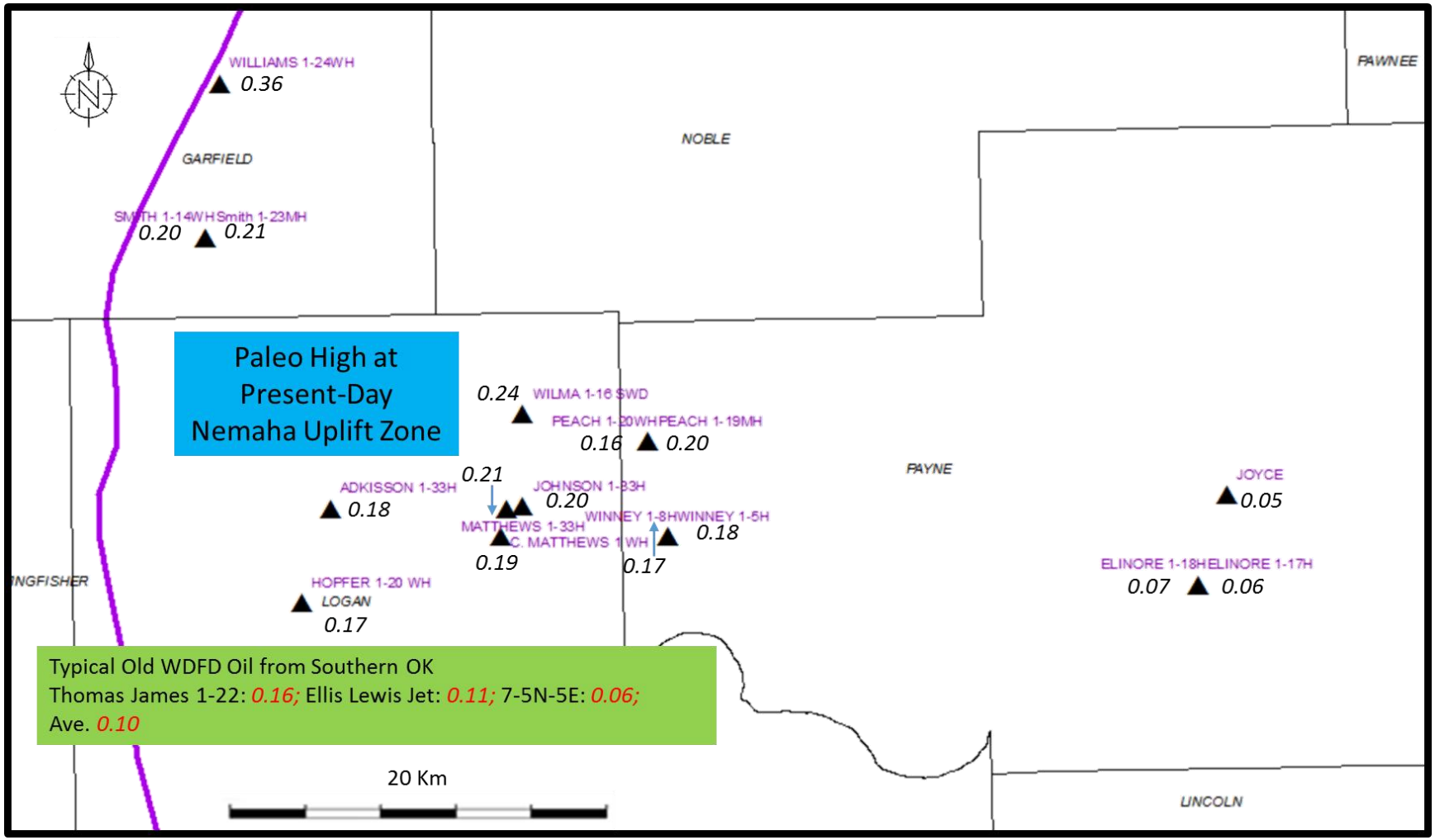

Figure 73. Map of Logan and Payne with C_{30} diahopane/C_{30} hopane ratios for the tight oil samples (condensates not shown due to this ratio couldn't be measured)

5.2.3 Isorenieratane and related compounds (m/z 134)

Analysis of paleorenieratanes and isorenieratanes was performed on the aromatic fractions of the oils by SIM/GC-MS using the ion *m/z* 134.1 (Figure 74). Identification of these compounds was achieved by comparison with reference mass chromatograms published by Brown and Kenig (2004); Schwark and Frimmel (2004); Miceli Romero and Philp (2012), and Connock (2015). The compounds identified in this study were paleorenieratane (P) and isorenieratane (I), the origin of which and their indicative of PZA have been discussed in section 4.2.3. The paleorenieratanes were in high abundance in all of the analyzed oil samples, whereas the isorenieratanes were present in lower concentrations. Attention should be paid to the fact that those Woodford-sourced oil samples produced from Southern Oklahoma contain abundant paleorenieratane and isorenieratane as well, including: Ford-1, "A", "F", and Thomas James 1-22. The condensate, Lingo 1-13WH, has no paleorenieratane nor isorenieratane detected but alkyl benzenes probably attributing to its high maturity. The tight oil samples, including: C. Matthews 1-8WH, Hopfer 1-20WH, Joyce 1-32WH, and Peach 1-20Wh, all have detectable paleorenieratane and isorenieratane. Since paleorenieratane and isorenieratane found in both the Woodford and Mississippian extracts as discussed previously in section 4.2.3, these two compounds are not Woodford source-specific. Therefore, the identification of these compounds do not help grouping the oil families in this study but suggest the PZA occurred within the water column during deposition the of the possible source rock for the oils in this study.

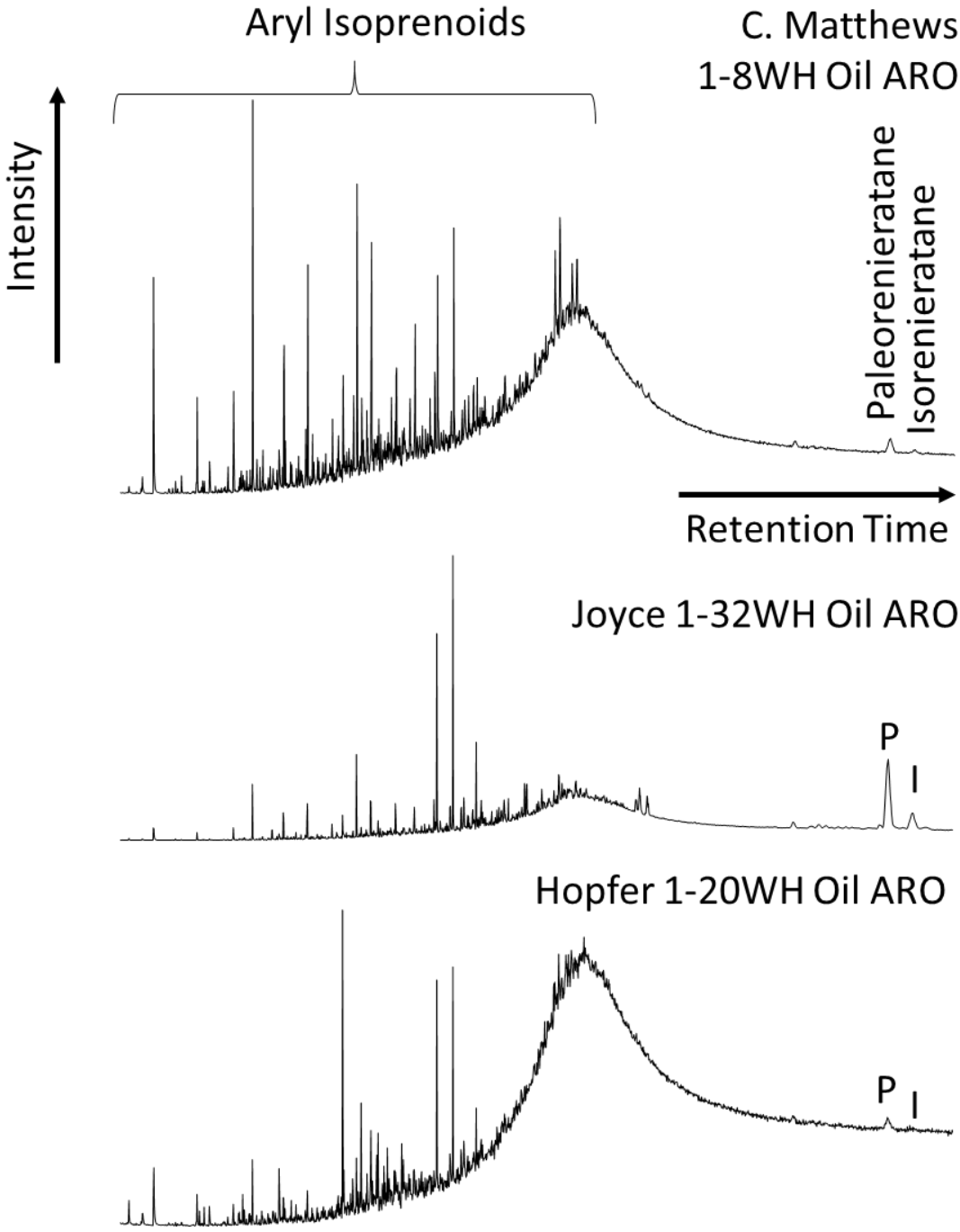

Figure 74. Mass chromatograms of *m/z* 134 of the aromatic fractions showing the aryl isoprenoids and isorenieratane related compounds distributions of the oil samples in this study (P = Paleorenieratane; I = Isorenieratane)

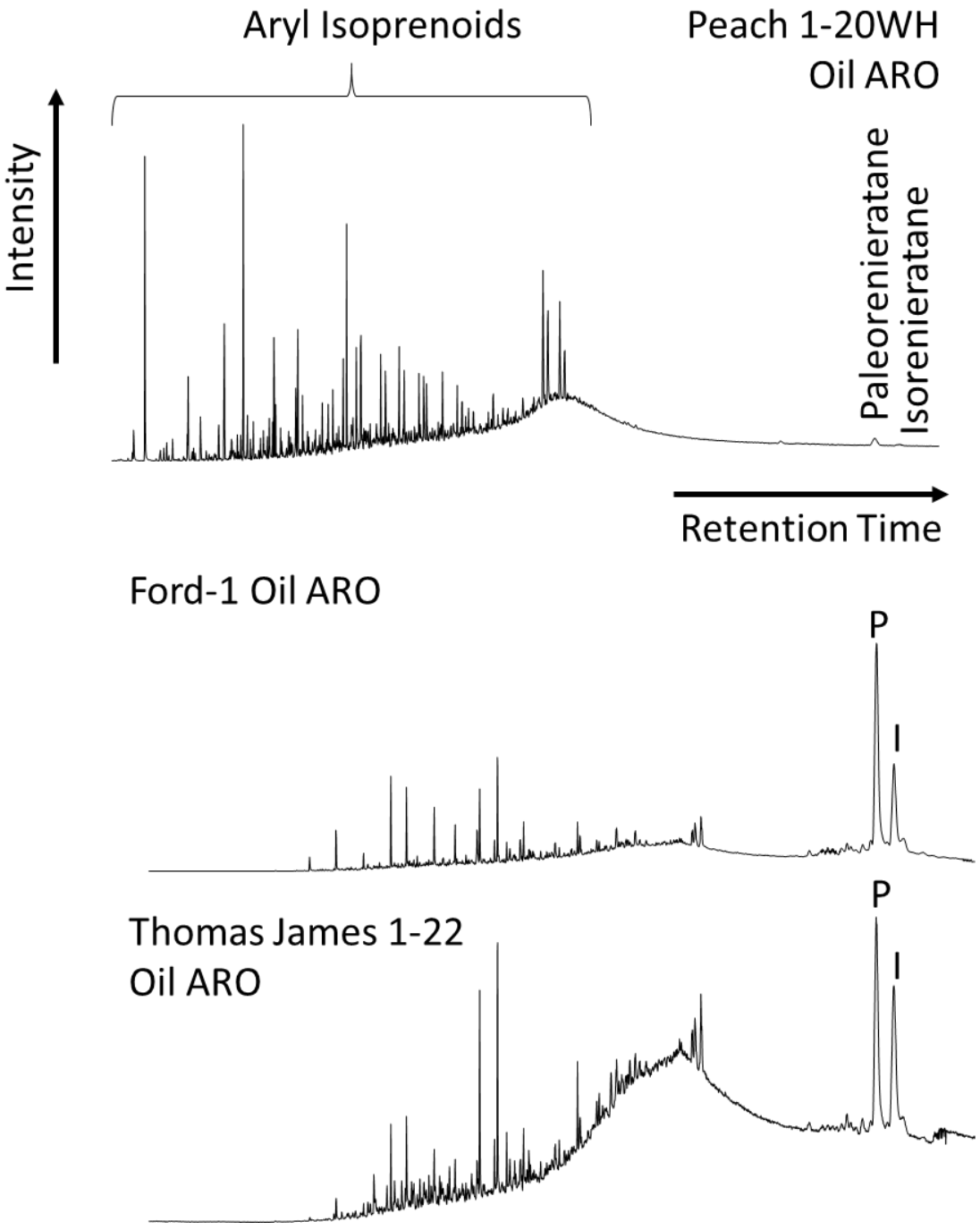

Figure 75. Mass chromatograms of *m/z* 134 of the aromatic fractions showing the aryl isoprenoids and isorenieratane related compounds distributions of the oil samples in this study (P = Paleorenieratane; I = Isorenieratane)

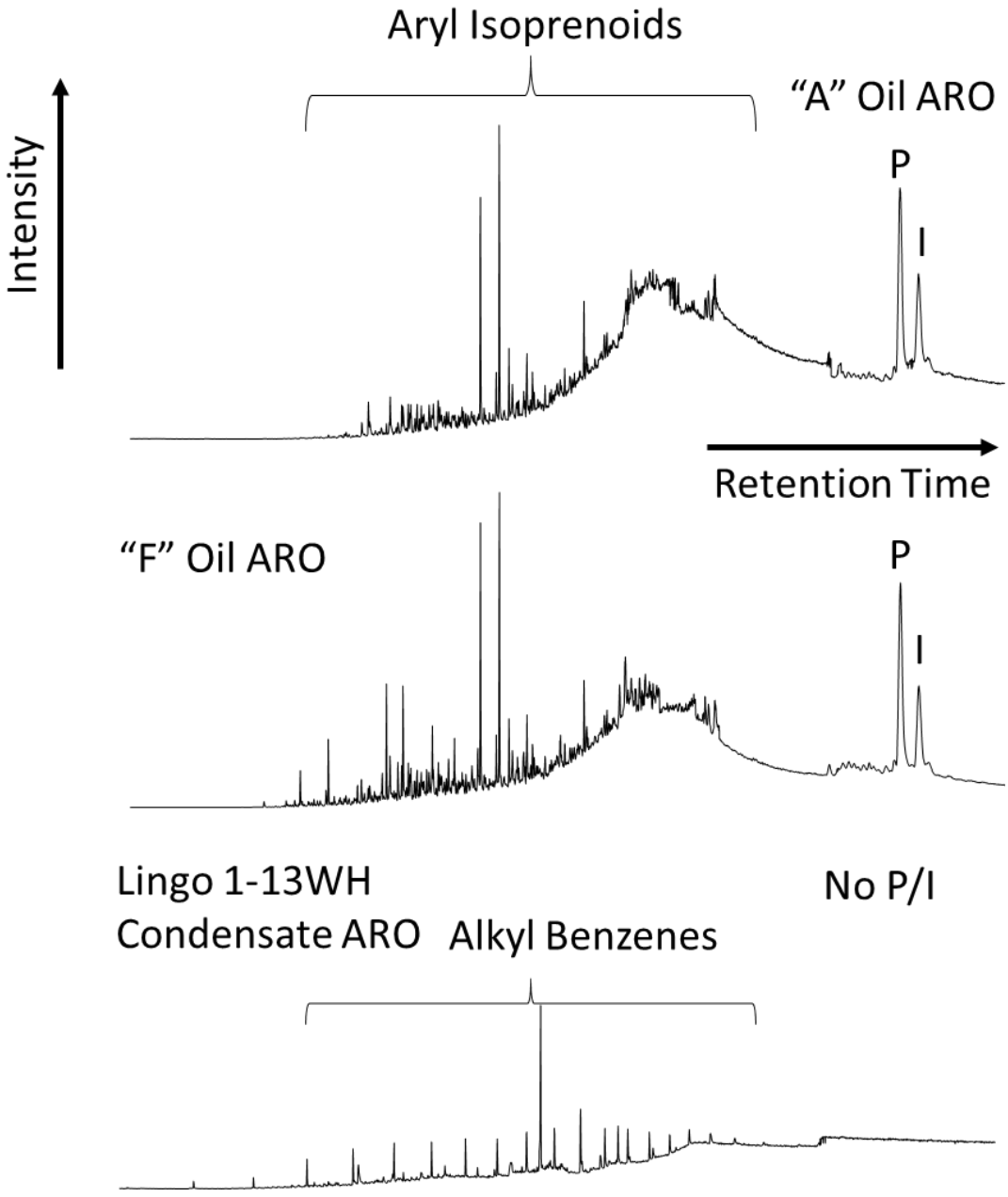

Figure 76. Mass chromatograms of *m/z* 134 of the aromatic fractions showing the aryl isoprenoids and isorenieratane related compounds distributions of the oil samples in this study (P = Paleorenieratane; I = Isorenieratane)

5.2.4 Monoaromatic Steroids (m/z 253)

Monoaromatic steroids (MAS) are a group of biomarkers derived from sterols containing a side-chain double bond during diagenesis (Riolo et al., 1986; Moldowan and Fago, 1986). These biomarkers were identified in the B&C fraction of Woodford Shale rock extracts and oils through SIM/GC-MS by analysis of the *m/z* 253.3 ion (Figure 77). The ternary diagram of C_{27}, C_{28}, and C_{29} monoaromatic steroids (MAS) has been used to characterize the variations in depositional environments, and are particularly useful for distinguishing marine from non-marine oils (Moldowan et al., 1985). Moldowan et al. found the oils and rock extracts derived from marine organic matter contain greater amounts of C_{28} MAS than those of non-marine origin. In addition, Moldowan et al. (1985) observed that some oils derived from marine carbonate source rocks contain higher amounts of C_{29} MAS than that from marine shale. The Woodford rock extracts and the tight oil samples have a greater concentration of C_{28} MAS, followed by C_{27} and C_{29} MAS and their distributions are similar to that of the regular steranes (Figure 78), indicating a marine source for these samples.

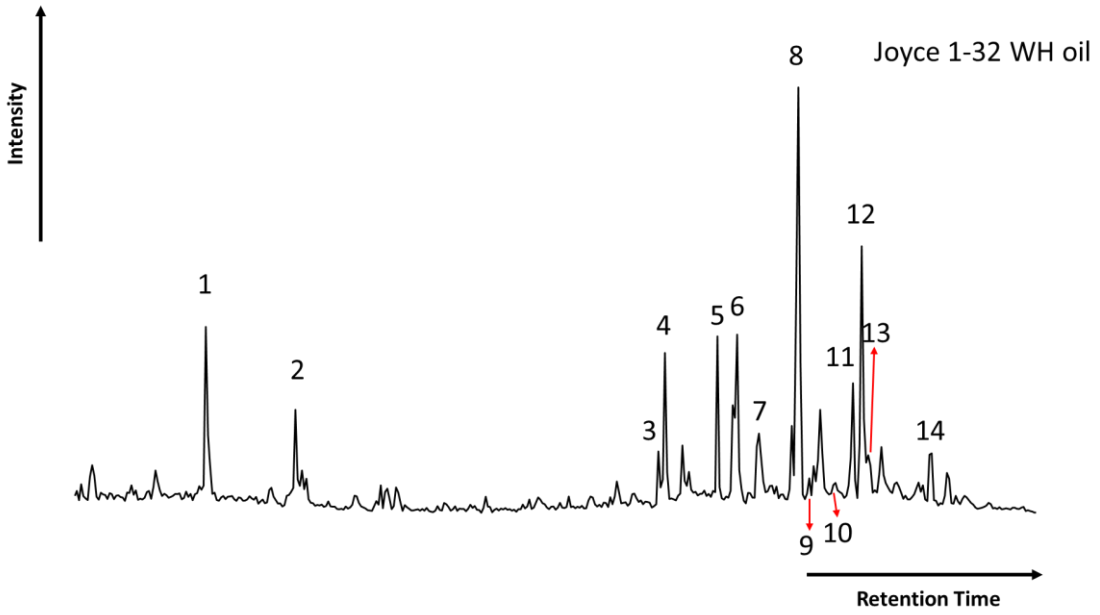

Figure 77. SIM mass chromatograms of the *m/z* 253.3 ion showing distributions of the monoaromatic steroids (MAS) in the B&C fractions of Joyce 1-32 WH oil. Peak identification is presented in Table 14.

Table 14. Identification of monoaromatic steroids (MAS) in the SIM *m/z* 253.3 mass chromatogram of the B&C fractions

Peak #	Compound
1	C_{21} Pregnane
2	C_{22} 20-Methylpregnane
3	C_{27} 5β-Cholestane 20S
4	C_{27} Diacholestane 20S
5	C_{27} Monoaromatic steroid
6	C_{28} 5β-Ergostane 20S + C_{28} Diaergostane 20S
7	C_{27} 5α-Cholestane 20R
8	C_{28} 5α-Ergostane 20S
9	C_{28} 5β-Ergostane 20R + C_{28} Diaergostane 20R
10	C_{29} 5β-Stigmastane 20S + C_{29} Diastigmastane 20S
11	C_{29} 5α-Stigmastane 20S
12	C_{28} 5α-Ergostane 20R
13	C_{29} 5β-Stigmastane 20R + C_{29} Diastigmastane 20R
14	C_{29} 5α-Stigmastane 20R

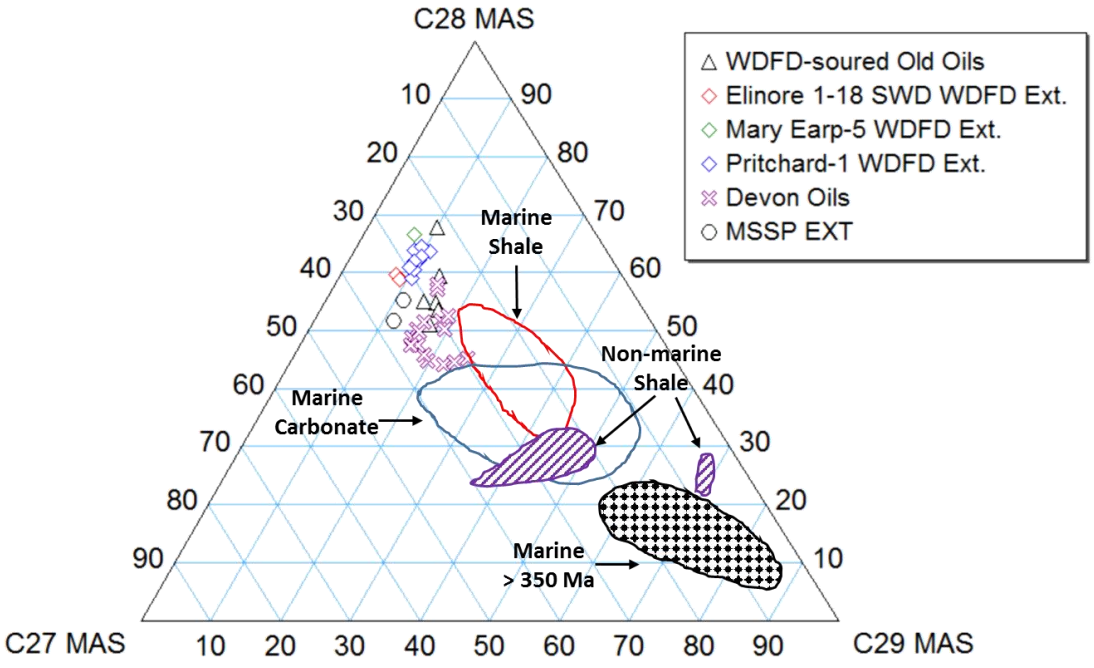

Figure 78. Ternary diagram of C_{27}, C_{28}, and C_{29} monoaromatic steroids for the Woodford Shale rock extracts and oils (Plot template from Moldowan et al., 1985)

5.3 Evaluation of Oil and Condensates Thermal Maturity

5.3.1 Steranes (m/z 217)

The map of Logan and Payne with C_{29} ββ/(ββ+αα) sterane ratios of the tight oil samples (Figure 79) shows the variation of thermal maturity for these oils. Devon oil samples can be divided into two groups: the eastern most three samples with C_{29} ββ/(ββ+αα) sterane ratios below 0.60, equivalent to the beginning of oil window, include Joyce 1-32 WH, Elinore 1-17 H and Elinore 1-18 H, and the fourteen oil samples located closer to the Nemaha Uplift have C_{29} ββ/(ββ+αα) sterane ratios above 0.60, which are more mature than the eastern most three ones. The oils produced in southern Oklahoma, which have been reported to be sourced from the Woodford Shale, have an average C_{29}

ββ/(ββ+αα) sterane ratio of 0.43, which is closer to that of the eastern most three oil samples.

5.3.2 Terpanes (m/z 191)

5.3.2.1 Hopanes

All of the oil samples show their 22S/(22S+22R) ratio (0.57-0.62; Table 9) approaching to the equilibrium range (early oil window). While, from the other biomarker maturity proxies, such as C_{29} ββ/(ββ+αα) sterane ratio, it is reasonable to infer the majority of the sample sets are equivalent to around 0.80% Ro. Therefore the 22S/(22S+22R) ratio couldn't give additional thermal maturity information on the oils.

5.3.2.2 Ts and Tm

The oil samples could be divided into two groups based on their Ts/(Ts+Tm) ratios (Figure 81): the three oil samples in the eastern-most region of the study area with Ts/(Ts+Tm) ratio below 0.50, equivalent to the beginning of oil window, including Joyce 1-32 WH, Elinore 1-17 H and Elinore 1-18 H, and the fourteen oil samples located closer to the Nemaha Uplift with Ts/(Ts+Tm) ratio above 0.60, which are more mature. The oils produced in southern Oklahoma, which have been reported to be sourced from the Woodford Shale, have an average Ts/(Ts+Tm) ratio of 0.43, which is closer to that of the three oil samples in the eastern-most region of the study area.

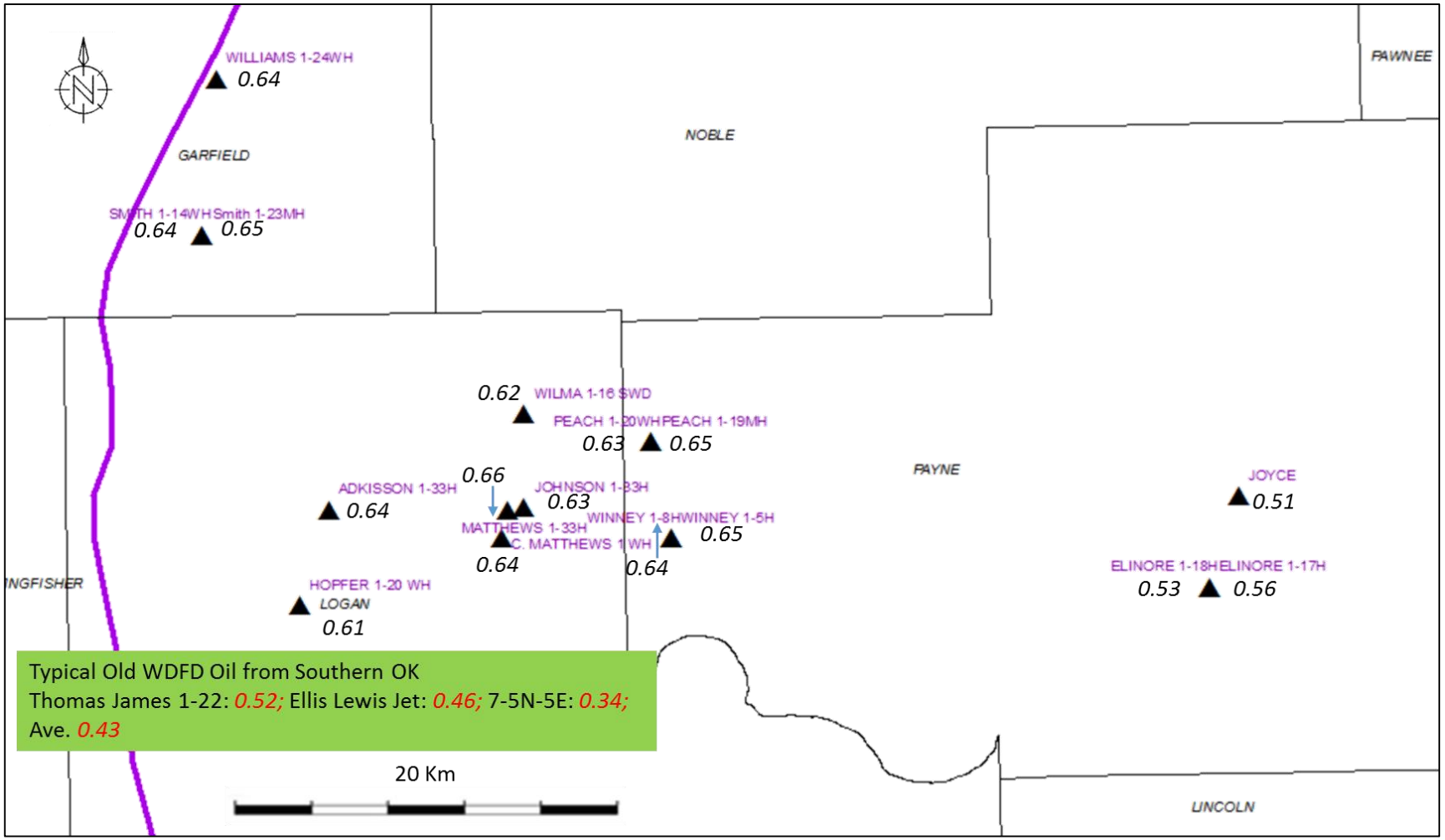

Figure 79. Map of Logan and Payne with C_{29} ββ/(ββ+αα) steranes ratios of the oil samples showing variations in thermal maturity (Condensates not shown due to this ratio couldn't be measured)

Table 15. Average C_{32} 22S/(22S+22R) hopane ratios for the Woodford Shale rock extracts and the studied oils

Sample	C_{32} 22S/(22S+22R)
Adkisson 1-33H	0.61
Smith 1-14H	0.56
Winney 1-8H	0.57
Elinore 1-18H	0.59
Johnson 1-33H	0.64
Smith 1-23MH	0.63
Wilma 1-16SWD	0.61
Winney 1-5H	0.69
Matthews 1-33H	0.59
Elinore 1-17H	0.61
Peach 1-19 MH	0.56
Joyce 1-32 WH	0.59
Hopfer 1-20 WH	0.62
Peach 1-20 WH	0.56
C. Matthews 1-8 WH	0.62
Ford-1	0.60
Thomas James 1-22	0.60
Anadarko Taylor 2118	0.60
A	0.54
Ellis Lewis Jet	0.58
F	0.59
7-5N-5E	0.59

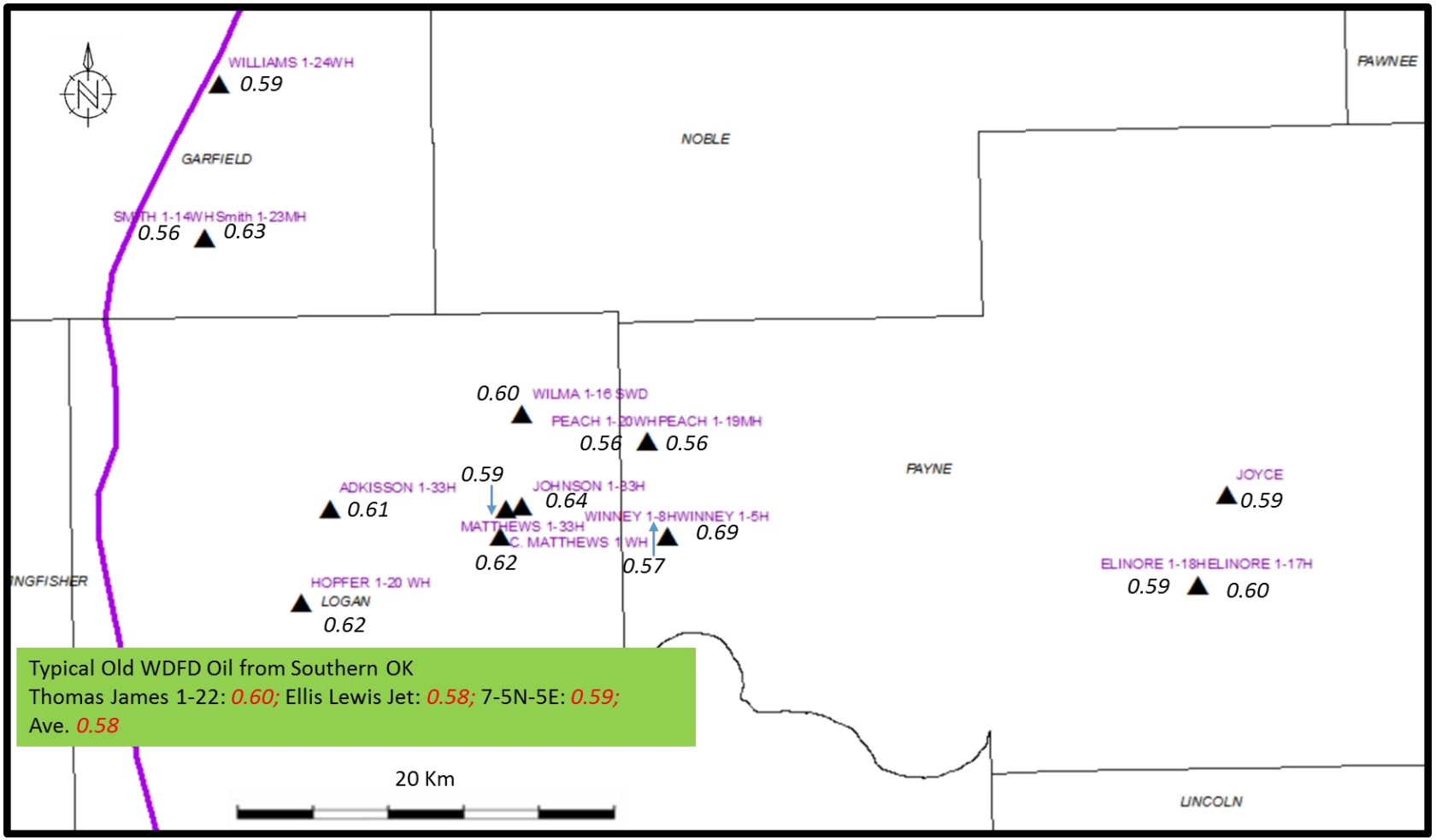

Figure 80. Map of Logan and Payne with C_{32} 22S/(22S+22R) hopanes ratios of the oil samples showing thermal maturity (Devon condensates not shown due to this ratio couldn't be measured)

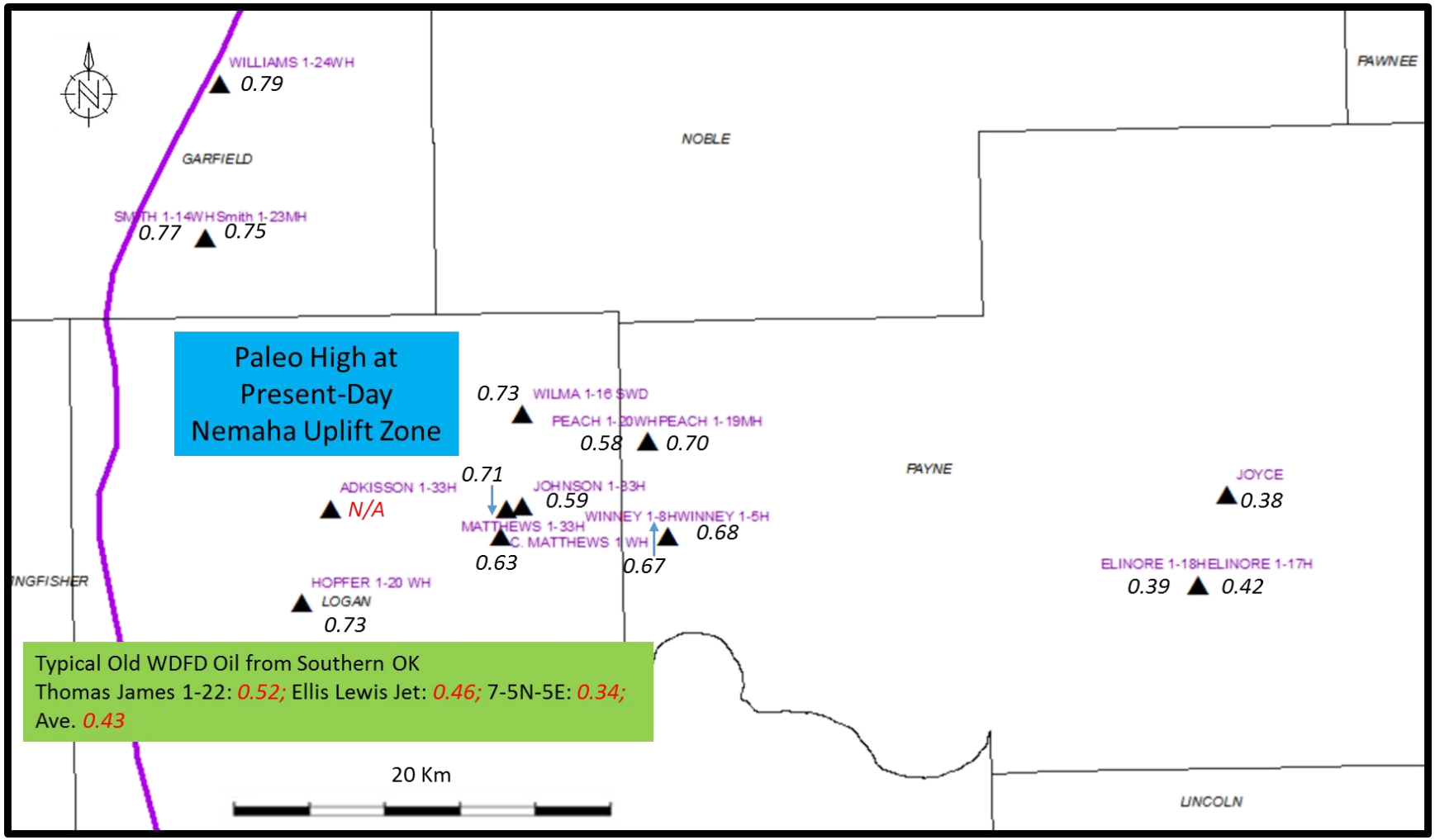

Figure 81. Map of Logan and Payne with Ts/Tm ratios of the oil samples showing variation in thermal maturity (Devon condensates not shown due to this ratio couldn't be measured)

5.3.3 Phenanthrenes

Phenanthrenes and methylphenanthrenes were determined in the aromatic fraction of the oils by SIM/GC-MS monitoring the ions *m/z* 178.3, 192.3, and 206.3 (Figure 82). Values of MPI-1 ratios were obtained for the oil samples in this study, and used to calculate a vitrinite reflectance equivalent (Rc) values (Figure 82). The equation from Radke and Welte (1981), corresponding to low maturity levels, was used to calculate vitrinite reflectance (Rc) values for the oil samples. The vitrinite reflectance equivalent (Rc) values calculated from the MPI-1 parameters of the oil samples in this study show no trend covary with any geological or geochemical parameters (Figure 83). This anomalous behavior may be attributed to the oil samples not being derived from a single source or the fact that the MPI-1 and vitrinite reflectance relationship was based on shale and coals containing type III organic matter (Radke and Welte, 1983). As a result it may not be directly applicable for the other types of source rocks, such as the Woodford Shale, containing mainly type II organic matter. Lithology of the source rock can also affect MPI ratios. It was reported by Cassani et al. (1988) that high MPI-1 values corresponded to high carbonate content in the La Luna Shale but did not reflect the true maturity level. A hypothesis to interpret the anomalous behavior of MPI in these oil samples would be they are not single sourced and may have contributions from carbonate sources, or more mature oils, accounting for the high MPI-1 values.

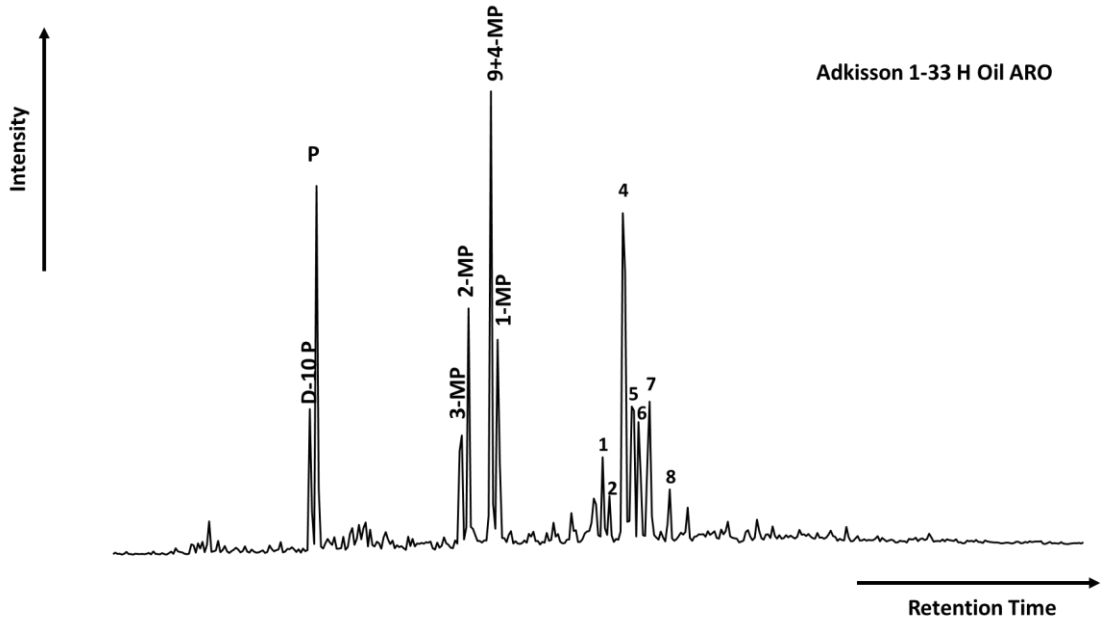

Figure 82. Summed mass chromatograms of *m/z* 178.2, 192.3, 206.3, 188.2 ions showing distributions of phenanthrenes compounds in the aromatic fractions of sample Adkisson 1-33 H Oil. Peak identifications are presented in Table 11.

Table 16. Calculated vitrinite reflectance (Rc) for the studied oils from MPI-1 values

Sample	R_c
Adkisson 1-33H	0.75
Smith 1-14H	1.03
Winney 1-8H	0.85
Elinore 1-18H	0.83
Johnson 1-33H	0.90
Smith 1-23MH	0.77
Wilma 1-16SWD	0.76
Winney 1-5H	1.03
Matthews 1-33H	1.12
Elinore 1-17H	0.79
Williams 1-24 WH	0.77
Peach 1-19 MH	0.76
Joyce 1-32 WH	0.74
Hopfer 1-20 WH	0.74
Peach 1-20 WH	0.73

C. Matthews 1-8 WH	0.73
Ford-1	0.74
Thomas James 1-22	0.81
Anadarko Taylor 2118	0.90
A	0.71
Ellis Lewis Jet	0.82
F	0.88
7-5N-5E	0.79

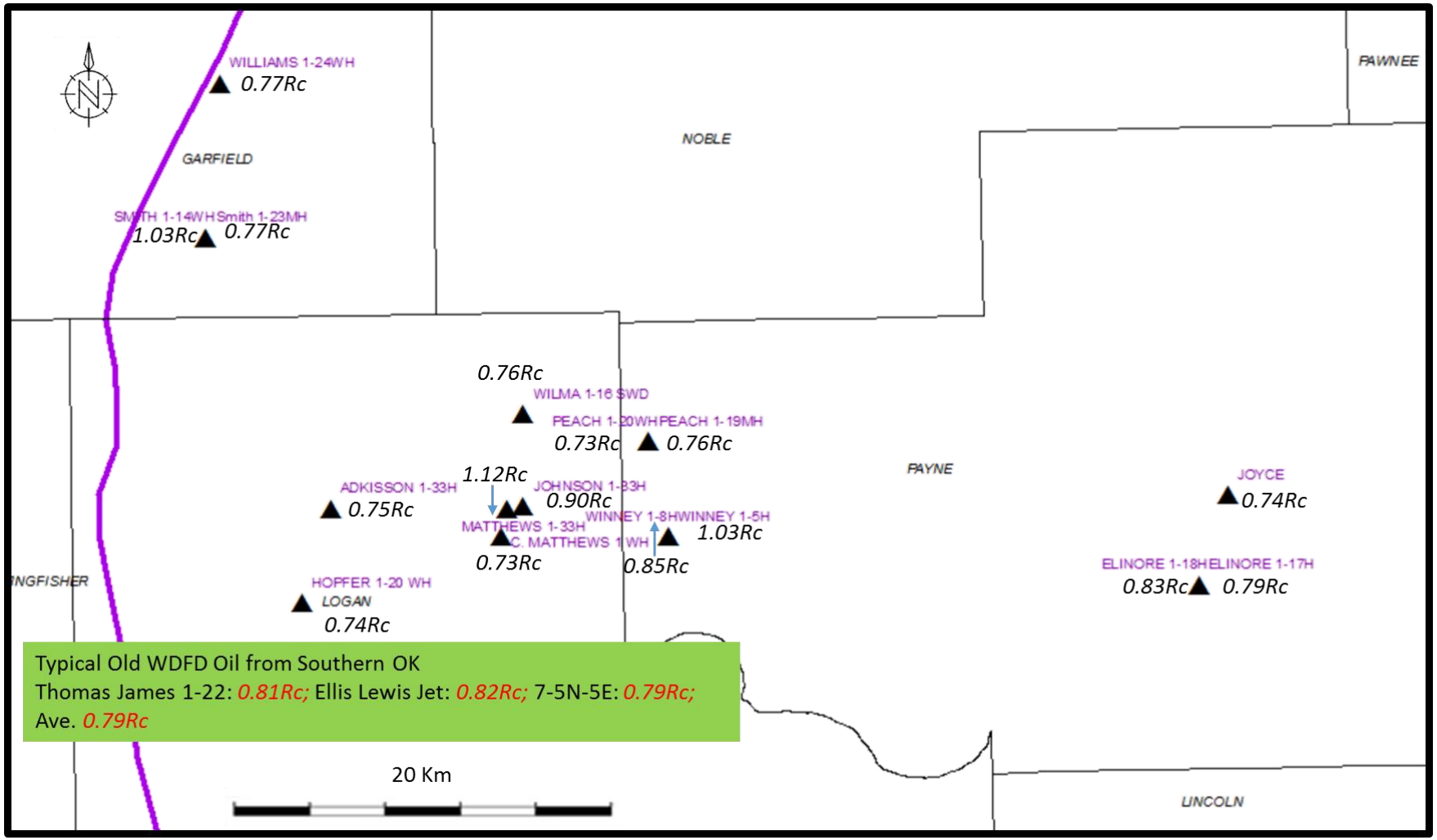

Figure 83. Map of Logan and Payne with the vitrinite reflectance equivalent (Rc) values calculated from the MPI ratios of the oil samples showing variation in thermal maturity (Condensates are not shown due to lack of phenanthrenes)

5.3.3 Diamondoids

Diamondoids are rigid fused-ring cycloalkanes with a diamond-like structure that shows high thermal stability initially and commonly precipitate directly from the gas to the solid phase during crude oil production (Williams et al., 1986; Wingert, 1992; Lin and Wilk, 1995; Dahl et al., 2002). Diamondoids are not found in living organisms but have been demonstrated to be synthesized from a wide variety of organic precursors via Lewis acid catalysis (Schleyer, 1990; Wingert, 1992). Considering their ubiquitous occurrence, even in oils of low thermal maturity, this mode of formation suggests diamondoids form by hydrocarbon rearrangement reactions on acidic clay minerals in petroleum source rocks (Schleyer, 1990). Unlike biomarkers, diamondoids in crude oils and source rocks are structurally very different from their probable precursors in living organisms. Diamondoids are good thermal maturity indicators for high-maturity samples (over 1.1% Ro) when biomarker thermal maturity indicators already thermally destroyed. Diamondoids are more applicable as thermal maturity proxies (Sweeney and Burnham, 1990; Dahl et al., 1999), although they were reported to be able to distinguish rock extracts from different organofacies (Schulz et al., 2001). Various diamondoid maturity parameters have been proposed to measure highly mature samples (Sweeney and Burnham, 1990; Dahl et al., 1999), but their usefulness remains unclear. A representative work was Chen et al. (1996) used two diamondoid indices, methyladamantane index (MAI) and methyldiamantane index (MDI), to evaluate the thermal maturity of crude oils and condensates from several basins in China. MAI showed a better linear relationship related to VRo than MDI in his study, especially in the highly mature section (Ro > 2.0%).

In this study the condensate sample Wion 1-29 H with predominance of the admantanes in the detected key ion fragmentograms (*m/z* 136.1, 135.1, 149.1, 163.1, 177.1) was used as reference sample (Figure 84). Identification of the admantanes in the reference sample was performed by direct comparison in distributions of the admantanes in the reference sample at the key ion fragments with those published by Wingert et al. (1992). Subsequently, the reference sample was then used for the diamondoid identification of the other oil/condensate samples by matching retention time (Figure 85). Determination of the diamondoid ratios such as MAI (1-MA/(1-MA + 2-MA)) was conducted using peak areas. The formula, Rc = 3.27*MAI - 0.86, to calculate Rc (vitrinite reflectance equivalent) from MAI was courtesy of Dr. Thanh Nguyen (University of Oklahoma). The formula was obtained from the fitting curve between measured VRo and MAI of the original data sets published by Chen et al. (1996). It was not surprisingly observed Rc from MAI is out of the maturity scope of regular oils, therefore the majority of Devon tight oils are around 0.9%Ro, the tiny difference between which couldn't be resolved by MAI. Not surprisingly either to observe the Rc of Devon condensates are over 1.2% Ro and seems to increase towards the deep part of the Anadarko Basin following the regional dip of the Woodford Shale.

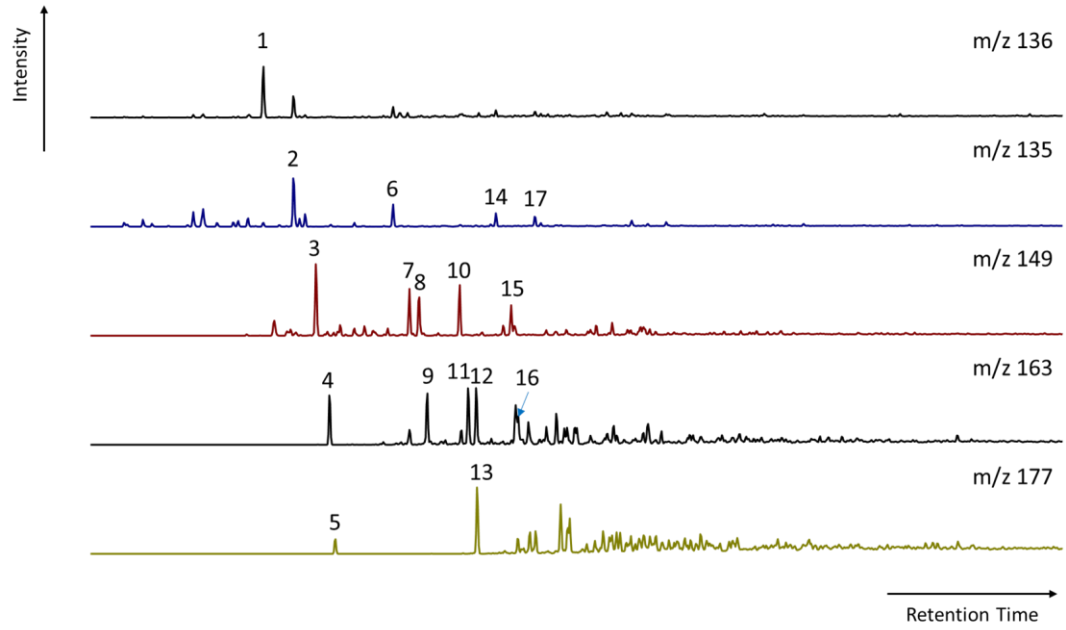

Figure 84. Mass chromatograms of *m/z* 136.1, 135.1, 149.1, 163.1, 177.1 ions showing distributions of adamantanes in the Wion 1-29H condensate

Table 17. Diamondoid hydrocarbon compounds identification

Peak #	Compound
1	Adamantane
2	l-Methyladamantane
3	1,3-Dimethyladamantane
4	1,3,5-Trimethyladamantane
5	1,3,5,7-Tetramethyladamantane
6	2-Methyladamantane
7	1,4-Dimethyladamantane, *cis*
8	1,4-Dimethyladamantane, *trans*
9	1,3,6-Trimethyladamantane
10	1,2-Dimethyladamantane
11	1,3,4-Trimethyladamantane, *cis*
12	1,3,4-Trimethyladamantane, *trans*
13	1,2,5,7-Tetramethyladamantane
14	1-Ethyladamantane
15	1-Ethyl-3-methyladamantane
16	l-Ethyl-3,5-dimethyladamantane
17	2-Ethyladamantane

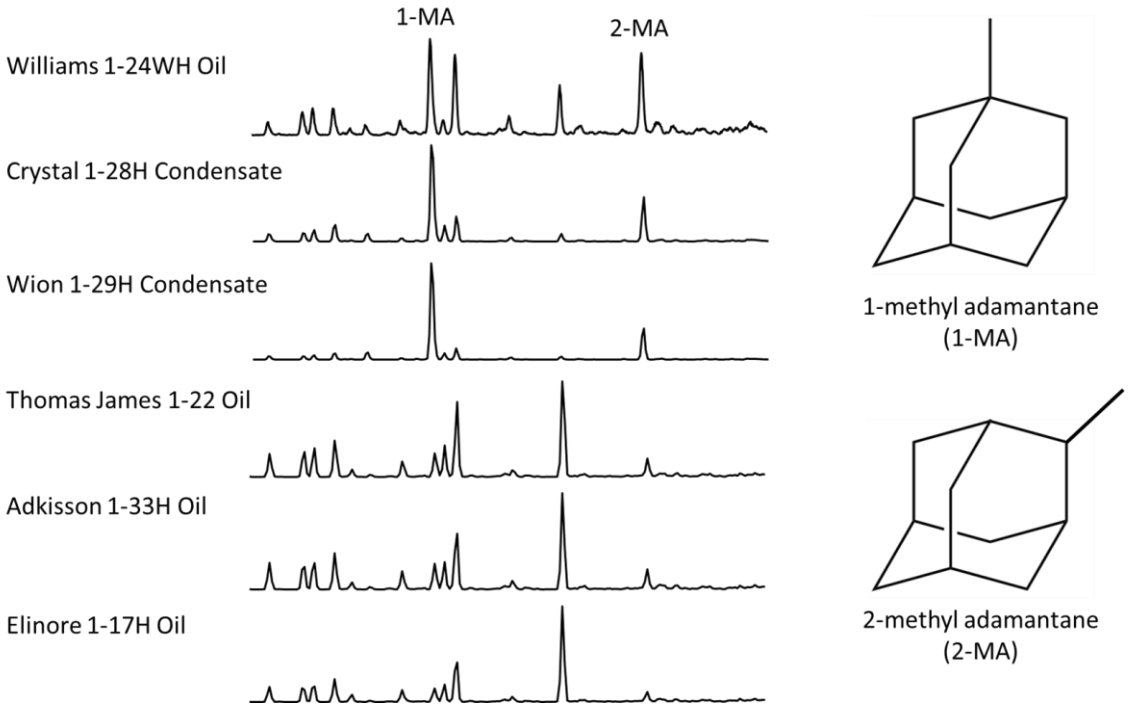

Figure 85. Mass chromatograms of *m/z* 135.1 ion showing distributions of adamantanes in the whole oil of representative crude oils and condensates

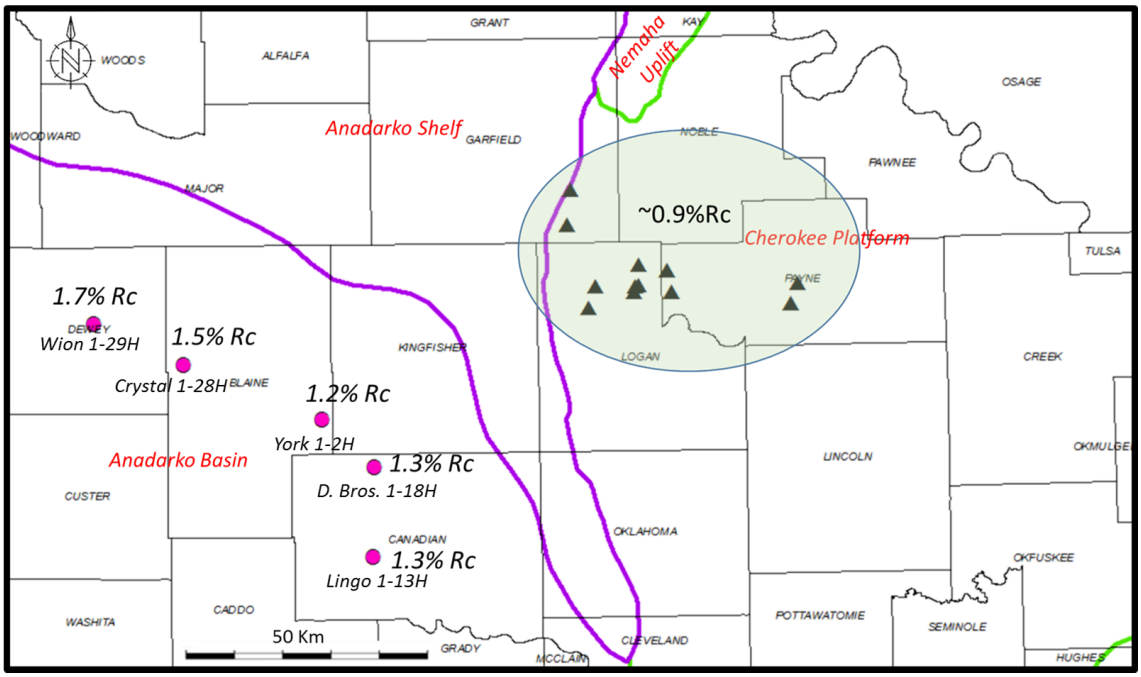

Figure 86. Devon oils & condensates sample location map with Rc (Vitrinite Reflectance calculated) from MAI (Methyl Adamantane Index) (oils denoted by black triangles; condensates denoted by pink dots)

Table 18. Rc of Devon oils & condensates calculated from MAI

Sample	Status	MAI	R_c
Adkisson 1-33H	Oil	0.59	1.1
Smith 1-14H	Oil	0.58	1.0
Winney 1-8H	Oil	0.57	1.0
Elinore 1-18H	Oil	0.61	1.1
Johnson 1-33H	Oil	0.60	1.1
Smith 1-23MH	Oil	0.58	1.0
Winney 1-5H	Oil	0.57	1.0
Matthews 1-33H	Oil	0.53	0.9
Elinore 1-17H	Oil	0.63	1.2
Williams 1-24 WH	Oil	0.54	0.9
Peach 1-19 MH	Oil	0.54	0.9
Joyce 1-32 WH	Oil	0.54	0.9
Hopfer 1-20 WH	Oil	0.54	0.9
Peach 1-20 WH	Oil	0.54	0.9
C. Matthews 1-8 WH	Oil	0.55	0.9
Thomas James 1-22	Oil	0.62	1.2
A	Oil	0.56	1.0
Ellis Lewis Jet	Oil	0.62	1.2
F	Oil	0.56	1.0
7-5N-5E	Oil	0.62	1.2
Crystal 1-28H	Condensate	0.72	1.5
York 1-2H	Condensate	0.64	1.2
Wion 1-29H	Condensate	0.77	1.7
D. Bros. 1-18H	Condensate	0.64	1.3
Lingo 1-13H	Condensate	0.67	1.3

5.4 Oil-Oil and Oil-Source Rock Correlations

5.4.1 Oil-Oil Correlations

The data sets of this study provide a very good chance to investigate whether the oils produced from the horizontal well drilled into the Mississippian strata are genetically related to the oil produced from the horizontal well drilled into the Woodford Shale at a

same well site. The three well locations shown on the map in Figure 87 are: Winney 1-5H, a horizontal well drilled into the Woodford Shale; Winney 1-8H, a horizontal well drilled into the Mississippian Limestone overlying the Woodford Shale from the same well site; and Winney 1-8 SWD, a vertical well drilled into the Arbuckle Group carbonates for salt water disposal, with the Mississippian and Woodford cores samples at several depth. Oil samples were obtained from Winney 1-5H and 1-8H.

The SIM *m/z* 191.3 and *m/z* 217.3 ion mass chromatograms of two oils were shown below (Figure 88): Winney 1-5H oil produced from Woodford and Winney 1-8H oil from Mississippian. By comparing their fingerprints, these two oils' terpanes and steranes characteristics are almost exactly the same. Taking into account of these three wells are drilled from a same well site, only 12 meters apart, it's reasonable to infer the overlying Mississippian strata is connected with the Woodford Shale in this well.

If these two oils originate from a same source, what is that source: Woodford, Mississippian, or some other source? The similarity of *m/z* 191 traces of Winney 1-5H oil, Winney 1-8 SWD 5155' Mississippian rock extract and Winney 1-8 SWD 5360' Woodford rock extract were compared in Figure 89. It would appear that the oil more closely resembles the Mississippian extract than the Woodford extract. Several characteristics of the Winney 1-8 SWD 5155 ft Mississippian rock extract in terms of *m/z* 191 traces are consistent with that from the Mississippian rock in Oklahoma reported by Wang (1993) and Kim (1999). These characteristics include: 1) extended tricyclic terpanes (TT33 ~ TT39) dominate over homohopanes (H31 ~ H35); 2) very abundant tricyclic terpanes (TT28 ~ TT31); 3) C_{30} diahopane moderately detectable (C_{30} 17α-diahopane/hopane ratio around 0.20). As discussed in the section 4.2.2, Kim (1999)

proposed the relative abundance of extended tricyclic terpanes (> C_{30}) over homohopanes (C_{31} ~ C_{35}) appeared to be associated with several events of algal bloom during deposition of the Lower Mississippian Limestone. Wang (1993) and Kim (1999) found dominant extended tricyclic terpanes are diagnostic biomarker fingerprints for the Lower Mississippian Limestone in the Anadarko Basin. Based on these findings, the oils contain significant Mississippian source contribution.

Very similar terpanes and steranes fingerprints (Figure 91) between two oils produced from Woodford and Mississippian from a same well site were also observed in the center of Payne County with the well locations shown in Figure 90. From the SIM *m/z* 191.3 mass chromatograms, several characteristics can be documented: 1) extended tricyclic terpanes (TT33 ~ TT38) could be detected until C_{38} but homohopanes (H31 ~ H35) still dominate over extended tricyclic terpanes (TT33 ~ TT38) in this range (Table 19); 2) abundant tricyclic terpanes (TT19 ~ TT31), especially distinct distribution pattern of TT28 ~ TT31 (Table 19); 3) Ts/Tm ratio close to 1; 4) C_{30} diahopane almost non-detectable compared to C_{30} regular hopane (C_{30} 17α-diahopane/hopane ratio around 0.05). Taking into account that these three wells are drilled at a same well site, only about 10 meters apart, it's reasonable to infer that the overlying Mississippian strata is connected with the Woodford Shale in this well.

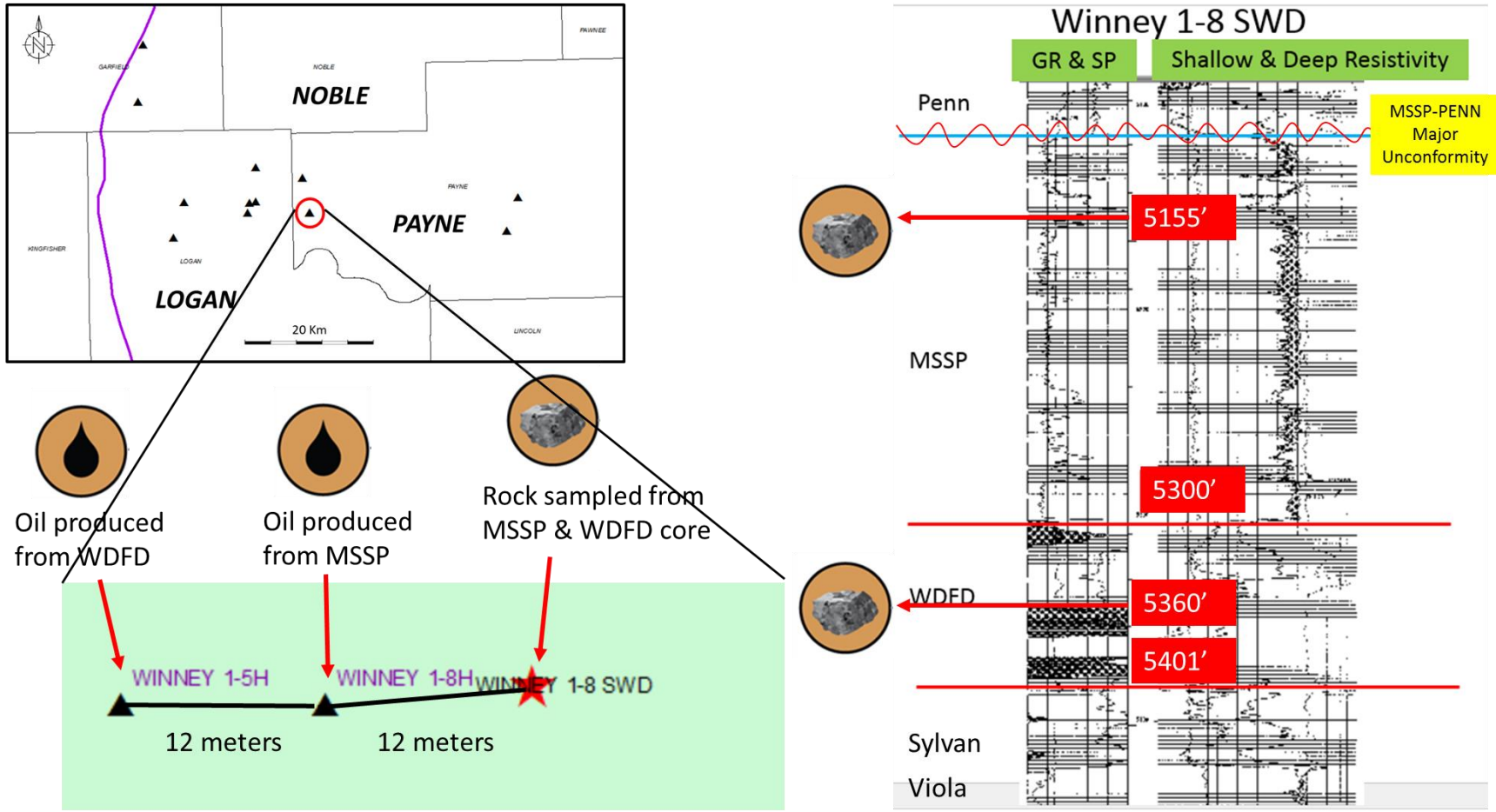

Figure 87. Map of Logan and Payne with the well site highlighted for oil-to-oil correlation study and the well log of Winney 1-8 SWD showing Mississippian and Woodford rock sampling depth

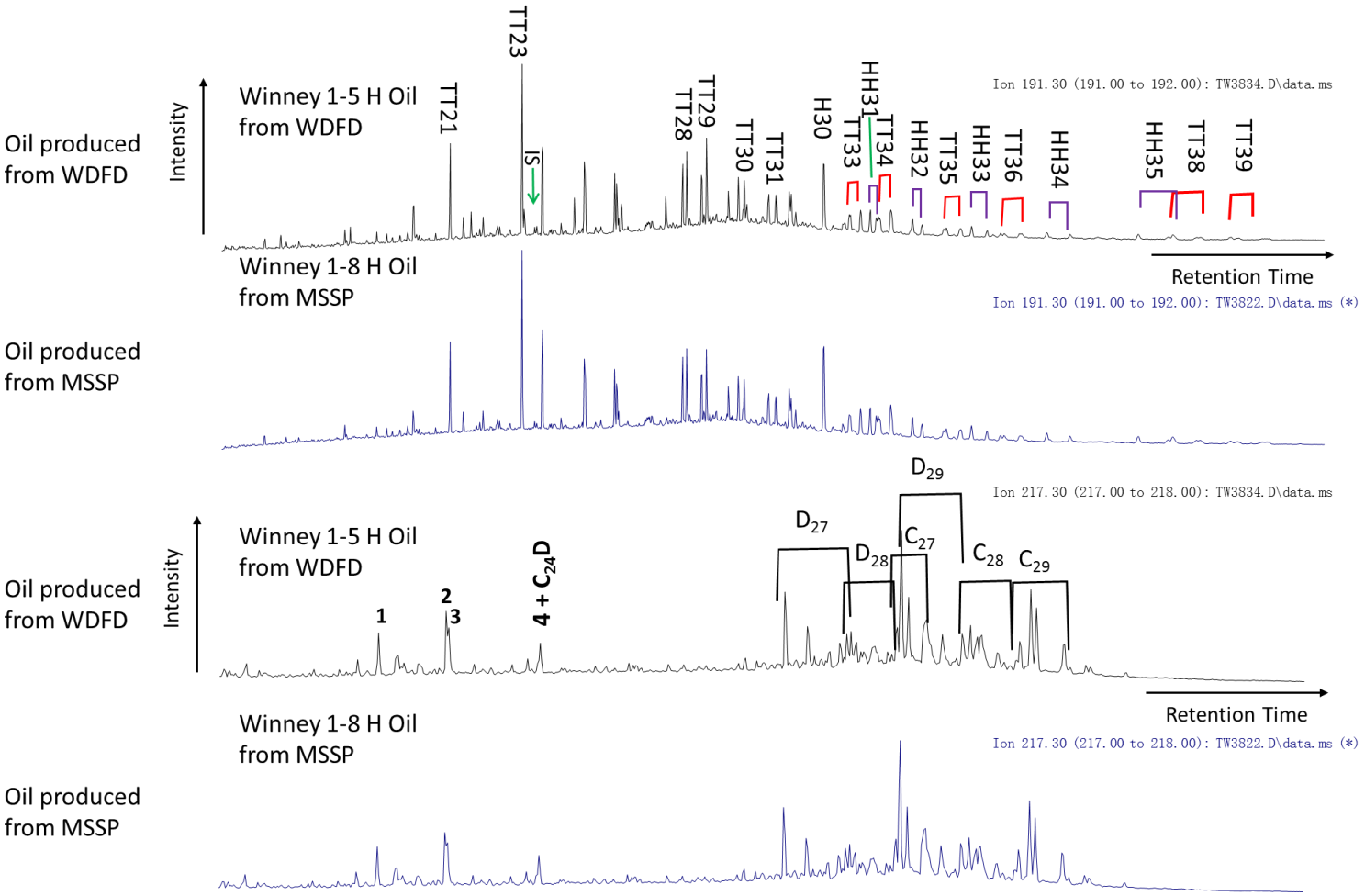

Figure 88. Correlation between an oil produced from the Woodford Shale and an oil produced from the Mississippian Limestone at a same well site (Red brackets denote tricyclic terpane (TT) isomers and purple brackets denote homohopane (HH) isomers; Steranes peak identification is listed in Table 6)

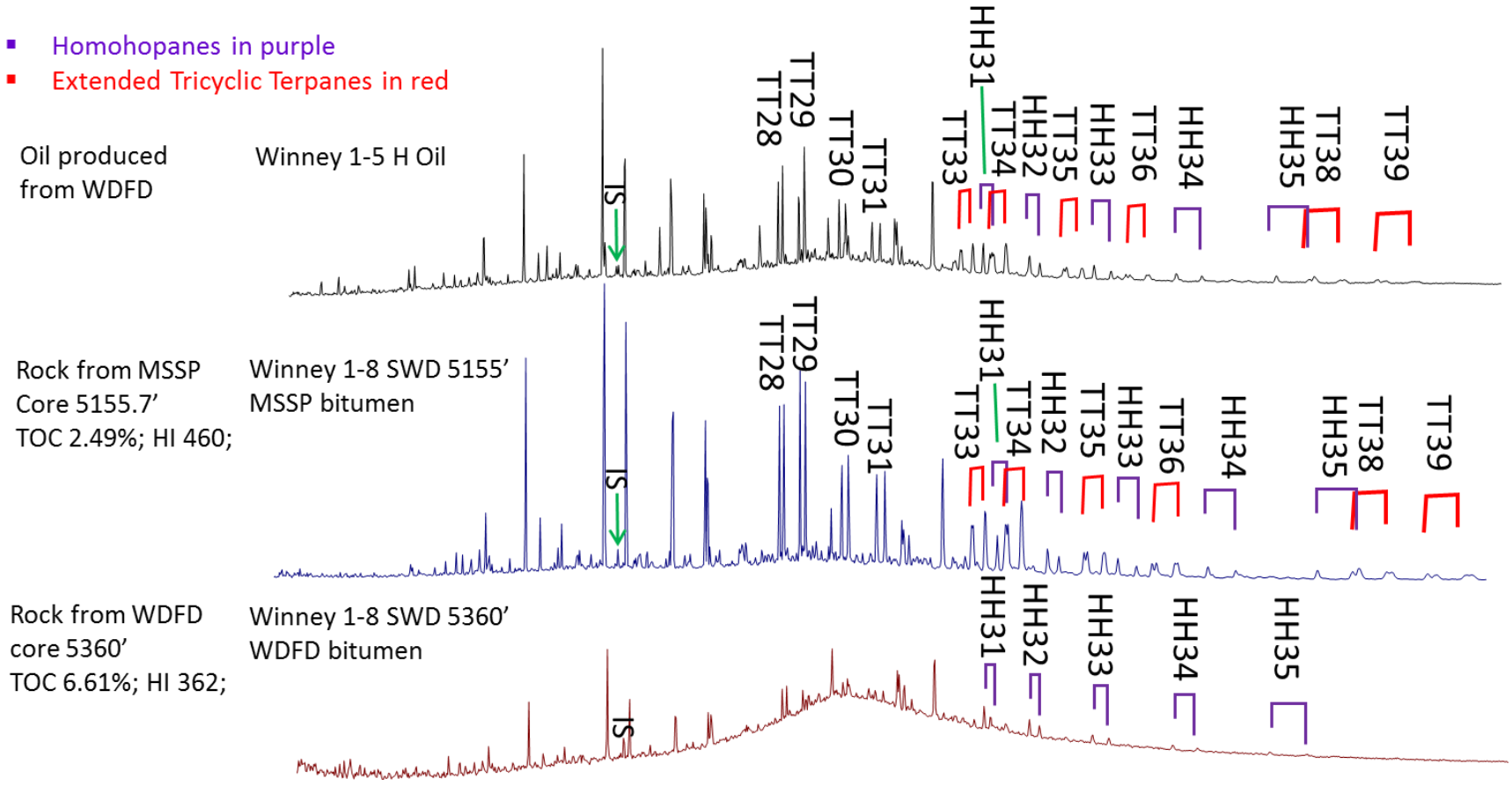

Figure 89. SIM *m/z* 191.3 mass chromatograms showing distributions of terpanes in the B&C fractions of the oil samples and rock extract (Red brackets denote tricyclic terpane (TT) isomers and purple brackets denote homohopane (HH) isomers)

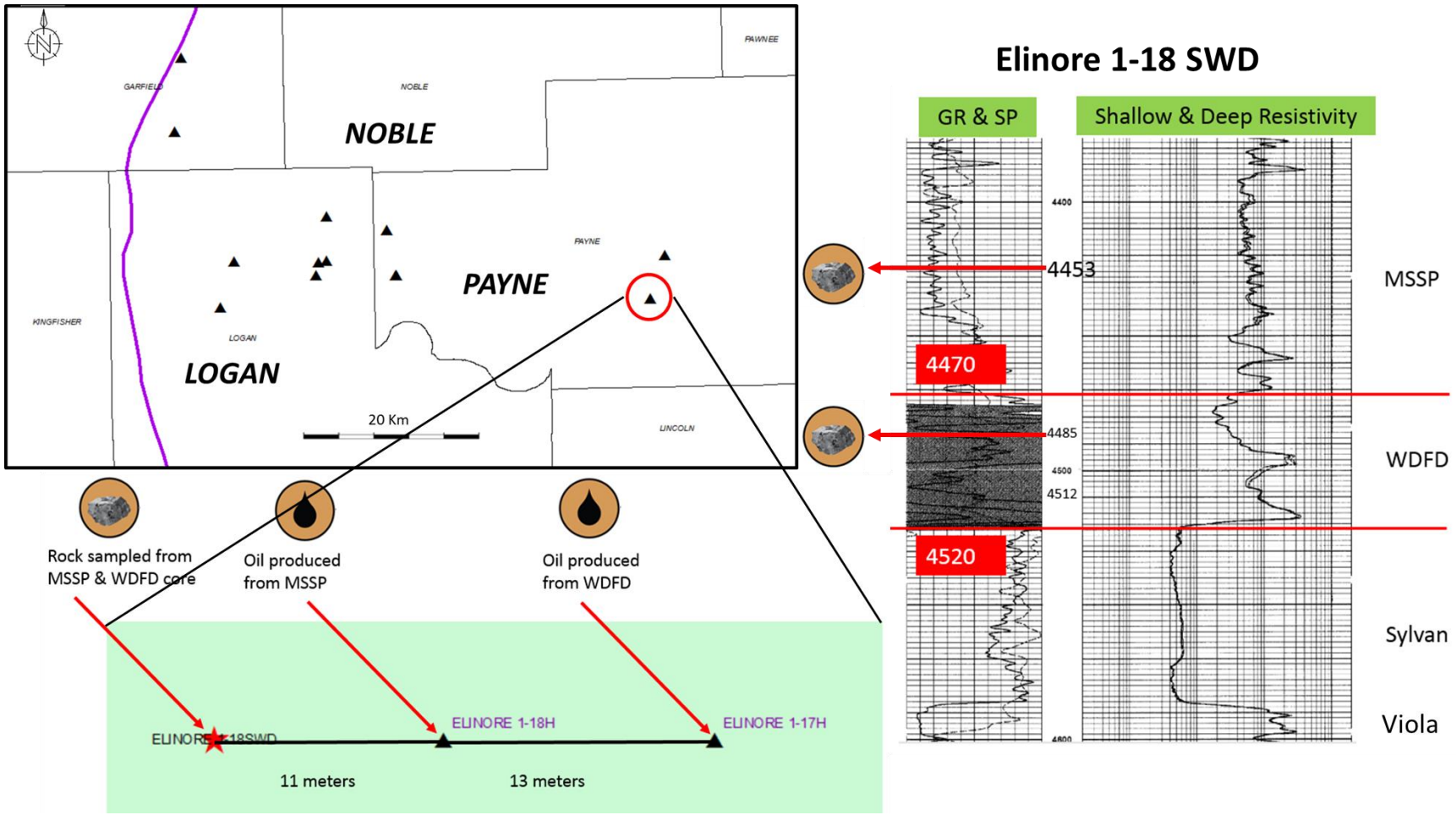

Figure 90. Map of Logan and Payne with the well site highlighted for oil-to-oil correlation study and the well log of Elinore 1-18 SWD showing the Mississippian and Woodford rock sampling depth

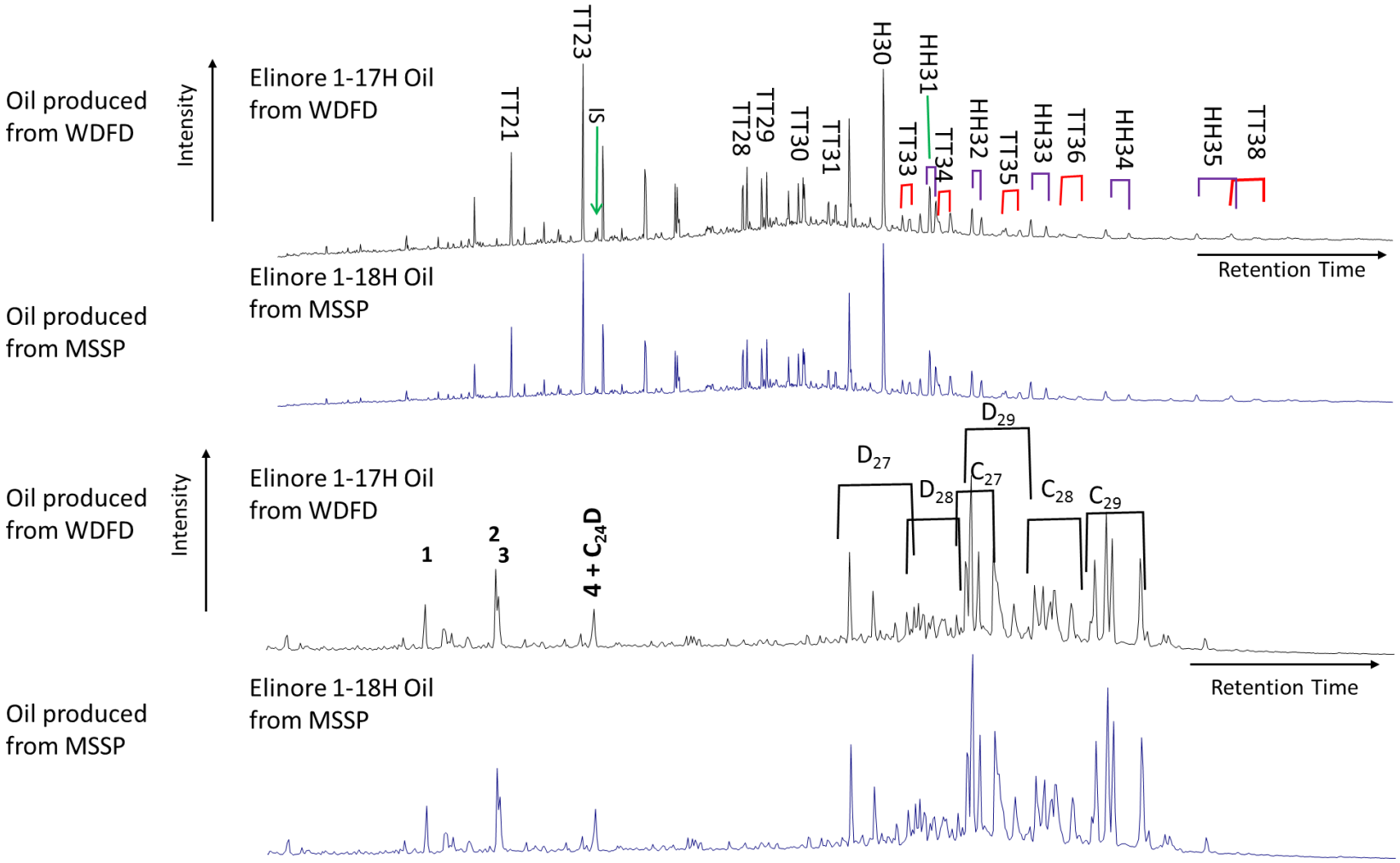

Figure 91. Correlation between an oil produced from the Woodford Shale and an oil produced from the Mississippian Limestone at a same well site

Table 19. Absolute Concentrations of Terpanes (m/z 191) of the oils and rock extracts in Figure 90 (Concentrations are expressed as µg biomarkers/g TOC)

Well Name	TT19	TT20	TT21	TT22	TT23	TT24	TT25	TT26	24/4	TT28S	TT28R	TT29S	TT29R	Ts	TT30S	Tm	TT30R	TT31S	TT31R	H29	29Ts
Elinore 1-17H Oil	2	11	19	5	41	23	25	23	3	12	14	12	12	7	10	10	8	8	6	30	4
Elinore 1-18H Oil	9	34	58	15	119	72	73	68	10	39	42	39	40	22	30	35	26	27	21	104	15
Elinore 1-18 SWD 4453’	2	7	19	5	52	26	34	33	3	23	26	16	19	18	19	23	11	16	15	37	16
Elinore 1-18 SWD 4486’	2	3	8	2	14	5	6	7	2	3	3	2	1	6	2	5	2	2	1	13	4

Well Name	D30	H30	TT33R	H31S	H31R	TT34S	H32S	H32R	TT35S	TT35R	H33S	H33R	TT36S	TT36R	H34S	H34R	H35S	H35R
Elinore 1-18 SWD 4453’	11	92	18	36	24	0	30	22	25	18	21	14	20	21				
Elinore 1-18 SWD 4486’	3	15	2	4	4	0	4	3	2	2	2	1	2	1				

Well Name	D30	H30	TT33S	TT33R	H31S	H31R	TT34S	TT34R	H32S	H32R	TT35S	TT35R	H33S	H33R	TT36S	TT36R	H34S	H34R	H35S	TT38S	H35R	TT38R	TT39S	TT39R
Elinore 1-17H Oil	3	49	8	8	16	11	8	11	11	7	7	5	8	5	5	4	6	4	4	2	6	3	0	ND
Elinore 1-18H Oil	13	173	28	28	61	49	24	45	43	30	25	20	30	22	20	17	22	15	17	9	22	16	14	10

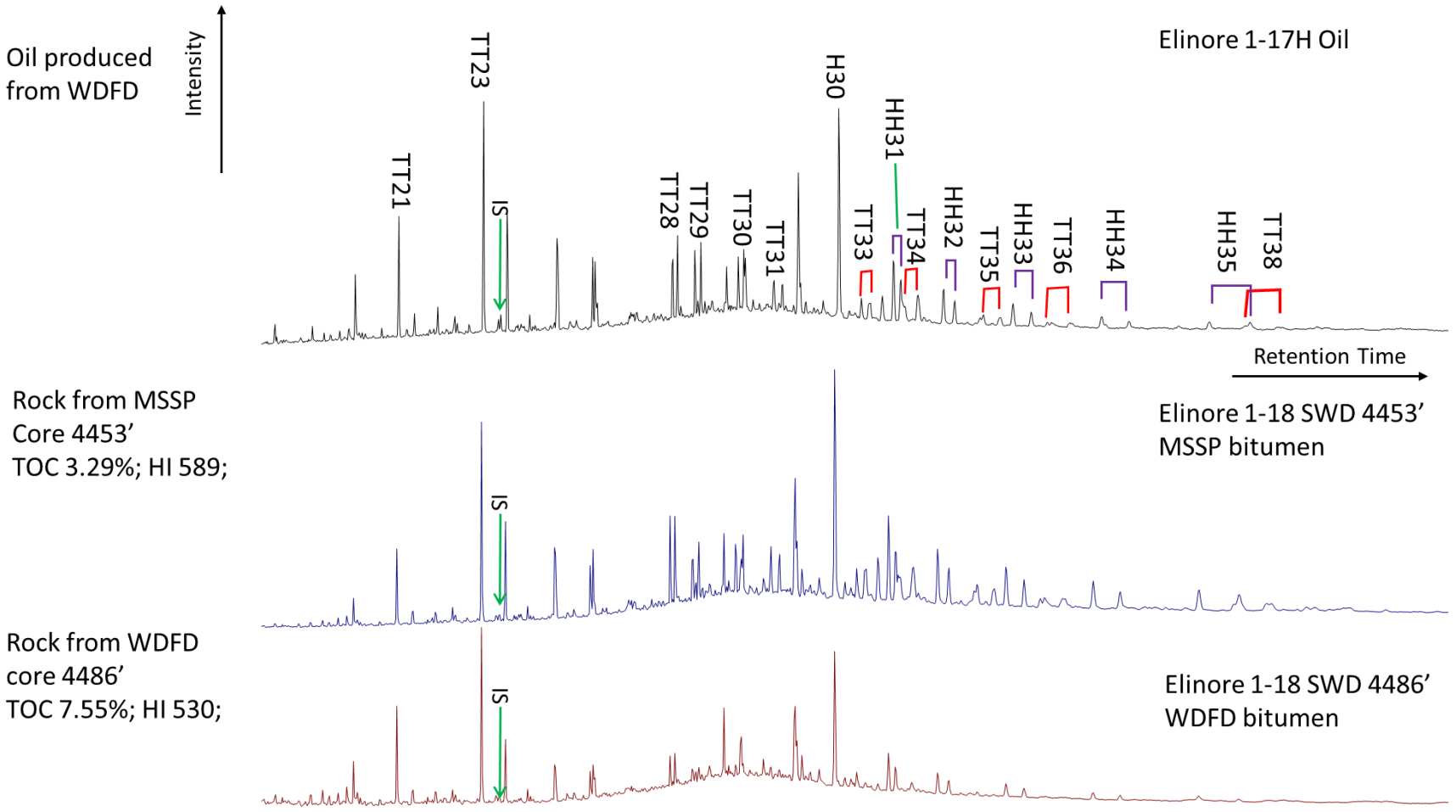

Figure 92. SIM *m/z* 191.3 mass chromatograms showing distributions of terpanes in the B&C fractions of the studied oil samples and rock extract

If these two oils are from a same source, what is that source: Woodford, Mississippian, or some other source? The similarity of *m/z* 191 traces of Elinore 1-17H oil, Elinore 1-18 SWD 4453 ft Mississippian rock extract and Elinore 1-18 SWD 4486 ft Woodford rock extract were compared in Figure 92. It's hard to determine whether the oil fingerprints resembles the Mississippian rock extract or the Woodford rock extract. From the tricyclic terpanes (TT28-TT29 and (TT30-TT31) distribution pattern, the oil neither resemble the Mississippian nor the Woodford. Moreover, the extended tricyclic terpanes (TT33 ~ TT39) are not that abundant as the Mississippian rock extract but are more detectable than the Woodford rock extract (Table 19). Lastly the C_{30} diahopane is more abundant in the Mississippian and Woodford rock extract but not in the oil sample (Table 19). By checking the maturity of these two source beds, both of them contain a very high HI value. Moreover the VRo measured from the Woodford Shale in the Elinore 1-18 SWD has a value of 0.56% Ro, which is lower than the Rc of the oil sample calculated from any biomarker maturity parameter. Moreover, the oil is around 45 ^{o}API gravity, which is lighter than a typical early mature petroleum product if expelled from the early mature source bed *in-situ*. From the reservoir quality perspective, it was recently reported by Kvale (2014) that abundant marine coarse-grained biogenic silica were found in the Woodford cores in this area. These coarse-grained materials may be the contributor to the good reservoir petrophysical properties suggesting the Woodford Formation may not be the source rock in this area but simply a tight reservoir. By integrating all of these facts, it is proposed that the oil produced from this well site are not generated *in-situ* either from the Woodford Shale or the Mississippian carbonate source rock but migrated from the Woodford Shale in some other places. The reason why the oil fingerprints looks like

in between these two source beds may be attributed to the fact that the migrated oil dissolved portions of both of the two sources' extracts as discussed below.

5.4.2 Oil-Source Rock Correlations

The distributions of steranes and terpanes have been widely used as correlation tools (Moldowan et al., 1985; Volkman, 1988; Philp et al., 1989; and Moldowan et al., 1992). Since steranes and terpanes are very common biomarkers existing in almost all of the source rocks and oils, there are possibilities that oils sourced from different source rocks may have similar distributions of hopanes and steranes. If the correlation can be supported by additional geochemical information, such as the results of carbon isotopic analysis, absolute concentration of biomarkers, the correlation will be less ambiguous. Special biomarkers and/or biomarker distributions are even better correlation tools.

Genetic relationships between an oil and a suspected source rock can be established by comparing the similarity of their fingerprints. The SIM *m/z* 191.3 mass chromatograms of three oils and two source rocks were displayed in Figure 93, including two oil samples, namely Adkisson 1-33H oil, Elinore 1-17H oil, and a typical Woodford-sourced oil produced from a conventional reservoir in Southern Oklahoma, and two source rocks, Winney 1-8 SWD 5155 ft Lower Mississippian Limestone rock extract and Mary Earp-5 4093 ft Woodford Shale rock extract and well locations shown in Figure 94. The Winney and Adkisson oils are two representative end-members in terms of their *m/z* 191 fingerprints. The other oils are intermediate between these end-members. One end-member is Adkisson 1-33H oil. The characteristics of *m/z* 191 fingerprints of Adkisson 1-33H oil include: 1) extended tricyclic terpanes (TT33 ~ TT39) dominate over homohopanes (H31 ~ H35) in the same chromatographic region; 2) unusually abundant

tricyclic terpanes (TT28 ~ TT31); 3) relatively higher (29Ts+D30)/H30 ratio. While, comparing with Adkisson 1-33H oil, the characteristics of *m/z* 191 fingerprints of Elinore 1-17H oil are: 1) extended tricyclic terpanes (TT33 ~ TT38) could be detected until C_{38} but homohopanes (H31 ~ H35) still dominate over extended tricyclic terpanes (TT33 ~ TT38) in this range; 2) abundant tricyclic terpanes (TT19 ~ TT31), especially distinct distribution pattern of TT28 ~ TT31; 3) Ts/Tm ratio close to 1; 4) relatively lower (29Ts+D30)/H30 ratio and C_{30} diahopane almost non-detectable compared to C_{30} regular hopane. 7-5N-5E oil, as one of the representative Woodford-sourced oil produced from a conventional reservoir in Southern Oklahoma, shows the characteristics of a typical Woodford-sourced oil, which are very similar to that of the Elinore 1-17H oil.

Adkisson 1-33H oil resemble the Winney 1-8 SWD 5155 ft Mississippian rock extract rather than Mary Earp-5 4093 ft Woodford rock extract in terms of their fingerprints, including: 1) extended tricyclic terpanes (TT33 ~ TT39) dominate over homohopanes (H31 ~ H35) in the same chromatographic region; 2) unusually abundant tricyclic terpanes (TT28 ~ TT31); and 3) relatively higher (29Ts+D30)/H30 ratio. The Elinore 1-17H oil appears to be genetically related to 7-5N-5E Woodford-sourced oil and Mary Earp-5 Woodford rock extract. The reason why an immature-to-early-mature Woodford rock extract, like the Mary Earp-5 4093 ft sample, was chosen to be compared for correlation is because, as discussed before in section 4.2.2.3, the regular hopanes, especially the homohopane series, in the Woodford source rock seriously thermally degraded during source rock maturation. Only a low-maturity ranking Woodford sample, like the Mary Earp-5 4093 ft, could show the original

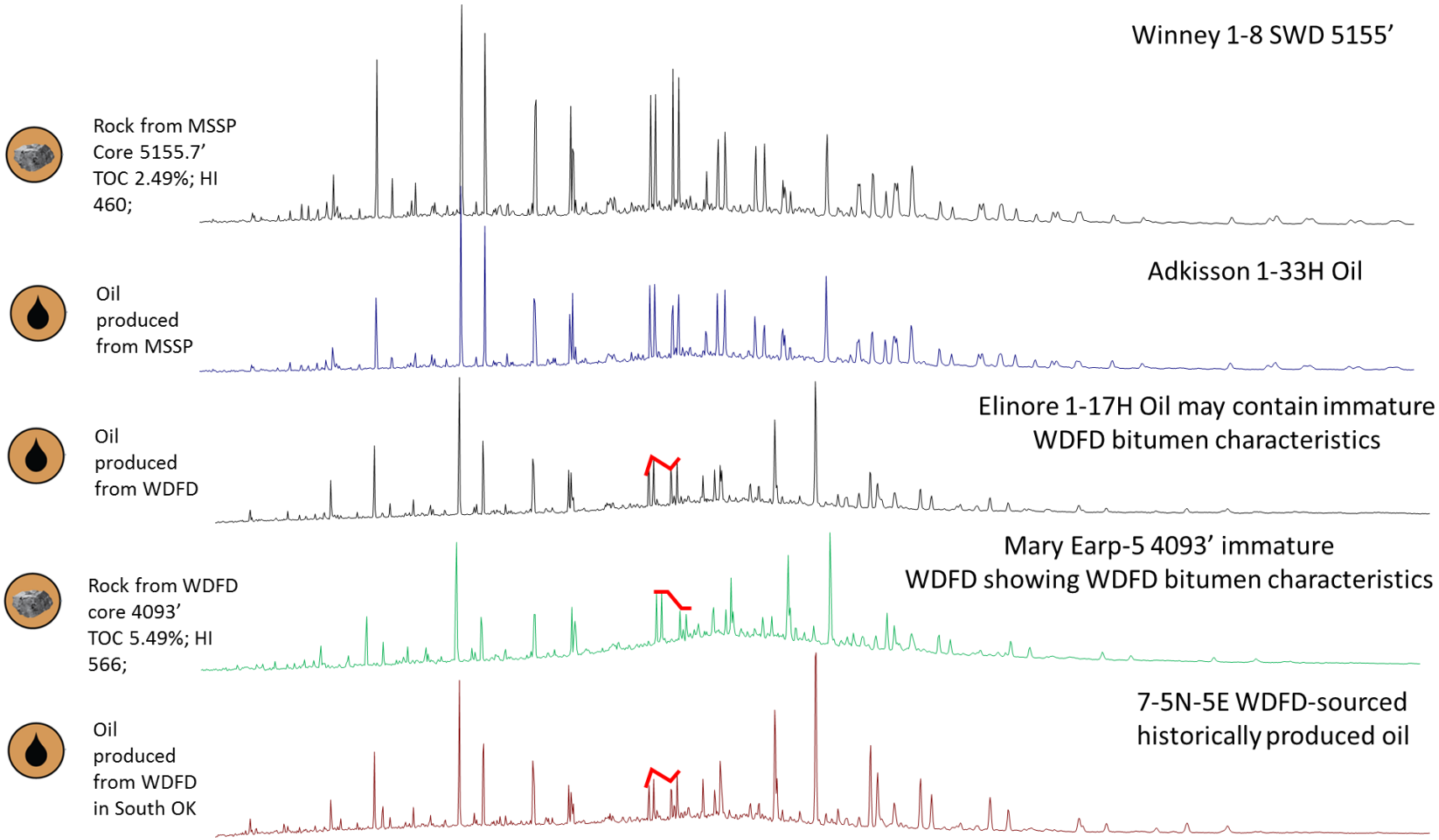

Figure 93. SIM *m/z* 191.3 mass chromatograms showing distributions of terpanes in the B&C fractions of the studied oil samples and rock extract.

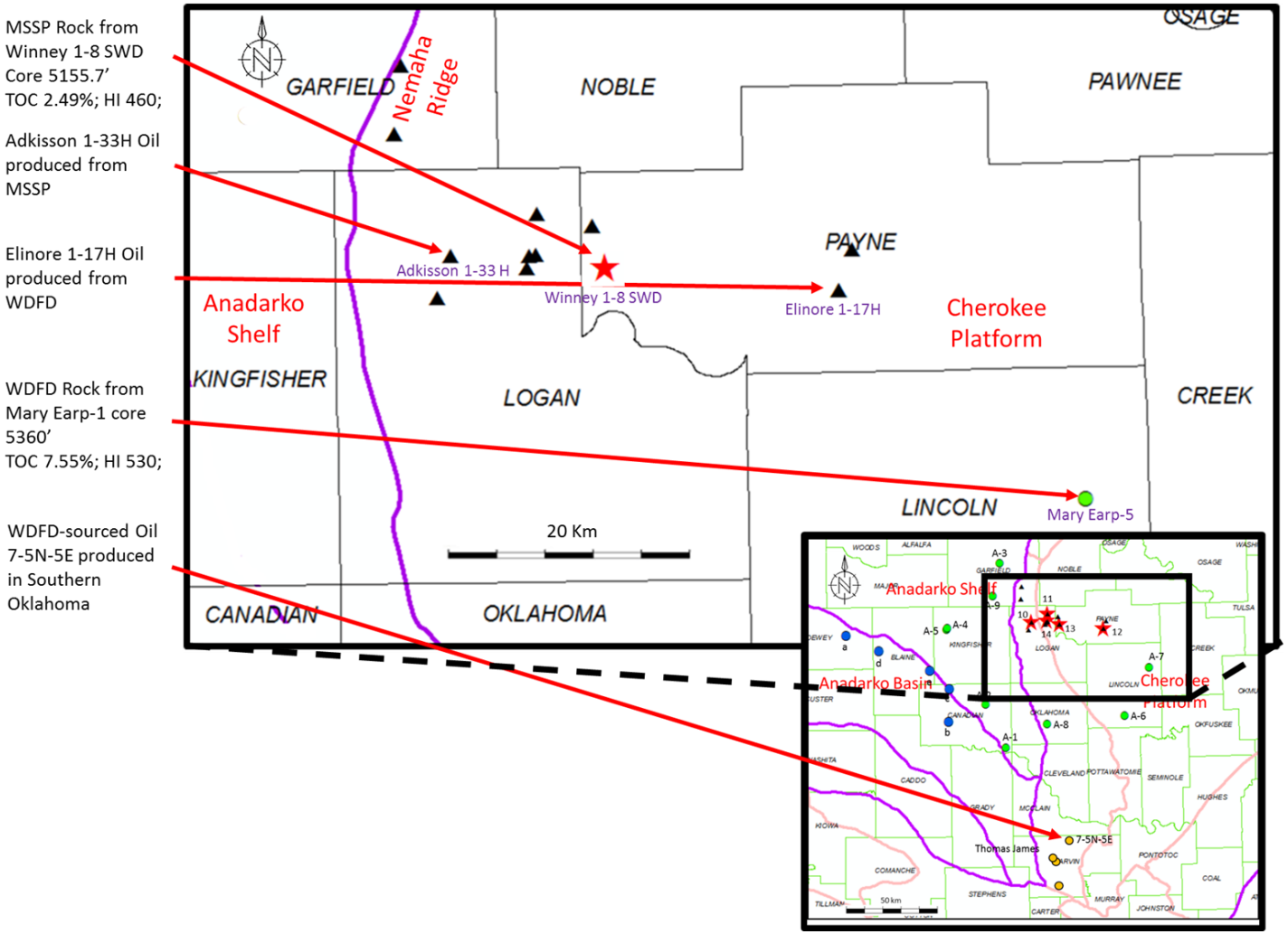

Figure 94. Map of Logan and Payne with the well site highlighted for oil-to-source rock correlation study

hopanes distributions for correlation with oil samples. Therefore, in summary, Adkisson 1-33H oil appears to have a great contribution from the Mississippian source rock and Elinore 1-17H oil is sourced primarily from the Woodford Shale.

The organic matter source and depositional environment information reflected by the biomarker distributions support this correlation as well. The unusually abundant distributions of extended tricyclic terpanes has been reported as one of the most diagnostic characteristics of Mississippian source rock extracts and Mississippian-sourced oils (Wang, 1993; Kim, 1999). As discussed before in the section 4.2.3, Kim (1999) proposed that the relative abundance of extended tricyclic terpanes (> C_{30}) over homohopanes (C_{31} ~ C_{35}) appeared to be associated with several events of algal bloom during the Lower Mississippian Limestone deposited (Kim, 1999). Another obvious characteristics in terms of *m/z* 191 fingerprints is the (29Ts+D30)/H30 ratios in the Winney 1-8 SWD 5155 ft Mississippian rock extract and Adkisson 1-33H oil are higher than those in the other samples in Figure 93. 18α-30-norneohopane (29Ts) and C_{30} 17α-diahopane (D30) are two rearranged hopanes. They were thought to be rearranged from regular hopanes and the rearrangement chemical reaction appeared to be associated with clay and/or acidic catalysis. Therefore the relatively high (29Ts+D30)/H30 ratio in either the Mississippian rock extracts or the Mississippian-sourced oil may infer that the clay content and/or acidity level of the Mississippian source rock depositional environment (Kim, 1999).

By applying the extended tricyclic terpanes vs. homohopanes ratio (TT33-TT39/H31-H35: the sum of C_{33} to C_{39} tricyclic terpanes divided by the sum of C_{31} to C_{35} homohopanes) as the correlation tool, sixteen Devon produced tight oil samples could be

subdivided into two major groups: Group-A gathers Elinore 1-17H, Elinore 1-18H and Joyce 1-32H, which are located in the eastern-most region of the study area and most far away from the Nemaha Uplift; and Group-B encompasses the left thirteen wells, which are closer to the Nemaha Uplift Zone towards the West (Figure 95). The oil samples in Group-A have no Mississippian source characteristics but the typical Woodford-sourced oil characteristics. The oil samples in Group-B have the Mississippian source characteristics in variable extents, which infer at least these oil samples have the Mississippian source contribution but the Woodford source contribution couldn't be excluded.

The terpane series biomarker distributions of either oil samples (Figure 96) or source rock samples (Figure 97) support the oil-to-source rock correlation as well. In this type of figure, more biomarkers are utilized as correlation tools. The idea is the data points of the genetically related samples should fall into an "envelope" in this type of figure. In Figure 96, it's obvious to subdivide the data points into two "envelopes". Envelope-A gathers the majority of the tight oil samples with the Mississippian source contribution and Envelope-B encompasses the Woodford-sourced oils. Not only the genetically related oil samples fall into the same envelope, the genetically related source rock samples should fall into the same envelope as well. In Figure 97, it's interesting to see the two Mississippian rock extract encompass the majority of the tight oil samples with the Mississippian source contribution. While, in the other envelope, the Woodford-sourced oils are within the Woodford source rock data points approximately.

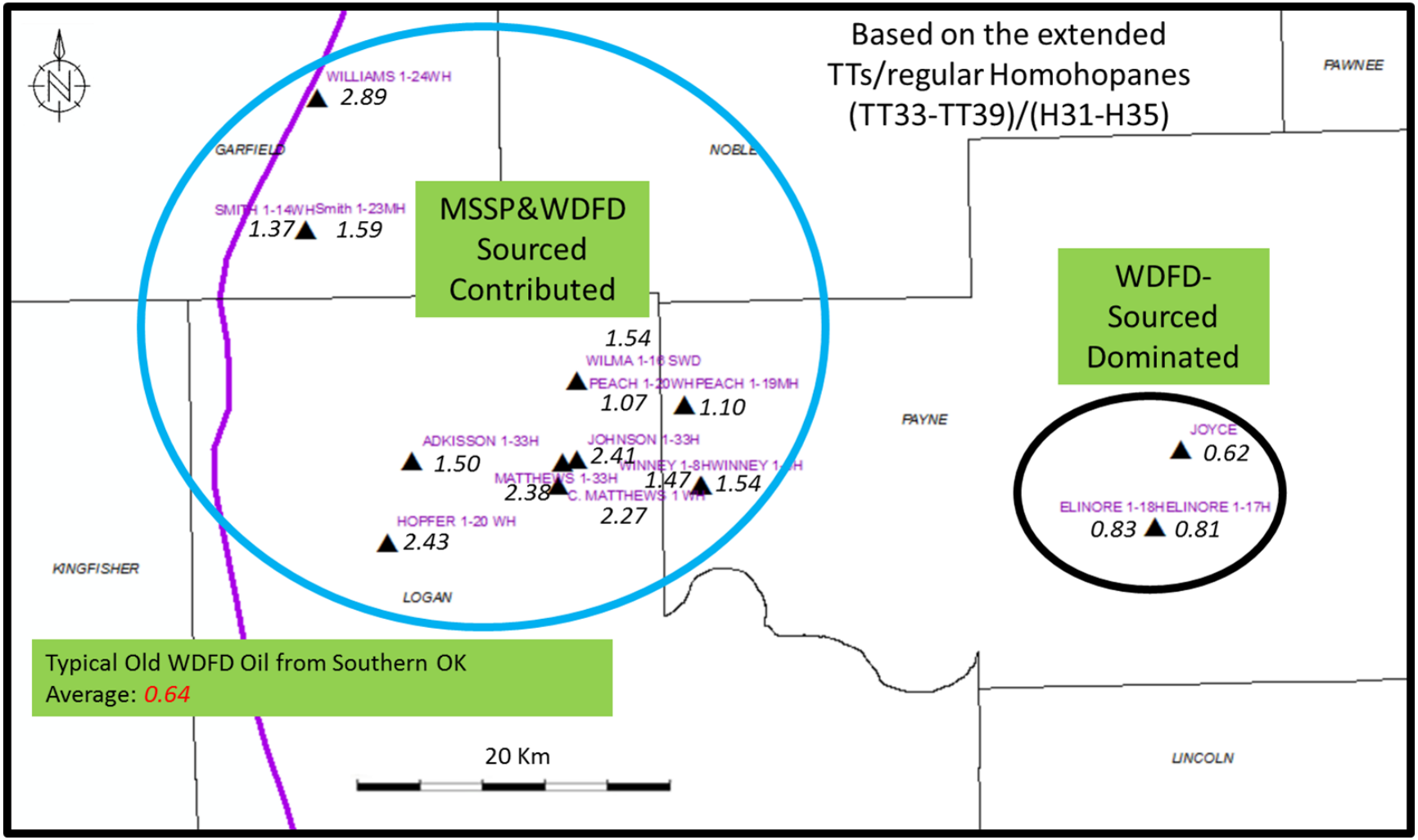

Figure 95. Well Location Map of Logan and Payne with the extended tricyclic terpanes vs. homohopanes ratios (TT33~TT39)/(H31~H35) for oil-to-source rock correlation

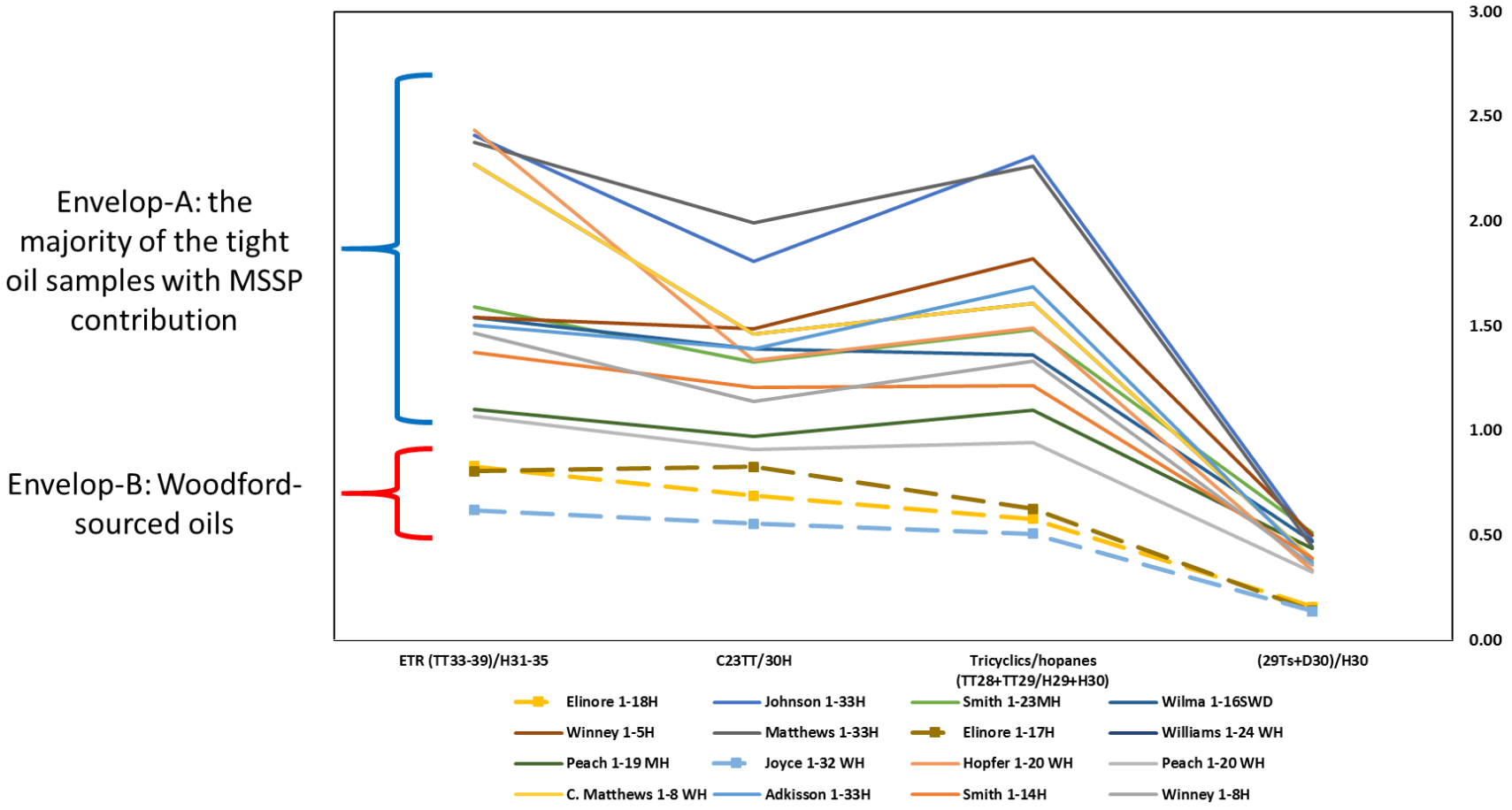

Figure 96. Biomarker (Terpanes) distributions of the studied tight oil samples for oil-oil correlation

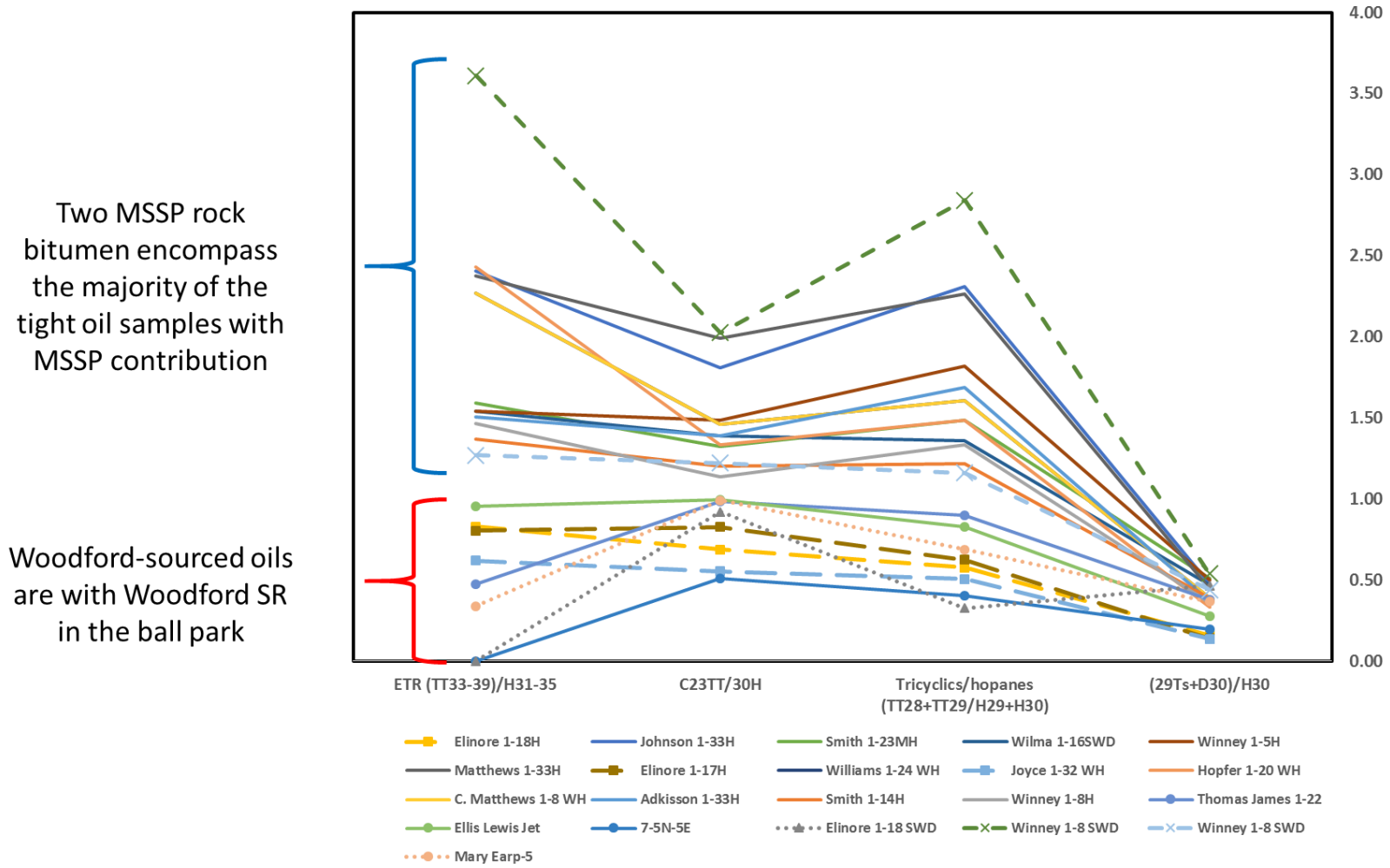

Figure 97. Biomarker (Terpanes) distributions of the studied tight oil samples and source rock extract for oil-to-source rock correlation

6. CONCLUSIONS

The Woodford Shale in central Cherokee Platform is a typical marine siliciclastic mudstone with excellent source rock potential demonstrated by the TOC and Rock-Eval parameters. Biomarker distributions of regular steranes, hopanes and monoaromatic steroids (MAS) are consistent with an interpretation that the Woodford Shale was deposited generally in a marine siliciclastic depositional environment. Aryl isoprenoids and paleorenieratanes/isorenieratanes detected in the Woodford extracts indicate the occurrence of episodic periods of photic zone anoxia (PZA) during deposition of the Woodford Shale. In addition, *n*-alkane and sterane distributions, and the tentative identification of gammacerane suggest deposition of the Woodford Shale under hypersaline conditions in Central Oklahoma. Source-dependent biomarker parameters, including diasteranes and diahopanes, indicate that in the area in the proximity of the Nemaha Uplift, the Woodford Shale was deposited under a condition rich in clay content, reflecting the influence of the paleo-Nemaha Uplift. Thermal maturity parameters based on the measured vitrinite reflectance values (% Ro), Rock-Eval and biomarker maturity parameters indicate that the Woodford Shale is immature to marginally mature in Payne County, and show a progressive increase in maturity towards the southeast following the regional dip. In the area in the proximity of the Nemaha Uplift, the Woodford Shale is in the main stage of oil generation.

Analysis of the geochemical profile shows a minimal range of vertical variation within the Woodford Shale in this study. The Woodford Shale in this study was subdivided into middle and upper members without a lower member found based on the integration of geochemical and geological data. The middle Woodford member has the

higher TOC values. Pristane and phytane (Pr/Ph) and biomarker ratios suggest the establishment of stronger anoxic conditions during deposition of the middle Woodford member than the upper Woodford member, where the latter may have received an additional siliciclastic organic matter input. In the area in the proximity of the Nemaha Uplift, Pr/Ph ratios indicate deposition under suboxic to dysoxic conditions for the Woodford Shale interval analyzed. Isotope data indicates a marine organic matter source for the Woodford Shale, but $\delta^{13}C$ values do not show significant organic facies, depositional environment, or thermal maturity changes.

The origin of the oils and condensates sampled in this study were related to their possible source beds based on oil-oil and oil-source rock correlation by comparing biomarker fingerprints. Three major conclusions were made: (i) oils produced from the Woodford Formation and that from the overlying Mississippian Formation share very similar fingerprints suggesting the Woodford Formation and the overlying Mississippian Formation are connected in the study area; (ii) oils produced in the area in the proximity of the Nemaha Uplift (Logan and West Payne Counties) were not only sourced by Woodford but also had a significant Mississippian source contribution based on the presence of abundant extended tricyclic terpanes and other source-specific biomarker characteristics; (iii) oils sampled from the East of the Cherokee Platform (Central-East Payne County) share strong Woodford source characteristics but were not generated *in-situ* from the Woodford Shale since the Woodford in that area is not mature enough. Therefore, the oil produced there may probably be migrated from the Woodford Shale in the deeper part of the Anadarko Basin in Southern Oklahoma. The results of this research are consistent with some new findings reported by the Devon geologists that abundant

marine coarse-grained biogenic silica (radiolarian-rich chert facies) found in Woodford cores (Central-East Payne County) in this area may be a contributor to good reservoir petrophysical properties suggesting the Woodford Formation may not be the source rock in this area but simply a tight reservoir.

7. REFERENCES

Alexander, R., Kagi, R. and Noble, R. (1983) Identification of the bicyclic sesquiterpanes, drimane, and eudesmane in petroleum: *Journal of the Chemical Society, Chemical Communication*, 226-228.

Algeo, T.J., Lyons, T.W., Blakey, R.C., and Over, D.J. (2007) Hydrographic conditions of the Devono-Carboniferous North American Seaway inferred from sedimentary Mo-TOC relationships: *Palaeogeography, Palaeoclimatology, Palaeoecology* **256**, 204–230.

Algeo, T.J., and Rowe, H. (2012) Paleoceanographic applications of trace-metal concentration data: *Chemical Geology* **324-325**, 6-18.

Althoff, C.D. (2012) Characterization of depositional megacycles in the Woodford trough of central Oklahoma: Norman, University of Oklahoma, unpublished M.S. thesis, 99p.

American Society for Testing and Materials (2011) Standard test method for microscopical determination of the reflectance of vitrinite dispersed in sedimentary rocks: West Conshohocken, PA, ASTM International, Annual book of ASTM standards: *Petroleum products, lubricants, and fossil fuels; Gaseous fuels; coal and coke,* Sec. 5, v. 5.06, D7708-11, 823-830.

Amorocho Sanchez, J.D. (2013) Sequence stratigraphy and seismic interpretation of the Upper Devonian-Lower Mississippian Woodford Shale in the Cherokee Platform; a characterization approach for unconventional resources: Norman, University of Oklahoma unpublished M.S. thesis, 109p.

Amsden, T.W. (1967) Silurian and Devonian strata in Oklahoma: Symposium—Silurian-Devonian rocks of Oklahoma and environs: *Tulsa Geological Society Digest* **35**, 25-34.

Amsden, T.W. and Klapper, G. (1972) Misener Sandstone (Middle-Upper Devonian), north-central Oklahoma: *American Association Petroleum Geologists Bulletin* **56**, 2323-2334.

Amsden, T.W. (1975) Hunton Group (Late Ordovician, Silurian, and Early Devonian) in the Anadarko basin of Oklahoma: *Oklahoma Geological Survey Bulletin* **121**, 214p.

Amsden, T.W. (1989) Depositional and post-depositional history of Middle Paleozoic (Late Ordovician through Early Devonian) strata in the Ancestral Anadarko Basin: *Anadarko Basin Symposium, 1988. Oklahoma Geological Survey Circular 90*, 143-146.

Anderson, H.M., Hiller, N. and Gess, R.W. (1995) Archaeopteris (Progymnospermopsida) from the Devonian of southern Africa: *Botanical Journal of the Linnean Society* **117**, 305 – 320.

Andrusevich, V.E., Engel, M.H., Zumberge, J.E., and Brothers, L.A. (1998) Secular, episodic changes in stable carbon isotope composition of crude oils: *Chemical Geology* **152**, 59–72.

Aquino Neto, F.R., Trendel, J.M., Restle, A., Connan, J. and Albrecht, P.A. (1983) Occurrence and formation of tricyclic and tetracyclic terpanes in sediments and petroleums: In Bjorøy M. et al. *Advances in organic geochemistry,* 659-667.

Azevedo, D. A., Aquino Neto, F. R., Simoneit, B. R. T. and Pinto, A. C. (1992) Novel series of tricyclic aromatic terpanes characterized in Tasmanian tasmanite: *Organic Geochemistry* **18**, 9-16.

Banner, J. L., 1995, Application of the trace element and isotope geochemistry of strontium to studies of carbonate diagenesis: *Sedimentology* **42**, 805–824.

Barker, C.E. and Pawlewicz, M.J. (1993) An empirical determination of the minimum number of measurements needed to estimate the mean random vitrinite reflectance of disseminated organic matter: *Organic Geochemistry* **20**, 643 ‑ 651.

Barron, L.S. and Ettensohn, F.R. (1981) Paleoecology of the Devonian-Mississippian black-shale sequence in eastern Kentucky with an atlas of some common fossils: U.S. Department of Energy, Morgantown Energy Technology Center, DOE/ET/12040-51, 75p.

Bechtel, A., Hamor-Vido, M., Sachsenhofer, R.F., Reischenbacher, D., Gratzer, R. and Puttmann, W. (2007) The middle Eocene Markushegy sub-bituminous coal (Hungary): paleoenvironmental implications from petrographic and geochemical studies. *International Journal of Coal Geology* **72,** 33-52.

Beck, C.B. (1988) Origin and evolution of gymnosperms: *Columbia University Press, New York*, 1-84.

Beck, C.B. and Wight, D.C. (1988) Progymnosperms. *In* C. B. Beck [ed.], Origin and evolution of gymnosperms, 1-84. Columbia University Press, New York, New York, USA.

Becker C.M. (1927) Geology of Caddo and Grady counties: *Oklahoma Geological Survey Bulletin* **40-I**, 18p.

Bernal A.S. (2013) Geological characterization of the Woodford Shale, McAlister Cemetery Quarry, Criner Hills, Ardmore Basin, Oklahoma: *University of Oklahoma, unpublished Master thesis*, 141p.

Blakey, R. C. (2008) Gondwana paleogeography from assembly to breakup - a 500 million year odyssey, in Fielding, Christopher R., Frank, Tracy D., and Isbell, John L. (eds), Resolving the Late Paleozoic Ice Age in Time and Space: *Geological Society of America, Special Paper* **441**, 1-28.

Blumer, M., Mullin, M.M., and Thomas, D.W. (1963) Pristane in zooplankton: *Science* **140,** 974.

Blumer, M. and Thomas, D.W. (1965) "Zamene", isomeric C_{19} monoolefins from marine zooplankton, fishes, and mammals: *Science* **148,** 370-371.

Bourbonniere, R. A. and Meyers, P. A. (1996) Sedimentary geolipid records of historical changes in the watersheds and productivities of Lakes Ontario and Erie: *Limnology and Oceanography* **41**, 352-359.

Badra, H. (2011) Field characterization and analog modeling of natural fractures in the Woodford Shale, southeast Oklahoma: Norman, University of Oklahoma, unpublished M.S. thesis, 78p.

Boon, J.J., Hines, H., Burlingame, A.L., Klok, J., Rijpsta, W.I.C., deLeeuw, J. W., Edmunds, K. E., and Eglinton, G. (1983) Organic geochemical studies of solar lake laminated cyanobacterial mats. *In* Bjoroy, H. (Ed.), *Advances in Organic Geochemistry* 1981*:* New York (Wiley), 207-227.

Branch, A.A. (2007) Comprehensive characterization of a core from an over-mature Woodford Shale in Le Flore County, Oklahoma, and comparison with data from

other studies of the Woodford Shale in the Arkoma Basin: Norman, OK, University of Oklahoma, unpublished M.S. thesis, 131p.

Bray, E.E. and Evans, E.D. (1961) Distribution of n-paraffins as a clue to recognition of source beds: *Geochimica et Cosmochimica Acta* **22**, 2-15.

Brocks, J.J. and Summons, R.E. (2013) Sedimentary Hydrocarbons, Biomarkers for Early Life. *2nd ed., Elsevier Ltd* **8**, 63-115.

Brooks, J. D., Gould, K. and Smith, J. W. (1969) Isoprenoid hydrocarbons in coal and petroleum: *Nature* **222**, 237-259.

Brown, T.C. and Kenig, F. (2004) Water column structure during deposition of Middle Devonian-Lower Mississippian black and green/gray shales of the Illinois and Michigan Basins: a biomarker approach: *Palaeogeography, Palaeoclimatology, Palaeoecology* **215,** 59-85.

Burruss, R. C. and Hatch, J.R. (1987) Regional variations in crude oil geochemistry, Anadarko basin, Oklahoma, Texas, and Kansas—evidence for multiple sources, mixing, and migration distances [abstract]: *American Association Petroleum Geologists Bulletin* **71**, 535.

Burruss, R.C. and Hatch, J.R. (1989) Geochemistry of oils and hydrocarbon source rocks, greater Anadarko basin: evidence for multiple sources of oils and long-distance oil migration, in K.S. Johnson, ed., Anadarko basin symposium, 1988: *Oklahoma Geological Survey Circular* **90**, 53-64.

Campbell J. A. and Northcutt R. A. (2001) Petroleum systems of sedimentary basins in Oklahoma: Johnson K. S. and Merrian D. F. (eds.) Petroleum systems of

sedimentary basins in the southern Midcontinent, 2000 symposium. *Oklahoma Geological Survey Circular* **106,** 1-5.

Cardott, B.J. and Lambert, M.W. (1985) Thermal maturation by vitrinite reflectance of Woodford Shale, Anadarko basin, Oklahoma: *American Association Petroleum Geologists Bulletin* **69**, 1982-1998.

Cardott, B.J. (1989) Thermal maturation of the Woodford Shale in the Anadarko basin: K.S. Johnson, ed., Anadarko basin symposium, 1988: *Oklahoma Geological Survey Circular* **90**, 32-46.

Cardott, B.J. (2005) Overview of unconventional energy resources of Oklahoma, in B.J. Cardott, ed., Unconventional energy resources in the southern Midcontinent, 2004 symposium: *Oklahoma Geological Survey Circular* **110**, 7-18.

Cardott, B.J. (2011) Application of Petrology to Shale Oil and Gas Potential of the Woodford Shale, Oklahoma, USA: *TSOP Annual Meeting, Halifax, Canada,* 2011.

Cardott, B.J. (2012) Thermal maturity of Woodford Shale gas and oil plays, Oklahoma, USA: *International Journal of Coal Geology* **103**, 109-119.

Cardott, B.J. (2013) Woodford Shale: From hydrocarbon source rock to reservoir: *AAPG Search and Discovery* Article #50817, 85 slides.

Cardott, B.J. (2014a) Woodford Shale play update: Expanded extent in the oil window: *AAPG Search and Discovery* Article #80409, 51 slides.

Cardott, B.J. (2014b) Determining the Thermal Maturity Level at Which Oil Can Be Economically Produced in the Woodford Shale: Woodford Oil Congress, Oklahoma City, 2014.

Cassani, F., Gallango, O., Talukdar, S., Vallejos, C., and Ehrmann, U. (1988) Methylphenanthrene maturity index of marine source rock extracts and crude oils from the Maracaibo Basin: *Organic Geochemistry* **13**, 73-80.

Chain, A.R. (2012) Stratigraphy and composition of the Woodford Shale in depositionally updip and downdip wells, Anadarko Basin, Oklahoma: Norman, University of Oklahoma, unpublished M.S. thesis, 118p.

Charpentier, R.R. (2001) Cherokee Platform Province (060): *U. S. Geological Survey, 1995 National Oil and Gas Resource Assessment Team, Circular* **1118**, 13p.

Chen, J., Fu, J., Sheng, G., Liu, D., and Zhang, J. (1996) Diamondoid hydrocarbon ratios: novel maturity indices for highly mature crude oils: *Organic Geochemistry* **25**, 179-190.

Clark, J.P. and Philp, R.P. (1989) Geochemical characterization of evaporite and carbonate depositional environments and correlation of associated crude oils in the Black Creek Basin, Alberta: *Canadian Geologists Bulletin* **37,** 401-416.

Clifford, D.J., Clayton, J.L. and Sinninghe Damste, J.S. (1997) 3,4,5-2,3,6 Substituted diaryl carotenoid derivatives (Chlorobiaceae) and their utility as indicators of photic zone anoxia in sedimentary environments: *Abstracts from the 18th International Meeting on Organic Geochemistry, September 22-26, 1997, Maastricht, The Netherlands* (B. Horsfield, ed.), Forschungszentrum Julich, Julich, Germany, 685-686.

Coffey, B. (2015) Recent exploration success in the Woodford shale, Payne-Logan Counties: finding 1000+ BOPD wells in an area peppered with dry holes: *AAPG Search and Discovery* Article #90230, 25 slides.

Comer, J.B. and Hinch, H.H. (1981) Petrologic factors controlling internal migration and expulsion of petroleum from source rocks: Woodford-Chattanooga of Oklahoma and Arkansas [abstract]: *American Association of Petroleum Geologists Bulletin* **65**, 912.

Comer, J.B. and Hinch, H.H. (1987) Recognizing and quantifying expulsion of oil from the Woodford Formation and age-equivalent rocks in Oklahoma and Arkansas: *American Association of Petroleum Geologists Bulletin* **71**, 844-858.

Comer, J. B. (1991) Stratigraphic analysis of the Upper Devonian Woodford Formation, Permian basin, West Texas and southeastern New Mexico: *Bureau of Economic Geology, Report of Investigations* **201**, 63p.

Comer, J.B. (1992) Organic geochemistry and paleogeography of Upper Devonian formations in Oklahoma and western Arkansas, in K.S. Johnson and B.J. Cardott, eds., Source rocks in the southern Midcontinent, 1990 symposium: *Oklahoma Geological Survey Circular* **93**, 70-93.

Comer, J.B. (2005) Facies distribution and hydrocarbon production potential of Woodford Shale in the southern Midcontinent, in B.J. Cardott, ed., Unconventional energy resources in the southern Midcontinent, 2004 symposium: *Oklahoma Geological Survey Circular* **110**, 51-62.

Comer, J.B. (2008) Woodford Shale in southern Midcontinent, USA—Transgressive system tract marine source rocks on an arid passive continental margin with persistent oceanic upwelling: *AAPG Annual Convention, San Antonio, TX*, poster, 3 panels.

Comer, J.B. (2012) Woodford Shale and the evaporate connection – the significance of aridity and hypersalinity in organic matter productivity and preservation: *Geological Society of America Abstracts with Programs* **44**, 6.

Connan, J., Buroullec, J., Dessort, D. and Albrecht, P. (1986) The microbial input in carbonate-anhydrite facies of a sabakha palaeoenvironment from Guatemala: a molecular approach. *Organic Geochemistry* **10**, 29-50.

Connock, G. (2015) Paleoenvironmental Interpretation of the Woodford Shale, Wyche Farm Shale Pit, Pontotoc County, Arkoma Basin, Oklahoma with Primary Focus on Water Column Structure: *University of Oklahoma, unpublished Master thesis*, 253p.

Corbett, R.E. and Smith, R.A. (1969) Lichens and fungi. Part VI. Dehydration rearrangements of 15-hydroxyhopanes: *Journal of the Chemical Society (C)* **1969**, 44-47.

Corbett, M.J., Lowery, C., Miceli Romero, A., Watkins, D.K., Leckie, R.M., Li, W., Pramudito, A., Donovan, A., Staerker, S. (2011) A bio-chemostratigraphic framework of Oceanic Anoxic Event 2 at Lozier Canyon, TX: correlations to the Western Interior Seaway and comparison to sequence stratigraphic surfaces. *GSA Annual Meeting Abstracts with Programs* **43**, 611.

Cornford, C., Gardner, P. and Burgess, C. (1998) Geochemical truths in large data sets. I: Geochemical screening data. *Organic Geochemistry* **29**, 519-530.

Curtis, J.B. (2002) Fractured shale-gas systems: *American Association of Petroleum Geologists Bulletin* **86**, 1921-1938.

Dahl, J.E., Moldowan, J.M., Peters, K.E., et al. (1999) Diamondoid hydrocarbons as indicators of natural oil cracking: *Nature* **399**, 54-57.

Dahl, J.E., Liu, S.G. and Carlson, R.M.K. (2002) Isolation and structure of higher diamondoids, nanometer-sized diamond molecules: *Science* **299**, 96-99.

DeGarmo, E.P. (2015) Geochemical characterization of the Woodford Shale (Devonian-Mississippian), McAlister Cemetery Quarry, Criner Hills Uplift, Ardmore Basin, Oklahoma: Norman, University of Oklahoma, unpublished M.S. thesis, 102p.

Derenne, S., Largeau, C., Casadevall, E. and Connan, J. (1988) Comparison of torbanites of various origins and evolutionary stages. Bacterial contribution to their formation. Cause of lack of botryococcane in bitumens: *Organic Geochemistry* **12**, 43-59.

Dembicki Jr, H. (2009) Three common source rock evaluation errors made by geologists during prospect or play appraisals: *American Association of Petroleum Geologists Bulletin* **93**, 341-356.

Denison, R.E., Kirkland, D.W., and Gormly, J.R. (1990) Criner Hills-Arbuckle Mountains field trip guidebook: Mobil Dallas Research Laboratory.

Didyk, B.M., Simoneit, B.R.T., Brassell, S.C., Eglinton, G. (1978) Organic geochemical indicators of palaeoenvironmental conditions of sedimentation: *Nature* **272,** 216-222.

Dow, W.G. (1977) Kerogen studies and geological interpretations: *Journal of geochemical exploration* **7**, 79-99.

Dutta, S., Greenwood, P.F., Brocke, R., Schaefer, R.G. and Mann, U. (2006) New insights into the relationship between Tasmanites and tricyclic terpenoids: *Organic Geochemistry* **37**, 117-127.

Energy Information Administration (EIA) (2015) Lower 48 states shale plays: http://www.eia.gov/oil_gas/rpd/shale_gas.pdf, accessed April 13th, 2015.

Engel, M.H., Imbus, S.W. and Zumberge, J.E. (1988) Organic geochemical correlation of Oklahoma crude oils using R- and Q-mode factor analysis: *Organic Geochemistry* **12**, 157-170.

Esther E.A. (2015) Integrated characterization of the Woodford Shale in south-west Cherokee Platform, Oklahoma: Norman, University of Oklahoma, unpublished M.S. thesis, 104p.

Freie, A.J. (1930) Sedimentation in the Anadarko Basin: *Oklahoma Geological Survey Bulletin* **48**, 80p.

Fritz, R.D., and Beaumont, E.A. (2001) Depositional environment and sequence stratigraphy of Silurian through Mississippian strata in the Midcontinent, in K.S. Johnson, ed., Silurian, Devonian, and Mississippian geology and petroleum in the southern Midcontinent, 1999 symposium: OGS Circular 105, p. 173.

Fu, J., Sheng, G. Peng. P., et al. (1986) Peculiarities of salt lake sediments as potential source rocks in China: *Organic Geochemistry* **10**, 119-126.

Gale, J.F.W., Reed, R.M. and Holder, J. (2007) Natural fractures in the Barnett Shale and their importance for hydraulic fracture treatments: *American Association of Petroleum Geologists Bulletin* **91**, 603-622.

Gao, S.S., Liu, K.H., Cao, A., Chen, C., Hubbard, M.S., Zachary, J.A., and Zhang, Y. (2002) Old Rifts Never Die: Crustal Thickening Across the Mid-Continent Rift and Its Possible Role in Post-Rifting Tectonics: *GSA Annual Meeting, Denver, Colorado*, Paper No. 30-6.

Gerhard, L.C. (2004) Review of the Nemaha Ridge: A New Look at An Old Structure: *Kansas Geological Survey, Current Research in Earth Science, Bulletin* **250**, part 1.

Grice, K., Schaeffer, P., Schwark, L. and Maxwell, J.R. (1996) Molecular indicators of paleoenvironmental conditions in an immature Permian shale (Kupferschiefer, Lower Rhine Basin, north-west Germany) from free and sulfide-bound lipids: *Organic Geochemistry* **25**, 131-147.

Grice, K., Schaeffer, P., Schwark, L. and Maxell, J.R. (1997) Changes in paleoenviromental conditions during deposition of the Permian Kupfeschiefer (Lower Rhine Basin, northwest Germany) inferred from molecular and isotopic compositions of biomarker components: *Organic Geochemistry* **26**, 677-690.

Grice, k., Audino, M., Boreham, C. J., Alexander, R. and Kagi, R. I. (2001) Distributions and stable carbon isotopic compositions of biomarkers in torbanites from different palaeogeographical locations: *Organic Geochemistry* **32**, 1195-1210.

Goosens, H., de Leeuw, J. W., Schenck, P. A. and Brassell, S. C. (1984) Tocopherols as likely precursors of pristane in ancient sediments and crude oils: *Nature* **312,** 440-442.

Gould, C.N. (1924) A new classification of the Permian red beds of southwestern Oklahoma: *American Association of Petroleum Geologists Bulletin* **8**, 322-341.

Hallam, A. (1967) *The depth significance of shales with bituminous laminae: Marine Geology* **5**, 481-492.

Hallam, A. (1981) Facies interpretation in the stratigraphic record: W.H. Freeman, San Francisco, 291p.

Ham, W.E., Denison, R.E., and Merritt, C.A. (1964) Basement rocks and structural evolution of southern Oklahoma: *Oklahoma Geological Survey Bulletin* **95**: 302. pp.

Haq, B.U. and Schutter, S.R. (2008) A Chronology of Paleozoic Sea-Level Changes: *Science* **322**, 64-68.

Hartgers, W.A., Sinninghe Damste, J.S., Requejo, A.G., et al. (1994) A molecular and carbon isotopic study towards the origin and diagenesis fate of diaromatic carotenoids: *Organic Geochemistry* **22**, 703-725.

Hass, W.H. and Huddle, J.W. (1965) Late Devonian-Early Mississippian age of the Woodford Shale in Oklahoma as determined by conodonts: *Geological Survey Research*. United States Geological Survey Professional Paper **525-D**, 124-132.

Hatch, J.R., Jacobson, S.R., Witzke, B.J., Risatti, J.B., Anders, D.E., Watley, W.L., Newell, K.D. and Vuletich, A.K. (1987) Possible late Middle Ordovician carbon isotope excursion: evidence from Ordovician oils and hydrocarbon source rocks, Midcontinent and east-central United States: *American Association of Petroleum Geologists Bulletin* **71**, 1342-1354.

Heckel, P.H. (1977) Origin of phosphatic black shale facies in Pennsylvanian cyclothems of Mid-Continent North America: *American Association of Petroleum Geologists Bulletin* **61**, 1045-1068.

Hester, T.C., H.L. Sahl, and Schmoker, J.W. (1988) Cross sections based on gamma ray, density, and resistivity logs showing stratigraphic units of the Woodford Shale, Anadarko basin, Oklahoma: U.S. Geological Survey Miscellaneous Field Studies Map MF-2054, 2 sheets.

Hester, T.C., Schmoker, J.W. and Sahl, H.L. (1990) Log-derived regional source-rock characteristics of the Woodford Shale, Anadarko basin, Oklahoma: *U.S. Geological Survey Bulletin* **1866-D**, 38p.

Hickey J.J. and Henk B. (2007) Lithofacies summary of the Mississippian Barnett Shale, Mitchell 2 T. P. Sims well, Wise County, Texas: *American Association of Petroleum Geologists Bulletin* **91**, 437-443.

Hill, R.J., Jarvie, D.M., Zumberge, J., Henry, M., and Pollastro, R.M. (2007a) Oil and gas geochemistry and petroleum systems of the Fort Worth Basin: *American Association of Petroleum Geologists Bulletin* **91**, 445-473.

Hill, R.J., Zhang, E., Katz, B.J., and Tang, Y. (2007b) Modeling of gas generation from the Barnett Shale, Fort Worth Basin, Texas: *American Association of Petroleum Geologists Bulletin* **91**, 501-521.

Huang, W.Y. and Meinschein, W.G. (1979) Sterols as ecological indicators: *Geochimica et Cosmochimica Acta* **43,** 739-745.

Hussain, M., and Bloom, M.A. (1991) Pyrolysis and hydrocarbon source bed potential of the Upper Devonian Woodford Shale, Hovey Channel, southern Permian basin, West Texas [abstract]: AAPG Bulletin, v. 75, p. 599.

Hunt, J.M. (1979) *Petroleum geochemistry and geology.* 617p. W.H. Freeman and Company. USA.

Hunt, J.M. (1984) Generation and Migration of Light Hydrocarbons: Science 226, 1265-1270.

Hunt, J.M. (1995) *Petroleum Geochemistry and Geology,* 2nd ed., Freeman: San Francisco, 1995.

International Energy Agency (IEA) (2015) World Energy Outlook 2015: http://www.worldenergyoutlook.org/media/weowebsite/2015/151110_WEO2015_presentation.pdf, accessed November 10th, 2015.

Irwin, M.L. (1965) General theory of epeiric clear water sedimentation: *American Association Petroleum Geologists Bulletin* **49**, 445-459.

Jacobson, S.R. (1991) Petroleum source rocks and organic facies, *in* Merrill, R.K., ed., Source and migration processes and evaluation techniques: American Association of Petroleum Geologists Handbook of Petroleum Geology, 1-11.

Jarvie, D.M., Hill, R.J., Ruble, T.E. and Pollastro, R.M. (2007) Unconventional shale-gas systems: The Mississippian Barnett Shale of north-central Texas as one model for thermogenic shale-gas assessment: *American Association of Petroleum Geologists Bulletin* **91**, 475-499.

Jarvie, D.M. (2010) Worldwide Shale Resource Plays and Potential: *American Association of Petroleum Geologists Search and Discover* Article #90104©2010 American Association of Petroleum Geologists Annual Convention and Exhibition 11-14 April 2010.

Jarvie, D.M. (2012a) Shale Resource Systems for Oil and Gas: Part 1—Shale-gas Resource Systems: in J. A. Breyer, ed., Shale reservoirs—Giant resources for the 21st century: *AAPG Memoir* **97**, 69-87.

Jarvie, D.M. (2012b) Shale Resource Systems for Oil and Gas: Part 2—Shale-gas Resource Systems: in J. A. Breyer, ed., Shale reservoirs—Giant resources for the 21st century: *AAPG Memoir* **97**, 89-119.

Johnson, K.S. (1989) Geological evolution of the Anadarko Basin: *Anadarko Basin Symposium, 1988. Oklahoma Geological Survey Circular* **90**, 3-12.

Jones, R.W. and Demaison, G.J. (1982) Organic facies-stratigraphic concept and exploration tool: *Proc. 2nd ASCOPE Conf. Exhibit* **1982**, 51-68.

Jones, R.W. (1983) Organic matter characteristics near the shelf-slope boundary, in Stanley, D.J. and Moore, G.T. (eds.), The shelf break: critical interface on continental margins: *Society of Economic Paleontologists and Mineralogists Special Publication* **33**, 391-405.

Jones, P.J. (1986) The petroleum geochemistry of the Pauls Valley area, Anadarko Basin, Oklahoma: *University of Oklahoma, unpublished M.S. Thesis*, 175p.

Jones, P.J. and Philp, R.P. (1990) Oils and source rocks from Pauls Valley, Anadarko basin, Oklahoma, U.S.A.: *Applied Geochemistry* **5**, 429-448.

Kareem, M.R. (1992) Geological constrained modeling of the temporal and spatial evolution of hydrocarbon generation in the Anadarko Basin: *University of Oklahoma, unpublished M.S. Thesis*, 191p

Kelley, S.A. (1991) Thermal condition in the Anadarko Basin, Oklahoma: *American Association of Petroleum Geologists Bulletin* **75**, 607.

Kilian, B.J. (2012) Sequence stratigraphy of the Woodford Shale, Anadarko Basin, Oklahoma: Implications on regional Woodford target correlation: Norman, University of Oklahoma, unpublished M.S. thesis, 102p.

Kim, D. (1999) Organic geochemistry of Mississippian age rocks from the Northeastern margin of the Anadarko Basin, Oklahoma: *University of Oklahoma, unpublished Ph.D. dissertation*, 147p.

Kirkland, D.W., Denison, R.E., Summers, D.M., and Gormly, J.R. (1992) Geology and organic geochemistry of the Woodford Shale in the Criner Hills and western Arbuckle Mountains, in K.S. Johnson and B.J. Cardott, eds., Source rocks in the southern Midcontinent, 1990 symposium: OGS Circular 93, p. 38-69.

Koopmans, M. P., Koster, J., Van Kaam-Peters, H. M. E. (1996) Diagenetic and catagenetic products of isorenieratene: molecular indicators for photic zone anoxia: *Geochimica et Cosmochimica Acta* **60**, 4467-4496.

Kvale, E.P. and Bynum, J. (2014) Regional upwelling during Late Devonian Woodford deposition in Oklahoma and its influence on hydrocarbon production and well completion: *AAPG Search and Discovery* Article #80410, 34p.

Lambert, M.W. (1994) Revised Upper Devonian and Lower Mississippian stratigraphic nomenclature in Kansas, in D.L. Baars, compiler, Revision of stratigraphic nomenclature in Kansas: *Kansas Geological Survey Bulletin* **230**, 75-77.

Lardner, J. E. (1984) Petrology, depositional environment, and diagenesis of Middle Pennsylvanian (Desmoinesian) "Lagoonal interval" Cherokee Group in east-central Kansas: M.S. thesis, University of Iowa, 156 p.

Lee, W. (1943) The stratigraphy and structural development of the Forest City basin: *Kansas State Geological Survey of Kansas Bulletin* **51**, 142 p.

Lewan, M.D., Winters, J.C. and McDonld, J.H. (1979) Generation of oil-like pyrolyzates from organic-rich shales: *Science* **203**, 897-899.

Lewan, M.D. (1983) Effects of thermal maturation on stable organic isotopes as determined by hydrous pyrolysis of Woodford Shale: *Geochimica et Cosmochimica Acta* **47**, 1471-1479.

Lin, R. and Wilk, Z.A. (1995) Natural occurrence of tetramantane ($C_{22}H_{28}$), pentamantane ($C_{26}H_{32}$) and hexamantane ($C_{30}H_{36}$) in a deep petroleum reservoir: *Fuel* **74**, 1512-1521.

Loucks R.G. and Ruppel S.C. (2007) Mississippian Barnett Shale: lithofacies and depositional setting of a deep-water shale-gas succession in the Fort Worth Basin, Texas: *American Association of Petroleum Geologists Bulletin* **91**, 579-601.

Mango, F.C. (1990) The origin of light hydrocarbons in petroleum: A kinetic test of the steady-state catalytic hypothesis: *Geochimica et Cosmochimica Acta* **54**, 1315-1323.

Mango, F.D. (1991) The stability of hydrocarbons under the time-temperature conditions of petroleum genesis: *Nature* **352**,146-148.

Mango, F.C. (1994) The origin of light hydrocarbons in petroleum: Ring preference in the closure of carbocylic rings: *Geochimica et Cosmochimica Acta* **58**, 895-901.

Mango, F.D. (1997) The light hydrocarbons in petroleum: a critical review: *Organic Geochemistry* **26**, 2641-2644.

Mann, E.A. (2014) Stratigraphic study of organic-rich microfacies of the Woodford Shale, Anadarko Basin, Oklahoma: Norman, OK, University of Oklahoma, unpublished M.S. thesis, 110p.

McCullough, B.J., and R.M. Slatt, 2014, Stratigraphic variability of the Woodford Shale across Oklahoma: *AAPG Search and Discovery Article* #80417, 24p. http://www.searchanddiscovery.com/pdfz/documents/2014/80417mccullough/ndx _mccullough.pdf.html

McKirdy, D.M., Aldridge, A.K. and Ypma, P.J.M. (1983) A geochemical comparison of some crude oils from Pre-Ordovician carbonate rocks. In: *Advances in Organic Geochemistry 1981* (M. Bjoroy, C. Albrecht, C. Cornford, et al., eds.), John Wiley & Sons, New York, 99-107.

McKirdy, D.M., Kanstler, A.J., Emmett, J.K. and Aldridge, A.K. (1984) Hydrocarbon genesis and organic facies in Cambrian carbonates of the Eastern Officer Basin, South Australia. In: *Petroleum Geochemistry and Source Rock Potential of Carbonate Rocks* (J.G. Palacas, ed.), American Association of Petroleum Geologists Geology, Tulsa, OK, 13-31.

Mello, M.R., Telnaes, N., Gaglianone, P.C., Chicarelli, M.I., Brassell, S.C., and Maxwell, J.R. (1988) Organic geochemical characterization of depositional paleoenvironments of source rocks and oils in Brazilian marginal basins: *Organic Geochemistry* **13,** 31-45.

Menchaca, M. (2014) Oklahoma Oil and Gas: Woodford SCOOP Wells Have Stamina: in DI BLOG, *drillinginfo website*.

Merriam, D.F. (1963) The Geologic History of Kansas: *State Geological Survey of Kansas Bull.* **162**, 317 p.

Miall, A.D. (2008) The Southern Midcontinent, Permian Basin, and Ouachitas: *The Sedimentary Basins of the United States and Canada* **5**, 297-327.

Miceli Romero, A. (2010) Geochemical characterization of the Woodford Shale, central and southeastern Oklahoma: Norman, OK, University of Oklahoma, unpublished M.S. thesis, 133p.

Miceli Romero, A. and Philp, R.P. 2012, Organic geochemistry of the Woodford Shale, southeastern Oklahoma: How variable can shales be?: *American Association Petroleum Geologists Bulletin* **96**, 493-517.

Miceli Romero, A. (2014) Subsurface and outcrop organic geochemistry of the Eagle Ford Shale (Cenomanian-Coniacian) in West, Southwest, Central, and East Texas: University of Oklahoma, unpublished Ph.D. dissertation, 323p.

Miller, R.C. (2006) Characterization of the Woodford Shale in outcrop and subsurface in Pontotoc and Coal Counties, Oklahoma: Norman, OK, University of Oklahoma, unpublished M.S. thesis, 110p.

Moldowan, J.M., Seifert, W.K., and Gallegos, E.J. (1985) Relationship between petroleum composition and depositional environment of petroleum source rocks: *American Association of Petroleum Geologists Bulletin* **69**, 1255-1268.

Moldowan, J.M. and Fago, F.J. (1986) Structure and significance of a novel rearranged monoaromatic steroid hydrocarbon in petroleum: *Geochimica et Cosmochimica Acta* **50**, 343-351.

Moldowan, J.M., Sundararaman, P., and Schoell, M. (1986) Sensitivity of biomarker properties to depositional environment and/or source input in the Lower Toarcian of S.W. Germany: *Organic Geochemistry* **10,** 915-926.

Moldowan, J. M., Fago, F.J., Lee, C.Y. (1990) Sedimenatary 24-n-propylcholestanes, molecular fossils diagnostic of marine algae: *Science* **247**, 309-312.

Moldowan, J. M., Fago, F. J., Carlson, R. M. K., et al. (1991) Rearranged hopanes in sediments and petroleum: *Geochimica et Cosmochimica Acta* **55**, 3333-3353.

Moldowan, J.M., Lee, C.Y., Sundararaman, P., Salvatori, T., Alajbeg, A., Gjukić, B., Demaison, G.J., Slougui, N., and Watt, D. (1992) Source correlation and maturity assessment of selected oils and rocks from the Central Adriatic Basin (Italy and Yugoslavia): In Moldowan, J.M., Albrecht, P. and Philp R.P. (eds.) *Biological Markers in Sediments and Petroleum* **1992**, 370-401.

Moldowan, J.M., Peters, K.E., Carlson, R.M.K., Schoell, M., and Abu-Ali, M.A. (1994) Diverse applications of petroleum biomarker maturity parameters: *The Arabian Journal for Science and Engineering* **19**, 273-298.

Molinares Blanco, C. E. (2013) Stratigraphy and palynomorphs composition of the Woodford Shale in the Wyche Farm Shale Pit, Pontotoc County, Oklahoma: *University of Oklahoma, unpublished Master thesis*, 90p.

Northcutt R. A. and Campbell J. A. (1996) Geologic provinces of Oklahoma: *Shale Shaker* **46**, 99-103.

Northcutt, R. A., Johnson, K. S., and Hinshaw, G. C. (2001) Geology and petroleum reservoirs in Silurian, Devonian, and Mississippian rocks in Oklahoma: In Johnson K. S. (ed.) Silurian, Devonian, and Mississippian geology and petroleum in the southern Midcontinent, 1999 symposium. *Oklahoma Geological Survey Circular* **105,** 1-29.

O'Brien, N.R., and Slatt, R.M. (1990) Woodford Formation, *in* Argillaceous rock atlas: New York, Springer-Verlag, 104-105.

Oklahoma Geological Survey (2009) *Oklahoma geologic provinces map* (in jpg), http://www.ogs.ou.edu/level2-earthscied.php, accessed on October 5, 2009.

Ourisson, G., Albrecht, P., and Rohmer, M. (1979) The hopanoids. Paleochemistry and biochemistry of a group of natural products: *Pure and Applied Chemistry* **51**, 709-729.

Ourisson, G., Albrecht, P., and Rohmer, M. (1982) Predictive microbial biochemistry – from molecular fossils to prokaryotic membranes: *Trends in biochemical sciences* **7**, 236-239.

Palacas, J.G., Anders, D.E., and King, J.D. (1984) South Florida Basin – a prime example of carbonate source rocks in petroleum: In Palacas, J.G. (ed.) Petroleum geochemistry and source rock potential of carbonate rocks. *AAPG Special Publication* **18,** 71-96.

Parrish, J.T. (1982) Upwelling and petroleum source beds, with reference to Paleozoic: *American Association of Petroleum Geologists Bulletin* **66**, 750-774.

Pawlewicz, M.J. (1989) Thermal maturation of the eastern Anadarko basin, Oklahoma: *U.S. Geological Survey Bulletin* **1866-C**, C1-C12.

Pearce, T.J., and Jarvis, I. (1992) Applications of geochemical data to modeling sediment dispersal patterns in distal turbidites: Late Quaternary of the Madeira Abyssal Plain: *Journal of Sedimentary Petrology* 62, 1112–1129.

Pearce, T.J., Besly, B.M., Wray, D.S. and Wright, D.K. (1999) Chemostratigraphy: A method to improve interwell correlation in barren sequences — A case study using onshore Duckmantian/Stephanian sequences (West Midlands, U.K.): *Sedimentary Geology* **124**, 197–220.

Pepper, A.S. and Corvi, P.J. (1995) Simple kinetic models of petroleum formation. Part I: oil and gas generation from kerogen: *Marine and Petroleum Geology* **12**, 291-319.

Perry, W.J. (1989) Tectonic evolution of the Anadarko Basin region, Oklahoma: *United States Geological Survey Bulletin* **1866-A**, 19p.

Peters, K.E. (1986) Guidelines for evaluating petroleum source rock using programmed pyrolysis: *American Association of Petroleum Geologists Bulletin* **70**, 318-329.

Peters, K.E., Moldowan, J.M., Sundararaman, P. (1990) Effects of hydrous pyrolysis on biomarker thermal maturity parameters: Monterey Phosphatic and Siliceous members: *Organic Geochemistry* **15**, 249-265.

Peters, K.E. and Moldowan, J.M. (1991) Effects of source, thermal maturity, and biodegradation on the distribution and isomerization of homohopanes in petroleum: *Organic Geochemistry* **17**, 47-61.

Peters, K.E., and Cassa, M.R. (1994) Applied source rock geochemistry, *in* Magoon, L.B., and Dow, W.G., eds., The petroleum system—From source to trap: Tulsa, Okla., *American Association of Petroleum Geologists Memoir* **60**, 93-117.

Peters, K.E., Cluston, M.J. and Robertson, G. (1999) Mixed marine and lacustrine input to an oil-cemented sandstone breccia from Brora, Scotland: *Organic Geochemistry* **30**, 237-248.

Peters, K.E., Walters, C.C., and Moldowan, J.M. (2005) *The biomarker guide, Volumes 1 and 2: biomarkers and isotopes in petroleum exploration and earth history.* Second Edition, 1155p. Cambridge University Press. USA.

Philp, R.P. and Gilbert, T.D. (1986) Biomarker distributions in oils and predominantly derived from terrigenous source material: In Leythaeuser, D. and Rullkötter, J. (eds.) *Advances in Organic Geochemistry,* 73-84.

Philp, R.P., Jones, P.J., Lin, L.H., Michael, G.E., and Lewis, C.A. (1989) An organic geochemical study of oils, source rocks, and tar sands in the Ardmore and Anadarko basins: in K.S. Johnson, ed., Anadarko basin symposium, 1988: *Oklahoma Geological Survey Circular* **90**, 65-76.

Philp, R.P., Chen, J.H., Galvez-Sinibaldi, A., Wang, H.D., and Allen, J.D. (1992) Effects of weathering and maturity on the geochemical characteristics of the Woodford Shale: In Johnson, K.S. and Cardott. B.J. (eds.) Source rocks in the Southern Midcontinent. *Oklahoma Geological Survey Circular* **93,** 106-121.

Philp, R.P. (2003) Petroleum Geochemistry, with a brief introduction to applications to exploration and production in Oklahoma: *The Shale Shaker* **54**, 69-79.

Philp, R.P. (2007) The role of geochemistry in characterization of gas shales and produced gas: *Geological Society of America Annual Meeting and Exposition – Abstracts with programs,* pp. 356.

Picha, F.J., and Peters, K.E. (1998) Biomarker oil-to-source rock correlation in the Western Carpathians and their foreland, Czech Republic: *Petroleum Geoscience* **4**, 289 – 302.

Pollastro, R.M. (2007) Total petroleum system assessment of undiscovered resources in the giant Barnett Shale continuous (unconventional) gas accumulation, Fort Worth Basin, Texas: *American Association of Petroleum Geologists Bulletin* **91**, 551-578.

Powell, T. G. and McKirdy, D. M. (1973) Relationship between ratio of pristane to phytane, crude oil composition and geological environment in Australia: *Nature*, **243**, 37-39.

Rangel, A., Parra, P., and Niño, C. (2000) The La Luna Formation: chemostratigraphy and organic facies in the Middle Magdalena Basin: *Organic Geochemistry* **31,** 1267-1284.

Radke, M. and Welte, D.H. (1981) The Methylphenanthrene Index (MPI): A maturity parameter based on aromatic hydrocarbons: *Advances in Organic Geochemistry*, 504-512.

Radke, M., Welte, D.H., and Willsch, H. (1982) Geochemical study on a well in the Western Canada Basin: relation of the aromatic distribution pattern to maturity of organic matter: *Geochimica et Cosmochimica Acta* **46**, 1–10.

Radke, M., Leythaeuser, D., and Teichmüller, M. (1984) Relationship between rank and composition of aromatic hydrocarbons for coal of different origins: *Organic Geochemistry* **6,** 423-430.

Radke, M., Welte, D.H., and Willsch, H. (1986) Maturity parameters based on aromatic hydrocarbons: influence of the organic matter type: *Organic Geochemistry* **10,** 51-63.

Rascoe, B.Jr. and Hyne, N.J. (1988) Petroleum Geology of the Mid-Continent: *Tulsa Geological Society Special Publication* **3**, 162p.

Reber, J.J. (1988) Correlation and biomarker characterization of Woodford-type oil and source rock, Aylesworth field, Marshall County, Oklahoma: University of Tulsa, unpublished M.S. thesis, 96p.

Reiser, J., McGregor, E., Jones, J., Enick, R. and Holder, G. (1996) Adamantane and Diamantane; Phase Diagrams, Solubilities, and Rates of Dissolution: *Fluid Phase Equilibria* **117**, 160-167.

Requejo, A.G. (1992) Quantitative analysis of triterpene and sterane biomarkers: methodology and applications in molecular maturity studies: *Biological Markers in Sediments and Petroleum* (J.M. Moldowan, P. Albrecht and R.P. Philp, eds.), Prentice-Hall, Englewood Cliffs, NJ, 222-240.

Riolo, J., Hussler, G., Albrecht, P. and Connan, J. (1986) Distribution of aromatic steroids in geological samples: their evaluation as geochemical parameters: *Organic Geochemistry* **10,** 981-990.

Roberts, C.T., and Mitterer, R.M. (1992) Laminated black shale-bedded chert cyclicity in the Woodford Formation, southern Oklahoma: K. S. Johnson and B. J. Cardott, eds., Source rocks in the southern Midcontinent, 1990 symposium: *Oklahoma Geological Survey Circular* **93**, 330-336.

Rowland, S.J. (1990) Production of acyclic isoprenoids hydrocarbons by laboratory maturation of methanogenic bacteria: *Organic Geochemistry* **15,** 9-16.

Rubinstein, I., Sieskind, O., and Albrecht, P. (1975) Rearranged sterenes in a shale: occurrence and stimulated formation: *Journal of Chemical Society, Perkin Transaction I,* 1833-1836.

Rullkötter, J., Spiro, B. and Nissenbaum, A. (1985) Biological marker characteristics of oils and asphalts from carbonate source rocks in a rapidly subsiding graben, Dead Sea, Israel: *Geochimica et Cosmochimica Acta* **49**, 1357-1370.

Schamel, S. (2015) Shale oil resource play potential of the Green River Formation, Uinta Basin, Utah: *Utah Geological Survey. Open-file report*, 639.

Schenk, C.J. (2005) Geologic Definition of Conventional and Continuous Accumulations in Select U.S. Basins – The 2001 Approach. In 2005 AAPG Hedberg Conference: Understanding, Exploring and Developing Tight Gas Sands: *AAPG Search and Discovery* article #90042.

Schleyer, P. von R. (1990) My thirty years in hydrocarbon cages: from adamantine to dodecahedrane. In: *Cage Hydrocarbons* (G.A. Olah, ed.), John Wiley & Sons, New York, pp. 1-38.

Schmoker, J.W. (1986) Oil generation in the Anadarko Basin, Oklahoma and Texas: Modeling using Lopatin's method: *Oklahoma Geological Survey Special Publication* **86-3**.

Schmoker, J.W. (1989) Thermal maturity of the Anadarko Basin: *Anadarko Basin Symposium, 1988. Oklahoma Geological Survey Circular* **90**, 25-31.

Schmoker, J.W. (2002) Resource-assessment perspectives for unconventional gas systems: *American Association of Petroleum Geologists Bulletin* **86**, 1993-1999.

Schopf, T.J.M. (1980) *Paleoceanography.* Harvard University Press, Cambridge.

Schulz, L.K., Wilhelms, A., Rein, E., Steen, A.S. (2001) Application of diamondoids to distinguish source rock facies: *Organic Geochemistry* **32**, 365-375.

Schwark, L. and Frimmel, A. (2004) Chemostratigraphy of the Posidonia Black Shale, SW Germany II. Assessment of extent and persistence of photic-zone anoxia using aryl isoprenoids distributions: *Chemical Geology* **206,** 231-248.

Seifert, W.K. and Moldowan, J.M. (1978) Applications of steranes, terpanes and monoaromatics to the maturation, migration and source of crude oils: *Geochimica et Cosmochimica Acta* **42**, 77-95.

Seifert, W.K. and Moldowan, J.M. (1986) Use of biological markers in petroleum exploration: In Johns, R.B. (ed.) *Methods in geochemistry and geophysics* **24**, 261-290.

Shanmugam, G. (1985) Significance of coniferous rain forests and related organic matter in generating commercial quantities of oil, Gippsland Basin, Australia: *American Association of Petroleum Geologists Bulletin* **69**, 1241-1254.

Shaw, A.B. (1964) Time in stratigraphy: McGraw-Hill, New York, 365 pp.

Singh P. (2008) Lithofacies and sequence stratigraphic framework of the Barnett Shale, Northeast Texas: *University of Oklahoma, unpublished Ph.D. dissertation,* 181p.

Sinninghe Damsté, J.S., Kenig, F., Koopmans, M.P., Koster, J.; Schouten, S., Hayes, J.M. and de Leeuw, J.W. (1995) Evidence for gammacerane as an indicator of water column stratification: *Geochimica et Cosmochimica Acta* **59**, 1895-1900.

Sinninghe Damsté J.S., Mueller, A., van Bentum, E., Reichart, G.J., and Schouten, S. (2009) Oceanic anoxia, organic carbon burial and climate change during OAE-2: *Goldschmit Conference Abstracts* **2009**, 1230.

Simoneit, B. R. T., Schoell, M., Dias, R. F., and Aquino Neto, F. R. (1993) Unusual carbon isotope compositions of biomarker hydrocarbons in a Permian tasmanite: *Geochimica et Cosmochimica Acta* **57**, 4205-4211.

Slatt, R.M., Singh, P., Philp R.P., Marfurt K.J., Abousleiman, Y. and O'Brien, N.R. (2009a) Workflow for stratigraphic characterization of unconventional gas shales:

2008 Society of Petroleum Engineers Shale Gas Production Conference, Fort Worth, Texas. SPE 119891.

Slatt, R.M., Singh, P., Philp R.P., Marfurt, K.J., Abousleiman, Y., O'Brien, N.R. and Eslinger, E.V. (2009b) Workflow for stratigraphic characterization of unconventional gas shales: *Gulf Coast Association of Geological Transactions* **59,** 699-710.

Slatt, R.M., Singh, P., Philp, R.P., Saison, A, Abousleiman, Y., O'Brien, N. R. and Eslinger, E.V. (2009c) Workflow for stratigraphic characterization of unconventional gas shales: *Geological Society of America, Abstracts with Programs* **41**, 12p.

Slatt, R.M., Singh, P., Borges, G., Perez, R., Portas, R., Vallejo, J., Ammerman, M., Coffey, W. and Eslinger, E. (2009d) Reservoir characterization of unconventional gas shales: example from the Barnett Shale, Texas, USA: *AAPG Search and Discovery, article* #30075.

Slatt, R.M., and O'Brien, N.R. (2011) Pore types in the Barnett and Woodford gas shales: Contribution to understanding gas storage and migration pathways in fine-grained rocks: *American Association Petroleum Geologist Bulletin* **95**, 2017-2030.

Sofer, Z. (1984) Stable carbon isotope compositions of crude oils: application to source depositional environments and petroleum alteration: *American Association of Petroleum Geologists Bulletin* **68**, 31-49.

Sullivan, K.L. (1983) Organic facies variation of the Woodford Shale in Western Oklahoma: *University of Oklahoma, Norman, unpublished M.S. thesis* **1983**, 101p.

Summons, R.E. and Powell, T.G. (1987) Identifiaction of aryl isoprenoids in a source rock and crude oils: biological markers for the green sulfur bacteria. *Geochimica et Cosmochimica Acta* **51,** 557-566.

Sweeney, J.J. and Burnham, A.K. (1990) Evaluation of a simple model of vitrinite reflectance based on chemical kinetics: *American Association of Petroleum Geologists Bulletin* **74**, 1559-1570.

ten Haven, H.L., de Leeuw, J.W., and Schenck, P.A. (1985) Organic geochemical studies of a Messinian evaporitic basin, northern Apennines (Italy) I: Hydrocarbon biological markers for a hypersaline environment: *Geochimica et Cosmochimica Acta* **49,** 2181-2191.

ten Haven, H.L., de Leeuw, J.W., Rullkötter, J., and Sinninghe Damsté, J.S. (1987) Restricted utility of the pristane/phytane ratio as a paleoenvironmental indicator: *Nature* **330,** 641-643.

ten Haven, H.L., de Leeuw, J.W., Sinninghe Damsté, J.S., Schenck, P.A., Palmer, S.E., and Zumberge, J.E. (1988) Application of biological markers in the recognition of palaeohypersaline environments: *Geological Society of London Special Publications* **40,** 123-130.

ten Haven, H.L., Rohmer, M., Rullkötter, J., and Bisseret, P. (1989) Tetrahymanol, the most likely precursor of gammacerane, occurs ubiquitously in marine sediments: *Geochimica et Cosmochimica Acta* **53,** 3073-3079.

Thompson, K.F.M. (1983) Classification and thermal history of petroleum based on light hydrocarbons: *Geochimica et Cosmochimica Acta* **47**, 303-316.

Thompson, K.F.M. (1987) Fractionated aromatic petroleums and the generation of gas-condensates: *Organic Geochemistry* **11**, 573-590.

Tissot, B.P., Durand, B., Espitalié, J., and Combaz, A. (1974) Influence of nature and diagenesis of organic matter in formation of petroleum*: American Association of Petroleum Geologists Bulletin* **58**, 499-506.

Tissot, B.P. and Welte, D.H. (1984) *Petroleum formation and occurrence.* Springer-Verlag Berlin Heidelberg, Germany, 699p.

Tissot, B.P. and Espitalie, J. (1975) L'evolution thermique de la matiere organique des sediments: aplications d'une simulation mathematique: *Rev. IFP* **30**, 743-777.

Tréanton, J.A. (2014) Outcrop-derived Chemostratigraphy of the Woodford Shale, Murray County, Oklahoma: M.S. Thesis, University of Oklahoma, Norman, OK.

Tréanton, J.A., B.W. Turner, and Slatt, R.M. (2014) Outcrop Derived Inorganic Geochemistry of the Woodford Shale, Murray County, Oklahoma: Houston Geological Society Applied Geoscience Conference (Mudrocks), Houston, TX.

Trendel, J.M., Restle, A., Cnnan, j. and Albrecht, P. (1982) Identification of a novel series of tetracyclic terpene hydrocarbons (C_{24}-C_{27}) in sediments and petroleums: *Journal of the Chemical Society, Chemical Communications*, 304-306.

Tribovillard, N., Algeo, T.J., Lyons, T. and Riboulleau, A. (2006) Trace metals as paleoredox and paleoproductivity proxies: An update: *Chemical Geology* **232**, 12–32.

Turner, B.W., Molinares-Blanco, C.E., and Slatt, R.M. (2015a) Chemostratigraphic, palynostratigraphic, and sequence stratigraphic analysis of the Woodford Shale, Wyche Farm Quarry, Pontotoc County, Oklahoma: *Interpretation* **3**, SH1-SH9.

Turner, B.W., Treanton, J.A., and Slatt, R.M. (2015b) The use of chemostratigraphy to refine ambiguous sequence stratigraphic correlations in marine shales: an example from the Woodford Shale, Oklahoma: *AAPG Search and Discovery* Article #51181, 17 slides.

Tyson, R.V. (1987) The genesis and palynofacies characteristics of marine petroleum source rocks. In: Brooks, J. and Fleet, A.J. (eds), Marine petroleum source rocks. Geol. Soc. Spec. Publ., 26, Blackwell, Oxford, 47-67.

Urban, J.B. (1960) Microfossils of the Woodford Shale (Devonian) of Oklahoma: *University of Oklahoma, Norman, unpublished M.S. thesis* **1960**, 77p.

Van Dorsselacer, A., Albrecht, P. and Ourisson, G. (1977) Identification of novel 17α (H)-hopanes in shales, coals, lignites, sediments and petroleum: *Bulletin e la Societ Chimique de France* **1-2**, 165-170.

Van Kaam-Peters, H.M.E., Heidy, M.E., Kostter, J., et al. (1998) The effect of clay minerals on diasterane/sterane ratios: *Geochimica et Cosmochimica Acta* **62,** 2923-2929.

Van Krevelen, D.W. (1961) Coal: typology-chemistry-physics-constitution: Elsevier Science, Amsterdam, 514 p.

Volkman, J. K., Alexander, R., Kagi, R. I., Noble, R. A., and Woodhouse, G. W. (1983) A geochemical reconstruction of oil generation in the Barrow Sub-basin of Western Australia: *Geochimica et Cosmochimica Acta* **51,** 1625-1637.

Volkman, J.K. (1986) A review of sterol markers for marine and terrigenous organic matter: *Organic Geochemistry* **47**, 2091-2106.

Volkman, J.K., Banks, M.R., Denwer, K., and Aquino Neto, F.R. (1989) Biomarker composition and depositional setting of *Tasmanite* oil shale from northern Tasmania, Australia: *14th International Meeting of Organic Geochemistry, Paris, France*.

Walper, J.L. (1977) Paleozoic tectonics of the southern margin of North America: *Gulf Coast Association of Geological Societies Transactions* **27**, 230-239.

Walters, C.C., Isaksen, G.H., Peters, K.E., (2003) Applications of light hydrocarbon molecular and isotopic compositions in oil and gas exploration: *Analytical Advances for Hydrocarbon Research*, Springer, pp. 247-266.

Waples, D.W., Machihara, T. (1990) Application of sterane and triterpanes biomarkers in petroleum exploration: *Bulletin of Canadian Petroleum Geology* **38**, 357-380.

Waples, D.W., Machihara, T. (1991) Biomarkers for geologists: *AAPG Methods in Exploration Series* **9**, 91.

Wang, H.D. (1993) A geochemical study of potential source rocks and crude oils in the Anadarko basin, Oklahoma: *University of Oklahoma, unpublished Ph.D. dissertation*, 296p.

Wang, H.D. and Philp, R.P. (1997) Geochemical study of potential source rocks and crude oils in the Anadarko Basin, Oklahoma: *American Association of Petroleum Geologists Bulletin* **81**, 249-275.

Waples, D.W. (1985) *Geochemistry in petroleum exploration.* International Human Resources Development Corporation. USA.

Waples, D.W. and Machihara T. (1991) Biomarkers for geologists – A practical guide to the application of steranes and triterpanes in petroleum geology: *AAPG Methods in Exploration* **9,** 85.

Welte, D.H., Hagemann, H.W., Hollerbach, A., and Leythaeuser, D. (1975) Correlation between petroleum and source rock, in J.A. Momper, chairman, Time and temperature relations affecting the origin, expulsion, and preservation of oil and gas: 9th World Petroleum Congress Proceedings **2**, Applied Science publishers, London, 179-191.

West, N., Alexander, R. and Kagi, R. (1990) The use of silicalite for rapid isolation of branched and cyclic alkane fractions of petroleum: *Organic Geochemistry* **15**, 499-501.

Williams, J.A., Bjoroy, M., Dolcater, D.L. and Winters, J.C. (1986) Biodegradation in South Texas Eocene oil effects on aromatics and biomarkers: *Organic Geochemistry* **10**, 451-462.

Wingert, W.S. (1992) GC-MS analysis of diamondoid hydrocarbons in Smackover petroleum: *Fuel* **71**, 37-43.

Zhang, S., Huang, H., Su, J., Zhu, G., Wang, X., and Larter, S. (2014) Geochemistry of Paleozoic marine oils from the Tarim Basin, NW China. Part 4: Paleobiodegradation and oil charge mixing: *Organic Geochemistry* **67,** 41-57.

Zumberge, J.E. (1987) Prediction of source rocks characteristics based on terpane biomarkers in crude oils: a multivariate statistical approach: *Geochimica et Cosmochimica Acta* **51,** 1625-1637.

8. APPENDIX

A. Abbreviations and formulas used for calculation of geochemical biomarker ratios

n-Alkanes

Carbon Preference Index (CPI)

$$CPI = \frac{1}{2}\left[\frac{C_{25} + C_{27} + C_{29} + C_{31} + C_{33}}{C_{26} + C_{28} + C_{30} + C_{32} + C_{34}} + \frac{C_{25} + C_{27} + C_{29} + C_{31} + C_{33}}{C_{24} + C_{26} + C_{28} + C_{30} + C_{32}}\right]$$

Terrigenous/Aquatic Ratio (TAR):

$$TAR = \left[\frac{C_{27} + C_{29} + C_{31}}{C_{15} + C_{17} + C_{19}}\right]$$

Steranes

C_{27}%, C_{28}%, C_{29}% = C_{27}, C_{28}, C_{29} [14α(H),17α(H)- + 14β (H),17β (H)-Cholestane (20S+ 20R)]

C_{29} 20S/(20S + 20R) = C_{29} [14α(H),17α(H)-Cholestane (20S)]/[14α(H),17α(H)-Cholestane (20S+20R)]

C_{29} ββ/(ββ + αα) = C_{29} [14β(H),17β(H)-Cholestane (20S+20R)]/[14β(H),17β(H)- + 14α(H),17α(H)-Cholestane (20S+20R)]

Preg/Ster = C_{21} 14β(H),17β(H)-Pregnane/C_{27} 14α(H),17α(H)-Cholestane (20R)

C_{27} Dia/C_{27} Sterane = [C_{27} 13β(H),17α(H)- + C_{27} 13α(H),17β(H)-Diacholestane (20S+20R)]/[C_{27} 14α(H),17α(H)- + 14β(H),17β(H)-Cholestane (20S+20R)]

C_{27} Dia/(Dia+Reg) = [C_{27} 13β(H),17α(H)- + 13α(H),17β(H)-Diacholestane (20S+20R)]/ [C_{27} 13β(H),17α(H)- + 13α(H),17β(H)-Diacholestane (20S+20R) + C_{27} 14α(H),17α(H)- + 14β(H),17β(H)-Cholestane (20S+20R)]

Sterane Index = $C_{30}/(C_{27}-C_{30})$ = [C_{30} 14α(H),17α(H)- + 14β(H),17β(H)-Cholestane (20S+20R)]/ C_{27}, C_{28}, C_{29}, C_{30} [14α(H),17α(H)- + 14β(H),17β(H)-Cholestane (20S+20R)]

Hopanes

Sterane/17α-Hopanes = [C_{27}, C_{28}, C_{29}, C_{30} 14α(H),17α(H)- + 14β(H),17β(H)-Cholestane (20S+20R)]/[C_{29} 17α(H),21β(H)-30-Norhopane + C_{30} 17α(H),21β(H)-Hopane + C_{31}+C_{32}+C_{33} 17α(H),21β(H)-Homohopanes (22S+22R)]

TR/17α-H = C_{28} + C_{29} Tricyclic terpanes (20S+20R)/17α-Hopanes

C22/C21TR = C_{22}/C_{21} Tricyclic terpanes

C24/C23TR = C_{24}/C_{23} Tricyclic terpanes

C26/C25TR = C_{26}/C_{25} Tricyclic terpanes

C23TR/30H = C_{23} Tricyclic terpanes/C_{30} 17α(H),21β(H)-Hopane

C24TT/30H = C_{24} Tetracyclic terpane/C_{30} 17α(H),21β(H)-Hopane

H29/H30 = C_{29} 17α(H),21β(H)-30-Norhopane/C_{30} 17α(H),21β(H)-Hopane

31R/30H = C_{31} 17α(H),21β(H)-Homohopane (22R)/C_{30} 17α(H),21β(H)-Hopane

35S/34S = C_{35} 17α(H),21β(H)-Pentakishomohopane (22S)/C_{34} 17α(H),21β(H)-Tetrakishomohopane (22S)

HH Index = $C_{35}/(C_{31} – C_{35})$ = C_{35} 17α(H),21β(H)-Pentakishomohopane (22S+22R)/[C_{31}+C_{32}+C_{33}+C_{34}+C_{35} 17α(H),21β(H)-Homohopanes (22S+22R)]

C31 22S/22S+22R = C_{31} [17α(H),21β(H)-Homohopanes (22S)/17α(H),21β(H)-Homohopanes (22S+22R)]

Aryl Isoprenoids

Aryl Isoprenoid ratio (AIR):

AIR = (C_{13}-C_{17})/(C_{18}-C_{22}) 2,3,6-trimethyl substituted aryl isoprenoids

Aromatics

MPI-1:

$$MPI\ 1 = 1.5\ \times \frac{[2 - MP + 3 - MP]}{[P + 1 - MP + 9 - MP]}$$

Calculated vitrinite reflectance:

For 0.65 to 1.35%R_o: R_c = 0.60 MPI-1 + 0.40

For 1.35 to 2.00%R_o: R_c = -0.60 MPI-1 + 2.30

MA(I):

$$MA(I) = \sum C_{27} - C_{29}\ MAS$$

MA(II):

$$MA\ (II) = \sum C_{21} - C_{22}\ MAS$$

MA29 = C_{29} [5α- + 5β-Stigmastane (20S+20R)]

%C_{27}, %C_{28}, %C_{29} MAS = ΣC_{27}, ΣC_{28}, ΣC_{29} MAS

B. Total Organic Carbon (TOC) and Rock-Eval (RE) parameters for the Woodford Shale and Mississippian Limestone samples

Frank 1-33 SWD core

Well Name	Depth (ft)	TOC	S_1	S_2	S_3	T_{max}	HI	OI	S_2/S_3	S_1/TOC	PI	$S_1 + S_2$
Frank 1-33SWD	5572.5	2.11	2.56	7.72	0.84	430	366	40	9.2	121	0.25	10.28
Frank 1-33SWD	5573.7	4.91	6.18	22.84	0.79	441	465	16	28.9	126	0.21	29.02
Frank 1-33SWD	5577.1	5.84	6.65	25.86	0.86	441	443	15	30.1	114	0.20	32.51
Frank 1-33SWD	5578.5	5.68	5.61	24.28	0.68	435	427	12	35.7	99	0.19	29.89
Frank 1-33SWD	5585.9	7.69	6.57	30.71	0.86	435	399	11	35.7	85	0.18	37.28
Frank 1-33SWD	5612.7	1.39	1.29	4.64	0.74	434	334	53	6.3	93	0.22	5.93
Frank 1-33SWD	5625.1	4.36	3.75	18.58	0.64	435	426	15	29.0	86	0.17	22.33
Frank 1-33SWD	5549.4	0.52	1.09	2.21	0.67	413	422	128	3.3	208	0.33	3.30
Frank 1-33SWD	5553.7	0.53	0.53	1.59	0.68	422	301	129	2.3	100	0.25	2.12
Frank 1-33SWD	5561.4	2.77	1.84	10.01	0.92	435	362	33	10.9	67	0.16	11.85
Frank 1-33SWD	5570.0	1.37	2.26	4.49	0.95	426	328	69	4.7	165	0.33	6.75
Frank 1-33SWD	5576.6	4.12	4.70	18.90	0.73	437	458	18	25.9	114	0.20	23.60
Frank 1-33SWD	5586.0	8.19	6.94	33.60	0.63	434	410	8	53.3	85	0.17	40.54
Frank 1-33SWD	5595.0	7.57	6.08	31.30	0.52	436	414	7	60.2	80	0.16	37.38
Frank 1-33SWD	5598.7	7.53	5.77	32.44	0.61	438	431	8	53.2	77	0.15	38.21
Frank 1-33SWD	5603.3	11.04	7.72	40.19	0.65	438	364	6	61.8	70	0.16	47.91
Frank 1-33SWD	5610.0	4.12	3.50	18.63	0.61	440	452	15	30.5	85	0.16	22.13
Frank 1-33SWD	5616.4	2.49	2.46	9.86	0.75	442	396	30	13.1	99	0.20	12.32
Frank 1-33SWD	5620.2	1.57	1.33	4.92	0.95	437	314	61	5.2	85	0.21	6.25
Frank 1-33SWD	5628.0	4.48	3.31	18.66	0.93	439	416	21	20.1	74	0.15	21.97
Frank 1-33SWD	5632.1	5.55	3.40	23.10	0.64	442	416	12	36.1	61	0.13	26.50

Elinore 1-18 SWD core

Well Name	Depth (ft)	TOC	S_1	S_2	S_3	T_{max}	HI	OI	S_2/S_3	S_1/TOC	PI	$S_1 + S_2$
Elinore 1-18SWD	4484.8	5.37	2.43	29.60	0.22	443	552	4	134.5	45	0.08	32.03
Elinore 1-18SWD	4486.7	7.55	3.12	40.03	0.58	438	530	8	69.0	41	0.07	43.15
Elinore 1-18SWD	4488.8	7.01	3.22	39.52	0.29	439	564	4	136.3	46	0.08	42.74
Elinore 1-18SWD	4490.9	6.77	3.30	42.78	0.34	437	632	5	125.8	49	0.07	46.08
Elinore 1-18SWD	4495.5	8.38	4.04	45.50	0.21	435	543	3	216.7	48	0.08	49.54
Elinore 1-18SWD	4499.1	9.08	4.45	47.18	0.21	435	520	2	224.7	49	0.09	51.63
Elinore 1-18SWD	4500.2	12.47	6.01	66.08	0.29	437	530	2	227.9	48	0.08	72.09
Elinore 1-18SWD	4500.8	9.04	4.42	55.68	0.25	435	616	3	222.7	49	0.07	60.10
Elinore 1-18SWD	4508.5	6.44	4.00	39.17	0.27	439	609	4	145.1	62	0.09	43.17
Elinore 1-18SWD	4512.6	5.06	3.68	33.92	0.21	435	670	4	161.5	73	0.10	37.60
Elinore 1-18SWD	4513.3	5.77	3.61	29.92	0.29	438	518	5	103.2	63	0.11	33.53
Elinore 1-18SWD	4519.4	7.96	4.49	45.09	0.39	436	566	5	115.6	56	0.09	49.58
Elinore 1-18SWD	4521.4	8.30	3.92	38.91	0.37	436	469	4	105.2	47	0.09	42.83
Elinore 1-18SWD	4525.4	9.39	4.73	50.62	0.21	437	539	2	241.0	50	0.09	55.35

Wilma 1-16 SWD core

Well Name	Depth (ft)	TOC	S_1	S_2	S_3	T_{max}	HI	OI	S_2/S_3	S_1/TOC	PI	$S_1 + S_2$
Wilma 1-16SWD	5326.3	4.23	1.95	11.14	0.30	443	263	7	37.1	46	0.15	13.09
Wilma 1-16SWD	5331.9	3.78	1.39	10.39	0.24	440	275	6	43.3	37	0.12	11.78
Wilma 1-16SWD	5339.0	6.87	3.27	24.17	0.17	448	352	2	142.2	48	0.12	27.44
Wilma 1-16SWD	5347.7	5.20	2.18	17.65	0.17	444	340	3	103.8	42	0.11	19.83
Wilma 1-16SWD	5349.0	7.21	3.64	25.46	0.11	442	353	2	231.5	51	0.13	29.10
Wilma 1-16SWD	5351.9	8.09	4.43	29.22	0.22	440	361	3	132.8	55	0.13	33.65

Wilma 1-16SWD	5358.4	5.56	2.84	18.95	0.18	444	341	3	105.3	51	0.13	21.79
Wilma 1-16SWD	5359.5	7.49	3.91	27.80	0.17	445	371	2	163.5	52	0.12	31.71
Wilma 1-16SWD	5364.5	7.59	3.73	27.48	0.17	446	362	2	161.6	49	0.12	31.21
Wilma 1-16SWD	5366.0	7.15	3.72	23.58	0.32	444	330	4	73.7	52	0.14	27.30
Wilma 1-16SWD	5369.5	1.64	1.63	6.35	0.26	440	388	16	24.4	100	0.20	7.98
Wilma 1-16SWD	5389.0	5.59	2.74	22.02	0.16	445	394	3	137.6	49	0.11	24.76
Wilma 1-16SWD	5400.0	15.51	5.67	67.76	0.15	446	437	1	451.7	37	0.08	73.43

Winney 1-8 SWD core

Well Name	Depth (ft)	TOC	S_1	S_2	S_3	T_{max}	HI	OI	S_2/S_3	S_1/TOC	PI	$S_1 + S_2$
Winney 1-8SWD	5298.5	0.18	0.15	0.28	0.39	445	156	218	1	84	0.35	0.43
Winney 1-8SWD	5305.4	0.08	0.07	0.13	0.19	445	165	241	1	89	0.35	0.20
Winney 1-8SWD	5309.6	0.43	1.10	0.95	0.40	428	223	94	2	258	0.54	2.05
Winney 1-8SWD	5312.8	3.27	3.99	11.39	0.10	442	349	3	114	122	0.26	15.38
Winney 1-8SWD	5319.3	3.93	2.85	12.49	0.30	442	318	8	42	73	0.19	15.34
Winney 1-8SWD	5328.8	0.72	0.47	2.04	0.41	450	284	57	5	65	0.19	2.51
Winney 1-8SWD	5339.0	0.71	0.32	1.91	0.23	452	271	33	8	45	0.14	2.23
Winney 1-8SWD	5350.5	3.38	4.02	13.44	0.24	447	398	7	56	119	0.23	17.46
Winney 1-8SWD	5360.1	6.61	4.64	23.93	0.21	439	362	3	114	70	0.16	28.57
Winney 1-8SWD	5370.0	6.39	4.03	24.38	0.35	443	382	5	70	63	0.14	28.41
Winney 1-8SWD	5380.4	11.68	6.15	45.11	0.17	443	386	1	265	53	0.12	51.26
Winney 1-8SWD	5381.3	7.10	4.38	30.73	0.09	447	433	1	341	62	0.12	35.11
Winney 1-8SWD	5390.2	6.99	4.86	28.53	0.16	446	408	2	178	70	0.15	33.39
Winney 1-8SWD	5390.5	1.19	0.88	1.60	0.09	398	134	8	18	74	0.35	2.48
Winney 1-8SWD	5400.0	0.53	0.74	1.18	0.41	442	222	77	3	139	0.39	1.92

Adkisson 1-33 SWD core

Well Name	Depth (ft)	TOC	S_1	S_2	S_3	T_{max}	HI	OI	S_2/S_3	S_1/TOC	PI	$S_1 + S_2$
Adkisson 1-33 SWD	5786.5	0.20	0.18	0.43	1.29	446	214	648	0	91	0.30	0.6
Adkisson 1-33 SWD	5796.4	0.78	0.56	1.54	1.68	443	197	215	1	72	0.27	2.1
Adkisson 1-33 SWD	5810.4	0.18	0.12	0.30	1.74	457	168	972	0	68	0.29	0.4
Adkisson 1-33 SWD	5820.5	1.95	1.01	3.36	1.23	441	172	63	3	52	0.23	4.4
Adkisson 1-33 SWD	5830.3	3.07	3.37	12.32	1.41	444	402	46	9	110	0.21	15.7
Adkisson 1-33 SWD	5840.6	6.35	3.92	22.92	0.29	445	361	5	79	62	0.15	26.8
Adkisson 1-33 SWD	5850.9	7.30	3.78	25.95	0.25	444	355	3	104	52	0.13	29.7
Adkisson 1-33 SWD	5860.5	9.84	3.90	34.29	0.27	446	348	3	127	40	0.10	38.2
Adkisson 1-33 SWD	5870.8	14.36	3.77	58.85	0.24	445	410	2	245	26	0.06	62.6
Adkisson 1-33 SWD	5873.1	9.60	1.83	39.38	0.33	450	410	3	119	19	0.04	41.2
Adkisson 1-33 SWD	5786.5	0.20	0.18	0.43	1.29	446	214	648	0	91	0.30	0.6
Adkisson 1-33 SWD	5796.4	0.78	0.56	1.54	1.68	443	197	215	1	72	0.27	2.1
Adkisson 1-33 SWD	5810.4	0.18	0.12	0.30	1.74	457	168	972	0	68	0.29	0.4
Adkisson 1-33 SWD	5820.5	1.95	1.01	3.36	1.23	441	172	63	3	52	0.23	4.4

OGS Woodford cores

Well Name	Depth (ft)	TOC	S_1	S_2	S_3	T_{max}	HI	OI	S_2/S_3	S_1/TOC	PI	$S_1 + S_2$
Mary Earp - 5	4087.0	9.19	3.87	56.45	0.78	431	614	8	72	42	0.06	60.32
Mary Earp - 5	4093.0	5.49	2.34	31.07	0.70	434	566	13	44	43	0.07	33.41
Mary Earp - 5	4098.5	0.33	0.22	0.49	0.40	437	151	123	1	68	0.31	0.71
Mary Earp - 5	4105.0	0.02	0.01	0.01	0.14	0	50	700	0	50	0.50	0.02
Mary Earp - 5	4110.0	0.23	0.41	0.33	0.50	429	145	219	1	180	0.55	0.74
Mary Earp - 5	4115.5	0.27	0.89	0.53	0.53	427	199	199	1	335	0.63	1.42

Mary Earp - 5	4122.0	0.13	0.02	0.13	0.24	0	97	179	1	15	0.13	0.15
Mary Earp - 5	4126.5	0.13	0.01	0.16	0.22	0	124	171	1	8	0.06	0.17
Boyd Unit-1	6475.0	3.89	3.67	32.37	0.98	435	832	25	33	94	0.10	36.04
Boyd Unit-1	6481.0	7.07	4.45	36.17	0.56	429	512	8	65	63	0.11	40.62
Boyd Unit-1	6486.5	5.69	2.77	27.75	0.64	429	488	11	43	49	0.09	30.52
Boyd Unit-1	6493.0	0.02	0.01	0.05	0.13	0	231	602	0	46	0.17	0.06
Boyd Unit-1	6523.0	0.01	0.01	0.05	0.13	0	512	1,332	0	102	0.17	0.06
Boyd Unit-1	6533.0	0.03	0.01	0.06	0.15	0	199	498	0	33	0.14	0.07
Dannehl 2-16	8596.0	7.53	3.86	28.75	0.63	443	382	8	46	51	0.12	32.61
Dannehl 2-16	8602.5	7.00	4.74	26.61	0.64	442	380	9	42	68	0.15	31.35
Dannehl 2-16	8608.0	6.03	4.12	23.95	0.52	442	397	9	46	68	0.15	28.07
Dannehl 2-16	8615.5	6.92	4.24	26.60	0.61	444	384	9	44	61	0.14	30.84
Dannehl 2-16	8619.5	5.66	3.68	22.29	0.44	444	394	8	51	65	0.14	25.97
Pritchard-1	5107.0	6.38	3.49	41.78	0.75	441	655	12	56	55	0.08	45.27
Pritchard-1	5113.0	5.63	3.34	38.61	0.61	439	686	11	63	59	0.08	41.95
Pritchard-1	5119.0	7.83	3.97	48.04	0.77	438	614	10	62	51	0.08	52.01
Pritchard-1	5125.0	5.56	3.37	35.59	0.74	438	640	13	48	61	0.09	38.96
Pritchard-1	5131.0	7.32	4.17	49.37	0.83	438	674	11	59	57	0.08	53.54
Pritchard-1	5137.0	7.82	4.72	53.52	0.84	439	684	11	64	60	0.08	58.24
Pritchard-1	5141.0	6.72	4.02	46.92	0.90	440	698	13	52	60	0.08	50.94
Pritchard-1	5147.0	8.90	4.82	59.36	0.85	435	667	10	70	54	0.08	64.18
Pritchard-1	5153.0	7.21	5.75	49.72	0.89	439	690	12	56	80	0.10	55.47
Pritchard-1	5159.0	8.15	5.55	52.66	0.83	436	646	10	63	68	0.10	58.21
Robberson Ranch 10-1	8707.0	14.40	4.67	57.10	1.34	443	397	9	43	32	0.08	61.77
Robberson Ranch 10-1	8712.0	8.12	3.85	39.67	0.92	440	489	11	43	47	0.09	43.52
Robberson Ranch 10-1	8723.0	2.99	2.01	13.16	0.58	441	440	19	23	67	0.13	15.17

Robberson Ranch 10-1	8726.0	5.26	2.74	30.22	0.72	443	575	14	42	52	0.08	32.96
Robberson Ranch 10-1	8731.0	0.31	1.55	0.92	0.64	428	296	206	1	498	0.63	2.47
Robberson Ranch 10-1	8759.0	0.14	0.43	0.40	0.43	422	290	312	1	312	0.52	0.83
Robberson Ranch 10-1	8774.5	0.02	0.01	0.01	0.06	0	44	262	0	44	0.50	0.02
Robberson Ranch 10-1	8787.5	0.04	0.01	0.05	0.10	0	122	244	1	24	0.17	0.06
Anderson 12-1	6824.0	4.89	2.28	19.08	0.56	448	390	11	34	47	0.11	21.36
Anderson 12-1	6833.0	3.69	2.06	11.09	0.48	449	301	13	23	56	0.16	13.15
Anderson 12-1	6836.0	3.91	2.06	16.62	0.54	448	425	14	31	53	0.11	18.68
Anderson 12-1	6842.0	6.80	3.94	27.78	0.53	445	409	8	52	58	0.12	31.72
Anderson 12-1	6848.0	6.16	3.26	21.62	0.60	440	351	10	36	53	0.13	24.88
Anderson 12-1	6857.0	5.36	2.62	19.49	0.65	449	364	12	30	49	0.12	22.11
Anderson 12-1	6869.0	5.01	2.79	17.84	0.68	445	356	14	26	56	0.14	20.63
Anderson 12-1	6875.0	4.83	2.79	15.89	0.65	442	329	13	24	58	0.15	18.68
Anderson 12-1	6881.0	6.74	3.66	23.08	0.64	440	342	9	36	54	0.14	26.74
Anderson 12-1	6887.0	6.25	3.26	22.53	0.57	443	360	9	40	52	0.13	25.79
Anderson 12-1	6893.0	7.00	4.29	26.70	0.70	443	381	10	38	61	0.14	30.99
Anderson 12-1	6897.0	7.42	3.43	25.60	0.49	448	345	7	52	46	0.12	29.03
Anderson 12-1	6903.0	1.45	0.75	4.77	0.36	448	329	25	13	52	0.14	5.52
Anderson 12-1	6912.0	5.34	2.37	19.70	0.47	448	369	9	42	44	0.11	22.07
Anderson 12-1	6918.0	4.37	2.02	14.23	0.62	445	326	14	23	46	0.12	16.25
Anderson 12-1	6923.0	8.51	5.21	35.64	0.63	446	419	7	57	61	0.13	40.85
Anderson 12-1	6929.0	6.28	3.95	23.69	0.67	444	377	11	35	63	0.14	27.64
Anderson 12-1	6933.0	0.78	1.00	1.51	0.44	445	193	56	3	128	0.40	2.51
Anderson 12-1	6935.0	0.63	0.58	1.27	0.44	448	201	70	3	92	0.31	1.85
Anderson 12-1	6941.0	0.22	0.08	0.19	0.21	0	85	94	1	36	0.30	0.27

Anderson 12-1	6944.0	0.25	0.17	0.33	0.15	434	130	59	2	67	0.34	0.50
Chenoweth-1	6505.0	0.89	1.42	0.98	0.66	438	110	74	1	160	0.59	2.40
Chenoweth-1	6512.0	6.22	3.67	15.25	0.61	440	245	10	25	59	0.19	18.92
Chenoweth-1	6518.0	3.33	1.86	8.11	0.45	442	244	14	18	56	0.19	9.97
Chenoweth-1	6525.0	4.04	3.22	10.29	0.63	438	255	16	16	80	0.24	13.51
Chenoweth-1	6530.0	4.18	3.27	12.89	0.72	439	308	17	18	78	0.20	16.16
Chenoweth-1	6536.0	7.52	3.24	16.72	0.50	443	222	7	33	43	0.16	19.96
Chenoweth-1	6541.0	4.09	2.67	10.33	0.66	443	253	16	16	65	0.21	13.00
Chenoweth-1	6546.0	0.78	0.73	1.51	0.57	433	193	73	3	93	0.33	2.24
Chenoweth-1	6553.5	0.17	0.05	0.11	0.17	0	64	99	1	29	0.31	0.16
Chenoweth-1	6559.5	0.25	0.08	0.35	0.18	430	141	73	2	32	0.19	0.43
Chenoweth-1	6562.0	0.23	0.11	0.14	0.28	0	61	122	1	48	0.44	0.25
York-1	8523.0	5.51	1.64	15.49	0.58	444	281	11	27	30	0.10	17.13
York-1	8525.0	5.24	1.88	16.41	0.60	443	313	11	27	36	0.10	18.29
York-1	8531.0	4.13	1.30	10.83	0.38	444	262	9	29	31	0.11	12.13
York-1	8537.0	0.04	0.01	0.02	0.11	0	49	272	0	25	0.33	0.03
York-1	8542.0	0.10	0.04	0.05	0.12	0	52	124	0	41	0.44	0.09
Pope Unit-1	8480.0	0.75	0.79	1.29	0.63	443	173	84	2	106	0.38	2.08
Pope Unit-1	8485.0	0.73	0.47	0.94	0.44	445	128	60	2	64	0.33	1.41
Pope Unit-1	8497.0	0.54	0.35	0.67	0.36	444	124	67	2	65	0.34	1.02
Pope Unit-1	8510.0	0.44	0.35	0.34	0.36	444	78	83	1	80	0.51	0.69
Pope Unit-1	8522.0	0.17	0.04	0.02	0.12	0	12	72	0	24	0.67	0.06
Pope Unit-1	8534.0	0.32	0.21	0.21	0.22	445	66	69	1	66	0.50	0.42
Pope Unit-1	8542.0	0.13	0.05	0.02	0.05	0	16	39	0	39	0.71	0.07
Pope Unit-1	8589.0	5.52	1.66	14.18	0.58	440	257	11	24	30	0.10	15.84
Pope Unit-1	8590.0	0.16	0.19	0.11	0.34	0	67	207	0	116	0.63	0.30
Pope Unit-1	8611.0	0.26	0.73	0.19	0.61	0	73	236	0	282	0.79	0.92
Pope Unit-1	8628.0	0.14	0.04	0.02	0.16	0	15	119	0	30	0.67	0.06

Mississippian cores

Well Name	Depth (ft)	TOC	S_1	S_2	S_3	T_{max}	HI	OI	S_2/S_3	S_1/TOC	PI	$S_1 + S_2$
Albert Severin-1	6445	2.78	1.54	6.52	0.29	447	235	10	22	55	0.19	8.06
Elinore 1-18 SWD	4453	3.29	1.44	19.39	0.58	441	589	18	33.4	44	0.07	20.8
Winney 1-8 SWD	5155	2.49	2.20	11.46	0.27	435	460	11	42	88	0.16	13.7
Winney 1-8 SWD	5166	3.13	1.12	15.12	0.36	446	483	12	42	36	0.07	16.2

C. Gas chromatograms of the saturate fractions for the Woodford Shale samples analyzed in this study (Pr = pristane; Ph = phytane, n-C_{25} = C_{25} normal alkane)

Pritchard-1 core (Woodford Formation)

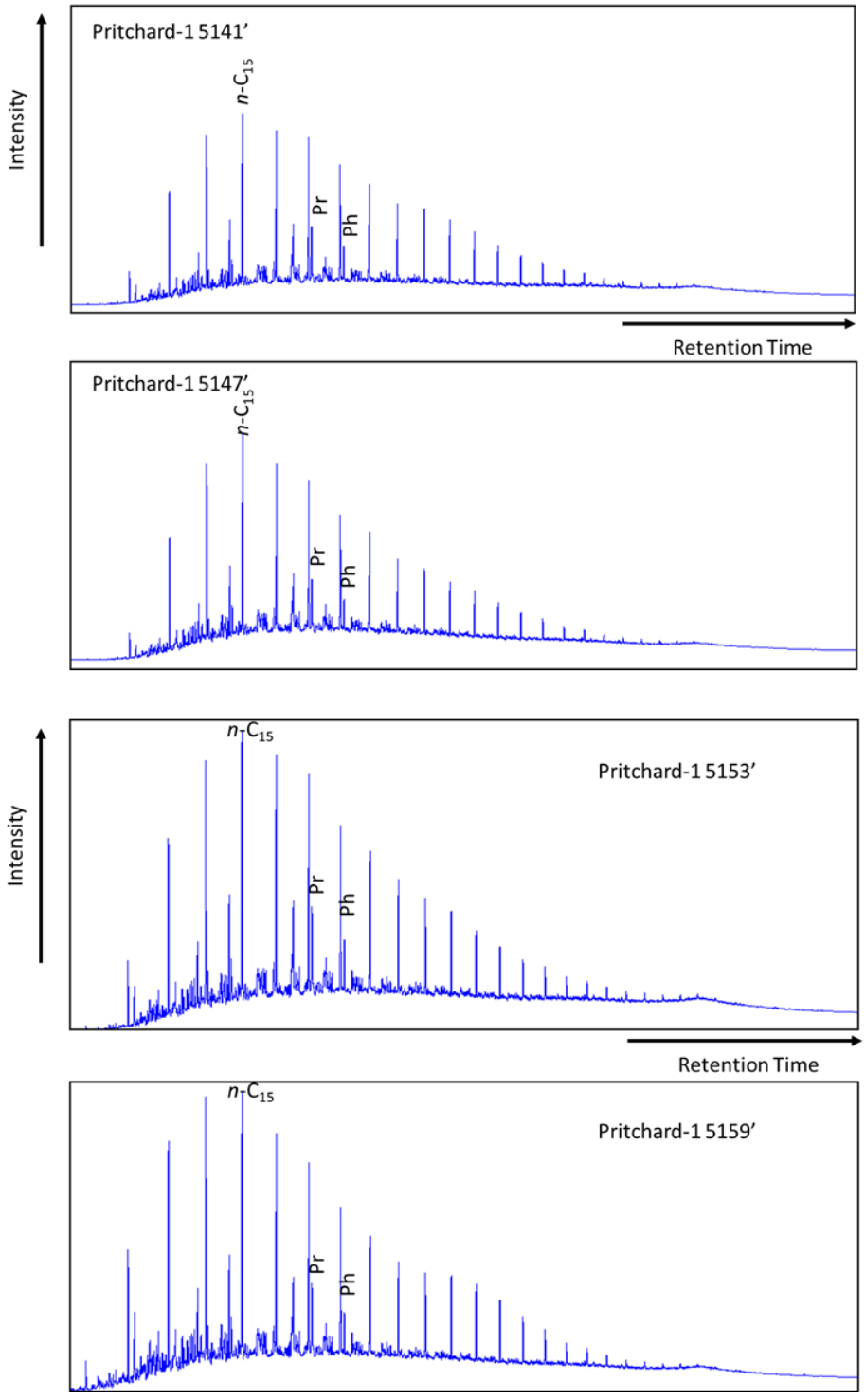

Frank 1-33 SWD core (Woodford Formation)

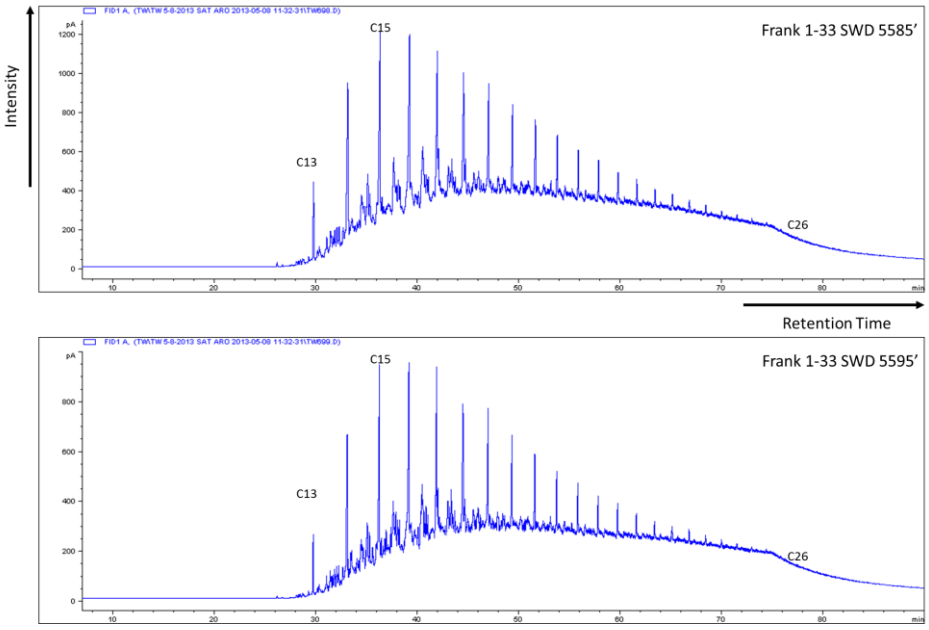

Wilma 1-16 SWD core (Woodford Formation)

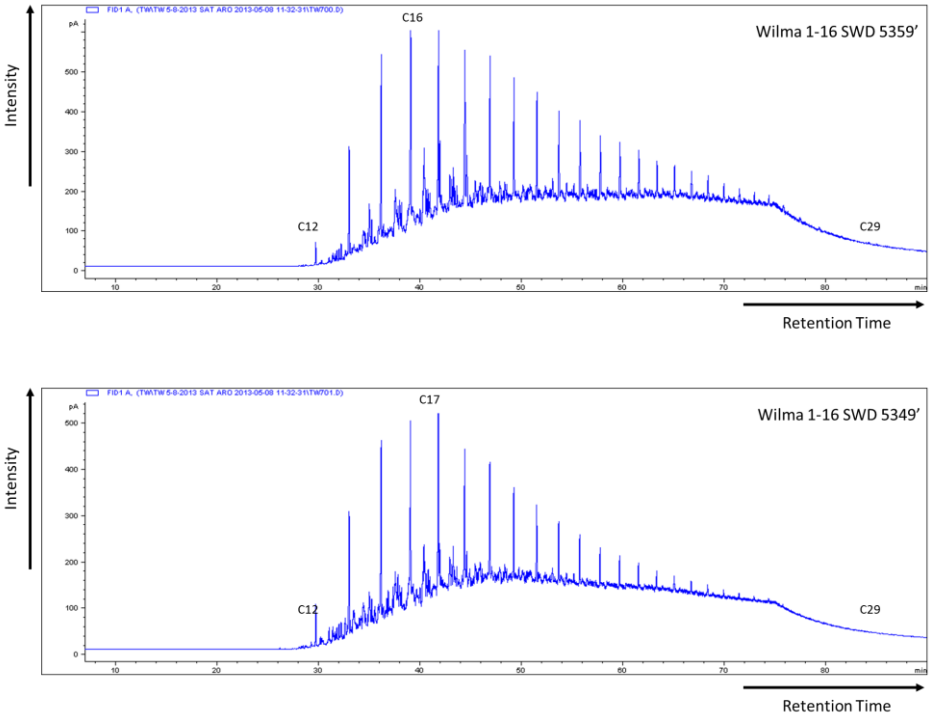

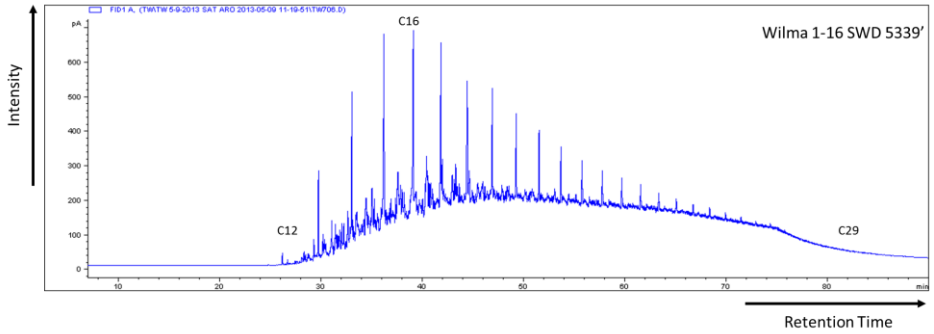

Adkisson 1-33 SWD core (Woodford Formation)

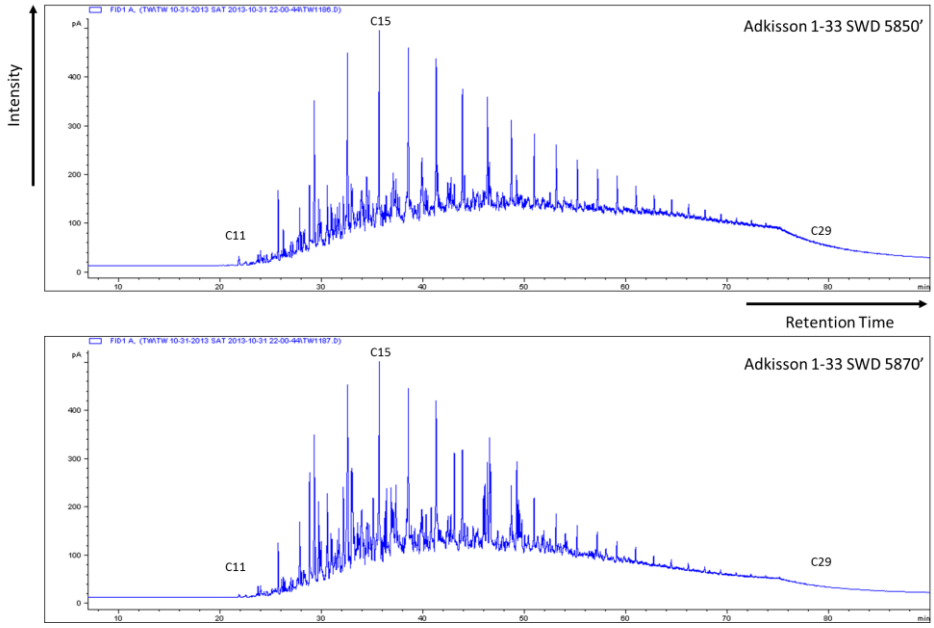

Elinore 1-18 SWD core (Woodford Formation)

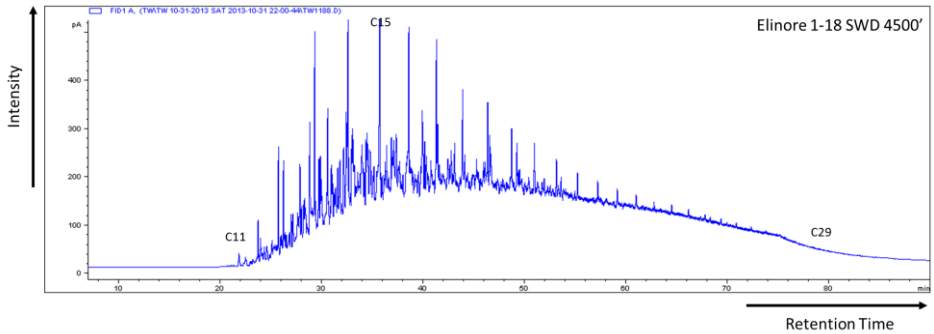

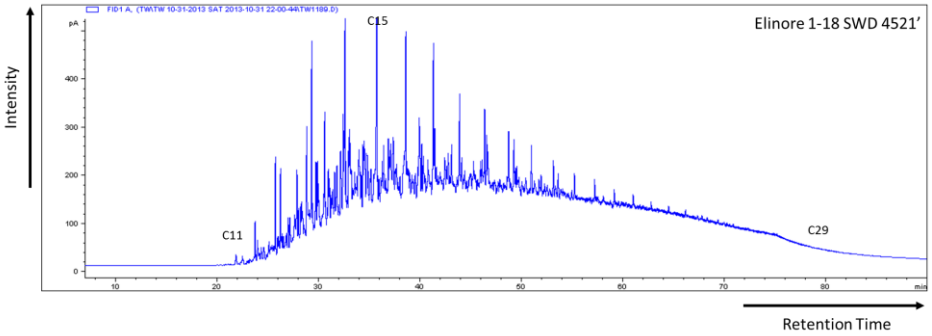

Ranch 10-1 core (Woodford Formation)

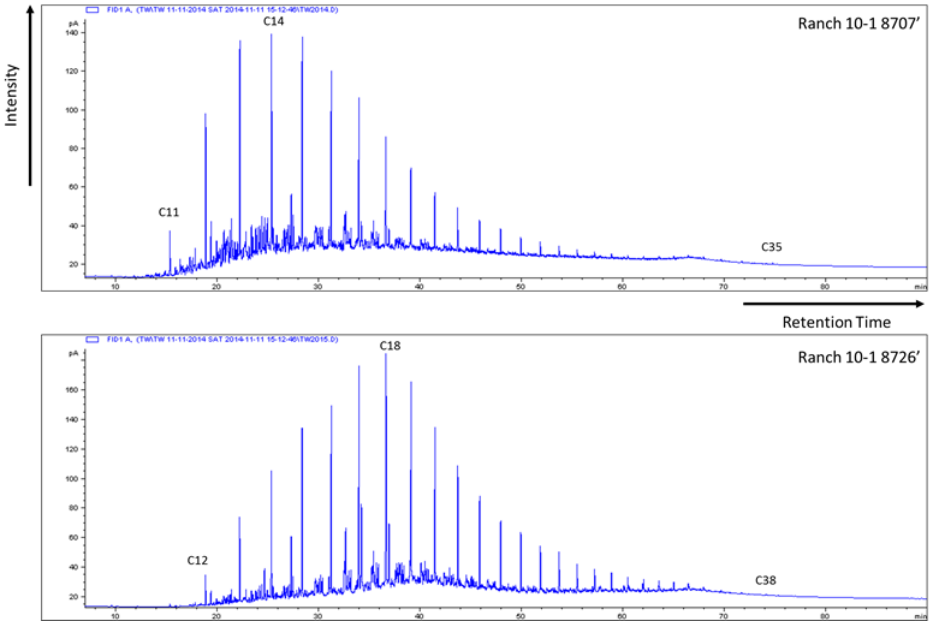

Anderson 12-1 core (Woodford Formation)

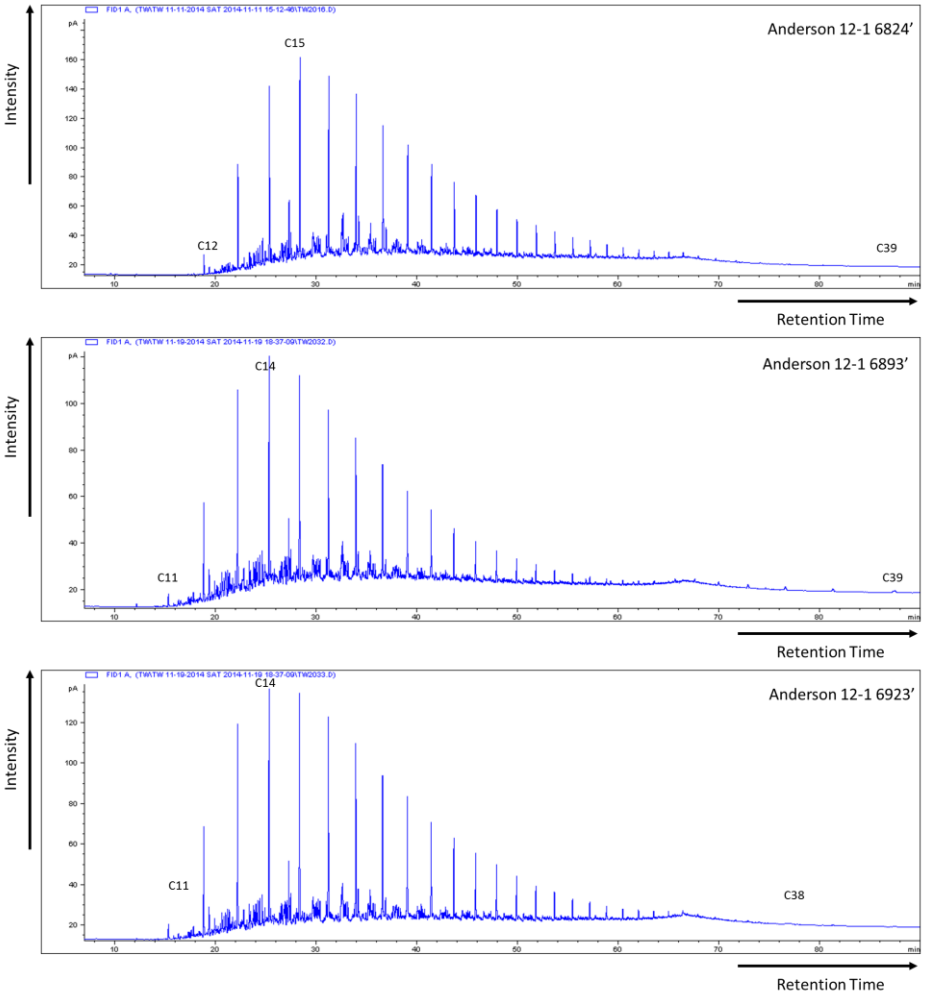

Chenoweth-1 (Woodford Formation)

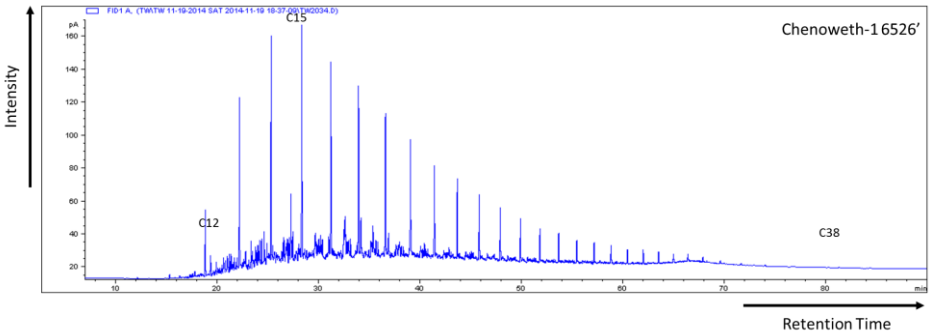

York-1 (Woodford Formation)

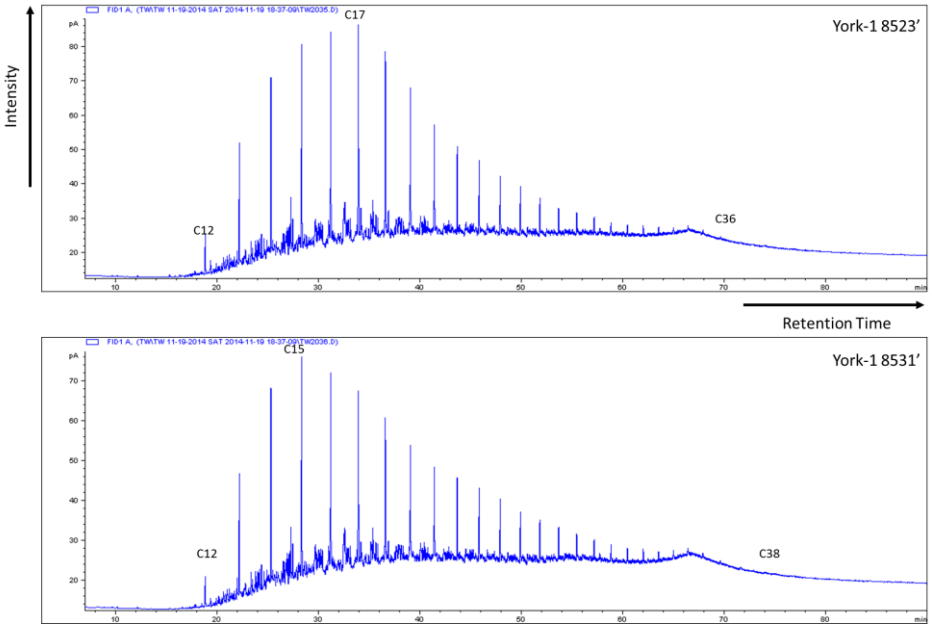

Pope Unit-1 (Woodford Formation)

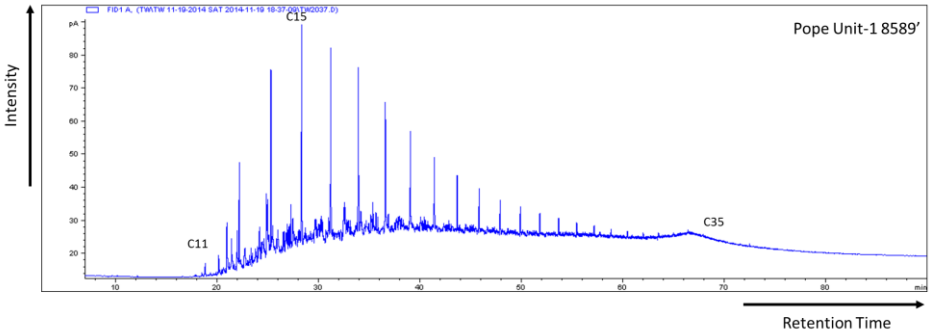

Mississippian cores

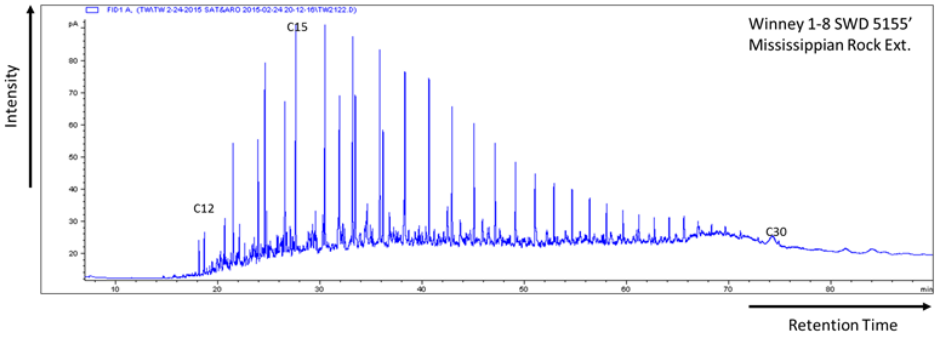

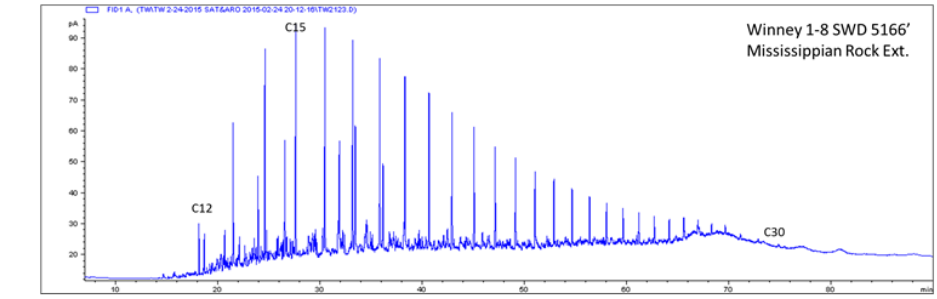

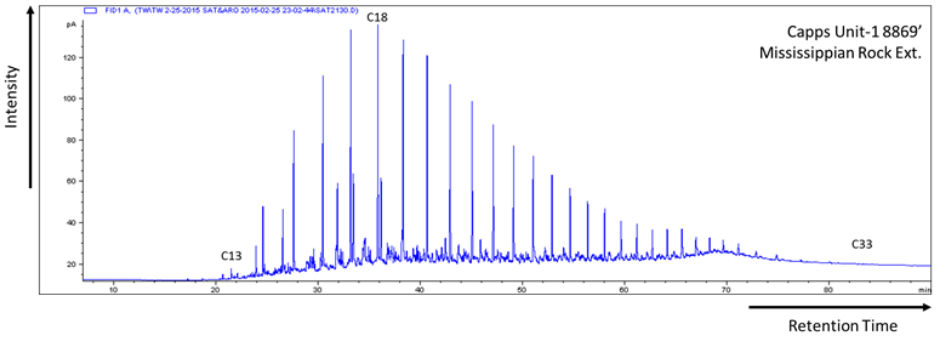

Smith 1-23 KO oil

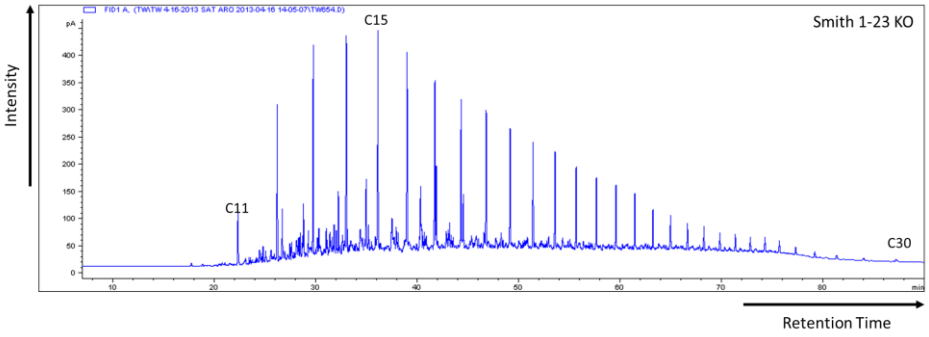

Wilma 1-16H oil

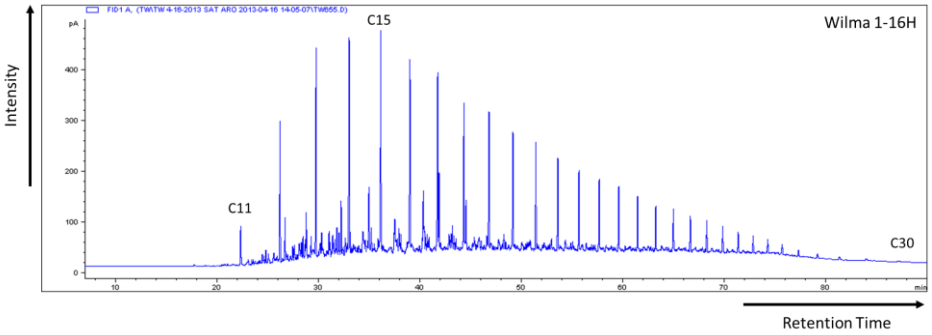

Matthews 1-33H oil

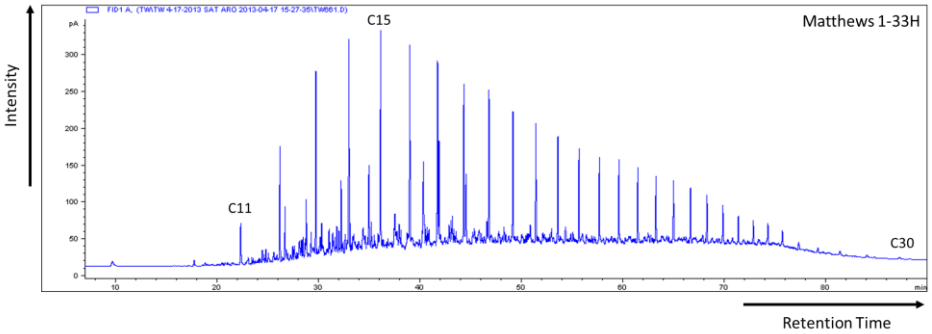

Winney 1-5H oil

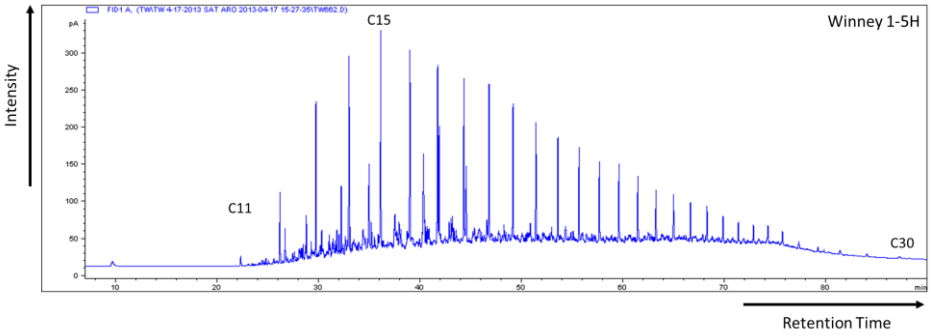

Smith 1-14H oil

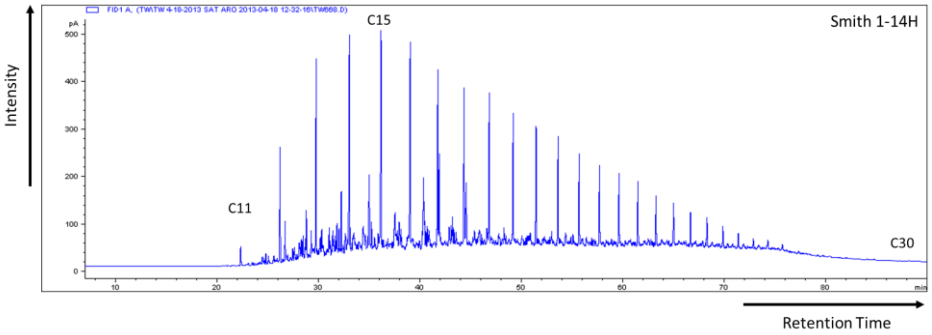

Johnson 1-33H oil

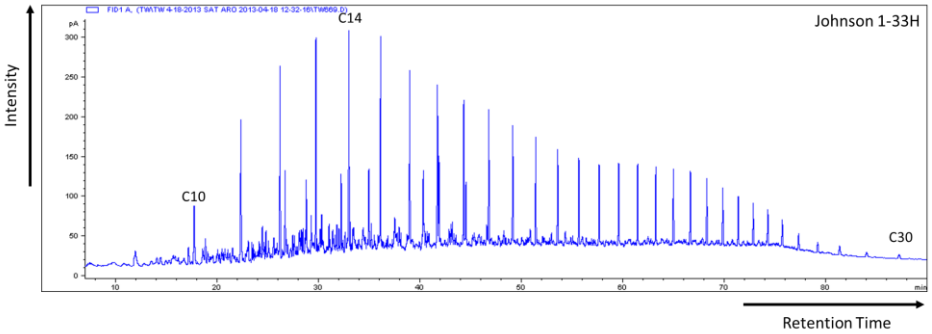

Elinore 1-18H oil

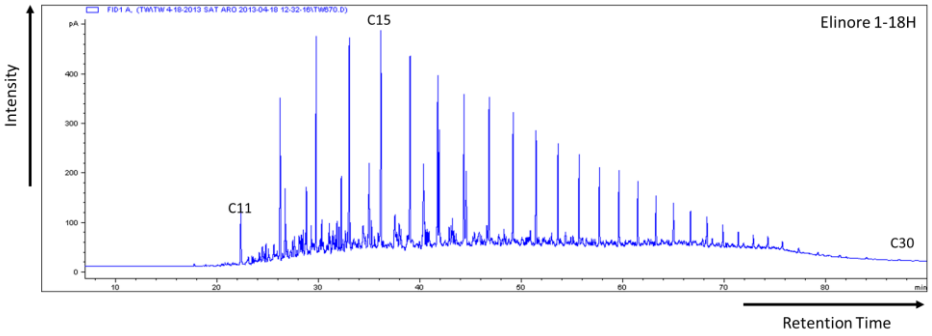

Winney 1-8H oil

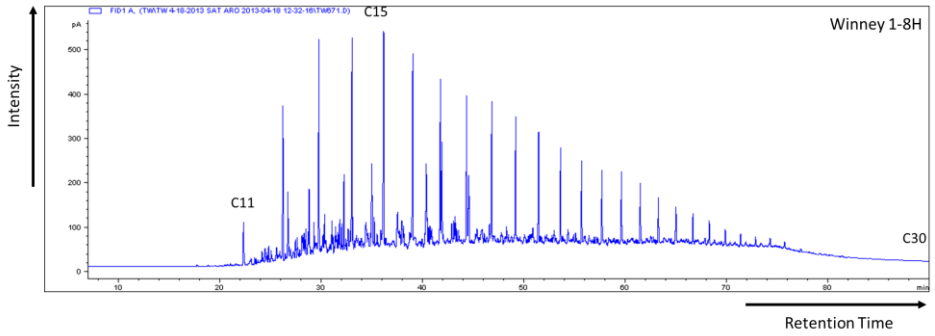

Adkisson 1-33H oil

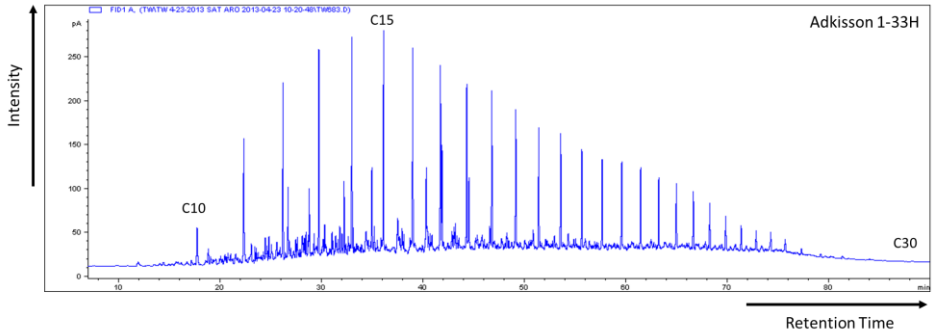

Elinore 1-17H oil

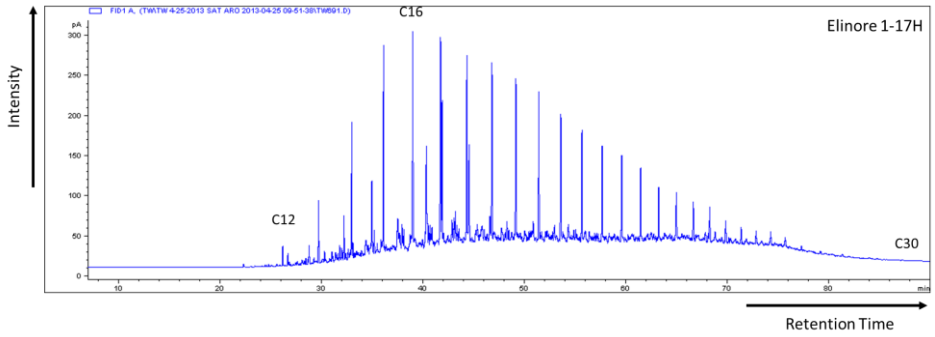

Williams 1-24WH oil

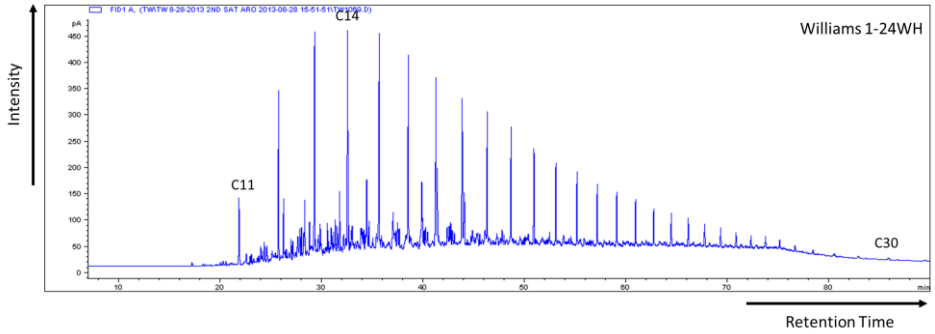

Peach 1-19H oil

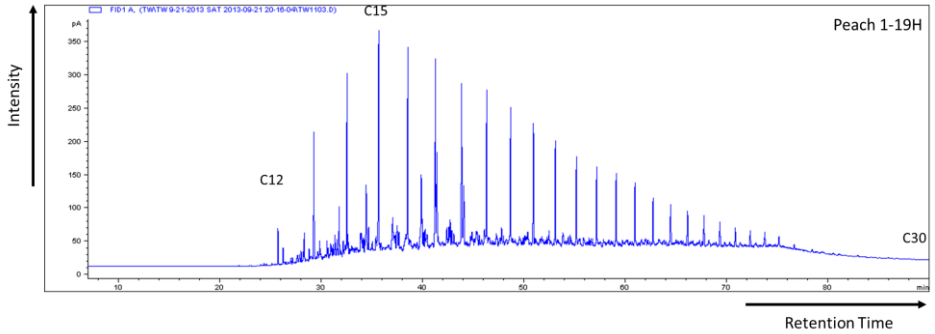

Joyce 1-32H oil

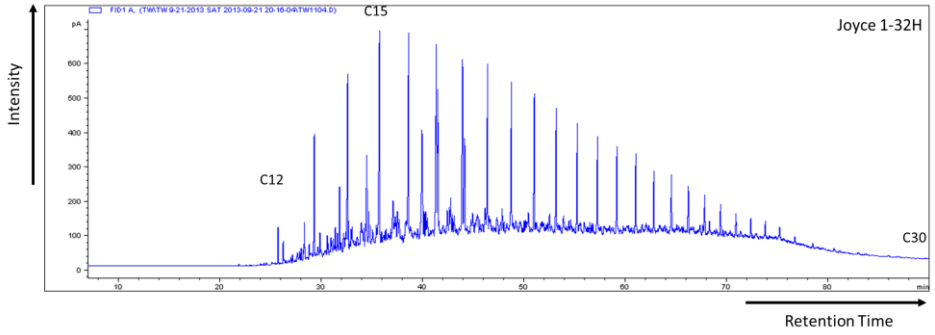

Hopfer 1-20H oil

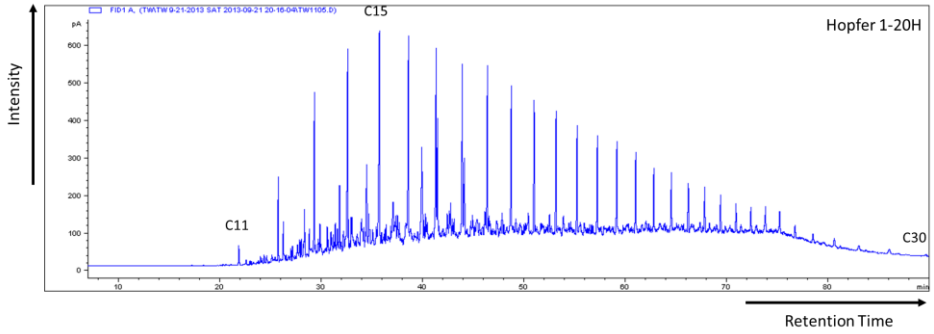

Peach 1-20WH oil

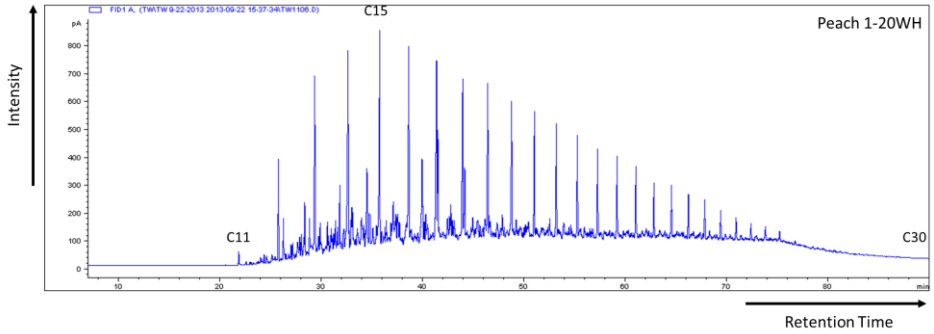

C. Matthews 1-8 oil

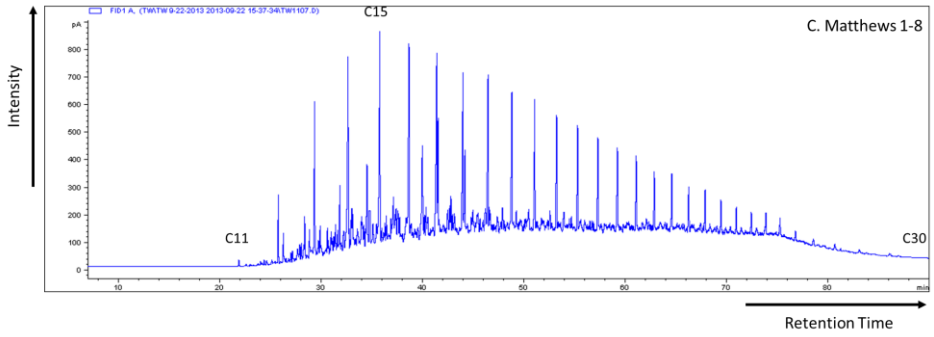

"A" oil

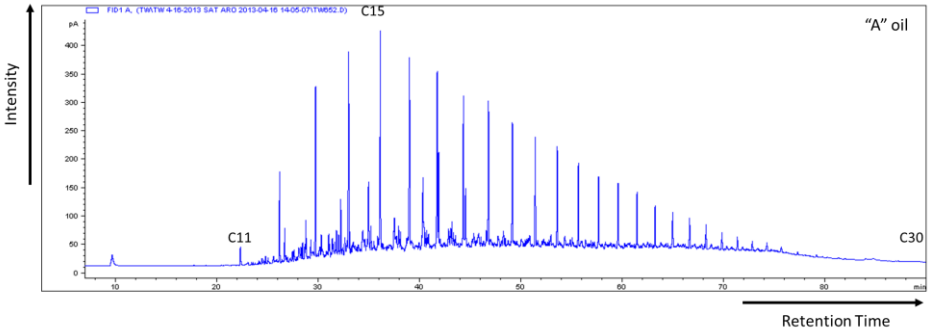

Ellis Lewis Jet oil

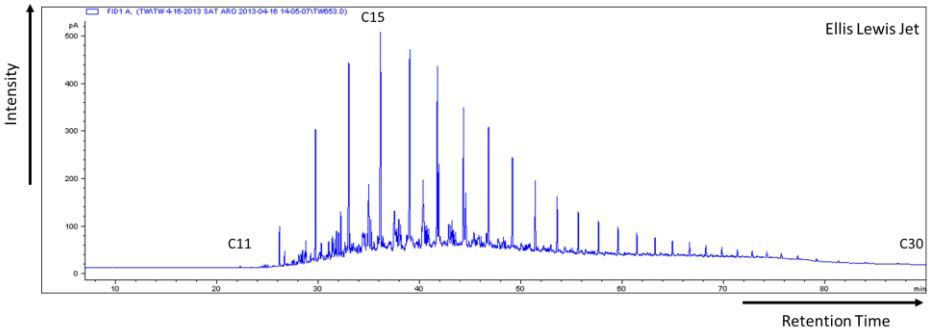

Anadarko Taylor 2118 oil

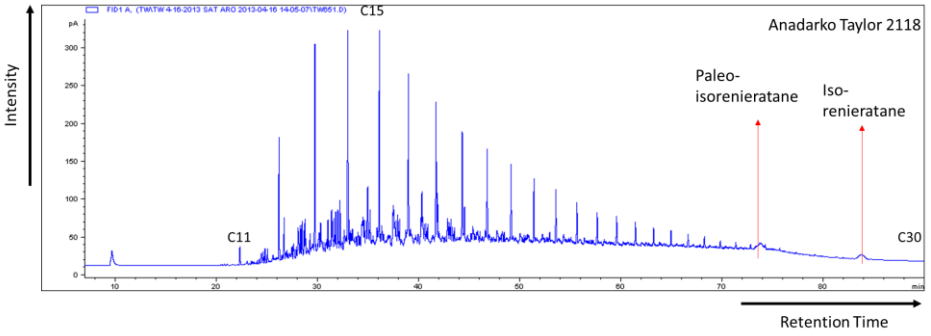

"F" oil

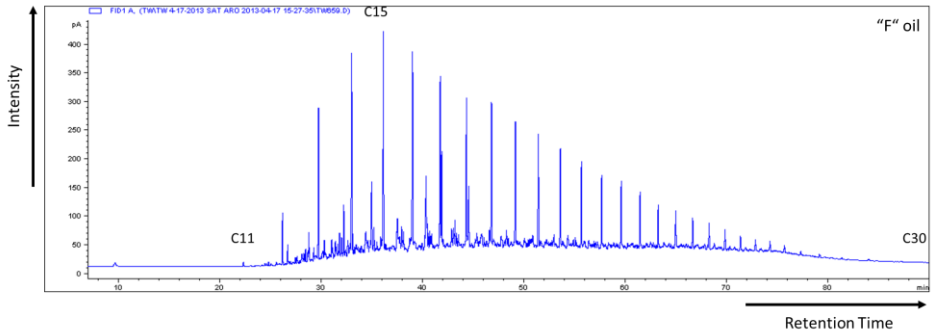

7-5N-5E oil

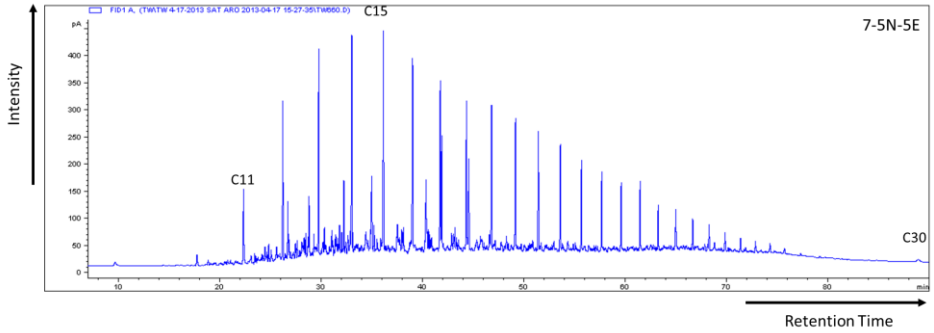

Ford-1 oil

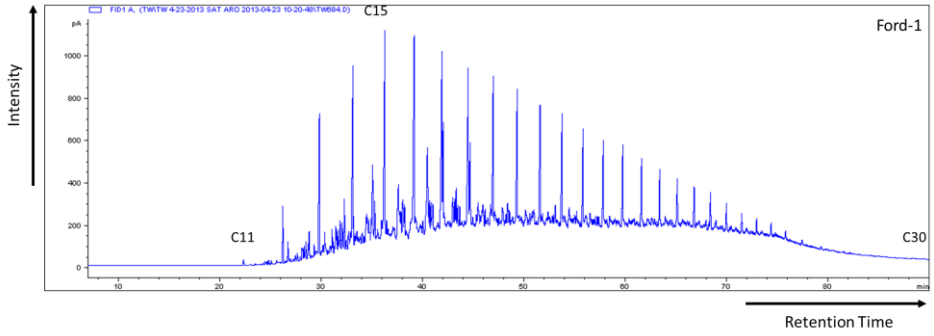

ST Mary Condensate

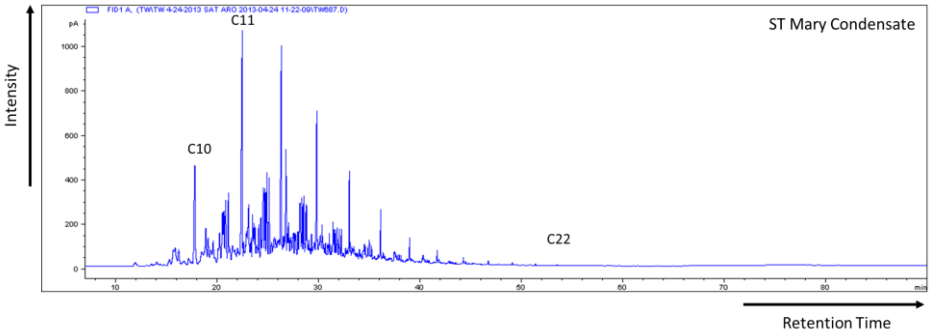

D. Geochemical ratios of steranes for the branched and cyclic fractions (B&C) of the Woodford/Mississippian extracts, oils, and condensate samples (N.D. = not determined)

Adkisson 1-33 SWD core

SAMPLE	DEPTH (ft)	C_{29} 20S/ (20S+20R)	C_{29} ββ/ (ββ + αα)	Preg/ Steranes	C_{27} Dia/ C_{27} Ster	C_{27} Dia/ (Dia+Reg)	Sterane Index
TW5005	5820	0.41	0.57	1.81	0.74	0.43	0.09
TW4920	5830	0.45	0.52	1.32	0.72	0.42	0.14
TW4921	5840	0.54	0.55	0.78	0.69	0.41	0.12
TW4922	5860	0.47	0.59	2.16	0.93	0.48	0.12
TW5005	5820	0.41	0.57	1.81	0.74	0.43	0.09

Elinore 1-18 SWD core

SAMPLE	DEPTH (ft)	C_{29} 20S/ (20S+20R)	C_{29} ββ/ (ββ + αα)	Preg/ Steranes	C_{27} Dia/ C_{27} Ster	C_{27} Dia/ (Dia+Reg)	Sterane Index
TW4923	4453	0.52	0.47	0.48	0.48	0.33	0.12
TW4924	4486	0.49	0.45	0.80	0.45	0.31	0.10
TW4925	4495	0.50	0.48	1.58	0.69	0.41	0.09
TW4926	4513	0.52	0.50	1.02	0.69	0.41	0.06
TW4927	4525	0.45	0.51	1.19	0.72	0.42	0.08

Frank 1-33 SWD core

SAMPLE	DEPTH (ft)	C_{29} 20S/ (20S+20R)	C_{29} ββ/ (ββ + αα)	Preg/ Steranes	C_{27} Dia/ C_{27} Ster	C_{27} Dia/ (Dia+Reg)	Sterane Index
TW4928	5573	0.48	0.58	2.13	0.89	0.47	0.10
TW4956	5578	0.46	0.59	2.69	0.87	0.47	0.05
TW3258	5585	0.35	0.45	2.71	0.87	0.47	N.D.
TW3259	5595	0.49	0.59	3.32	0.83	0.45	N.D.
TW2945	5603	0.35	0.54	2.24	0.96	0.49	N.D.
TW4957	5609	0.38	0.57	2.50	0.93	0.48	0.08
TW4958	5616	0.45	0.61	1.93	0.90	0.47	0.09
TW4959	5623	0.41	0.56	1.88	0.81	0.45	0.08
TW4960	5631	0.40	0.58	2.32	0.96	0.49	N.D.

Wilma 1-16 SWD core

SAMPLE	DEPTH (ft)	C_{29} 20S/ (20S+20R)	C_{29} ββ/ (ββ + αα)	Preg/ Steranes	C_{27} Dia/ C_{27} Ster	C_{27} Dia/ (Dia+Reg)	Sterane Index
TW4961	5326	0.40	0.59	2.50	0.96	0.49	0.10
TW3262	5339	0.46	0.59	3.25	0.90	0.47	N.D.
TW3260	5359	0.42	0.64	2.81	0.90	0.47	N.D.
TW4962	5366	0.52	0.43	3.00	0.97	0.49	0.06

Winney 1-8 SWD core

SAMPLE	DEPTH (ft)	C_{29} 20S/ (20S+20R)	C_{29} ββ/ (ββ + αα)	Preg/ Steranes	C_{27} Dia/ C_{27} Ster	C_{27} Dia/ (Dia+Reg)	Sterane Index
TW4964	5360	0.37	0.59	1.79	0.85	0.46	0.09
TW4965	5370	0.43	0.58	2.09	0.72	0.42	0.08
TW4182	5380	0.41	0.57	2.28	0.84	0.46	0.08

OGS Woodford cores

WELL	SAMPLE	DEPTH (ft)	C_{29} 20S/ (20S+20R)	C_{29} ββ/ (ββ + αα)	Preg/ Steranes	C_{27} Dia/ C_{27} Ster	C_{27} Dia/ (Dia+Reg)	Sterane Index
Mary Earp-5	TW4993	4087	0.59	0.36	1.08	0.66	0.40	0.14
Mary Earp-6	TW4994	4093	0.42	0.42	0.82	0.53	0.35	0.07
Boyd Unit-1	TW4995	6481	0.41	0.43	1.31	0.59	0.37	0.07
Boyd Unit-2	TW4996	6486	0.40	0.42	2.19	0.84	0.46	0.07
Dannehl 2-16	BC6590	8596	0.41	0.63	3.31	0.67	0.40	0.07
Dannehl 2-16	BC6591	8608	0.40	0.59	4.19	0.69	0.41	0.06
Dannehl 2-18	TW4999	8619	0.40	0.59	2.43	0.70	0.41	0.10
Pritchard-1	TW5000	5113	0.41	0.47	0.91	0.60	0.38	0.06
Pritchard-2	TW5001	5119	0.41	0.48	1.65	0.67	0.40	0.05
Pritchard-1	TW6002	5125	0.49	0.48	2.00	0.67	0.40	0.04
Pritchard-1	TW6003	5131	0.57	0.47	2.27	0.68	0.40	0.07
Pritchard-1	TW6056	5137	0.45	0.52	0.95	0.60	0.37	0.04
Pritchard-1	TW6057	5141	0.45	0.53	0.83	0.60	0.38	0.04
Pritchard-1	TW6058	5147	0.43	0.51	1.22	0.59	0.37	0.04
Pritchard-1	TW6059	5153	0.45	0.53	0.94	0.67	0.40	0.04
Pritchard-1	TW6060	5159	0.50	0.49	1.70	0.80	0.44	0.04

Robberson Ranch 10-1	TW6061	8707	0.43	0.58	2.01	0.58	0.37	0.06
Robberson Ranch 10-1	TW6081	8726	0.39	0.63	1.95	0.45	0.31	0.08
Anderson 12-1	TW6082	6824	0.40	0.63	3.91	0.65	0.39	0.07
Anderson 12-1	TW6106	6893	0.40	0.57	4.26	0.68	0.41	0.06
Anderson 12-1	TW6107	6923	0.47	0.60	3.00	0.76	0.43	0.08
Chenoweth-1	TW6108	6526	0.43	0.60	3.28	0.77	0.44	0.05
York-1	TW6109	8523	0.42	0.56	2.82	0.62	0.38	0.07
York-1	TW6110	8531	0.41	0.55	2.98	0.84	0.46	0.06
Pope Unit-1	BC6615	8589	0.40	0.60	4.01	0.84	0.46	0.01
Mary Earp-5	TW4993	4087	0.59	0.36	1.08	0.66	0.40	0.14

Mississippian cores

WELL	SAMPLE	DEPTH (ft)	C_{29} 20S/ (20S+20R)	C_{29} ββ/ (ββ + αα)	Preg/ Steranes	C_{27} Dia/ C_{27} Ster	C_{27} Dia/ (Dia+Reg)	Sterane Index
Albert Severin-1	BC6633	6444.7	0.42	0.66	1.89	0.65	0.40	0.01
Albert Severin-1	SAT3149	6445	0.40	0.62	2.87	0.74	0.43	0.06
Winney 1-8 SWD	BC6566	5155	0.40	0.65	0.71	0.65	0.39	0.08
Winney 1-8 SWD	BC6567	5166	0.41	0.66	1.60	0.66	0.40	0.12
Capps Unit-1	BC6568	8869	0.42	0.70	1.27	0.95	0.49	0.08

Oils and condensates from Devon Energy

SAMPLE	STATUS	C_{29} 20S/ (20S+20R)	C_{29} ββ/ (ββ + αα)	Preg/ Steranes	C_{27} Dia/ C_{27} Ster	C_{27} Dia/ (Dia+Reg)	Sterane Index
Adkisson 1-33H	Oil	0.46	0.67	1.56	0.50	0.33	0.10
Smith 1-14H	Oil	0.43	0.64	1.40	0.61	0.38	0.09
Winney 1-8H	Oil	0.40	0.64	0.47	0.46	0.32	0.08
Elinore 1-18H	Oil	0.43	0.53	0.49	0.41	0.29	0.09
Johnson 1-33H	Oil	0.48	0.63	0.99	0.64	0.39	0.11
Smith 1-23MH	Oil	0.48	0.66	0.81	0.46	0.32	0.08
Wilma 1-16SWD	Oil	0.39	0.62	0.59	0.51	0.34	0.08
Winney 1-5H	Oil	0.41	0.65	0.55	0.51	0.34	0.08
Matthews 1-33H	Oil	0.40	0.67	0.54	0.54	0.35	0.09
Elinore 1-17H	Oil	0.40	0.56	0.58	0.38	0.28	0.09
Williams 1-24 WH	Oil	0.44	0.69	0.97	0.55	0.35	0.08
Peach 1-19 MH	Oil	0.41	0.65	0.87	0.46	0.31	0.06
Joyce 1-32 WH	Oil	0.46	0.56	0.92	0.38	0.28	0.08
Hopfer 1-20 WH	Oil	0.45	0.67	0.81	0.42	0.30	0.08
Peach 1-20 WH	Oil	0.45	0.68	0.93	0.45	0.31	0.07
C. Matthews 1-8 WH	Oil	0.46	0.64	1.58	0.57	0.36	0.07
Wion 1-29 WH	Condensate	0.38	0.47	0.40	0.66	0.40	N.D.
Lingo 1-13 WH	Condensate	N.D.	N.D.	N.D.	N.D.	N.D.	N.D.
Dougherty Bros 1-18 WH	Condensate	N.D.	N.D.	N.D.	N.D.	N.D.	N.D.
Crystal 1-28 WH	Condensate	0.41	0.61	1.64	0.74	0.42	N.D.
York 1-2H	Condensate	0.31	0.62	1.90	0.94	0.48	N.D.

Conventionally Produced Woodford-Sourced Oils and condensates from Southern Oklahoma

SAMPLE	STATUS	C_{29} 20S/ (20S+20R)	C_{29} ββ/ (ββ + αα)	Preg/ Steranes	C_{27} Dia/ C_{27} Ster	C_{27} Dia/ (Dia+Reg)	Sterane Index
Ford-1	Oil	0.42	0.56	1.09	0.42	0.30	0.08
Thomas James 1-22	Oil	0.44	0.60	1.24	0.57	0.36	0.07
Anadarko Taylor 2118	Oil	0.48	0.61	1.68	0.63	0.38	0.12
A	Oil	0.47	0.62	1.18	0.62	0.38	0.09
Ellis Lewis Jet	Oil	0.43	0.60	2.07	0.50	0.33	0.09
F	Oil	0.44	0.61	1.58	0.53	0.35	0.09
7-5N-5E	Oil	0.40	0.57	0.69	0.47	0.32	0.06
ST Mary	Condensates	N.D.	N.D.	N.D.	N.D.	N.D.	N.D.

E. Geochemical ratios of terpanes for the branched and cyclic fractions (B&C) of the Woodford Shale extracts, oils, and condensates samples (ND = not determined)

Devon Woodford cores

Well Name	DEPTH (ft)	TT22 /TT21	TT24 /TT23	TT26 /TT25	C23TT /30H	24/4 vs. 30H	H29 /H30	H31R /H30	H35S /H34S	Homo Hopane Index	Ts /(Ts+Tm)	22S /(22S+22 R) H32	ETR	D30 /H30	29Ts+D30 /H30
Adkisson 1-33 SWD	5820	0.32	0.59	0.97	0.84	0.17	0.56	0.21	0.92	0.13	0.78	0.54	0.63	0.79	1.12
Adkisson 1-33 SWD	5830	0.38	0.56	0.92	1.94	0.21	0.42	0.28	1.43	0.18	0.69	0.49	0.70	0.63	0.90
Adkisson 1-33 SWD	5840	0.30	0.62	0.88	1.68	0.16	0.45	0.22	0.84	0.12	0.75	0.57	0.70	0.63	1.04
Adkisson 1-33 SWD	5860	0.32	0.56	0.87	3.03	0.20	0.50	0.28	1.14	0.09	0.67	0.53	0.68	0.70	1.15
Elmore 1-18 SWD	4453	0.28	0.50	0.97	0.56	0.03	0.40	0.26	0.94	0.18	0.45	0.58	0.82	0.12	0.30
Elmore 1-18 SWD	4486	0.26	0.37	1.19	0.92	0.12	0.84	0.24	0.94	0.10	0.56	0.58	0.60	0.20	0.47
Elmore 1-18 SWD	4495	ND	0.40	1.23	1.64	0.20	0.82	0.26	0.69	0.07	0.54	0.60	0.77	0.34	0.58
Elmore 1-18 SWD	4500	ND	ND	ND	0.00	0.00	0.84	0.28	0.24	0.04	ND	0.59	ND	0.29	0.53

Elinore 1-18 SWD	4513	0.39	0.42	1.74	1.10	0.12	0.49	0.20	0.84	0.12	0.60	0.53	0.76	0.23	0.46
Elinore 1-18 SWD	4521	ND	ND	ND	0.00	0.00	0.86	0.31	0.43	0.07	ND	0.62	ND	0.32	0.75
Elinore 1-18 SWD	4525	0.32	0.40	1.30	1.01	0.12	0.52	0.27	1.02	0.10	0.60	0.50	0.70	0.23	0.45
Frank 1-33 SWD	5573	0.20	0.64	1.11	2.79	0.34	0.89	0.40	0.54	0.12	0.80	0.62	0.74	0.72	1.02
Frank 1-33 SWD	5578	0.55	0.67	1.18	2.98	0.13	0.80	0.40	0.60	0.11	0.77	0.61	0.68	0.64	1.07
Frank 1-33 SWD	5609	0.57	0.66	0.83	2.15	0.40	0.57	0.47	1.01	0.14	0.77	0.61	0.71	0.72	1.01
Frank 1-33 SWD	5616	0.49	0.67	1.21	1.63	0.11	0.46	0.31	0.64	0.14	0.74	0.56	0.71	0.57	0.93
Frank 1-33 SWD	5623	0.35	0.59	1.41	1.38	0.07	0.40	0.26	0.42	0.08	0.69	0.51	0.69	0.60	0.92
Frank 1-33 SWD	5631	0.44	0.64	1.44	1.66	0.16	0.50	0.21	1.14	0.17	0.74	0.48	0.68	0.60	0.94
Wilma 1-16 SWD	5326	0.36	0.69	1.13	1.83	0.15	0.56	0.33	1.55	0.17	0.73	0.51	0.74	0.58	0.99
Wilma 1-16 SWD	5359	0.28	0.73	0.99	2.69	0.16	0.42	0.29	1.29	0.14	0.73	0.52	0.82	0.66	1.06
Wilma 1-16 SWD	5366	0.39	0.67	1.09	3.00	0.25	0.57	0.29	1.29	0.15	0.75	0.55	0.71	0.83	1.34
Winney 1-8 SWD	5350	0.34	0.67	0.86	1.13	0.24	0.46	0.31	0.42	0.07	0.73	0.53	0.69	0.39	0.74
Winney 1-8 SWD	5360	0.44	0.63	0.94	1.26	0.11	0.51	0.47	0.53	0.10	0.67	0.56	0.72	0.42	0.82
Winney 1-8 SWD	5370	0.38	0.54	1.15	1.23	0.11	0.46	0.20	1.20	0.14	0.74	0.55	0.64	0.37	0.71
Winney 1-8 SWD	5380	0.25	0.59	1.04	1.27	0.07	0.47	0.34	0.80	0.10	0.75	0.54	0.65	0.41	0.77
Winney 1-8 SWD	5390	ND	0.56	1.21	1.02	0.13	0.44	0.24	0.54	0.05	0.71	0.62	0.62	0.36	0.67

OGS Woodford cores

Well Name	DEPTH (ft)	TT22 /TT21	TT24 /TT23	TT26 /TT25	C23TT /30H	24/4 vs. 30H	H29 /H30	H31R /H30	H35S /H34S	Homo Hopane Index	Ts /(Ts+Tm)	22S /(22S+22R)	H32 ETR	D30 /H30	29Ts+D30 /H30
Mary Earp-5	4093	0.29	0.39	1.36	0.99	0.05	0.72	0.25	0.76	0.15	0.47	0.55	0.77	0.15	0.37
Boyd Unit-1	6481	0.33	0.39	1.15	2.10	0.08	0.91	0.34	0.92	0.08	0.46	0.56	0.76	0.26	0.51
Boyd Unit-1	6486	0.35	0.35	1.05	2.12	0.18	0.81	0.29	0.64	0.09	0.46	0.62	0.73	0.23	0.46
Dannehl 2-16	8596	0.39	0.74	1.21	2.03	0.40	0.53	0.10	ND	0.00	0.50	0.61	0.78	0.29	0.50
Dannehl 2-16	8608	0.32	0.67	1.00	3.39	0.69	0.82	0.08	ND	0.00	0.41	0.59	0.82	0.50	0.85
Dannehl 2-16	8619	ND	0.54	1.22	1.07	0.10	0.63	0.30	0.61	0.11	0.62	0.59	0.70	0.29	0.50
Pritchard-1	5113	0.51	0.32	1.45	0.50	0.04	0.71	0.28	1.14	0.14	0.52	0.54	0.54	0.12	0.32
Pritchard-1	5119	0.36	0.37	1.34	0.78	0.04	0.73	0.24	0.74	0.12	0.52	0.54	0.61	0.16	0.38
Pritchard-1	5125	0.68	0.39	0.59	0.98	0.31	0.71	0.13	0.92	0.13	0.50	0.69	0.67	0.18	0.37
Pritchard-1	5131	0.72	0.45	0.59	1.32	0.42	0.74	0.30	0.66	0.11	0.50	0.52	0.73	0.22	0.44
Pritchard-1	5137	0.32	0.42	1.17	1.22	0.42	0.73	0.33	0.56	0.11	0.41	0.45	0.69	0.21	0.46
Pritchard-1	5141	0.34	0.48	1.12	0.72	0.16	0.63	0.33	0.83	0.12	0.39	0.56	0.74	0.14	0.34
Pritchard-1	5147	0.36	0.48	0.97	1.27	0.28	0.66	0.36	0.74	0.09	0.39	0.54	0.73	0.19	0.38
Pritchard-1	5153	0.39	0.53	1.11	1.06	0.23	0.62	0.35	0.97	0.10	0.37	0.58	0.76	0.15	0.34

Pritchard-1	5159	0.40	0.49	1.10	1.14	0.29	0.72	0.40	1.06	0.10	0.40	0.57	0.71	0.17	0.38
Ranch 10-1	8707	0.36	0.60	1.34	1.02	0.43	0.64	0.29	0.71	0.10	0.50	0.59	0.65	0.19	0.40
Ranch 10-1	8726	0.41	0.63	1.20	0.27	0.06	0.50	0.24	0.87	0.11	0.54	0.55	0.65	0.10	0.23
Anderson 12-1	6824	0.33	0.75	1.26	0.96	0.24	0.48	0.24	0.79	0.12	0.59	0.54	0.68	0.38	0.60
Anderson 12-1	6893	0.38	0.55	1.08	2.84	0.82	0.56	0.40	0.65	0.09	0.55	0.60	0.71	0.75	1.11
Anderson 12-1	6923	0.34	0.64	1.03	3.00	0.84	0.66	0.53	1.16	0.12	0.57	0.61	0.76	0.91	1.49
Chenoweth-1	6526	0.20	0.61	1.10	4.72	1.09	0.85	0.89	0.98	0.11	0.62	0.56	0.72	1.76	2.48
York-1	8523	0.33	0.70	1.15	5.09	1.25	0.76	0.80	0.98	0.10	0.55	0.55	0.77	1.20	1.91
York-1	8531	0.29	0.66	1.17	4.50	1.59	0.74	0.50	0.91	0.14	0.54	0.52	0.80	0.94	1.48
Pope Unit-1	8589	0.30	0.76	1.10	6.34	0.75	0.85	0.00	ND	ND	0.59	ND	0.80	1.20	1.67

Mississippian cores

Well Name	TT22 /TT21	TT24 /TT23	TT26 /TT25	C23TT /30H	24/4 vs. 30H	H29 /H30	H31R /H30	H35S /H34S	Homo Hopane Index	Ts /(Ts+Tm)	22S /(22S+22 R) H32	TT33-39) /H31-35	ETR	D30 /H30	29Ts+D30 /H30
AFS-126	6444.7	0.25	0.64	1.14	4.83	0.56	0.82	0.37	ND	0.00	0.80	0.47	0.00	0.76	1.09
Winney 1-8 SWD	5155	0.20	0.74	0.95	2.03	0.16	0.35	0.00	0.95	0.09	1.00	0.60	3.61	0.93	0.25
Winney 1-8 SWD	5166	0.26	0.64	0.92	1.22	0.13	0.39	0.36	0.99	0.16	0.45	0.59	1.27	0.82	0.18
C8869	8869	0.24	0.91	1.06	6.78	0.53	0.71	ND	ND	ND	0.28	ND	ND	0.91	1.29

Oils and condensates from Devon Energy

Well Name	TT22 /TT21	TT24 /TT23	TT26 /TT25	C23TT /30H	24/4 vs. 30H	H29 /H30	H31R /H30	H35S /H34S	Homo Hopane Index	Ts /(Ts+Tm)	22S /(22S+22 R) H32	TT33-39) /H31-35	ETR	D30 /H30	29Ts+D30 /H30
Adkisson 1-33H	0.24	0.72	1.06	1.39	0.13	0.47	0.96	0.99	0.14	0.35	0.61	1.50	0.87	0.18	0.37
Smith 1-14H	0.37	0.78	1.09	1.20	0.16	0.54	0.23	0.98	0.19	0.77	0.56	1.37	0.78	0.20	0.39
Winney 1-8H	0.29	0.71	0.88	1.14	0.08	0.45	0.23	1.21	0.22	0.67	0.57	1.47	0.88	0.17	0.36
Elinore 1-18H	0.26	0.60	0.93	0.69	0.06	0.60	0.28	0.76	0.13	0.39	0.59	0.83	0.88	0.07	0.16
Johnson 1-33H	0.33	0.76	0.88	1.81	0.19	0.42	0.24	0.84	0.21	0.59	0.64	2.41	0.87	0.20	0.48
Smith 1-23MH	0.23	0.80	0.95	1.33	0.21	0.48	0.25	1.06	0.21	0.75	0.63	1.59	0.81	0.21	0.51
Wilma 1-16SWD	0.27	0.70	0.96	1.39	0.17	0.49	0.19	0.84	0.17	0.73	0.61	1.54	0.81	0.24	0.47
Winney 1-5H	0.26	0.72	0.86	1.49	0.08	0.48	0.26	1.00	0.18	0.68	0.69	1.54	0.90	0.18	0.50

Matthews 1-33H	0.23	0.72	0.88	1.99	0.12	0.47	0.22	1.29	0.23	0.71	0.59	2.38	0.90	0.22	0.45
Elinore 1-17H	0.29	0.58	0.94	0.83	0.06	0.61	0.23	0.65	0.12	0.42	0.61	0.81	0.87	0.06	0.14
Williams 1-24 WH	0.29	0.72	0.90	1.46	0.15	0.45	0.00	1.26	0.22	0.35	0.62	2.27	0.87	0.19	0.39
Peach 1-19 MH	0.23	0.75	0.95	0.97	0.10	0.46	0.25	1.16	0.19	0.70	0.56	1.10	0.84	0.20	0.44
Joyce 1-32 WH	0.25	0.62	0.87	0.56	0.06	0.55	0.33	0.91	0.11	0.35	0.59	0.62	0.81	0.05	0.14
Hopfer 1-20 WH	0.24	0.63	0.94	1.34	0.10	0.47	0.00	1.13	0.20	0.36	0.62	2.43	0.86	0.17	0.33
Peach 1-20 WH	0.33	0.72	0.89	0.91	0.13	0.48	0.40	0.90	0.14	0.43	0.56	1.07	0.82	0.16	0.32
C. Matthews 1-8 WH	0.29	0.72	0.90	1.46	0.15	0.45	0.00	1.26	0.22	0.35	0.62	2.27	0.87	0.19	0.39
Wion 1-29 WH	0.35	0.98	ND	0.29	0.00	0.96	0.42	1.86	0.18	ND	0.52	0.00	ND	0.00	0.11
Crystal 1-28 WH	0.46	0.80	0.97	1.99	0.17	1.02	0.62	1.30	0.20	0.60	0.57	0.57	0.88	0.10	0.32

Conventionally Produced Woodford-Sourced Oils and condensates from Southern Oklahoma

Well Name	TT22 /TT21	TT24 /TT23	TT26 /TT25	C23TT /30H	24/4 vs. 30H	H29 /H30	H31R /H30	H35S /H34S	Homo Hopane Index	Ts /(Ts+Tm)	22S /(22S+22 R) H32	TT33-39) /H31-35	ETR	D30 /H30	29Ts+D30 /H30
Ford-1	0.36	0.69	1.00	0.58	0.10	0.60	0.28	0.84	0.14	0.36	0.60	0.53	0.83	0.07	0.21
Thomas James 1-22	0.38	0.71	0.98	0.98	0.18	0.57	0.31	1.40	0.16	0.52	0.60	0.47	0.83	0.16	0.38
Anadarko Taylor 2118	0.34	0.74	1.11	3.40	0.25	0.60	0.38	1.40	0.21	0.73	0.60	1.73	0.86	0.41	0.73
A	0.33	0.69	0.84	0.80	0.12	0.47	0.25	0.96	0.15	0.58	0.54	0.96	0.81	0.14	0.36
Ellis Lewis Jet	0.31	0.66	1.02	1.00	0.13	0.55	0.25	0.98	0.16	0.46	0.58	0.96	0.85	0.11	0.28
F	0.27	0.69	0.93	0.90	0.11	0.48	0.22	0.89	0.14	0.40	0.59	0.91	0.83	0.13	0.27
7-5N-5E	0.33	0.73	0.71	0.51	0.06	0.57	0.39	0.78	0.12	0.34	0.59	0.00	0.81	0.06	0.20

Oils and condensates from Devon Energy

F. Quantitative biomarker analysis results for steranes (Concentrations are expressed as µg biomarkers/g TOC or µg biomarkers/g whole oil; ND = not determined)

Sample Name	Preg	Homopreg	C_{27} β α-Dia (20S)	C_{27} β α-Dia (20R)	C_{27} αβ -Dia (20S)	C27 αβ -Dia (20R)	C_{27} αα (20S)	C_{29} β α-Dia (20S)+ C_{27} β β (20R)	C_{27} β β (20S)	C_{27} αα (20R)	C_{29} β α-Dia (20R)	C_{29} α β -Dia (20S)	C_{29} α β -Dia (20R)	C_{29} α α-Dia (20S)	C_{29} β β -Dia (20R)	C_{29} β β -Dia (20S)	C_{29} α α-Dia (20R)
Adkisson 1-33H	20.1	5.4	14.6	9.7	3.1	6.3	11.3	28.7	14.8	12.9	10.4	9.4	10.7	9.5	25.3	17.9	11.3
Smith 1-14H	63.8	24.6	83.4	56.9	28.7	40.5	55.5	154.4	85.7	45.7	85.4	72.8	64.3	36.7	88.5	63.5	48.9
Winney 1-8H	49.2	22.6	63.5	43.6	20.3	26.9	42.1	125.1	62.7	103.9	42.5	57.9	50.1	30.9	80.0	59.4	45.8
Elinore 1-18H	45.1	35.1	56.4	38.5	27.3	23.3	72.9	128.2	65.2	91.9	67.3	53.4	69.3	72.4	106.5	80.2	95.0
Johnson 1-33H	38.7	19.5	47.7	37.9	16.0	27.1	25.8	84.6	51.4	39.0	42.3	43.1	37.7	28.7	61.7	40.9	31.0
Smith 1-23MH	30.9	7.9	21.9	14.8	6.7	9.0	13.1	42.3	19.4	38.1	9.5	18.6	18.5	10.6	25.3	16.8	11.6
Wilma 1-16SWD	15.4	7.1	17.6	12.2	5.9	7.5	10.8	31.9	15.4	26.1	11.4	14.3	13.7	7.8	18.1	13.9	12.1
Winney 1-5H	30.2	13.2	37.1	23.7	14.6	18.1	24.4	69.1	35.4	54.9	21.5	25.0	26.0	17.1	44.8	33.6	24.9
Matthews 1-33H	26.3	11.8	34.5	21.8	16.1	18.8	21.8	63.4	33.9	49.2	22.5	21.6	21.3	15.1	42.8	32.2	22.5
Elinore 1-17H	14.6	8.8	16.4	10.7	4.5	6.7	20.1	36.2	18.9	25.3	19.3	12.6	16.8	16.9	31.6	22.2	25.7

Williams 1-24 WH	9.2	2.2	7.1	4.9	1.7	2.7	4.4	10.8	5.3	9.5	3.2	4.7	3.8	2.3	6.7	4.7	2.9
Peach 1-19 MH	12.3	3.6	9.2	5.9	2.5	4.2	6.0	18.1	9.3	14.1	5.8	6.2	6.6	4.3	11.3	8.5	6.2
Joyce 1-32 WH	17.1	5.2	12.4	8.9	3.0	5.3	15.7	27.3	15.7	18.5	10.9	9.0	13.1	16.0	24.5	19.9	18.7
Hopfer 1-20 WH	22.3	6.1	16.0	11.5	3.7	8.0	14.1	32.0	19.7	27.6	9.2	10.3	12.1	10.5	28.1	20.1	13.0
Peach 1-20 WH	23.1	5.5	14.6	10.8	3.3	6.9	11.8	29.2	13.0	24.8	8.4	10.5	11.3	8.6	24.0	16.1	10.6
C. Matthews 1-8 WH	63.2	26.4	52.8	35.3	12.4	23.3	31.1	103.2	44.6	40.0	45.3	43.5	40.5	30.3	70.2	48.0	35.1
Wion 1-29 WH	0.2	0.1	0.4	0.3	0.3	0.3	0.3	0.6	0.4	0.6	0.3	0.5	0.4	0.2	0.2	0.2	0.3
Crystal 1-28 WH	0.5	0.1	0.2	0.2	0.1	0.1	0.1	0.3	0.1	0.3	0.1	0.2	0.1	0.1	0.1	0.1	0.1
York 1-2H	4.1	0.6	2.1	1.3	1.2	1.1	0.6	2.5	0.8	2.2	0.9	1.2	0.8	0.2	0.6	0.4	0.4

Conventionally Produced Woodford-Sourced Oils and condensates from Southern Oklahoma

Sample Name	Preg	Homopreg	C_{27} β α-Dia (20S)	C_{27} β α-Dia (20R)	C_{27} αβ -Dia (20S)	C27 αβ -Dia (20R)	C_{27} αα (20S)	C_{29} β α-Dia (20S)+ C_{27} β β (20R)	C_{27} β β (20S)	C_{27} αα (20R)	C_{29} β α-Dia (20R)	C_{29} α β -Dia (20S)	C_{29} α β -Dia (20R)	C_{29} α α-Dia (20S)	C_{29} β β -Dia (20R)	C_{29} β β -Dia (20S)	C_{29} α α-Dia (20R)
Ford-1	41.3	14.5	28.5	19.3	9.4	13.6	29.4	65.6	34.4	37.9	28.3	25.6	25.9	33.7	58.0	45.6	46.9
Thomas James 1-22	5.5	3.0	5.0	3.7	1.6	2.7	3.7	10.3	4.4	4.4	5.0	4.1	4.2	3.5	6.9	5.0	4.4
Anadarko Taylor 2118 A	48.4	19.9	32.3	20.1	9.4	15.3	12.6	55.8	26.1	28.9	16.9	29.8	20.9	18.3	32.8	26.7	20.0
Ellis Lewis Jet F	38.3	18.4	43.7	30.3	13.3	17.9	23.3	74.7	40.0	32.4	40.9	28.4	29.9	30.0	63.1	42.9	33.8
7-5N-5E	21.0	6.3	9.3	6.5	3.5	4.4	7.8	19.3	10.3	10.1	9.2	9.5	8.0	7.8	15.0	12.4	10.3
	35.8	11.1	24.6	17.3	8.1	10.5	17.3	50.3	23.1	22.6	22.2	19.7	18.5	17.2	34.7	26.8	22.2
	8.6	6.5	16.1	10.7	4.3	5.9	13.3	35.8	16.5	12.5	22.0	13.4	13.5	14.3	27.0	20.5	21.7

Woodford Cores from Devon Energy

Sample Name	Depth/ft	Preg	Homopreg	C_{27} β α-Dia (20S)	C_{27} β α-Dia (20R)	C_{27} αβ -Dia (20S)	C27 αβ -Dia (20R)	C_{27} αα (20S)	C_{29} β α-Dia (20S)+ C_{27} β β (20R)	C_{27} β β (20S)	C_{27} αα (20R)	C_{29} β α-Dia (20R)	C_{29} α β -Dia (20S)	C_{29} α β -Dia (20R)	C_{29} α α-Dia (20S)	C_{29} β β -Dia (20R)	C_{29} β β -Dia (20S)	C_{29} α α-Dia (20R)
Adkisson 1-33 SWD	5820	7.8	4.6	6.6	5.7	3.3	4.5	4.6	12.7	5.3	4.3	9.2	5.5	5.7	3.7	6.6	5.1	5.3
Adkisson 1-33 SWD	5830	4.6	3.8	6.6	4.8	2.7	3.0	3.4	11.7	5.2	3.5	7.9	6.4	6.7	4.6	6.7	4.5	5.7
Adkisson 1-33 SWD	5840	11.3	8.3	12.4	8.3	7.0	5.7	5.4	21.8	6.9	14.6	3.9	10.0	11.3	8.8	12.5	8.0	7.6
Adkisson 1-33 SWD	5860	12.4	8.7	11.0	8.9	6.3	6.8	5.8	17.6	6.3	5.7	13.7	9.4	7.4	4.8	9.0	6.0	5.5
Elinore 1-18 SWD	4453	11.7	9.3	25.3	17.9	11.4	11.3	25.4	60.0	26.1	24.3	45.0	25.7	29.5	41.3	42.9	26.8	37.9
Elinore 1-18 SWD	4486	9.7	7.2	6.9	5.1	3.1	3.8	8.3	14.5	6.6	12.1	7.6	7.0	10.1	10.3	10.6	6.8	10.9
Elinore 1-18 SWD	4495	15.8	11.3	12.1	8.8	5.6	6.1	9.9	18.7	8.7	10.0	10.6	10.3	9.8	9.3	10.6	6.8	9.5
Elinore 1-18 SWD	4513	7.5	5.6	9.7	7.3	3.7	6.0	7.3	17.4	6.5	7.3	12.8	8.0	8.9	8.7	10.4	6.5	8.1

Elinore 1-18 SWD	4525	0.0	0.0	0.0	0.0	0.0	0.0	0.0	0.0	0.0	0.0	0.0	0.0	0.0	0.0	0.0	0.0	0.0
Frank 1-33 SWD	5573	4.7	3.3	4.8	3.3	2.0	2.2	2.0	6.5	3.1	2.2	4.8	3.1	3.7	2.0	3.4	2.4	2.2
Frank 1-33 SWD	5578	7.2	3.7	5.3	4.0	2.2	3.1	3.1	7.6	3.4	2.7	5.1	3.3	2.5	2.0	3.6	2.7	2.3
Frank 1-33 SWD	5585	2.2	1.1	1.4	0.9	0.5	0.6	0.7	1.5	0.8	0.8	1.3	0.9	0.6	0.6	0.9	0.5	1.1
Frank 1-33 SWD	5595	4.7	2.7	3.2	1.9	0.9	1.1	1.5	3.9	1.9	1.4	2.8	1.9	1.5	1.0	1.7	1.2	1.0
Frank 1-33 SWD	5609	7.3	4.0	7.0	4.9	2.9	3.8	3.4	9.8	4.1	2.9	7.9	4.3	4.0	2.4	4.6	3.9	3.9
Frank 1-33 SWD	5616	6.1	3.7	7.1	4.8	2.7	3.6	2.9	10.8	3.3	3.1	7.3	4.7	5.4	2.5	4.9	4.0	3.1
Frank 1-33 SWD	5623	4.2	2.5	4.4	3.3	2.0	1.9	2.0	7.1	3.0	2.3	4.8	3.5	3.4	2.0	3.6	2.8	2.9
Frank 1-33 SWD	5631	8.7	5.2	8.4	5.8	3.5	4.5	3.5	12.3	3.7	3.7	8.0	4.9	4.7	3.1	6.1	4.7	4.6
Wilma 1-16 SWD	5326	4.3	2.4	3.5	2.4	1.4	2.4	1.6	5.0	1.8	1.7	4.0	2.0	2.1	1.5	3.0	2.4	2.3
Wilma 1-16 SWD	5339	4.0	1.7	3.0	1.9	1.0	1.3	1.6	3.4	1.7	1.2	3.1	1.8	1.1	0.7	1.3	0.9	0.8
Wilma 1-16 SWD	5359	3.4	2.0	4.2	2.5	1.3	1.7	1.6	5.9	2.1	1.2	3.8	2.5	2.0	1.0	2.3	1.7	1.3
Wilma 1-16 SWD	5366	8.8	4.9	6.3	4.8	2.6	2.6	2.6	2.7	8.6	2.9	2.8	6.4	4.2	3.6	2.1	3.1	3.3
Winney 1-8 SWD	5360	5.6	3.7	6.3	4.6	2.6	3.8	2.8	10.1	4.4	3.1	7.7	4.4	4.5	2.6	5.8	4.4	4.3
Winney 1-8 SWD	5370	12.6	7.9	9.8	6.8	4.2	4.4	5.6	15.8	7.6	6.0	13.6	8.2	6.9	5.4	9.6	8.0	7.2

Woodford Cores from OGS

Sample Name	Depth/ft	Preg	Homopreg	C_{27} β α-Dia (20S)	C_{27} β α-Dia (20R)	C_{27} αβ -Dia (20S)	C27 αβ -Dia (20R)	C_{27} αα (20S)	C_{29} β α-Dia (20S)+ C_{27} β β (20R)	C_{27} β β (20S)	C_{27} αα (20R)	C_{29} β α-Dia (20R)	C_{29} α β -Dia (20S)	C_{29} α β -Dia (20R)	C_{29} α α-Dia (20S)	C_{29} β β -Dia (20R)	C_{29} β β -Dia (20S)	C_{29} α α-Dia (20R)
Mary Earp-5	4087	5.3	3.0	4.2	3.3	1.9	2.8	3.9	6.6	3.2	4.9	4.6	2.5	3.6	8.0	4.1	3.5	5.5
Mary Earp-6	4093	11.1	5.5	11.1	7.2	3.9	5.6	12.8	17.4	8.6	13.6	12.6	6.9	10.8	10.8	11.3	7.8	15.2
Boyd Unit-1	6481	13.0	4.2	9.3	5.8	3.3	5.3	10.0	12.7	7.4	9.9	9.5	5.4	7.4	7.4	8.1	5.5	10.5
Boyd Unit-2	6486	3.1	1.8	1.8	1.2	0.9	1.0	1.5	1.9	1.1	1.4	1.5	0.8	1.0	1.1	1.1	0.9	1.6
Dannehl 2-16	8596	13.7	4.2	5.7	4.1	1.4	3.0	3.8	9.3	4.0	4.1	5.0	3.4	3.2	2.9	6.7	5.1	4.1
Dannehl 2-16	8608	8.7	2.5	3.0	2.0	0.8	1.5	1.9	4.5	2.0	2.1	2.4	1.7	1.6	1.5	3.4	2.1	2.3
Dannehl 2-18	8619	9.4	5.1	6.0	3.9	2.0	3.0	3.8	8.8	4.7	3.9	7.9	4.1	4.2	3.0	6.1	4.8	4.6
Pritchard-1	5113	18.4	9.6	21.7	15.5	7.3	11.1	18.9	36.9	16.3	20.3	25.8	18.4	21.6	19.3	25.7	17.2	28.1
Pritchard-2	5119	10.0	3.7	6.8	4.8	2.7	3.9	6.0	10.2	4.9	6.1	7.3	5.0	5.6	4.9	6.3	4.6	7.1
Pritchard-1	5125	2.9	1.1	1.9	1.4	0.7	1.0	1.5	3.1	1.4	1.5	2.2	1.3	1.5	1.7	1.9	1.3	1.8
Pritchard-1	5131	3.9	1.5	2.2	1.6	0.9	1.3	1.9	3.4	1.9	1.7	2.5	1.5	1.7	2.6	2.4	1.6	2.0
Pritchard-1	5137	2.0	1.0	1.8	1.2	0.8	1.2	1.5	3.2	1.7	2.1	1.9	1.2	1.5	1.2	1.6	1.3	1.5
Pritchard-1	5141	2.2	1.0	2.8	1.7	0.8	1.3	1.7	4.6	2.0	2.7	2.3	1.8	2.2	1.9	2.7	2.0	2.3
Pritchard-1	5147	3.2	1.3	2.7	1.8	0.9	1.5	2.3	4.4	2.3	2.6	2.1	1.8	1.9	1.7	2.7	1.5	2.3
Pritchard-1	5153	1.3	0.6	1.5	1.1	0.5	0.8	1.1	2.3	1.1	1.4	1.2	1.0	1.0	0.9	1.3	1.0	1.1
Pritchard-1	5159	1.8	0.8	2.1	1.4	0.7	1.0	1.4	2.7	1.3	1.0	1.8	1.1	1.3	1.3	1.5	1.1	1.4

Robberson Ranch 10-1	8707	1.4	0.6	0.7	0.5	0.3	0.4	0.6	1.2	0.7	0.7	0.7	0.4	0.5	0.5	0.8	0.6	0.6
Robberson Ranch 10-1	8726	2.7	1.1	2.0	1.1	0.5	0.9	1.8	4.4	2.2	1.4	2.5	1.5	1.8	1.7	4.3	3.2	2.7
Anderson 12-1	6824	4.9	1.4	2.3	1.4	0.7	1.3	1.6	4.1	1.8	1.3	2.6	1.5	1.8	1.2	2.9	2.1	1.8
Anderson 12-1	6893	0.5	0.1	0.2	0.2	0.1	0.1	0.2	0.3	0.2	0.1	0.2	0.1	0.1	0.1	0.2	0.1	0.1
Anderson 12-1	6923	1.6	0.4	0.9	0.7	0.2	0.5	0.5	1.4	0.6	0.5	0.9	0.7	0.6	0.4	0.8	0.5	0.5
Chenoweth-1	6526	1.2	0.2	0.6	0.5	0.2	0.4	0.4	0.9	0.4	0.4	0.6	0.5	0.4	0.2	0.5	0.3	0.3
York-1	8523	1.5	0.4	0.7	0.5	0.2	0.4	0.7	1.2	0.7	0.5	0.8	0.6	0.5	0.4	0.7	0.5	0.5
York-1	8531	1.4	0.6	0.7	0.6	0.3	0.7	0.6	1.0	0.6	0.5	0.9	0.6	0.4	0.3	0.5	0.3	0.4
Pope Unit-1	8589	9.4	2.5	3.4	2.6	1.0	2.3	2.2	4.4	2.1	2.4	3.2	1.7	1.7	1.3	2.7	2.0	1.9

Mississippian Cores

Sample Name	Depth/ft	Preg	Homopreg	C_{27} β α-Dia (20S)	C_{27} β α-Dia (20R)	C_{27} αβ -Dia (20S)	C27 αβ -Dia (20R)	C_{27} αα (20S)	C_{29} β α-Dia (20S)+ C_{27} β β (20R)	C_{27} β β (20S)	C_{27} αα (20R)	C_{29} β α-Dia (20R)	C_{29} α β -Dia (20S)	C_{29} α β -Dia (20R)	C_{29} α α-Dia (20S)	C_{29} β β -Dia (20R)	C_{29} β β -Dia (20S)	C_{29} α α-Dia (20R)
ALBERT SEVERIN-1	6445	5.8	1.3	2.3	1.7	0.5	1.5	1.5	3.2	1.5	3.1	0.8	1.5	1.2	0.7	1.7	1.3	0.9
Winney 1-8 SWD	5155	11.9	8.6	21.9	12.3	4.5	8.2	10.7	28.4	16.6	16.8	13.9	8.9	11.5	6.9	19.6	12.9	10.4

Winney 1-8 SWD	5166	15.8	7.5	14.3	10.4	4.0	8.3	9.9	23.5	12.3	9.9	11.0	8.2	7.5	6.0	16.7	11.1	8.5
Capps Unit-1	8869	3.4	1.1	3.9	2.6	0.8	1.6	1.2	3.8	1.9	2.7	2.0	1.6	1.5	0.7	2.3	1.4	0.9

G. Quantitative biomarker analysis results for terpanes (Concentrations are expressed as µg biomarkers/g TOC or µg biomarkers/g whole oil; ND = not determined)

Woodford cores from Devon Energy

Well Name	Depth/ft	TT19	TT20	TT21	TT22	TT23	TT24	TT25	TT26	24/4	TT28S	TT28R	TT29S	TT29R	Ts	TT30S
Adkisson 1-33 SWD	5820	3.24	5.22	11.00	3.56	19.99	11.71	11.97	11.64	3.98	5.30	5.05	7.75	7.28	15.17	5.54
Adkisson 1-33 SWD	5830	5.45	4.60	14.41	5.54	27.96	15.77	15.21	14.07	2.97	5.22	6.07	7.51	5.95	10.38	5.01
Adkisson 1-33 SWD	5840	4.61	3.63	9.79	2.97	17.29	10.65	8.80	7.70	1.61	4.64	4.75	5.53	4.42	8.30	4.52
Adkisson 1-33 SWD	5860	1.54	1.64	4.21	1.35	7.25	4.03	3.40	2.95	0.48	1.69	1.62	0.99	1.58	2.75	1.01
Elmore 1-18 SWD	4453	2.08	6.68	18.58	5.25	51.73	25.79	34.43	33.43	3.16	23.37	25.89	15.99	19.33	18.19	19.24
Elmore 1-18 SWD	4486	1.72	3.32	8.32	2.18	13.98	5.11	5.56	6.64	1.81	2.89	2.67	2.18	1.38	5.96	1.68
Elmore 1-18 SWD	4495	N.D.	N.D.	N.D.	N.D.	1.17	0.48	0.49	0.60	0.14	0.26	0.31	0.14	0.24	0.28	0.11
Elmore 1-18 SWD	4513	2.01	4.45	9.88	3.84	24.54	10.41	8.52	14.85	2.69	7.64	8.78	5.17	3.67	8.12	4.37

Frank 1-33 SWD	5573	1.32	1.03	2.78	0.56	4.13	2.64	2.37	2.63	0.50	1.12	1.16	1.09	1.00	1.52	0.74
Frank 1-33 SWD	5578	0.38	0.31	0.79	0.43	1.46	0.98	0.84	0.99	0.06	0.42	0.45	0.35	0.38	0.76	0.30
Frank 1-33 SWD	5609	0.42	0.52	0.92	0.52	1.76	1.16	1.05	0.88	0.33	0.48	0.58	0.47	0.43	0.80	0.36
Frank 1-33 SWD	5616	0.46	0.49	1.04	0.51	2.21	1.48	1.29	1.55	0.15	0.67	0.76	0.65	0.61	1.11	0.53
Frank 1-33 SWD	5623	0.81	0.73	2.18	0.76	3.61	2.12	1.83	2.58	0.18	1.04	1.23	1.18	0.98	2.01	0.94
Frank 1-33 SWD	5631	0.27	0.31	0.70	0.31	1.21	0.77	0.63	0.90	0.12	0.39	0.39	0.31	0.33	0.66	0.24
Wilma 1-16 SWD	5326	0.08	0.09	0.24	0.08	0.36	0.25	0.24	0.27	0.03	0.13	0.13	0.09	0.11	0.16	0.08
Wilma 1-16 SWD	5359	0.26	0.24	0.37	0.10	0.58	0.42	0.35	0.34	0.03	0.16	0.18	0.17	0.15	0.15	0.12
Wilma 1-16 SWD	5366	0.21	0.67	0.39	0.15	0.57	0.38	0.31	0.34	0.05	0.17	0.15	0.13	0.13	0.23	0.10
Winney 1-8 SWD	5350	0.08	0.09	0.17	0.06	0.31	0.21	0.21	0.18	0.07	0.10	0.10	0.09	0.10	0.17	0.06
Winney 1-8 SWD	5360	0.16	0.23	0.43	0.19	0.83	0.52	0.58	0.54	0.07	0.28	0.32	0.24	0.26	0.43	0.22
Winney 1-8 SWD	5370	0.35	0.42	0.90	0.34	1.67	0.91	0.96	1.11	0.15	0.39	0.38	0.30	0.32	0.79	0.25
Winney 1-8 SWD	5390	N.D.	N.D.	N.D.	N.D.	1.64	0.92	0.79	0.96	0.21	0.37	0.37	0.34	0.31	0.84	0.32

Woodford cores from Devon Energy (cont.-1)

Well Name	Depth/ft	Tm	TT30R	TT31S	TT31R	H29	29Ts	D30	H30	TT33R	H31S	H31R	TT34S	H32S
Adkisson 1-33 SWD	5820	4.37	4.29	6.69	3.76	13.22	7.92	18.70	23.67	4.27	7.36	4.87	0.00	7.83
Adkisson 1-33 SWD	5830	4.57	5.89	7.29	4.48	5.97	3.90	9.02	14.38	3.23	6.56	4.03	0.00	4.69
Adkisson 1-33 SWD	5840	2.80	2.50	3.91	4.11	4.64	4.18	6.54	10.31	2.91	4.18	2.27	0.00	4.45
Adkisson 1-33 SWD	5860	1.34	0.64	0.63	0.88	1.21	1.08	1.67	2.40	0.55	1.09	0.67	0.00	0.96
Adkisson 1-33 SWD	5870	N.D.	N.D.	N.D.	N.D.	N.D.	N.D.	N.D.	N.D.	N.D.	N.D.	N.D.	N.D.	N.D.
Elinore 1-18 SWD	4453	22.51	10.67	15.83	15.38	36.57	16.49	11.47	92.16	18.46	36.15	23.71	0.00	30.28

Elinore 1-18 SWD	4486	4.65	1.67	1.88	1.08	12.69	4.07	3.01	15.17	2.02	4.43	3.64	0.00	3.67
Elinore 1-18 SWD	4495	0.24	0.07	0.16	0.13	0.59	0.17	0.24	0.71	0.08	N.D.	N.D.	N.D.	0.15
Elinore 1-18 SWD	4513	5.35	3.44	5.39	2.94	11.05	5.16	5.20	22.35	3.36	7.26	4.44	0.00	4.80
Frank 1-33 SWD	5573	0.37	0.70	0.70	0.63	1.32	0.44	1.07	1.48	0.55	0.71	0.59	0.00	0.81
Frank 1-33 SWD	5578	0.22	0.26	0.27	0.22	0.39	0.21	0.31	0.49	0.14	0.25	0.19	0.00	0.30
Frank 1-33 SWD	5609	0.24	0.39	0.32	0.24	0.47	0.24	0.59	0.82	0.26	0.30	0.38	0.00	0.34
Frank 1-33 SWD	5616	0.38	0.47	0.50	0.48	0.63	0.48	0.78	1.36	0.35	0.47	0.42	0.00	0.40
Frank 1-33 SWD	5623	0.89	0.74	0.94	0.66	1.06	0.83	1.58	2.62	0.54	0.84	0.69	0.00	0.83
Frank 1-33 SWD	5631	0.24	0.26	0.29	0.25	0.37	0.25	0.44	0.73	0.17	0.21	0.15	0.00	0.18
Wilma 1-16 SWD	5326	0.06	0.07	0.08	0.07	0.11	0.08	0.11	0.20	0.04	0.08	0.06	0.00	0.06
Wilma 1-16 SWD	5359	0.05	0.09	0.14	0.08	0.09	0.09	0.14	0.21	0.05	0.10	0.06	0.00	0.08
Wilma 1-16 SWD	5366	0.08	0.12	0.08	0.07	0.11	0.10	0.16	0.19	0.04	0.05	0.06	0.00	0.06
Winney 1-8 SWD	5350	0.06	0.06	0.09	0.06	0.13	0.10	0.11	0.28	0.05	N.D.	N.D.	N.D.	0.08
Winney 1-8 SWD	5360	0.21	0.26	0.26	0.17	0.33	0.26	0.28	0.66	0.14	0.33	0.31	0.00	0.27
Winney 1-8 SWD	5370	0.28	0.26	0.22	0.18	0.63	0.47	0.50	1.37	0.25	0.45	0.28	0.00	0.40
Winney 1-8 SWD	5390	0.35	0.27	0.32	0.23	0.71	0.51	0.58	1.61	0.39	N.D.	N.D.	N.D.	0.46

Woodford cores from Devon Energy (cont.-2)

Well Name	Depth/ft	H32R	H33S	H33R	H34S	H34R	H35S	H35R
Adkisson 1-33 SWD	5820	6.63	5.61	4.27	4.43	3.68	4.07	2.79
Adkisson 1-33 SWD	5830	4.87	4.50	3.23	3.07	2.36	4.39	2.72

Adkisson 1-33 SWD	5840	3.33	3.93	2.91	2.79	3.44	2.35	1.25
Adkisson 1-33 SWD	5860	0.83	0.57	0.55	0.37	0.44	0.42	0.13
Elinore 1-18 SWD	4453	21.76	24.59	18.46	21.35	13.51	19.97	21.05
Elinore 1-18 SWD	4486	2.65	2.12	2.02	1.70	1.22	1.60	0.88
Elinore 1-18 SWD	4513	4.20	4.83	3.36	3.19	2.37	2.67	2.24
Elinore 1-18 SWD	4525	N.D.	0.00	0.00	0.00	0.00	0.00	0.00
Frank 1-33 SWD	5573	0.49	0.61	0.55	0.52	0.45	0.28	0.34
Frank 1-33 SWD	5578	0.19	0.15	0.14	0.17	0.11	0.10	0.08
Frank 1-33 SWD	5609	0.22	0.23	0.26	0.26	0.30	0.26	0.11
Frank 1-33 SWD	5616	0.32	0.43	0.35	0.43	0.19	0.28	0.22
Frank 1-33 SWD	5623	0.78	0.71	0.54	0.53	0.46	0.22	0.23
Frank 1-33 SWD	5631	0.20	0.16	0.17	0.15	0.14	0.17	0.11
Wilma 1-16 SWD	5326	0.06	0.05	0.04	0.03	0.03	0.05	0.04
Wilma 1-16 SWD	5359	0.08	0.05	0.05	0.04	0.03	0.05	0.03
Wilma 1-16 SWD	5366	0.05	0.08	0.04	0.03	0.02	0.04	0.03
Winney 1-8 SWD	5360	0.21	0.22	0.14	0.16	0.15	0.09	0.10
Winney 1-8 SWD	5370	0.33	0.34	0.25	0.20	0.30	0.24	0.17

Woodford cores from OGS

Well Name	Depth/ft	TT19	TT20	TT21	TT22	TT23	TT24	TT25	TT26	24/4	TT28S	TT28R	TT29S	TT29R	Ts	TT30S
Mary Earp-5	4093	0.14	0.42	0.92	0.27	2.34	0.91	1.21	1.65	0.12	0.91	0.83	0.51	0.54	0.85	0.54
Boyd Unit-1	6481	0.12	0.22	0.43	0.14	1.13	0.44	0.47	0.54	0.04	0.25	0.30	0.13	0.14	0.27	0.17
Boyd Unit-1	6486	0.04	0.05	0.10	0.04	0.27	0.10	0.10	0.11	0.02	0.05	0.04	0.03	0.02	0.05	0.03
Dannehl 2-16	8596	0.00	0.73	1.13	0.44	2.22	1.65	1.22	1.48	0.43	0.62	0.68	0.52	0.49	0.64	0.42
Dannehl 2-16	8608	0.00	1.16	1.62	0.52	3.08	2.07	1.82	1.82	0.62	0.83	0.93	0.86	0.66	0.70	0.54
Dannehl 2-16	8619	N.D.	N.D.	N.D.	0.00	0.57	0.31	0.29	0.35	0.05	0.16	0.15	0.14	0.11	0.24	0.13
Pritchard-1	5113	0.21	0.56	0.74	0.38	2.10	0.68	0.85	1.23	0.19	0.41	0.41	0.31	0.47	1.33	0.37
Pritchard-1	5119	0.05	0.10	0.17	0.06	0.41	0.15	0.17	0.23	0.02	0.08	0.10	0.05	0.06	0.19	0.06
Pritchard-1	5125	0.06	0.11	0.04	0.03	0.24	0.09	0.11	0.06	0.08	0.05	0.06	0.03	0.04	0.09	0.04
Pritchard-1	5131	0.05	0.12	0.05	0.03	0.23	0.10	0.12	0.07	0.07	0.06	0.07	0.03	0.03	0.07	0.02
Pritchard-1	5137	0.02	0.03	0.09	0.03	0.18	0.08	0.08	0.10	0.06	0.04	0.04	0.03	0.02	0.05	0.02
Pritchard-1	5141	0.03	0.05	0.11	0.04	0.28	0.13	0.14	0.16	0.06	0.08	0.09	0.06	0.05	0.10	0.05
Pritchard-1	5147	0.03	0.04	0.09	0.03	0.19	0.09	0.09	0.09	0.04	0.04	0.05	0.03	0.02	0.05	0.02
Pritchard-1	5153	0.02	0.04	0.09	0.03	0.21	0.11	0.11	0.12	0.05	0.05	0.06	0.06	0.04	0.07	0.04
Pritchard-1	5159	0.03	0.04	0.09	0.04	0.20	0.10	0.10	0.11	0.05	0.05	0.05	0.04	0.03	0.07	0.03
Ranch 10-1	8707	0.01	0.02	0.03	0.01	0.06	0.04	0.04	0.05	0.03	0.01	0.02	0.01	0.01	0.03	0.01
Ranch 10-1	8726	0.05	0.10	0.17	0.07	0.49	0.31	0.30	0.37	0.11	0.20	0.21	0.17	0.17	0.41	0.16
Anderson 12-1	6824	0.04	0.05	0.11	0.03	0.20	0.15	0.12	0.16	0.05	0.07	0.08	0.07	0.06	0.14	0.05
Anderson 12-1	6893	0.01	0.00	0.01	0.00	0.03	0.02	0.02	0.02	0.01	0.01	0.01	0.01	0.00	0.01	0.00
Anderson 12-1	6923	0.02	0.02	0.05	0.02	0.09	0.06	0.06	0.06	0.03	0.03	0.03	0.03	0.03	0.04	0.02
Chenoweth-1	6526	0.02	0.01	0.04	0.01	0.08	0.05	0.05	0.05	0.02	0.03	0.03	0.03	0.02	0.04	0.01

York-1	8523	0.01	0.01	0.03	0.01	0.06	0.04	0.03	0.04	0.01	0.02	0.02	0.01	0.01	0.02	0.01
York-1	8531	0.01	0.01	0.03	0.01	0.04	0.03	0.03	0.03	0.01	0.01	0.01	0.01	0.01	0.01	0.01
Pope Unit-1	8589	0.06	0.08	0.18	0.05	0.28	0.21	0.16	0.17	0.03	0.07	0.07	0.06	0.05	0.06	0.05

Woodford cores from OGS (cont.-1)

Well Name	Depth/ft	Tm	TT30R	TT31S	TT31R	H29	29Ts	D30	H30	TT33S	TT33R	H31S	H31R	TT34S	TT34R	H32S
Mary Earp-5	4093	0.97	0.56	0.54	0.46	1.70	0.51	0.36	2.36	0.45	0.39	0.797	0.577	0.30	0.35	0.56
Boyd Unit-1	6481	0.31	0.13	0.17	0.11	0.49	0.14	0.14	0.54	0.00	0.09	0.266	0.181	N.D.	N.D.	0.15
Boyd Unit-1	6486	0.06	0.03	0.02	0.01	0.10	0.03	0.03	0.13	0.00	0.02	0.063	0.037	N.D.	N.D.	0.04
Dannehl 2-16	8596	0.64	0.00	0.45	0.43	0.58	0.22	0.32	1.09	0.41	0.22	0.260	0.174	0.36	0.25	0.30
Dannehl 2-16	8608	1.00	0.00	0.52	0.43	0.74	0.32	0.45	0.91	0.50	0.00	N.D.	N.D.	0.00	0.00	0.25
Dannehl 2-16	8619	0.14	0.11	0.12	0.12	0.34	0.11	0.15	0.54	0.00	0.07	N.D.	N.D.	N.D.	N.D.	0.13
Pritchard-1	5113	1.25	0.32	0.40	0.30	3.00	0.85	0.49	4.23	0.00	0.63	1.420	1.181	N.D.	N.D.	0.85
Pritchard-1	5119	0.18	0.06	0.06	0.05	0.39	0.12	0.08	0.53	0.00	0.07	0.168	0.126	N.D.	N.D.	0.11
Pritchard-1	5125	0.09	0.04	0.03	0.02	0.17	0.05	0.04	0.25	0.00	0.03	0.084	0.032	N.D.	N.D.	0.05
Pritchard-1	5131	0.07	0.02	0.02	0.03	0.13	0.04	0.04	0.17	0.00	0.03	0.071	0.051	N.D.	N.D.	0.05
Pritchard-1	5137	0.08	0.00	0.02	0.02	0.11	0.04	0.03	0.15	0.00	0.04	0.057	0.050	N.D.	N.D.	0.04
Pritchard-1	5141	0.16	0.00	0.06	0.05	0.24	0.08	0.05	0.38	0.00	0.07	0.160	0.128	N.D.	N.D.	0.10
Pritchard-1	5147	0.08	0.00	0.02	0.02	0.10	0.03	0.03	0.15	0.00	0.02	0.061	0.053	N.D.	N.D.	0.04
Pritchard-1	5153	0.11	0.00	0.04	0.03	0.12	0.04	0.03	0.20	0.00	0.04	0.082	0.070	N.D.	N.D.	0.05
Pritchard-1	5159	0.10	0.00	0.04	0.03	0.13	0.04	0.03	0.18	0.00	0.03	0.075	0.071	N.D.	N.D.	0.05
Ranch 10-1	8707	0.03	0.00	0.01	0.01	0.04	0.01	0.01	0.06	0.00	0.01	0.025	0.018	N.D.	N.D.	0.02

Ranch 10-1	8726	0.35	0.00	0.19	0.13	0.89	0.22	0.18	1.78	0.00	0.26	0.543	0.426	N.D.	N.D.	0.42
Anderson 12-1	6824	0.09	0.00	0.06	0.05	0.10	0.05	0.08	0.21	0.00	0.03	0.062	0.050	N.D.	N.D.	0.06
Anderson 12-1	6893	0.01	0.00	0.01	0.00	0.01	0.00	0.01	0.01	0.00	0.00	0.005	0.004	N.D.	N.D.	0.00
Anderson 12-1	6923	0.03	0.00	0.02	0.02	0.02	0.02	0.03	0.03	0.00	0.01	0.019	0.016	N.D.	N.D.	0.02
Chenoweth-1	6526	0.03	0.00	0.02	0.02	0.01	0.01	0.03	0.02	0.00	0.01	0.014	0.015	N.D.	N.D.	0.01
York-1	8523	0.02	0.00	0.01	0.01	0.01	0.01	0.01	0.01	0.00	0.00	0.007	0.009	N.D.	N.D.	0.01
York-1	8531	0.01	0.00	0.01	0.01	0.01	0.01	0.01	0.01	0.00	0.00	0.004	0.005	N.D.	N.D.	0.00
Pope Unit-1	8589	0.04	0.00	0.04	0.04	0.04	0.02	0.05	0.04	0.06	0.00	0.000	N.D.	N.D.	N.D.	0.00

Woodford cores from OGS (cont.-2)

Well Name	Depth/ft	H32R	TT35S	TT35R	H33S	H33R	TT36S	TT36R	H34S	H34R	H35S	TT38S	H35R
Mary Earp-5	4093	0.46	0.00	N.D.	0.534	0.393	N.D.	N.D.	0.371	0.277	0.284	N.D.	0.394
Boyd Unit-1	6481	0.12	0.00	N.D.	0.118	0.092	N.D.	N.D.	0.053	0.058	0.049	N.D.	0.042
Boyd Unit-1	6486	0.03	0.00	N.D.	0.036	0.021	N.D.	N.D.	0.013	0.019	0.009	N.D.	0.018
Dannehl 2-16	8596	0.19	0.43	0.23	0.151	0.125	0.19	0.29	0.142	0.081	0.083	N.D.	0.072
Dannehl 2-16	8608	0.17	0.00	N.D.	N.D.	N.D.	N.D.	N.D.	N.D.	N.D.	N.D.	N.D.	N.D.
Dannehl 2-16	8619	0.09	0.00	N.D.	N.D.	N.D.	N.D.	N.D.	N.D.	N.D.	N.D.	N.D.	N.D.
Pritchard-1	5113	0.71	0.00	N.D.	0.737	0.628	N.D.	N.D.	0.532	0.468	0.609	N.D.	0.495
Pritchard-1	5119	0.09	0.00	N.D.	0.106	0.073	N.D.	N.D.	0.083	0.062	0.061	N.D.	0.051
Pritchard-1	5125	0.02	0.00	N.D.	0.041	0.032	N.D.	N.D.	0.027	0.023	0.025	N.D.	0.020
Pritchard-1	5131	0.04	0.00	N.D.	0.039	0.030	N.D.	N.D.	0.028	0.025	0.019	N.D.	0.024
Pritchard-1	5137	0.05	0.00	N.D.	0.055	0.036	N.D.	N.D.	0.027	0.031	0.015	N.D.	0.026

Pritchard-1	5141	0.08	0.00	N.D.	0.098	0.065	N.D.	N.D.	0.066	0.051	0.055	N.D.	0.049
Pritchard-1	5147	0.03	0.00	N.D.	0.034	0.022	N.D.	N.D.	0.022	0.019	0.016	N.D.	0.010
Pritchard-1	5153	0.04	0.00	N.D.	0.048	0.040	N.D.	N.D.	0.026	0.020	0.025	N.D.	0.019
Pritchard-1	5159	0.04	0.00	N.D.	0.039	0.029	N.D.	N.D.	0.024	0.020	0.025	N.D.	0.014
Ranch 10-1	8707	0.01	0.00	N.D.	0.012	0.010	N.D.	N.D.	0.010	0.009	0.007	N.D.	0.006
Ranch 10-1	8726	0.34	0.00	N.D.	0.332	0.256	N.D.	N.D.	0.225	0.175	0.196	N.D.	0.142
Anderson 12-1	6824	0.05	0.00	N.D.	0.038	0.029	N.D.	N.D.	0.026	0.022	0.020	N.D.	0.023
Anderson 12-1	6893	0.00	0.00	N.D.	0.003	0.003	N.D.	N.D.	0.002	0.003	0.002	N.D.	0.001
Anderson 12-1	6923	0.01	0.00	N.D.	0.014	0.012	N.D.	N.D.	0.008	0.009	0.009	N.D.	0.006
Chenoweth-1	6526	0.01	0.00	N.D.	0.007	0.007	N.D.	N.D.	0.005	0.004	0.004	N.D.	0.004
York-1	8523	0.01	0.00	N.D.	0.006	0.004	N.D.	N.D.	0.003	0.003	0.003	N.D.	0.002
York-1	8531	0.00	0.00	N.D.	0.003	0.003	N.D.	N.D.	0.002	0.003	0.002	N.D.	0.003

Mississippian cores

Well Name	TT19	TT20	TT21	TT22	TT23	TT24	TT25	TT26	24/4	TT28S	TT28R	TT29S	TT29R	Ts	TT30S
Albert Severin-1	6444.7	0.49	0.69	1.80	0.58	2.74	1.63	1.33	1.40	0.37	0.75	0.84	0.48	0.48	0.95
Winney 1-8 SWD	5155	0.42	1.24	3.98	0.81	7.45	5.53	5.90	5.60	0.58	3.35	3.51	3.87	3.33	1.05
Winney 1-8 SWD	5166	0.00	0.92	2.45	0.62	4.51	2.90	2.88	2.65	0.50	1.57	1.78	1.35	1.28	1.35
C8869	8869	0.30	0.63	1.71	0.41	3.12	2.83	2.70	2.86	0.24	1.57	1.70	1.83	1.81	0.68

Mississippian cores (cont.-1)

Well Name	Tm	TT30R	TT31S	TT31R	H29	29Ts	D30	H30	TT33S	TT33R	H31S	H31R	TT34S	TT34R	H32S
Albert Severin-1	6444.7	0.55	0.00	0.49	0.39	0.48	0.26	0.73	0.66	0.38	0.00	0.00	N.D.	N.D.	N.D.
Winney 1-8 SWD	5155	0.00	N.D.	2.67	2.47	1.27	1.07	0.91	3.67	2.78	0.77	0.42	0.00	N.D.	N.D.
Winney 1-8 SWD	5166	1.63	0.00	0.97	0.86	1.45	0.95	0.67	3.70	1.08	0.65	0.84	0.78	0.37	0.76
C8869	8869	1.74	0.00	1.52	1.39	0.32	0.20	0.60	0.46	1.63	1.79	0.00	N.D.	2.22	2.09

Mississippian cores (cont.-2)

Well Name	H32R	TT35S	TT35R	H33S	H33R	TT36S	TT36R	H34S	H34R	H35S	TT38S	H35R	TT38R	TT39S	TT39R
Albert Severin-1	6444.7	N.D.	N.D.	N.D.	N.D.	N.D.	N.D.	N.D.	N.D.	N.D.	N.D.	N.D.	N.D.	N.D.	N.D.
Winney 1-8 SWD	5155	1.01	2.44	2.21	1.05	0.77	1.77	1.71	0.80	0.59	0.75	2.08	0.00	N.D.	N.D.
Winney 1-8 SWD	5166	0.80	0.87	0.66	0.81	0.65	0.68	0.57	0.73	0.54	0.73	0.39	0.72	0.63	0.56
C8869	8869	N.D.	N.D.	N.D.	N.D.	N.D.	N.D.	N.D.	N.D.	N.D.	N.D.	N.D.	N.D.	N.D.	N.D.

Oils and condensates from Devon Energy

Well Name	TT19	TT20	TT21	TT22	TT23	TT24	TT25	TT26	24/4	TT28S	TT28R	TT29S	TT29R	Ts	TT30S
Adkisson 1-33H	11	26	65	16	129	93	88	93	12	58	60	55	56	35	55
Smith 1-14H	22	44	79	29	137	106	97	105	19	50	53	54	56	60	40
Winney 1-8H	10	26	67	19	131	93	96	85	9	57	58	51	56	30	43
Elinore 1-18H	9	34	58	15	119	72	73	68	10	39	42	39	40	22	30
Johnson 1-33H	7	24	51	17	99	75	77	68	11	43	43	47	47	26	42
Smith 1-23MH	6	13	24	6	39	31	29	27	6	14	15	16	19	15	14
Wilma 1-16SWD	4	19	16	5	28	20	20	19	4	10	11	10	10	10	8
Winney 1-5H	7	30	45	12	84	61	63	55	5	34	36	32	51	18	29
Matthews 1-33H	7	20	49	11	86	62	64	57	5	35	37	35	37	17	28
Elinore 1-17H	2	11	19	5	41	23	25	23	3	12	14	12	12	7	10
Williams 1-24 WH	3	5	11	3	23	17	16	15	2	9	9	9	10	6	8
Peach 1-19 MH	2	4	9	2	15	11	11	10	2	6	7	6	6	5	5
Joyce 1-32 WH	4	10	15	4	32	20	19	16	4	12	12	11	10	11	9
Hopfer 1-20 WH	2	7	15	4	34	21	23	22	3	15	14	13	13	9	14
Peach 1-20 WH	1	2	4	1	8	5	5	4	1	3	3	3	3	2	2
C. Matthews 1-8 WH	3	6	13	4	26	19	18	17	3	10	11	11	11	6	9

Oils and condensates from Devon Energy (cont.-1)

Well Name	Tm	TT30R	TT31S	TT31R	H29	29Ts	D30	H30	TT33S	TT33R	H31S	H31R	TT34S	TT34R	H32S
Adkisson 1-33H	65	N.D.	47	38	43	18	16	92	51	56	37	88	71	3	33
Smith 1-14H	18	32	39	31	62	22	22	114	38	37	40	26	40	51	34
Winney 1-8H	15	34	36	30	52	21	20	115	42	42	40	27	47	61	31
Elinore 1-18H	35	26	27	21	104	15	13	173	28	28	61	49	24	45	43
Johnson 1-33H	18	45	38	30	23	15	11	55	35	33	18	13	40	46	18
Smith 1-23MH	5	17	11	10	14	9	6	29	11	10	9	7	10	14	8
Wilma 1-16SWD	3	11	7	6	10	5	5	20	7	7	6	4	8	9	6
Winney 1-5H	8	23	22	19	27	18	10	57	22	23	19	15	26	33	24
Matthews 1-33H	7	32	22	20	20	10	9	43	25	26	13	9	30	33	12
Elinore 1-17H	10	8	8	6	30	4	3	49	8	8	16	11	8	11	11
Williams 1-24 WH	10	N.D.	7	6	7	3	3	16	8	8	6	N.D.	N.D.	N.D.	6
Peach 1-19 MH	2	5	4	3	7	4	3	16	5	5	5	4	5	7	5
Joyce 1-32 WH	20	N.D.	9	7	32	5	3	57	10	10	17	19	4	13	15
Hopfer 1-20 WH	15	N.D.	12	9	12	4	4	25	8	9	10	N.D.	N.D.	N.D.	8
Peach 1-20 WH	3	N.D.	2	2	4	1	1	8	2	2	3	3	1	3	2
C. Matthews 1-8 WH	12	N.D.	8	7	8	3	3	18	10	9	7	N.D.	N.D.	N.D.	7

Oils and condensates from Devon Energy (cont.-2)

Well Name	H32R	TT35S	TT35R	H33S	H33R	TT36S	TT36R	H34S	H34R	H35S	TT38S	H35R	TT38R	TT39S	TT39R
Adkisson 1-33H	21	47	40	22	15	33	28	17	16	17	15	22	30	31	30
Smith 1-14H	26	32	25	26	20	28	23	24	20	23	14	26	28	23	21
Winney 1-8H	24	37	29	28	23	29	22	21	15	26	15	32	24	21	20
Elinore 1-18H	30	25	20	30	22	20	17	22	15	17	9	22	16	14	10
Johnson 1-33H	11	26	25	14	9	23	18	14	13	12	14	17	22	33	19
Smith 1-23MH	5	9	7	5	4	7	7	5	4	5	3	7	7	5	4
Wilma 1-16SWD	4	6	5	4	3	4	4	4	3	3	2	4	5	4	3
Winney 1-5H	10	17	14	11	7	11	11	10	8	10	7	13	12	10	8
Matthews 1-33H	8	19	16	10	6	15	13	8	5	11	7	11	15	14	11
Elinore 1-17H	7	7	5	8	5	5	4	6	4	4	2	6	3	0	N.D.
Williams 1-24 WH	4	8	6	4	3	5	5	3	2	4	3	4	5	4	4
Peach 1-19 MH	4	4	3	3	3	3	2	3	3	3	1	4	3	2	2
Joyce 1-32 WH	10	9	7	12	9	4	3	8	6	7	2	5	4	0	N.D.
Hopfer 1-20 WH	5	12	11	6	4	9	7	5	4	5	5	5	11	11	7
Peach 1-20 WH	2	2	2	2	1	1	1	1	1	1	1	1	1	1	1
C. Matthews 1-8 WH	4	9	7	5	4	6	6	3	2	4	3	5	5	5	4

Conventionally Produced Woodford-Sourced Oils and condensates from Southern Oklahoma

Well Name	TT19	TT20	TT21	TT22	TT23	TT24	TT25	TT26	24/4	TT28S	TT28R	TT29S	TT29R	Ts	TT30S
Ford-1	4	15	26	9	49	34	32	32	8	17	19	16	17	14	14
Thomas James 1-22	1	3	4	1	8	6	6	6	2	3	3	3	3	2	3
Anadarko Taylor 2118	12	24	39	13	75	55	51	56	6	35	37	33	35	22	29
A	7	21	36	12	69	48	49	41	10	24	27	26	25	24	21
Ellis Lewis Jet	3	9	13	4	23	15	14	14	3	8	8	7	7	5	6
F	5	14	23	6	45	31	29	27	5	15	16	14	15	12	13
7-5N-5E	1	5	10	3	20	15	16	12	2	6	6	6	7	6	5

Conventionally Produced Woodford-Sourced Oils and condensates from Southern Oklahoma (cont.-1)

Well Name	Tm	TT30R	TT31S	TT31R	H29	29Ts	D30	H30	TT33S	TT33R	H31S	H31R	TT34S	TT34R	H32S
Ford-1	25	7	15	11	51	11	6	85	10	12	33	24	10	17	24
Thomas James 1-22	2	2	3	2	5	2	1	8	2	2	3	3	2	3	2
Anadarko Taylor 2118	8	22	25	22	13	7	9	22	21	22	11	8	24	22	8
A	17	15	18	14	41	18	12	86	17	17	28	22	16	26	21

Ellis Lewis Jet	6	3	6	4	12	4	2	23	5	5	8	6	4	6	5
F	18	2	10	8	24	7	6	50	9	10	16	11	9	14	12
7-5N-5E	12	2	4	3	22	5	2	39	N.D.	N.D.	N.D.	N.D.	N.D.	N.D.	13

Conventionally Produced Woodford-Sourced Oils and condensates from Southern Oklahoma (cont.-2)

Well Name	H32R	TT35S	TT35R	H33S	H33R	TT36S	TT36R	H34S	H34R	H35S	TT38S	H35R	TT38R	TT39S	TT39R
Ford-1	16	12	8	16	12	7	5	13	10	11	4	13	6	N.D.	N.D.
Thomas James 1-22	2	N.D.	N.D.	N.D.	N.D.	N.D.	N.D.	N.D.	N.D.	N.D.	N.D.	N.D.	N.D.	N.D.	N.D.
Anadarko Taylor 2118 A	5	17	14	12	7	12	13	8	6	12	N.D.	N.D.	N.D.	N.D.	N.D.
Ellis Lewis Jet F	17	15	11	16	11	11	10	12	8	11	5	13	10	8	7
7-5N-5E	4	4	3	4	4	3	2	3	2	3	1	4	3	3	2
	8	8	6	10	7	5	4	6	5	5	2	7	5	3	4